AD-A137 778 SPECTRAL ANALYSES OF HIGH-FREQUENCY PN SN PHASES FROM VERY SHALLOW FOCUS EARTHQUAKES(U) HAWAII INST OF GEOPHYSICS HONOLULU D A WALKER SEP 83 AFOSR-TR-84-0059 1/2

UNCLASSIFIED F49620-81-C-0065 F/G 8/11 NL

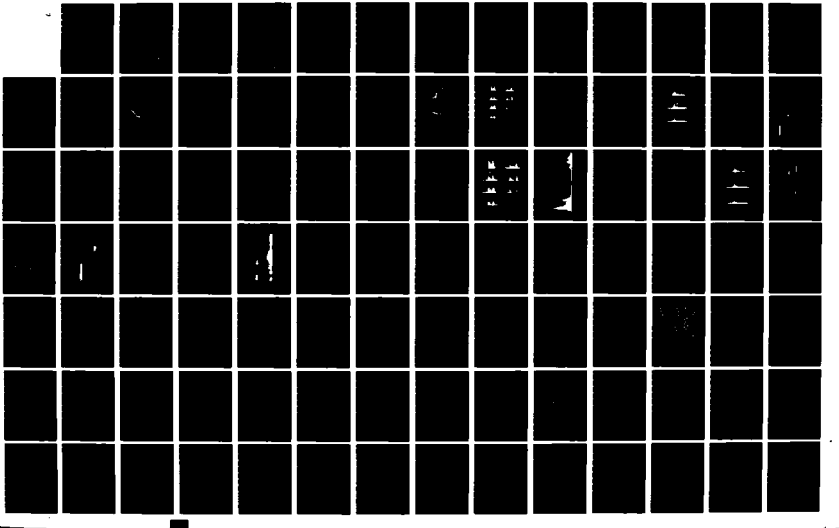

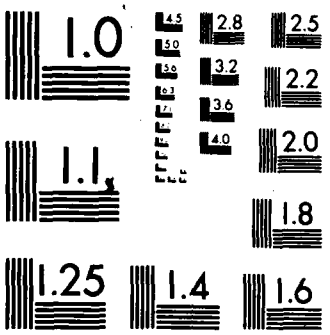

MICROCOPY RESOLUTION TEST CHART
NATIONAL BUREAU OF STANDARDS-1963-A

AFOSR-TR- 84-0059

FINAL

Technical Report

to the

Air Force Office of Scientific Research

from

Daniel A. Walker

Hawaii Institute of Geophysics
University of Hawaii
Honolulu, Hawaii 96822

Name of Contractor: University of Hawaii

Effective Date of Contract: 3 March 1981

Contract Expiration Date: 30 September 1983

Total Amount of Contract Dollars: $270,910

Contract Number: F49620-81-C-0065

Principal Investigator and Phone Number: Daniel A. Walker
808-948-8767

Program Manager and Phone Number: John W. Shupe
Interim Director of Research
808-948-7541

Title of Work: Spectral Analyses of High-Frequency Pn, Sn Phases from Very Shallow Focus Earthquakes

UNCLASSIFIED

SECURITY CLASSIFICATION OF THIS PAGE (When Data Entered)

REPORT DOCUMENTATION PAGE		READ INSTRUCTIONS BEFORE COMPLETING FORM
1. REPORT NUMBER AFOSR-TR- 84-0059	2. GOVT ACCESSION NO. AD-A137775	3. RECIPIENT'S CATALOG NUMBER
4. TITLE (and Subtitle) Spectral Analyses of High-Frequency Pn,Sn Phases from Very Shallow Focus Earthquakes		5. TYPE OF REPORT & PERIOD COVERED Final Report 6. PERFORMING ORG. REPORT NUMBER
7. AUTHOR(s) D. A. Walker		8. CONTRACT OR GRANT NUMBER(s) F49620-81-C-0065
9. PERFORMING ORGANIZATION NAME AND ADDRESS Hawaii Institute of Geophysics University of Hawaii Honolulu, Hawaii 96822		10. PROGRAM ELEMENT, PROJECT, TASK AREA & WORK UNIT NUMBERS 2309/A1 61102F
11. CONTROLLING OFFICE NAME AND ADDRESS Air Force Office of Scientific Research/NP Bolling AFB, Washington, D.C. 20301		12. REPORT DATE September 1983 13. NUMBER OF PAGES 182
14. MONITORING AGENCY NAME & ADDRESS(if different from Controlling Office)		15. SECURITY CLASS. (of this report) unclassified 15a. DECLASSIFICATION/DOWNGRADING SCHEDULE N/A

16 DISTRIBUTION STATEMENT (of this Report)

Approved for public release;
distribution unlimited.

17. DISTRIBUTION STATEMENT (of the abstract entered in Block 20, if different from Report)

18 SUPPLEMENTARY NOTES

19 KEY WORDS (Continue on reverse side if necessary and identify by block number)

Underground Nuclear Explosions; Body-Waves; Spectral Analyses; Hydrophone Recording; Discrimination; Noise Levels

20 ABSTRACT (Continue on reverse side if necessary and identify by block number)

The Wake Island Hydrophone Array has been successfully upgraded from a 3-channel slow-speed analog cassette system to an 11-channel computer controlled digital system for continuing research on Ocean P (Po) and Ocean S (So) phases, as well as normal, mantle-refracted P phases from underground nuclear explosions and earthquakes at great distances.

DD FORM 1 JAN 73 1473

UNCLASSIFIED

SECURITY CLASSIFICATION OF THIS PAGE (When Data Entered)

Features of the upgraded system are a large dynamic range (events from at least 4.0 to 8.0 mb can be recorded without distortion), absolute timing accuracy to 1 msec, interchannel timing accuracy to 1 msec, digital recording for ease of processing, and a 40 Hz Nyquist frequency for recording frequencies actually observed in Po/So at large distances.

Software development for compression and efficient management of the data has been successfully completed with master tapes sent to DARPA's Center for Seismic Studies for use by interested investigators.

Research papers on Po/So phases have reported on the frequency content and propagation velocities at the Wake hydrophones and across a 1600 km long deep ocean hydrophone array. At a distance of about 18° ($\simeq$2000 km) frequencies for Po/So are as high as 30 and 35 Hz, respectively; at a distance of about 30° ($\simeq$3,300 km), as high as 15 and 20 Hz, respectively. The travel time equations which successfully model all Northwestern Pacific shallow-focus Po/So first arrival data collected by the Hawaii Institute of Geophysics since 1963 at epicentral distances greater than 12° are $T = X/(7.96 \pm 0.05$ km/sec) - $(7.14 \pm 2.38$ sec) and $T = X/(4.57 \pm 0.04$ km/sec) - $(14.03 \pm 5.31$ sec), respectively. Values for a frequency dependent Q are found to range from 625 ± 469 at 2 Hz to $2106 + 473$ at 13 Hz for Po and from 1401 ± 296 at 5 Hz to 3953 ± 863 at 15 Hz for So. This could alternatively be described as an average attenuation of -21.5 ± 0.9 dB per 1000 km of travel path for both Po and So at all frequencies studied.

Regarding published research on normal-mantle refracted P phases, spectral comparisons for earthquakes and explosions have been completed and published. Expected differences between the spectral signatures of explosions and shallow focus earthquakes at great distances (the nuclear explosions being relatively stronger at high frequencies) are reported. The recording of a small explosion and improvement in its S/N ratio through some elementary enhancement techniques are also discussed.

TABLE OF CONTENTS

INTRODUCTION

General Objectives

General objectives of our research in deep ocean seismology can be summarized as follows:

(1) to determine the mechanism for the generation and propagation of Po/So phases; and

(2) to utilize the low noise levels at high frequencies (i.e., > 2 Hz) of the deep oceans and the relatively large amplitudes observed in P at those high frequencies from events at great distances (i.e., >> 30^{o}) to gain new insights into: (a) differences in spectra associated with source characeristics, and (b) the physical properties of the deep mantle.

In the past two years the principal means for achieving these objectives has been through the acquisition of data from hydrophones and ocean bottom seismometers located near Wake Island.

Specific Objectives

Specific objectives of an applied nature which we believe may be of interest to AFOSR are the following:

(1) the relationship of Po/So spectra to focal depth and source parameters;

(2) spectral comparisons of normal, mantle-refracted P phases at great distances from earthquakes and explosions;

(3) estimates of the coherence of seismic phases recorded on the deep ocean floor; and

(4) comparisons of S/N ratios for phases recorded on the Wake hydrophones, ocean bottom seismometers, and ocean sub-bottom seismometers.

The specific means by which AFOSR has contributed to our efforts to achieve these objectives has been major support for the upgrading of our Wake Island hydrophone array (partial support being derived from ACDA) and for the analysis of data acquired by: (a) the upgraded station, (b) the original three channel Wake system, and (c) other ocean bottom instrumentation in the Western Pacific.

Reasons for Interest

Reasons why these applied objectives may be of interest follow.

(1) For oceanic travel paths out to distances of about 3000 km, Po/So phases have signal-to-noise ratios generally at least ten times greater than the ratios of their respective normal, mantle-refracted P and S phases; and, in many instances, no P's or S's can be found in spite of

the presence of very strong Po's and So's. Therefore, the detection and discrimination of underground nuclear explosions at distances less than about 3000 km in an ocean environment requires an understanding of Po/So. Most important could be any possible relationship of Po/So spectra to focal depth and/or source parameters.

(2) Normal, mantle-refracted P phases recorded at great distances (i.e., 60° to 90°, or approximately 6700 km to 10,000 km) have substantial amounts of energy at high frequencies (i.e., 2 Hz to 10 Hz). Such phases from earthquakes and explosions are well recorded in the low noise environment of the deep ocean. [Estimates of noise levels on the Wake bottom hydrophones in the 2 to 10 Hz range are comparable to those of the best continental sites.]

(3) A major concern in the analysis of underground explosions by seismic methods is the reliability of yield estimates. Much of the scatter in yield estimates is due to inconsistencies between the waveforms from different stations, and even between the waveforms from elements of continental arrays with apertures the size of the Wake bottom array. These differences may be attributable to variations in the response of the continental crust underlying these arrays. Signals recorded in regions where the crust is very thin (i.e., under the deep ocean basins) may have higher coherencies--thereby providing a means for improved estimates of yield. The Wake array is an ideal tool for evaluating this hypothesis.

(4) In recent years some members of the "detection and discrimination" community have demonstrated a substantial amount of interest in ocean sub-bottom instrumentation. The level of this interest may be best manifested in DARPA's commitment to develop a working sub-bottom system--the "Marine Seismic System" or MSS. Anotner sub-bottom instrument which has been developed (this at HIG through ONR sponsorship) is called the "Ocean Sub-Bottom Seismometer" (OSS). A reasonable presumption is that S/N ratios for ocean sub-bottom systems would be greater than for existing bottom systems (i.e., ocean bottom seismometers or ocean bottom hydrophones), resulting in a higher sensitivity (or lower detection threshold) for the sub-bottom instrument. A possible alternative to a sub-bottom instrument is an array of bottom instruments such as ocean bottom seismometers or ocean bottom hydrophones, with enough elements to make up the difference in S/N. Essential requirements to achieve an increase in S/N are incoherent noise and coherent signals in the frequency band of interest. Advantages of such an array over a sub-bottom instrument may be in cost, in ease of deployment, and in studies requiring an array. With the continued operation of the eleven element deep-ocean hydrophone array near Wake Island. these questions may be answered through further comparisons between signals recorded by the sub-bottom systems and those recorded by the Wake hydrophones.

PROGRESS

Upgrading of the Wake Island Hydrophone Array Recording System

Upgrading of the recording system for the Wake Hydrophone Array, from a 3-channel slow-speed analog cassette system to an 11-channel, 16 bit, computer-controlled digital system, was accomplished by September, 1982. Some of the advantages of this new system are: (1) a large dynamic range to record, without distortion, events ranging from at least mb = 4.0 to mb = 8.0 (i.e., 16 bits = 96 dB); (2) absolute timing generally accurate to 1 msec (for ease in processing, no time correction needs to be applied to acheive this accuracy);(3) interchannel timing accurate to within 1 msec; (4) a digital recording format such that only a minimal amount of processing is necessary to convert the data to a widely useable format; (5) the capability to record all eleven available hydrophones; (6) the recording of frequencies at least as high as those already observed at Wake in Po and So (i.e., a 40 Hz Nyquist); (7) operation of the system so simple that it can be accomplished by the personnel at Wake who are untrained in computer hardware and software; (8) required servicing (i.e., changing tapes) no more than once per day; and (9) the capability of restarting automatically after power failures (which occur frequently at Wake).

The recording of data from all eleven available hydrophones produces four full-reel computer tapes per day requiring four tape drives to maintain a maximum of once per day servicing by an operator. Several problems which have occurred with the tape drives have made it necessary to record only eight of the eleven hydrophones (thus producing only three tapes per day) during most of the recording period. All other losses of data, including those caused by power-failures, amount to less than 3% of the total data collected.

Once the data on computer tape are received by HIG, an efficient compression and management of the data must be accomplished. Uncompressed, the data could amount to 1460 tapes per year, requiring a large space for storage and being inefficient to access for study, or to copy and transmit to other scientists. Software has been developed to compress this data to approximately 15% of its original volume and at the same time catalog all of the saved data for easy accessibility. Sections of data saved correspond to arrivals from events, and the raw data are also randomly sampled for future quantification of the temporal characteristics of ambient noise levels.

Compressed data tapes have been sent to the DARPA Center for Seismic Studies (CSS) for use by other scientists.

A complete description of the digital recording system at Wake, the data compression software used at HIG, and the tape format for data sent to CSS is contained in Appendix IX. A list of events for which the times of possible arrivals have been saved on the CSS compressed data tapes is contained in Appendix X.

Po/So Spectra vs. Focal Depth and Source Parameters

Although this was one of our original research objectives for AFOSR, no direct progress has been made in this area. Factors contributing to this lack of progress have been:

(a) the re-direction of efforts towards topics more readily resolved, of more immediate interest, and/or of greater apparent importance;

(b) anticipated improvements in instrumentation (i.e., the upgrading to a digital, rather than an analog system) which would greatly facilitate the data reduction required for this task; and

(c) the small number of events with very shallow focal depths (<10 km).

Indirectly, a great deal of progress may have been made towards the achievement of this objective. [It is unlikely that relationships of spectra to focal depths and source parameters could be postulated in the absence of a generally acceptable model for the generation and propagation of Po/So phases.] Evidence of continuing progress in Po/So research may be found in: (a) recent publications ("Oceanic Pn/Sn: a qualitative explanation and reinterpretation of the T-phase" by D. Walker; RIG Report 82-6; and "Spectral characteristics of high-frequency Pn. Sn phases in the Western Pacific" by D. Walker, C. McCreery, and G. Sutton; op. cit.); (b) the formation of an Ocean P Alliance with the publication of an OPA newletter; and, (c) important advances apparent in analyses of data acquired by the ONR sponsored OBS Wake array experiment reported at the recent fall AGU meeting and now in draft form in preparation for publication. ("Po/So Phases: Propagation Velocity and Attenuation Across A 1600 km Long Deep Ocean Hydrophone Array" by D. A. Walker and C. S. McCreery).

We should note that with the upgraded system we have recorded two shallow focus events (15 km and 17 km depth) from the Marianas at distances of about 18° and one intraplate (and presumably very-shallow focus) event from approximately 12° to the west of Wake. The Po/So phases from these, and other, events will be useful in evaluating Po/So as a possible discriminant.

Spectral Comparison for Earthquakes and Explosions

Spectral comparisons between earthquakes and explosions have been completed and are the subject of a pubished paper ("Spectra of nuclear explosions, earthquakes, and noise from Wake Island bottom hydrophones" by C. McCreery, D. Walker, and G. Sutton, Geophys. Res. Lett., 10, 59-62, 1983.) The data examined show expected differences between the spectral signatures of explosions and shallow focus earthquakes at great distances--the nuclear explosions being relatively stronger at high-frequencies (or weaker at low-frequencies) than earthquakes. Also, a small explosion has been recorded with a significant S/N ratio on the Wake hydrophones. A unique aspect of hydrophone recordings is that the ocean surface reflection (recorded at a time after the main P corresponding to twice the water depth divided by the velocity of sound in water) can be used to increase S/N ratios.

Estimates of Coherence

Comprehensive estimates of coherence and possible improvements in yield estimates are a major topic for investigation in the coming year using data acquired from the expanded hydrophone array. Some preliminary estimates of coherence have already been made. These estimates are appended to this report.

Comparisons of S/N Ratios

In September of 1982, DARPA and ONR conducted tests (the "Downhole Experiment") in the Northwestern Pacific relating to sub-bottom seismic instrumentation. Successful deployments included OBS's and HIG's ocean sub-bottom seismometer (OSS). During the same time the expanded Wake system became operational. Preliminary comparisons of S/N ratios for the Wake system and the available downhole data have been made. They are appended to this report. Additional comparisons were (and are being) made after the OSS data was retrieved from its recording package on the ocean bottom in the summer of 1983. These comparisons will be the subject of a future report.

SUMMARY OF ACCOMPLISHMENTS

Major accomplishments supported in whole, or in part, by AFOSR since 3 March 1982 follow.

(1) Successful upgrading of the Wake Hydrophone Array recording system from a three-channel analog cassette system to a sixteen-channel digital system. Some of the advantages of this new system are: (a) the ability to simultaneously record all of the active hydrophones in the array; (b) a 96 dB dynamic range; (c) millisecond accurate absolute and cross-channel timing; and (d) a digital format which allows immediate processing of the data.

(2) Development of software to compress and manage the digital data collected at Wake. This data is compressed by saving intervals of data in which seismic phases of interest are known or suspected to be present, and by saving regular intervals of data for sampling the ambient noise levels. These compressed data are stored on magnetic tape files which are catalogued on paper and in computer files for easy reference.

(3) Preparation of a report on items 1 and 2 above ("The Continuous Digital Data Collection System for the Wake Island Hydrophones" by C. S. McCreery).

(4) Distribution of the Wake digital data through the DARPA Center for Seismic Studies (CSS). Compressed data tapes containing known or suspected seismic phases are being routinely sent to CSS for access by others who may have an interest in this data. Investigators at Rondout Associates Inc. have successfully accessed the data through CSS. A list of intervals, and the events and phases, which they represent, is contained in Appendix X. The event format of the data also is described in Appendix IX.

(5) The observation and characterization of differences in spectral signature between P from explosions and P from shallow focus earthquakes recorded on the Wake bottom hydrophones. The observations reflect differences in source spectra between explosions and shallow focus earthquakes. For similar magnitudes, explosions had more energy at frequencies above 2.0 Hz and less energy at frequencies below 1.5 Hz.

(6) The enhancement of S/N of an extremely small explosion by signal stacking to a level near that for perfectly coherent signals.

(7) The publication of a report on items "4" and "5" above ("Spectra of nuclear explosions, earthquakes, and noise from Wake Island bottom hydrophones" by C. McCreery, G. Sutton, and D. Walker; op. cit.).

(8) Continuing analyses of Po/So phases with additional spectrograms and discussions submitted for publication ("Spectral characteristics of high-frequency Pn, Sn phases in the Western Pacific" by D. Walker, C. McCreery, and G. Sutton; op. cit.).

(9) The formation of an "Ocean P Alliance" with the publication of an OPA Newsletter to stimulate interest in, and research on, Po/So phases.

(10) The evolution of a qualitative explanation for the propagation of Po/So phases consistent with many observations of these phases throughout the western, northern, and central Pacific.

(11) The discovery of a probable relationship between Po/So and T phases.

(12) Publication of a report discussing item "9" and "10" above ("Oceanic Pn/Sn: a qualitative explanation and reinterpretation of the T-phase" by D. Walker; HIG Report 82-6.)

(13) Preliminary comparisons, with available data, of the Wake hydrophones to ocean bottom seismometers and the OSS. It should be noted that these are merely preliminary studies and in some cases the comparisons made are of an indirect nature. Nonetheless, it would appear that the Wake hydrophones may be comparable to the OSS in terms of S/N ratios, considering possible improvements through array processing. Direct comparisons to MSS are not possible since that system was not successfully deployed in the Pacific. Regarding the comparisons of Wake to ocean bottom seismographs, we have observed with data from an ONR sponsored OBS experiment near Wake Island in 1981 that the Wake hydrophones have higher S/N ratios than OBS's by about 10 dB over the range 1-20Hz.

(14) The presentation of studies on the spectra of nuclear explosions and earthquakes, as well as spectral studies of Po/So, at the 1982 DARPA/AFOSR annual review.

(15) Preparation of a report (Po/So Phases: Propagation Velocity and Attenuation Across a 1600 km Long Deep Ocean Hydrophone Array by D. Walker and C. McCreery) which quantifies the variations in velocity and spectra of Po/So phases across a long deep ocean array.

SIGNIFICANT TASKS REMAINING

(1) Consistent with our efforts to determine the mechanism for the generation and propagation of Po/So phases, a comprehensive investigation of the relationship of the T phase to Po/So will be made. This study will include spectral studies of the entire T phase coda (i.e., forerunners as well as peak signals) and comparisons of these spectra to the spectra of Po/So phases.

(2) Differences between the hydrophone/cable response (and possibly the lithosphere response) across the Wake array will be determined and removed from the data. This will be necessary to evaluate the stability of yield estimates from spectral or waveform data across the array. Such an evaluation will be made.

(3) Research on coherence across the Wake array will be completed with the coming year, and the significance of these studies in terms of possible improvements in S/N will be evaluated.

(4) S/N comparisons to the Wake hydrophones will be made with the OSS data which was retrieved from its recording package on the ocean bottom this past summer.

(5) Profiles of Po/So spectra as a function of focal depth will be made. If sufficient data is available for very shallow focus events, the possible significance of the relationships in terms of nuclear detection and/or discrimination will be evaluated.

The expanded Wake Island Hydrophone Array was successfully installed with funds provided primarily by AFOSR. However, since supplementary support of critical importance was provided by ACDA, all studies utilizing data acquired by the upgraded system should acknowledge both agencies. In the coming year ACDA funds will be used primarily on item #2 above, with the possibility that supplementary support for this task may be provided by AFOSR. On all other tasks AFOSR will be the principal supporter, with some supplementary funds provided by ACDA.

APPENDIX I

GEOPHYSICAL RESEARCH LETTERS, VOL. 10, NO. 1, PAGES 59-62, JANUARY 1983

SPECTRA OF NUCLEAR EXPLOSIONS, EARTHQUAKES, AND NOISE FROM WAKE ISLAND BOTTOM HYDROPHONES

Charles S. McCreery and Daniel A. Walker

Hawaii Institute of Geophysics, University of Hawaii, Honolulu, HI 96822

George H. Sutton

Rondout Associates, Inc., Stone Ridge, NY 12484

Abstract. Spectral characteristics of P phases from 4 shallow focus earthquakes and 8 underground explosions, and of 52 samples of ocean bottom background noise, are examined by using tape recordings of ocean bottom hydrophones near Wake Island from July 1979 through March 1981. Significant differences are found between spectra of large shallow focus earthquakes and explosions ($5.7 \leq mb \leq 6.3$) observed at 61° to 77° epicentral distance. For similar magnitudes, explosions were found to have less energy at frequencies below 1.5 Hz and more energy at frequencies above 2.0 Hz. Earthquakes were found to have a spectral slope of -28 dB/octave (relative to pressure) over the band 1 to 6 Hz. Explosions were found to have the same spectral slope over the band 2.2 to 6 Hz, but a different slope of -12 dB/octave over the band 1.1 to 2.2 Hz. High frequencies (>6 Hz) observed in the teleseismic P phases indicate high Q values for the deep mantle. Ambient noise levels on the ocean bottom near Wake are comparable to levels at the quietest continental sites for frequencies between 3 and 15 Hz. Also high levels of coherence (at least as high as 0.85) have been observed for P phases recorded on sensors with 40-km separation.

Introduction

In an earlier report (Walker, 1980), slow-speed paper recordings of hydrophones located near Wake Island were used in a study of P phases from underground nuclear explosions and earthquakes at comparable distances. That study was prompted by: (1) the work of Evernden (1977) and Evernden and Kohler (1979), which showed that P phases recorded in the 60° to 90° distance range from underground explosions were surprisingly rich in high-frequency energy (at least as high as 9 Hz); (2) the extreme sensitivity of the Wake hydrophones to high-frequency signals (Walker et al., 1978); and (3) the location of most known underground test sites in the 60° to 90° distance range from the Wake hydrophones. The major conclusion of Walker (1980) was that observable P phases were found for all Russian underground explosions with estimated yields in excess of 270 kilotons, whereas no such phases were found for earthquakes of comparable or greater magnitude at similar distances. Principal limitations of the investigation were that: (1) the slow-speed paper recordings were not suitable for detailed spectral analyses of either the recorded signals or the noise; and (2) the filtering was not optimized for the recording of distant earthquakes and explosions.

Paper number 2L1384.
0094-8276/83/ 002L-1384$3.00

This report discusses the spectra of P phases from underground explosions and earthquakes as well as the spectra of ambient noise derived from recent tape recordings of the Wake Island ocean bottom hydrophone array. This array consists of six hydrophones on relatively flat ocean bottom near Wake at about 5.5-km depth. The hydrophones are located at the vertices and center of a pentagon roughly 40 km across and are cabled directly to Wake Island. Only three of the hydrophones could be recorded simultaneously on the recording system used. This system was a four-channel (three data, one time code) slow-speed cassette recorder, with automatic gain-ranging amplifiers following low-noise preamps connected to the differential outputs (via cabling) of the moving coil hydrophones on the ocean bottom. These recorded signals were used to compute absolute spectra of the seismic phases and background noise by the following steps: (1) digitization at 80 samples per sec after anti-alias filtering; (2) normalization of the automatic gain levels; (3) computation of contiguous 512-point FFT's (6.4 sec per FFT) and their corresponding power spectra; (4) averaging of those spectra over the time window of interest; (5) normalization of the spectral bandwidth from 0.156 Hz to 1.0 Hz; and (6) removal of the hydrophone/recording system/anti-alias response. The recording system and anti-alias response were determined in situ. The hydrophone response was taken from the Columbia University OBS Calibration Manual (Thanos, 1966), which describes the estimated response between 0.05 and 100 Hz of an equivalent hydrophone. More specific information on the Wake hydrophone/cable responses at these frequencies is not available because of the age of the array (about 20 years), its formerly classified status, and the original bandwidth of interest (>10 Hz) to those who installed the array.

Spectra of Underground Explosions and Natural Earthquakes

The earthquakes and explosions investigated in this study are listed in Table 1. These events were chosen because they all occurred within 60° to 90° epicentral distance, were shallow focus, had large signal/noise ratios, and did not exceed the dynamic range of the recording system. Figure 1 shows the pressure spectra of some of these events, as well as composite pressure spectra for the earthquake and explosion groups. For purposes of comparison, pressure and vertical

Table 1. Description of Events Used in Figure 1

No.	Date	Location	Distance (degrees)	Depth (km)	Magnitude (mb)	Type	Number of Hydrophones
1	07/24/79	S. of Java	65.7	31	6.3	Earthquake	3
2	08/04/79	E. Kazakh	73.2	0	6.1	Explosion	3
3	08/18/79	E. Kazakh	73.2	0	6.1	Explosion	3
4	09/24/79	Novaya Zemlya	76.7	0	5.7	Explosion	1
5	09/29/79	N. Sumatera	72.9	27	6.2	Earthquake	1
6	10/18/79	Novaya Zemlya	76.8	0	5.8	Explosion	1
7	10/28/79	E. Kazakh	73.2	0	6.0	Explosion	1
8	12/23/79	E. Kazakh	73.3	0	6.1	Explosion	1
9	07/29/80	Nepal	76.4	18	6.1	Earthquake	2
10	09/14/80	E. Kazakh	73.2	0	6.2	Explosion	2
11	10/12/80	E. Kazakh	73.2	0	5.9	Explosion	2
12	11/19/80	Sikkim	70.4	17	6.0	Earthquake	2

displacement may be related using the expression: $P = \omega \rho v A$, where P is pressure, ω is angular frequency, ρ is seawater density, v is the speed of sound in seawater, and A is vertical displacement. This relationship holds for compressional energy arriving vertically from below the hydrophone. The following differences in the spectral signatures between explosions and shallow focus earthquakes are evident: (1) lack of energy in explosion P relative to earthquake P at frequencies below 1.5 Hz, (2) changes in spectral slope (corner frequency?) for explosions from -12 to -28 dB/octave (equivalent to -18 and -34 dB/octave in ground displacement) at about 2.2 Hz, and (3) greater energy in explosion P relative to earthquake P at frequencies above 2.0 Hz, despite smaller magnitude of the average explosion (6.03) than that of the average earthquake (6.16). Differences between the explosion and earthquake P phases observed at these frequencies is not surprising. The high frequencies observed and the actual shape of these curves have implications regarding Q along the travel path. Although these implications will not be discussed here, it is pointed out that the observation of frequencies in excess of 6 Hz (and up to 9 Hz) at distances greater than 60° implies a high Q at least along the deep mantle part of the P travel path.

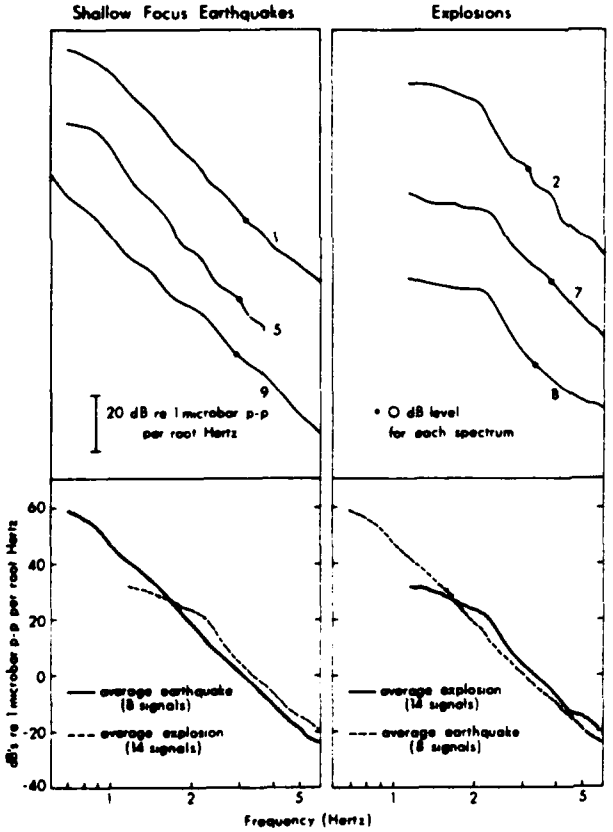

Figure 1. Sample spectra of P from some shallow focus earthquakes and nuclear explosions are shown in the upper portion of this figure. Numbers refer to the events as described in Table 1. The composite spectrum of each group, an average with ± 1 standard deviation, is shown in the lower portion of the figure. Before standard deviations were computed, individual spectrums were normalized by subtracting the difference between their mean dB value over the range 1.5-3.0 Hz and the mean dB value for all spectra over the same frequency range.

Although this study found a common high-frequency slope (-28 dB/octave) for both earthquakes and explosions, at least one other investigator (Evernden, 1977) has found earthquakes to fall off at least f^{-1} faster than explosions. This discrepancy might be explained by the small number of earthquakes used in the present study and the requirement in choosing those events of large signal/noise. Earthquakes having more high-frequency energy would have greater signal/noise because of much lower noise levels at high frequencies.

NTS events were not included in this study because they were rarely recorded with signal/noise greater than 2. Although signal levels near 1 Hz for NTS events are roughly equivalent to those observed for similar magnitude earthquakes and Soviet explosions, the signal fall-off above 1 Hz appears to be generally much greater for NTS. Therefore, little signal energy from NTS events is observed in the band above 2 Hz where lower ambient noise levels significantly enhanced the signal/noise of those events that were used. This rapid fall-off may be due to a recognized low Q effect in the source region (see for example Der et al., 1982).

Ocean Bottom Ambient Noise

The average background noise at the ocean bottom near Wake is shown in Figure 2 (labeled A). This average, along with its standard deviation, was determined from 52 samples of noise taken over 18 months of recording. Also plotted are an assortment of published noise curves for both ocean bottom and continental sites. When compared with noise levels from continental sites, the Wake ambient noise level could be described as: (1) high for frequencies between 0.2 Hz and 1.5 Hz; (2) average for frequencies between 1.5 Hz and 3.0 Hz; and (3) low for frequencies between 3.0 Hz and 15.0 Hz.

The observed low noise levels at higher frequencies affirm the ability of the Wake hydrophones to detect seismic signals at those frequencies. In addition, high-frequency phases recorded on the deep ocean bottom, which traverse only a few kilometers of homogeneous crust, may be less distorted than similar phases recorded on continents, which often traverse more than 40 km of crust. Consequently, coherence across the array appears to be high for telesiesmic P. These factors (low noise levels and a thin, homogeneous crust) have enabled the Wake array to acquire some impressive recordings of underground nuclear explosions. Shown in Figure 3 is an Eastern Kazakh explosion at 73° with a body wave magnitude of 5.9. Its signal/noise ratio is approximately 50/1. Also shown in Figure 3 is a Western Siberian explosion at 77° with a body wave magnitude of 4.6. This arrival is the weighted sum of signals from two of the hydrophones, as explained in the figure caption. Coherence between the two hydrophone signals in the band 1.5 to 5 Hz was measured at 0.85 for this arrival.

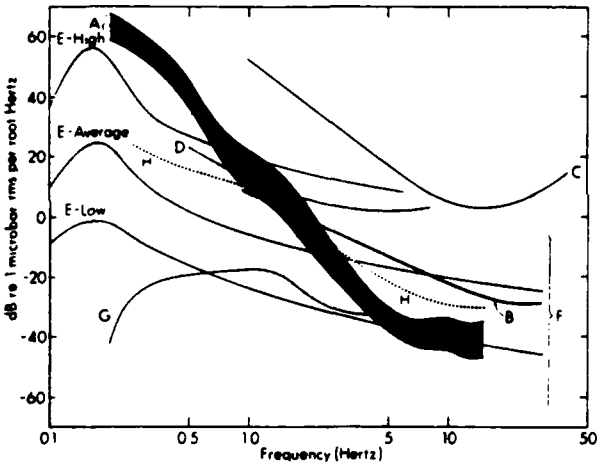

Figure 2. The average spectrum ± 1 standard deviation of 52 samples of background noise over 18 months from the Wake bottom hydrophones is labeled A. Also shown are some published noise curves for both ocean-bottom (B, C, D, and H) and continental (E, F, and G) environments, which have been converted from an assortment of units to the scale shown. B is a hypothetical "sample spectrum of deep-sea noise" (Urick, 1975; p. 188). C is a vertical seismometer measurement made in the Mariana Basin (Asada and Shimamura, 1976). D is a vertical seismometer measurement made at 46-km depth between Hawaii and California (Bradner and Dodds, 1964). H is a noise curve for a hydrophone bottomed off Eleuthera Island at 1200-m depth (Nichols, 1981). E represents low, average, and high noise levels estimated from curves compiled by Brune and Oliver (1959). F is an area bounded by the limits of noise curves measured on vertical seismometers for 16 locations within the United States and Germany (Frantti et al., 1962). G is the noise curve for the Oyer subarray of the Norwegian seismic array measured during a period "when most of the North Atlantic Ocean was very quiet" (Bungum et al., 1971).

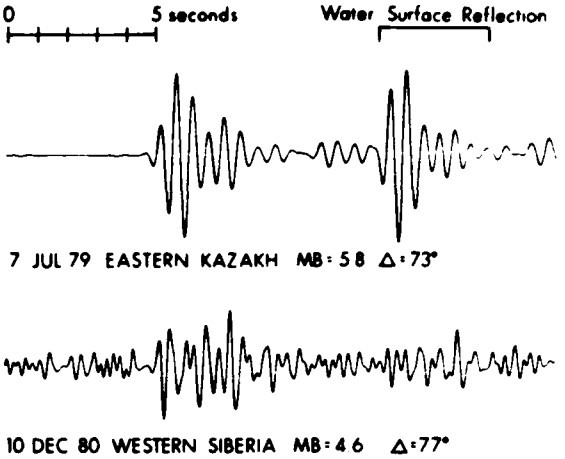

Figure 3. Sample time series of P, filtered to maximize signal/noise, from two nuclear explosions recorded on the Wake bottom hydrophones. The upper trace is from a single hydrophone and shows the direct arrival and its first water surface reflection. The lower trace is a composite of signals from two hydrophones with 40-km separation, obtained as follows: the filtered (1.5-5.0 Hz) time series from each hydrophone was inverted, shifted in time by the water surface reflection time, weighted to maximize the increase in signal/noise, and added to itself; the two resulting time series were then added with the appropriate propagation delay, and weighted to maximize the increase in signal/noise. Signal/noise was increased by 90% of the theoretical maximum with this method, indicating a high level of coherence between the signals added.

Summary

Significant differences are found between the spectra of P phases from explosions and from shallow focus earthquakes at 61° to 77° epicentral distance. Explosion spectra exhibit a change in spectral slope at about 2.2 Hz from -12 to -28 dB/octave relative to pressure. Earthquake spectra have a nearly constant slope of -28 dB/octave over the range of 1 to 6 Hz. High frequencies (>6 Hz) observed in these phases indicate a high Q in the deep mantle.

The ambient noise spectrum on the ocean bottom near Wake falls off at about -24 dB/octave over the range of 0.3 to 6 Hz. Between 3 and 15 Hz

the background noise levels are comparable to those at the quietest continental sites. Teleseismic P has been observed with a high level of coherence across a sensor separation of 40 km. The low level of ambient noise on the ocean floor at high frequencies and the high levels of coherence observed indicate that the ocean bottom may be an excellent observational regime for teleseismic P as well as other seismic phases rich in high frequencies.

Acknowledgments. This research was supported by the Advanced Research Projects Agency of the Department of Defense and was monitored by the Air Force Office of Scientific Research under Contract Nos. F 49620-79-C-0007 and F 49620-81-C-0065. Supplementary funds were provided by the U.S. Arms Control and Disarmanent Agency. Installation of the recording system was partially funded by the Office of Naval Research (Code 425GG). The authors express special thanks to the Air Force and Kentron International for assistance in installing and maintaining the recording station at Wake, and to Al David for diligently changing tapes and making repairs. The authors thank Neil Frazer for critically reviewing this report and Rita Pujalet for editorial assistance. Hawaii Institute of Geophysics Contribution No. 1316.

References

Asada, T., and H. Shimamura, Observation of earthquakes and explosions at the bottom of the western Pacific: Structure of oceanic lithosphere revealed by Longshot experiment, The Geophysics of the Pacific Ocean Basin and Its Margins, edited by G. H. Sutton, M. H. Manghnani, and R. Moberly, Am. Geophys. Union Monograph 19, p. 135-153, 1976.

Bradner, H., and J. Dodds, Comparative seismic noise on the ocean bottom and land, J. Geophys. Res., 69, 4339-4348, 1964.

Brune, J., and J. Oliver, The seismic noise of the earth's surface, Bull. Seismol. Soc. Amer., 49, 349-353, 1959.

Bungum, H., E. Rygg, and L. Bruland, Short-period seismic noise structure at Norwegian seismic array, Bull. Seismol. Soc. Amer., 61, 357-373, 1971.

Der, Z. A., T. W. McElfresh, and A. O'Donnell, An investigation of the regional variations and frequency dependence of anelastic attenuation in the mantle under the United States in the 0.5-4 Hz band, Geophys. J. R. astr. Soc., 69, 67-99, 1982.

Evernden, J., Spectral characteristics of the P codas of Eurasian earthquakes and explosions, Bull. Seismol. Soc. Amer., 67, 1153-1171, 1977.

Evernden, J. and W. Kohler, Further study of spectral characteristics of P codas of earthquakes and explosions, Bull. Seismol. Soc. Amer., 69, 483-511, 1979.

Frantti, G., D. Willis, and J. Wilson, The spectrum of seismic noise, Bull. Seismol. Soc. Amer., 52, 113-121, 1962.

Nichols, R. H., Infrasonic ambient ocean noise measurements: Eleuthera, J. Acoustic. Soc. Am., 69, 974-981,1981.

Thanos, S. N., OBS Calibration Manual, Lamont Geological Observatory, 1966.

Urick, R., Principles of Underwater Sound, McGraw-Hill, 1975.

Walker, D., Hydrophone recordings of underground nuclear explosions, Geophys. Res. Lett., 7, 465-467, 1980.

Walker, D., C. McCreery, G. Sutton, and F. Duennebier, Spectral analyses of high-frequency Pn and Sn phases observed at great distances in the western Pacific, Science, 199, 1333-1335, 1978.

(Received August 6, 1982;
accepted August 31, 1982.)

APPENDIX II

JOURNAL OF GEOPHYSICAL RESEARCH, VOL. 88, NO. B5, PAGES 4289-4298, MAY 10, 1983

SPECTRAL CHARACTERISTICS OF HIGH-FREQUENCY P_N, S_N PHASES IN THE WESTERN PACIFIC

Daniel A. Walker and Charles S. McCreery

Hawaii Institute of Geophysics, Honolulu, Hawaii 96822

George H. Sutton

Rondout Associates, Stone Ridge, New York 12484

Abstract. Pn and Sn phases from 25 selected earthquakes recorded since July of 1979 on ocean bottom hydrophones near Wake Island are used to complement and extend prior investigations of high-frequency Pn, Sn spectra in the Western Pacific. At a distance of about 18° (≈2000 km), frequencies for Pn and Sn are as high as 30 and 35 Hz, respectively; at a distance of about 30° (≈3300 km), as high as 15 and 20 Hz, respectively. Pn phases lose their high-frequency energy more rapidly than Sn phases do, yet Pn wavetrains are much longer than Sn wavetrains. Pn wavetrains of longer duration, more energy, and higher frequencies are found for travel paths primarily in the Northwestern Pacific Basin than for travel paths across the transition zone from the shallow Ontong-Java Plateau to the deep Northwestern Pacific Basin. Sn phases are extremely weak or absent for travel paths crossing this transition zone from the shallower Ontong-Java Plateau to the deeper Northwestern Pacific Basin, whereas Sn phases are well recorded for travel paths crossing the transition zone in the opposite direction. Although normal, mantle-refracted P phases are well recorded beyond about 21° (≈2300 km), available data indicate that detectable normal, mantle-refracted P phases may not exist at distances from about 17° to 21°.

Introduction

Recent investigations of high-frequency Pn, Sn in the Pacific [Walker, 1977; Walker et al., 1978; Sutton et al., 1978; Talandier and Bouchon, 1979; and McCreery, 1981] suggest that the real character of these phases is revealed at frequencies much higher than those traditionally associated with normal, mantle-refracted body waves at teleseismic distances (i.e., ≈ 1 Hz). For example, in one investigation [Walker et al., 1978], frequencies as high as 12 and 15 Hz were found for the Pn and Sn phases, respectively, of an earthquake recorded at a distance of 28.3° (3147 km).

In this report we offer a more comprehensive analysis of the spectral characteristics of Pn, Sn using additional data recorded since July of 1979 on ocean bottom hydrophones near Wake Island. Only undistorted arrivals with signal/noise ratios of at least 3/1 were used in this investigation. Epicentral distances, origin times, depths, and magnitudes are given in Table 1; and locations of epicenters are shown in Figure 1.

Paper number 3B0272.
0148-0227/83/003B-0272$05.00

Northwestern Pacific Basin Travel Paths

Spectrograms for some of the Pn, Sn phases having travel paths primarily under the deep Northwestern Pacific Basin (i.e., events 1 through 18) are shown in Figure 2. All reveal high frequencies, with values in excess of 20 Hz for both Pn and Sn at a distance of 18.0° (2000 km; event 2) and values of up to 15 and 20 Hz for Pn and Sn, respectively, at a distance of 29.4° (3270 km; event 17). (More detailed spectral analyses of the phases for event 2 at 18.0° indicate values as high as 30 and 35 Hz for Pn and Sn, respectively.)

Spectrograms for events 17 and 18 show the normal, mantle-refracted P phases as well as high-frequency Pn and Sn phases. Other events for which normal, mantle-refracted P phases have been clearly recorded are 11, 12, 13, 15, and 16. The fact that all of these events are at distances in excess of 21° is not coincidental, for it is only at these distances (the precise crossover depending, in part, on focal depth) that P phases begin to arrive ahead of the high-frequency Pn phase (Figure 3). With increasingly shorter distances, high-frequency Pn arrives increasingly ahead of the expected P.

Although it might seem reasonable to assume that P does arrive at distances less than about 21°, but is masked by Pn, such an assumption should be tested. One test is to compare spectrums where all of the P's energy, or large portions of it, might be suspected of being present within the Pn coda (i.e., events 1 through 10) to the spectrums where only Pn is known to exist (i.e., events 13 through 18; 11 and 12 could not be used due to Pn clipping). Composite spectrums have been made for the two groups of Pn arrivals (i.e., Pn with P suspected, at distances from about 17° to 22°; and Pn with P known to be absent, at distances from about 26° to 33°), as well as for all P phases, at distances from about 22° to 33°, either clearly arriving well ahead of Pn (events 11, 12, 13, 15, 16, 17, and 18) or suspected of arriving close to, but ahead of, Pn (events 9 and 10). These composites and the individual absolute spectrums from which they were derived are shown in Figure 4.

Individual and composite P spectrums are obviously, and not unexpectedly, very different in character from individual and composite Pn

TABLE 1. Epicentral Distances, Origin Times, Depths, and Magnitudes of Events 1-25 in Figure 1

Event Number	Distance, deg.	Date	Time	Depth, km	Magnitude, mb
1	17.8	July 8, 1980	1704:15.1	54	4.8
2	18.0	July 11, 1980	0942:00.2	33	5.3
3	18.7	June 9, 1980	1923:33.3	33	5.6
4	19.0	Dec. 8, 1979	1258:55.2	51	5.5
5	19.8	Dec. 16, 1979	1050:48.0	96	5.0
6	20.1	March 26, 1980	0722:37.0	45	5.5
7	20.7	Nov. 1, 1980	0440:37.7	109	5.6
8	20.9	Dec. 17, 1979	0728:48.2	33	5.1
9	21.2	Jan. 15, 1980	0523:25.7	120	5.1
10	21.7	Nov. 29, 1979	1708:21.3	109	5.4
11	24.9	Dec. 11, 1979	1726:22.1	161	5.9
12	25.4	Dec. 19, 1980	2332:41.6	79	6.2
13	26.5	Oct. 20, 1980	0329:21.3	81	5.5
14	27.1	Oct. 28, 1979	0539:36.0	88	5.4
15	28.5	Feb. 23, 1980	0551:03.5	47	6.4
16	28.5	Jan. 1, 1981	1032:13.1	53	6.2
17	29.4	Nov. 26, 1980	2348:59.9	77	5.8
18	32.7	Aug. 22, 1979	1828:55.7	128	5.5
19	28.0	Feb. 12, 1980	0320:23.2	75	5.9
20	28.0	Aug. 13, 1979	0303:47.9	88	5.8
21	28.6	May 14, 1980	1126:00.6	57	6.1
22	28.8	Sept. 28, 1980	1825:59.7	68	6.0
23	30.4	Nov. 6, 1979	1138:31.5	30	6.0
24	31.1	Oct. 23, 1979	0951:06.7	22	6.1
25	31.1	Feb. 22, 1980	2115:42.1	68	5.9

spectrums, in that the P has larger signal-to-noise ratios at lower frequencies (i.e., 1-2 Hz) than either Pn grouping (Figures 4 and 5), and the composite P is richer in lows, and weaker in highs, relative to the 26° to 33° Pn composite (Figure 5a). In comparing the composite 17° to 22° Pn spectrum to the composite 26° to 33° Pn spectrum (Figure 5b), we note that the 17° to 22° Pn is similar in character to the 26° to 33° Pn for frequencies higher than 2 Hz, but has lower signal-to-noise ratios at frequencies less than 2 Hz (i.e., values fall below the "4 dB above noise" requirement for plotting). This latter observation is also apparent in the individual spectrums (Figure 4). The fact that values for the 17° to 22° Pn spectrum fall below the 4 dB requirement for frequencies less that 2 Hz, coupled with values for the 22° to 33° P spectrum above the 4 dB level at those frequencies, suggests that detectable normal, mantle refracted P phases may not exist in the Pn codas of events at distances of 17° to 22°.

Another important, though not surprising, observation to be made from the composite plots (Figure 5b) is that Pn phases at great distances appear to be weaker at higher frequencies (≥10 Hz) than Pn phases at shorter distances.

Sn composite plots have also been made for the same events for which Pn composites have been made. These plots are shown in Figure 6. Although normal mantle-refracted P phases have been well recorded at great distances, normal mantle-refracted S phases from earthquakes have not been recorded by the Wake hydrophones. Presumably, this is due to the small pressure signal in the water resulting from S phases at

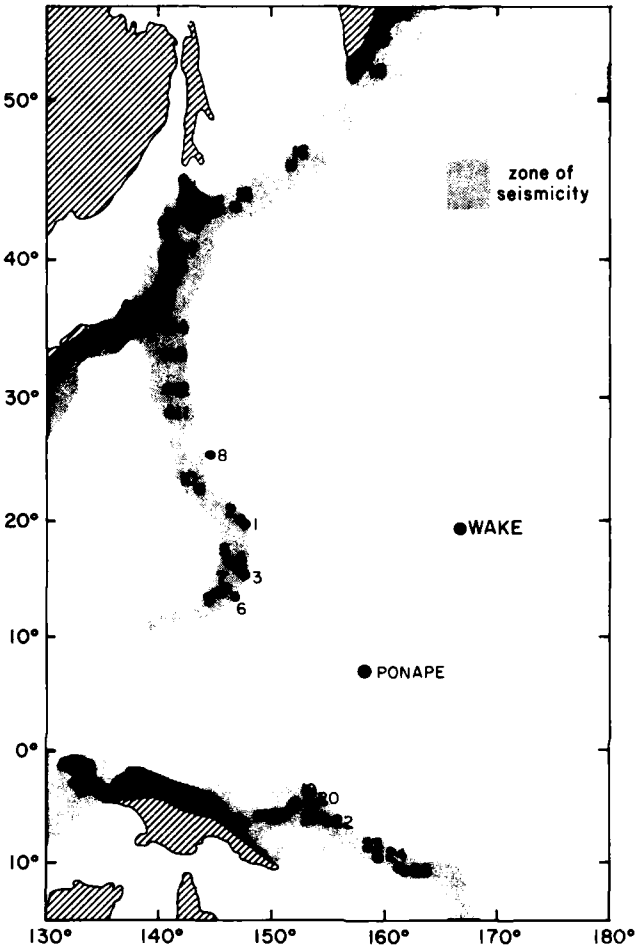

Fig. 1. Epicenter location map.

teleseismic distances. In addition, background noise levels are higher for those frequencies at which S would appear [McCreery et al., 1982].

In Figure 6a, Sn composite plots for the 17° to 22° and 26° to 33° distance ranges are compared to one another. Considering that the standard deviations of all of the composite plots presented in this paper are generally in the range of ± 3 dB, no significant differences are apparent in Figure 6a. In Figures 6b and 6c, Sn composite plots are compared to their respective Pn composite plots. Again, no statistically significant differences are indicated. In other words, Sn signal strength is generally comparable to Pn signal strength. This similarity of Pn and Sn spectrums was observed earlier for travel paths in the Western Pacific east of the Marianas [Ouchi, 1981].

Special mention should be made of the fact that the composite Sn plot in Figure 6c is 4 dB above background noise at frequencies well above 8 Hz while the composite Pn plot is not. Also it should again be noted that the individual Pn's and Sn's used to formulate the composite plots were for the same earthquakes. These considerations suggest that Sn phases do not lose their high frequencies as rapidly as Pn phases.

It has been pointed out that some high frequencies observed elsewhere might be the result of instrumental nonlinearities [Sacks, 1980] and/or nonlinear seismic interactions in the vicinity of a receiving station [Nakamura and Koyama, 1982]. As the lower frequencies are of comparable amplitude for both Pn and Sn at both distance ranges considered (Figures 6b and 6c), it is unlikely that such nonlinearities could explain the data discussed here. We also note that P, which has higher average amplitudes than

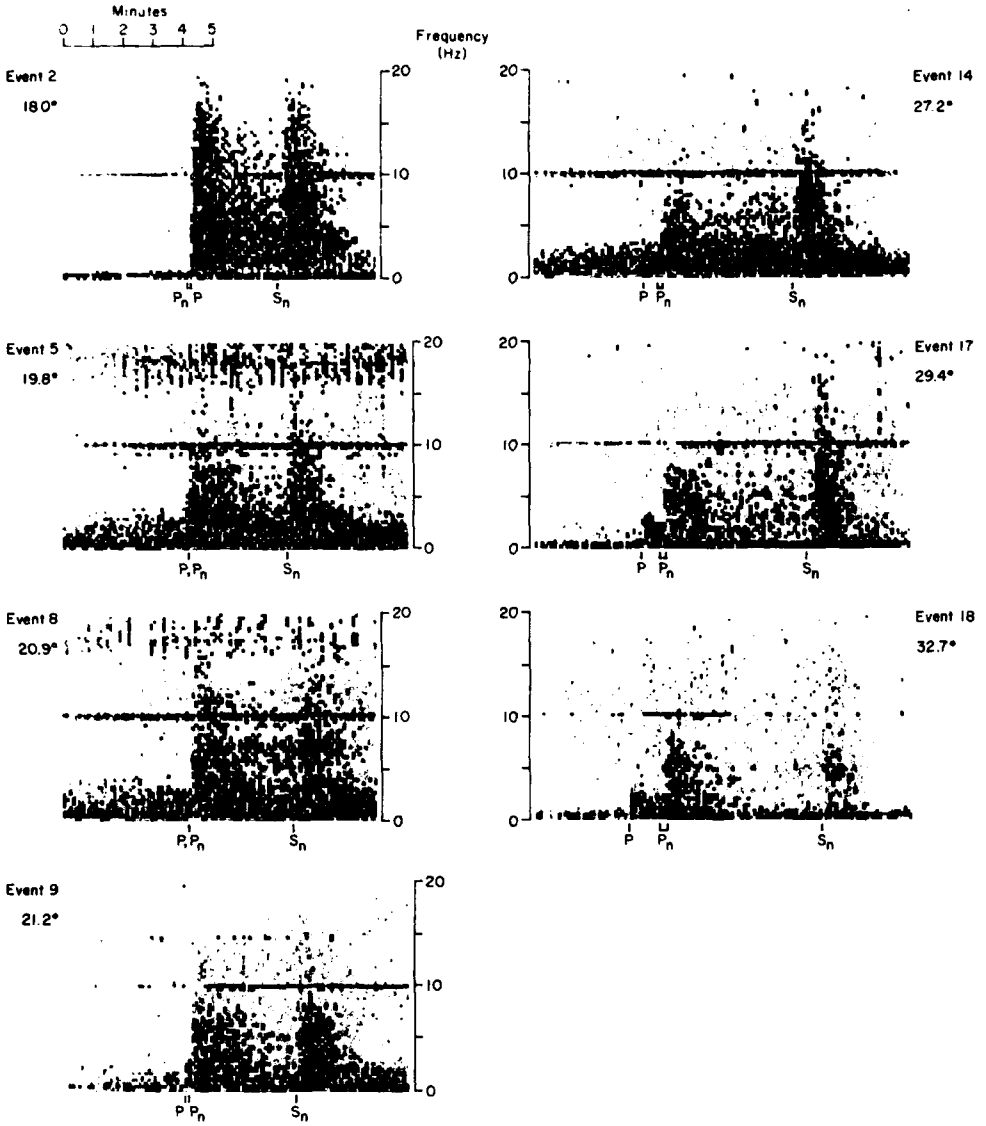

Fig. 2. Spectrograms for some earthquakes having travel paths to Wake under the Northwestern Pacific Basin. Expected times of arrivals are based on either the Jeffreys and Bullen [1958] tables for P or Pn/Sn travel time curves from Walker [1977]. These and succeeding spectrograms were made by dividing the time series into adjacent 512-point segments, Lanczos squared windowing the segments, and performing a fast Fourier transform (FFT) on each segment. In the horizontal direction, the width of each shaded block corresponds to one of the 512-point segments in the time series. In the vertical direction, each block is the average of two adjacent power spectral estimates out of the FFT. Only frequencies from 0 to 1/2 Nyquist are shown. The contour interval is 8 dB. The line at 10 Hz is due to time code cross talk. Instrument responses have not been removed.

Pn or Sn at the lower frequencies, has the most rapid falloff toward higher frequencies (Figure 5).

In all of these comparisons, another objection that could be made is that differences in source spectrums (and/or orientation of the source relative to the recording station) were not considered. Although all of the events occurred within the subducting margin of the Northwestern Pacific and the Pn, Sn phases used were generated by earthquakes having focal depths of 128 km or less, differences in source spectrums might be

significant. We believe, however, that overall trends of the individual spectrums (Figure 4) used for the composite plots are similar (as opposed to specific details that may differ) and that such similarities could justify the general conclusions drawn from that data. We also note that source effects are minimized in those comparisons of composite Pn's and Sn's from the same earthquakes (Figures 6b and 6c).

Another interesting feature of Pn, Sn phases is that the Pn wavetrain is much longer than the Sn wavetrain (Figure 2). Spectral analyses indicate that energy is lost at all frequencies in the later arriving portions of these wavetrains, and that this loss is much greater in the Sn wavetrains than in the Pn wavetrains.

Ontong-Java Plateau Travel Paths

Spectrograms for some of the more interesting Pn phases with travel paths to Wake under the shallow Ontong-Java Plateau (as well as portions of the deep Northwestern Pacific Basin) are shown in Figure 7. (Refer also to Table 1, Figure 1, and Figure 8.) The most conspicuous feature of these spectrograms is that Sn phases are extremely weak, or absent, even though Pn phases are prominent.

Figure 9 compares the composite Pn spectrum for events having Ontong-Java Plateau travel paths (events 19 through 25) to the composite Pn spectrum for events at comparable distances having Northwestern Pacific Basin travel paths (events 15 through 18). The Northwestern Pacific Basin events appear to have more Pn energy at higher frequencies than the Ontong-Java Plateau events. However, because of the approximate ± 3 dB standard deviation on each of these curves, this suggestion is not statistically significant. Comparing Figures 2 and 7, the duration of the Pn

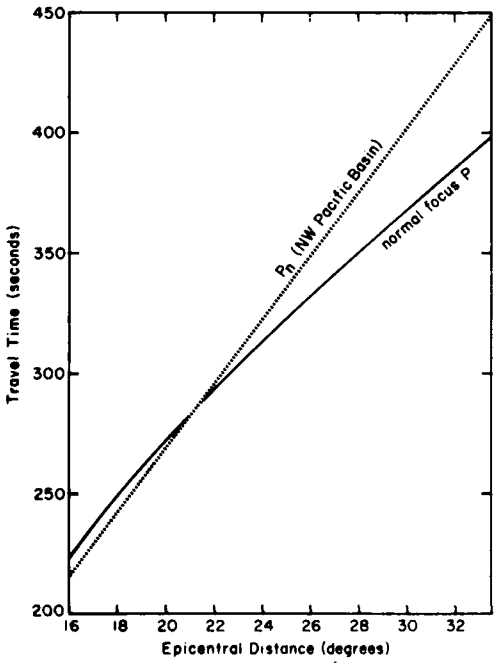

Fig. 3. Travel time curves for normal, mantle-refracted P phases and for Pn phases. P times are taken from Jeffreys and Bullen [1958], and Pn times are taken from Walker [1977].

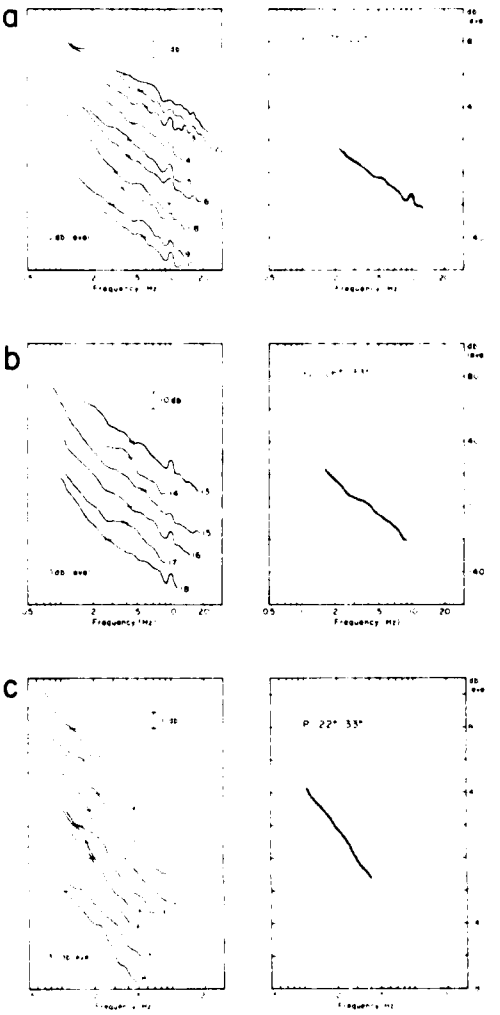

Fig. 4. Individual and composite spectrums for arrivals at Wake where (a) both Pn and P might be suspected of being present, at distances from about 17° to 22°, (b) only Pn is known to exist at distances from about 26° to 33°, and (c) only P is known to exist, at distances from about 22° to 33°. The spectrums are power level spectrums in decibels relative to one microbar peak-to-peak pressure per root hertz. Values for individual spectrums were plotted only if they were at least 4 dB above background noise. The composite curves are simply the averages for the individual curves, with the condition that composite values were used for those frequencies lacking at most only one individual curve. Standard deviations of composite values are indicated by shading. Values for standard deviations in these and succeeding spectrums are generally in the range of ± 3 dB. The peaks at 10 Hz are due to time code cross talk.

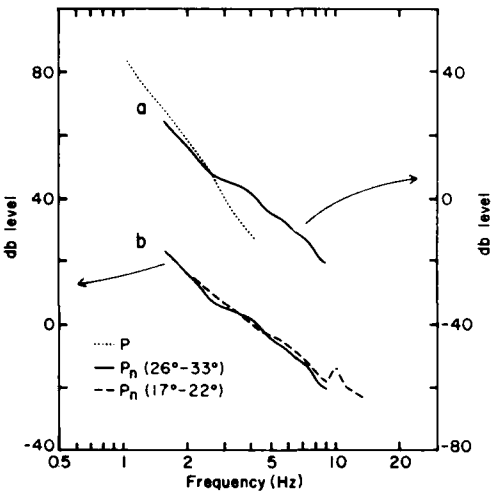

Fig. 5. Comparisons of composite spectrums: (a) P and the 26° to 33° Pn, and (b) the 17° to 22° Pn and the 26° to 33° Pn. Conclusions which can be drawn from these plots are (1) P and Pn spectrums are very different in character, (2) detectable P phases may not exist in the Pn codas of events at distances of 17° to 22°, and (3) Pn phases at great distances appear to be weaker at higher frequencies (≃10 Hz) than Pn phases at shorter distances.

wavetrains appears to be greater for the Northwestern Pacific Basin events.

In such comparisons, the important question again arises of differences in source characteristics, in this instance for New Ireland-Solomon Island earthquakes and for Japan-Kuril Islands-Kamchatka earthquakes. It is not possible, however, to attribute the absence of Sn to differences in source characteristics, as Sn phases from New Ireland and the Solomons have been well recorded at Ponape on the northern margin of the Ontong-Java Plateau [Walker, 1977]. Examples of such phases are shown in Figure 10. Of the more than forty events from the New Ireland-Solomon Islands area recorded at Ponape, amplitudes of Sn phases are at least comparable to, and frequently larger than, those of their respective Pn phases.

The absence of Sn at Wake would, therefore, appear to be a result of Sn's inability to propagate efficiently across the transition zone from the shallower Ontong-Java Plateau to the deeper Northwestern Pacific Basin, and would suggest that much of the energy in Sn travels through portions of the lithosphere involved in the transition. On the other hand, Sn's that have crossed this transition zone from the other direction (i.e., from earthquakes in the Marianas, Japan, the Kuriles, and Kamchatka) are well recorded at Ponape (Figure 10). Differences in the crustal structure of the Ontong-Java Plateau and the Northwestern Pacific Basin are indicated by the section profile [Hussong et al., 1979] shown in Figure 11.

Another comparison of spectrums at Wake for the two differing types of travel paths (Northwestern Pacific Basin and Ontong-Java Plateau travel paths) was made for the later arriving energy in the Pn wavetrains. For these comparisons, less energy at higher frequencies was present in those Pn's having travel paths that include the Ontong-Java Plateau. These deficiencies and the corresponding absence of Sn for paths across the transition zone from the shallow Ontong-Java Plateau to the deep Northwestern Pacific Basin suggest that the longer, stronger Pn phases observed for travel paths to Wake, primarily across the Northwestern Pacific Basin, may be the result of more efficient conversions of Pn to Sn (or Sn to Pn).

Concluding Remarks

The phenomenon of high-frequency Pn, Sn propagation is emerging as a major unresolved property of the oceanic crust and/or mantle. Others have described high-frequency Pn, Sn propagation as `a challenge remaining to the theoretician' [Richards, 1979] and as `the challenge to both explosion and earthquake

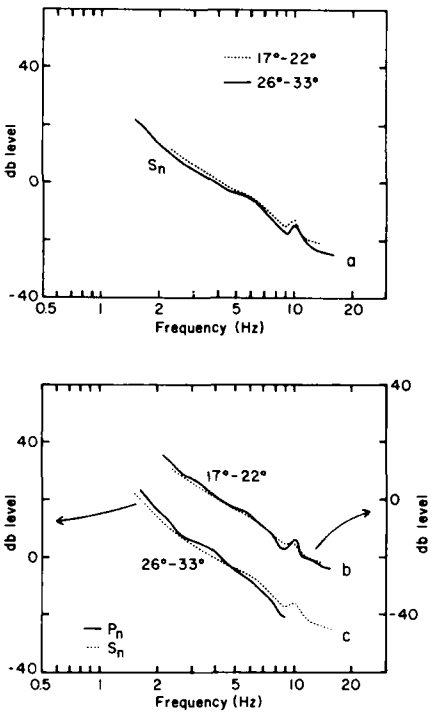

Fig. 6. Composite spectrums of Sn phases for those earthquakes with their Pn phases plotted in Figures 4a and 4b. Comparisons of spectrums are made (a) for the two Sn composites to one another, (b and c) and for each of the Sn composites to their respective Pn composite. A conclusion which can be drawn from these plots is that Sn signal strength is generally comparable to Pn signal strength except at high frequencies and large distances where Sn phases do not lose their energy as rapidly as Pn phases.

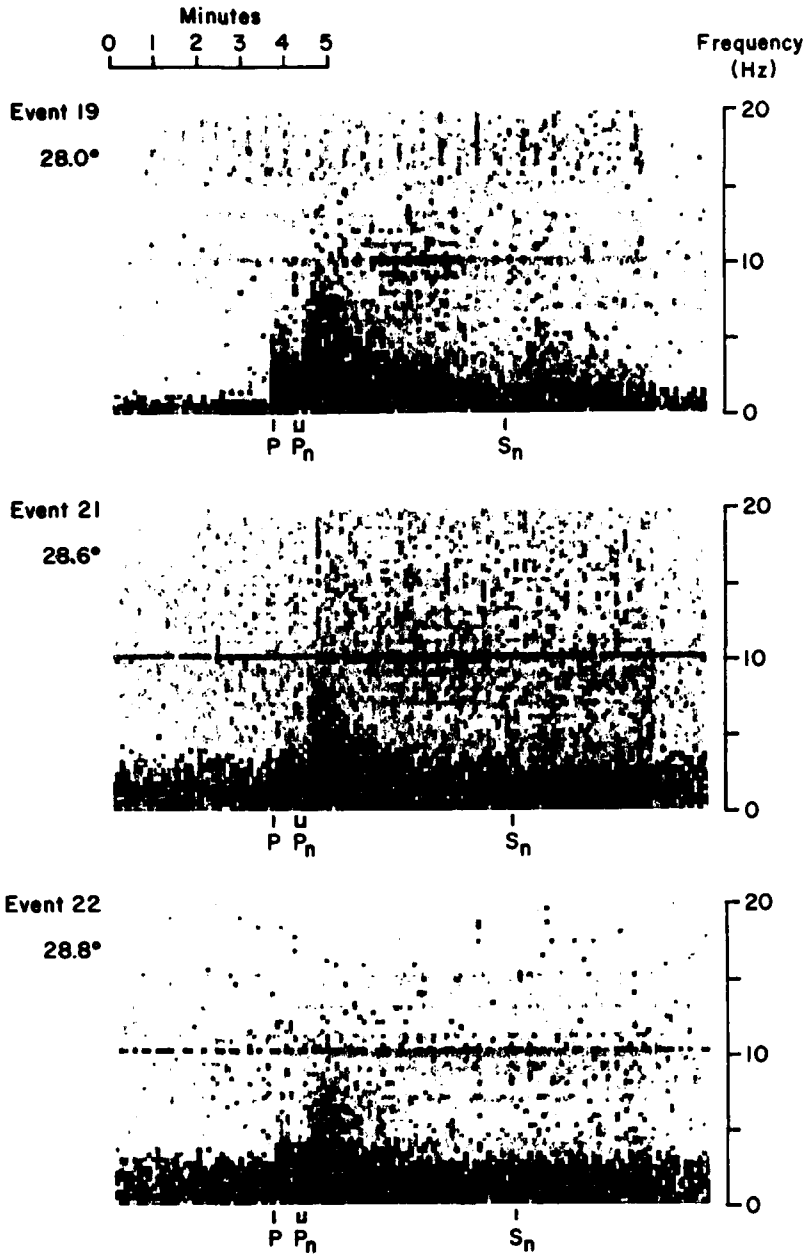

Fig. 7. Some spectrograms for earthquakes having portions of their travel paths to Wake under the Ontong-Java Plateau. In comparing these spectrograms to those of Figure 2, note the absence, or weakness, of Sn. Computational procedures are the same as used in Figure 2.

seismology for the coming decade' [Hirn et al., 1973]. These descriptions are supported not only by the unusual character of the phases but also by their probable occurrence throughout the world's oceans.

As important as recent efforts are to determine the mechanism of high-frequency Pn, Sn propagation [e.g., Stephens and Isacks, 1977; Menke and Richards, 1980; Sutton and Harvey, 1981; Gettrust and Frazer, 1981], we believe that many essential characteristics of Pn, Sn phases (especially at very high frequencies) are not well known, and that accurate quantification of those characteristics through the acquisition of additional high-quality data is greatly needed. We hope that this report will further familiarize seismologists with high-frequency Pn, Sn propagation and will be viewed as a preliminary attempt to quantify, in a relative sense, some of the essential characteristics of these phases.

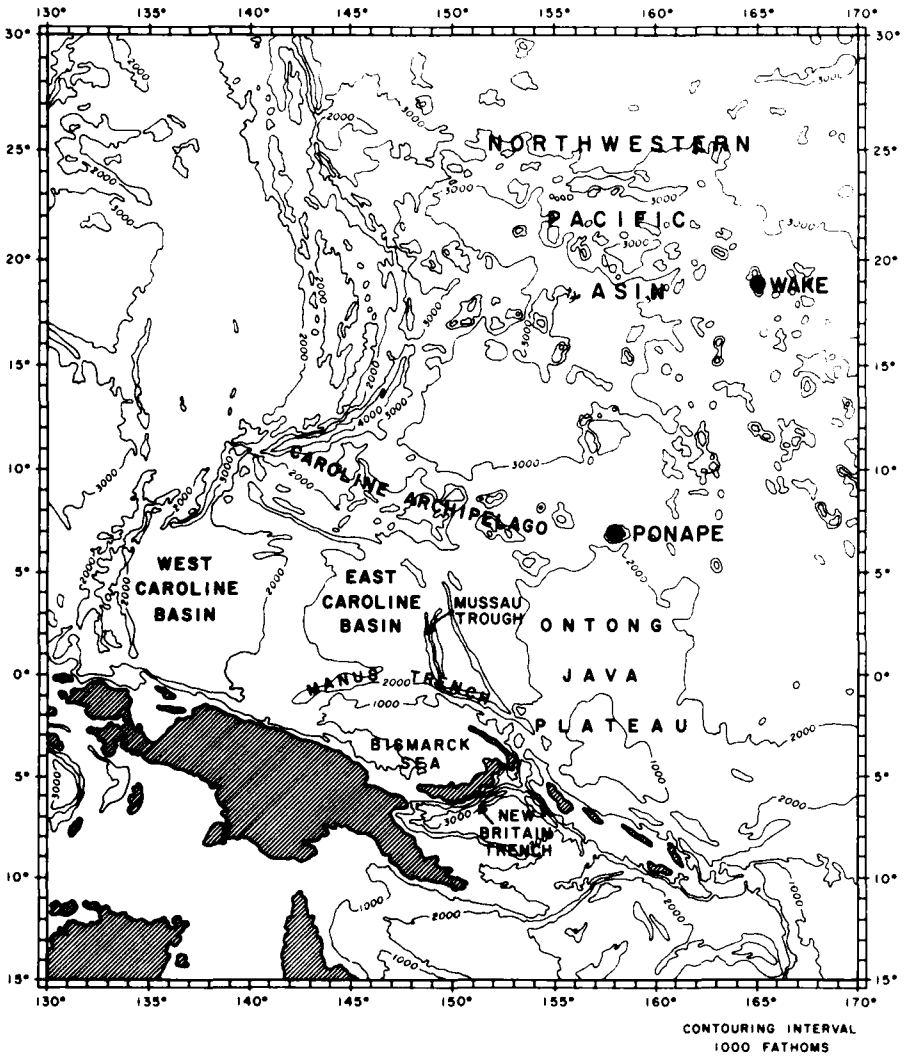

Fig. 8. Bathymetry map of the Northwestern Pacific area.

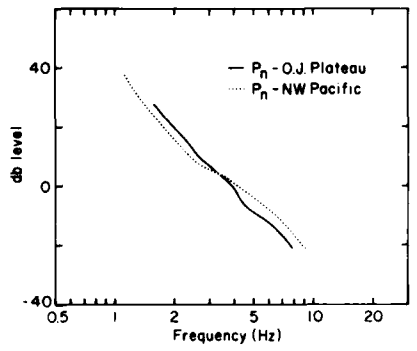

Fig. 9. Comparisons of composite Pn spectrums for events having travel paths across the Ontong-Java Plateau and the Northwestern Pacific Basin.

summary of principal observations contained in this report follows.

The apparent absence of normal, mantle-refracted P phases at distances less than about 21° (≃2300 km).

Frequencies as high as 30 and 35 Hz for Pn and Sn, respectively, at 18.0° (2000 km)

Frequencies as high as 15 and 20 Hz for Pn and Sn, respectively, at 29.4° (3270 km).

With increasing distance (i.e., from about 20° to 30°), Sn phases not losing their high frequencies as rapidly as Pn phases do.

Pn wavetrains longer than Sn wavetrains.

The extreme weakness or absence of Sn phases for travel paths across the transition zone from the Ontong-Java Plateau to the Northwestern Pacific Basin and the presence of Sn phases for travel paths in the opposite direction across this transition zone.

Longer, more energetic Pn wavetrains for travel paths primarily in the Northwestern Pacific Basin than for travel paths across the transition zone from the Ontong-Java Plateau to the Northwestern Pacific Basin.

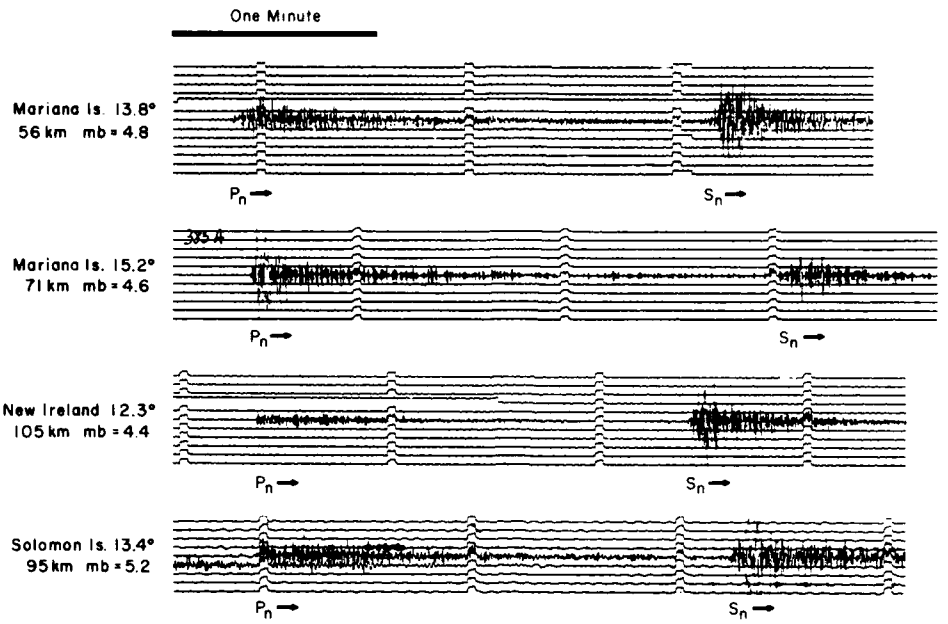

Fig. 10. Pn and Sn phases recorded at Ponape on the northern margin of the Ontong-Java Plateau.

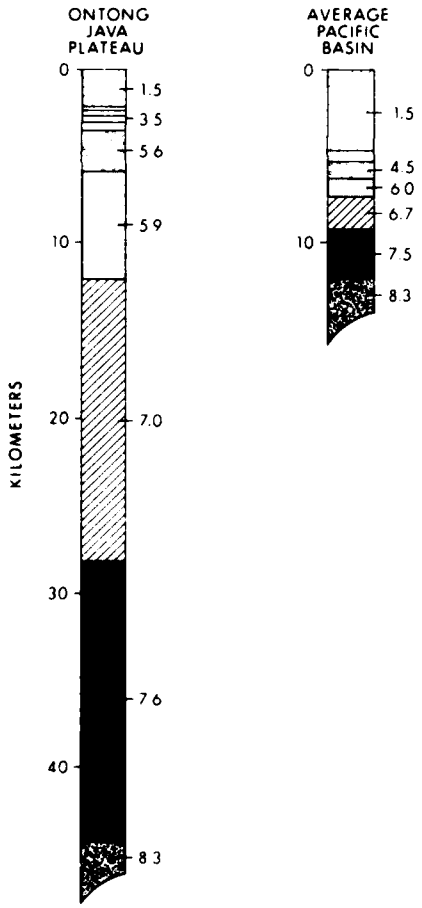

Fig. 11. Section profiles for the Ontong-Java Plateau and Pacific Basin as taken from Hussong et al. [1979].

Acknowledgments. This research was supported by the Advanced Research Projects Agency of the Department of Defense and was monitored by the Air Force Office of Scientific Research under contract F49620-79-C-0007. Supplementary funds were provided by the Air Force Office of Scientific Research (contract F49620-81-C-0065), the Office of Naval Research (Code 425GG), and the U.S. Arms Control and Disarmament Agency. The authors thank Fred Duennebier, Joe Gettrust, and Neil Frazer for reviewing a draft of this report. The editorial assistance of Rita Pujalet is also acknowledged. Hawaii Institute of Geophysics contribution 1354.

References

Gettrust, J., and L. Frazer, A computer model study of the propagation of the long-range Pn phase, Geophys. Res. Lett., 8, 749-752, 1981.

Hirn, A., L. Steinmetz, R. Kind, and K. Fuchs, Long range profiles in western Europe, II, Fine structure of the lower lithosphere in France (southern Bretagne), Z. Geophys., 39, 363-384, 1973.

Hussong, D., L. Wipperman, and L. Kroenke, The crustal structure of the Ontong-Java and Manihiki oceanic plateaus, J. Geophys. Res., 84, 6003-6010, 1979.

Jeffreys, H., and K. Bullen, Seismological Tables, Office of the British Association, Burlington House, London, 1958.

McCreery, C., High-frequency Pn, Sn phases recorded by ocean bottom seismometers on the Cocos Plate, Geophys. Res. Lett., 8, 489-492, 1981.

McCreery, C., D. Walker, and G. Sutton, Spectra of nuclear explosions, earthquakes, and noise from Wake Island bottom hydrophones, Geophys. Res. Lett., 10, 59-62, 1983.

Menke, W., and P. Richards, Crust-mantle whispering gallery phases: A deterministic model of teleseismic Pn wave propagation, J. Geophys. Res., 85, 5416-5422, 1980.

Nakamura, Y., and J. Koyama, Seismic Q of the lunar upper mantle, J. Geophys. Res., 87, 4855-4861, 1982.

Ouchi, T., Spectral structure of high frequency P and S phases observed by OBS's in the Mariana Basin, J. Phys. Earth, 29, 305-326, 1981.

Richards, P., Theoretical seismic wave propagation, Rev. Geophys. Space Phys., 17, 312-328, 1979.

Sacks, I., Mantle Qs from body waves-difficulties in determining frequency dependence, (abstract), Eos Trans. AGU, 61, 298, 1980.

Stephens, C., and B. Isacks, Toward an understanding of Sn: Normal modes of Love waves in an oceanic structure, Bull. Seismol. Soc. Am., 67, 69-78, 1977.

Sutton, G., and D. Harvey, Complete synthetic seismograms to 2 Hz and 1000 km for an oceanic lithosphere (abstract), Eos Trans. AGU, 62, 327, 1981.

Sutton, G., C. McCreery, F. Duennebier, and D. Walker, Spectral analyses of high-frequency Pn, Sn phases recorded on ocean bottom seismographs, Geophys. Res. Lett., 5, 745-747, 1978.

Talandier, J., and M. Bouchon, Propagation of high frequency Pn waves at great distances in the Central and South Pacific and its implications for the structure of the lower lithosphere, J. Geophys. Res., 84, 5613-5619, 1979.

Walker, D., High-frequency Pn and Sn phases recorded in the Western Pacific, J. Geophys. Res., 82, 3350-3360, 1977.

Walker, D., C. McCreery, G. Sutton, and F. Duennebier, Spectral analyses of high-frequency Pn and Sn phases observed at great distances in the Western Pacific, Science, 199, 1333-1335, 1978.

(Received July 14, 1982;
revised January 5, 1983;
accepted February 7, 1983.)

APPENDIX III

HIG-82-6

OCEANIC PN/SN PHASES: A QUALITATIVE EXPLANATION AND REINTERPRETATION OF THE T-PHASE

Daniel A. Walker

November 1982

Prepared for

OFFICE OF NAVAL RESEARCH
Contract N00014-75-C-0209
Project NR 083-603

Charles E. Helsley
Director
Hawaii Institute of Geophysics

ABSTRACT

The combined effects of: (1) differing efficiencies between Pn and Sn energy transmission across the basement-sediment interface; (2) ocean surface reflections; (3) Pn to Sn conversions; and, (4) large lateral variations in the crust and upper mantle are used to formulate a working hypothesis which appears to explain, qualitatively, many observations of high-frequency Pn/Sn phases throughout the western, northern, and central Pacific. Also, the concept of Pn/Sn phases as sources of energy at the basement-sediment interface is suggested as a possible mechanism for T-phase generation through scattering or Stoneley wave generation.

CONTENTS

FIGURES

INTRODUCTION

High-frequency Pn/Sn phases were first observed nearly fifty years ago for travel paths in the Atlantic from the West Indies to the northern east coast of the United States (Leet et al., 1951, reported that these observations were made as early as 1935). The history of research on these phases since that time has been given by several authors, with some of the more recent being Molnar and Oliver (1969) and Walker (1977a).

My interest in the phenomenon began in 1963 with the recording of long-range, high-frequency Pn/Sn phases on hydrophones of what was then known as the Pacific Missile Range facility. My efforts at trying to understand these unusual phases (Sn wavetrains greater than Pn wavetrains with frequencies as high as 15 Hz at distances in excess of 3000 km; Walker et al., 1978) has continued since those initial observations. A reasonable, concise summary of my accomplishments prior to this report might be that no answers were found--only more questions. Such methodology can only be rationally tolerated for a length of time much shorter than my tenure on the case. So, for the past few years, it has been hoped that a working hypothesis could be found that would permit many, if not all, of the diverse observational pieces to be fitted together in at least a qualitative sense. Such a hypothesis could then serve as an appropriate starting point for comprehensive and detailed quantitative analyses leading to a generally acceptable model for the generation and propagation of long-range, high-frequency Pn/Sn phases. A working hypothesis has now emerged and is the subject of this report.

SN SIGNAL STRENGTH

One of the most interesting aspects of long-range, high-frequency Pn/Sn propagation in the northwestern Pacific is the strength of the Sn phase (Walker et al., in press). Relative to Pn, Sn often appears stronger at great distances--even at high frequencies (Fig. 1). A possible explanation for these observations begins with considerations of: (1) the efficiencies of Pn/Sn energy transmission across the basement-unconsolidated sediment interface; (2) possible conversions of Pn and Sn at the basement-sediment interface; and, (3) ocean-surface reflections. Observations of conversions upward and across the basement-sediment interface, as well as ocean-surface reflections for short travel paths

off the coast of California are reported in Auld et al. (1969), where data indicate that the percentage of P (perhaps actually Pn) energy converted to S is greater than the percentage of S (perhaps actually Sn) energy converted to P. Examples of ocean-surface reflections are also given in Shimamura et al. (1975) and McCreery et al. (in press).

The very recording of "Pn/Sn" phases on ocean-bottom sediments is evidence that Pn and Sn energy does propagate, by some means, into the sediments. Energy losses above the basement-sediment interface will occur, i.e. not all of the energy passing into the sediments will be returned to the interface by way of reflections from the ocean surface. These losses could be much greater than those produced within that portion of the waveguide below the basement-sediment interface. Furthermore, if the percentage of Sn energy lost after propagation up through the basement-sediment interface, as S or converted P or both, is less than the percentage of Pn energy similarly lost up through this interface, then Sn would retain a greater percentage of its initial energy within that portion of the waveguide below the basement-sediment interface.

Under these assumptions Sn signal strength could increase with distance relative to Pn signal strength--even at high frequencies.

PN WAVETRAINS

In spite of Sn's greater signal strength, its wavetrain is considerably shorter than Pn's (Figs. 1 and 2). This seemingly peculiar observation can be explained by considering other types of conversions.

Any phases, originally Pn or Sn, that pass upward through the basement-sediment interface may eventually be reflected by the ocean surface (or the sediment-water interface) and returned to the basement-sediment interface to continue, somewhat weakened, in the waveguide as Pn or Sn or both. Throughout the travel path to the station, original Pn's returning to the interface and continuing in part as Sn's, as well as original Sn's returning to the interface and continuing in part as Pn's, would arrive between the main Pn and Sn phases. The net effect of such conversions would be Pn wavetrains greater in their duration than Sn wavetrains.

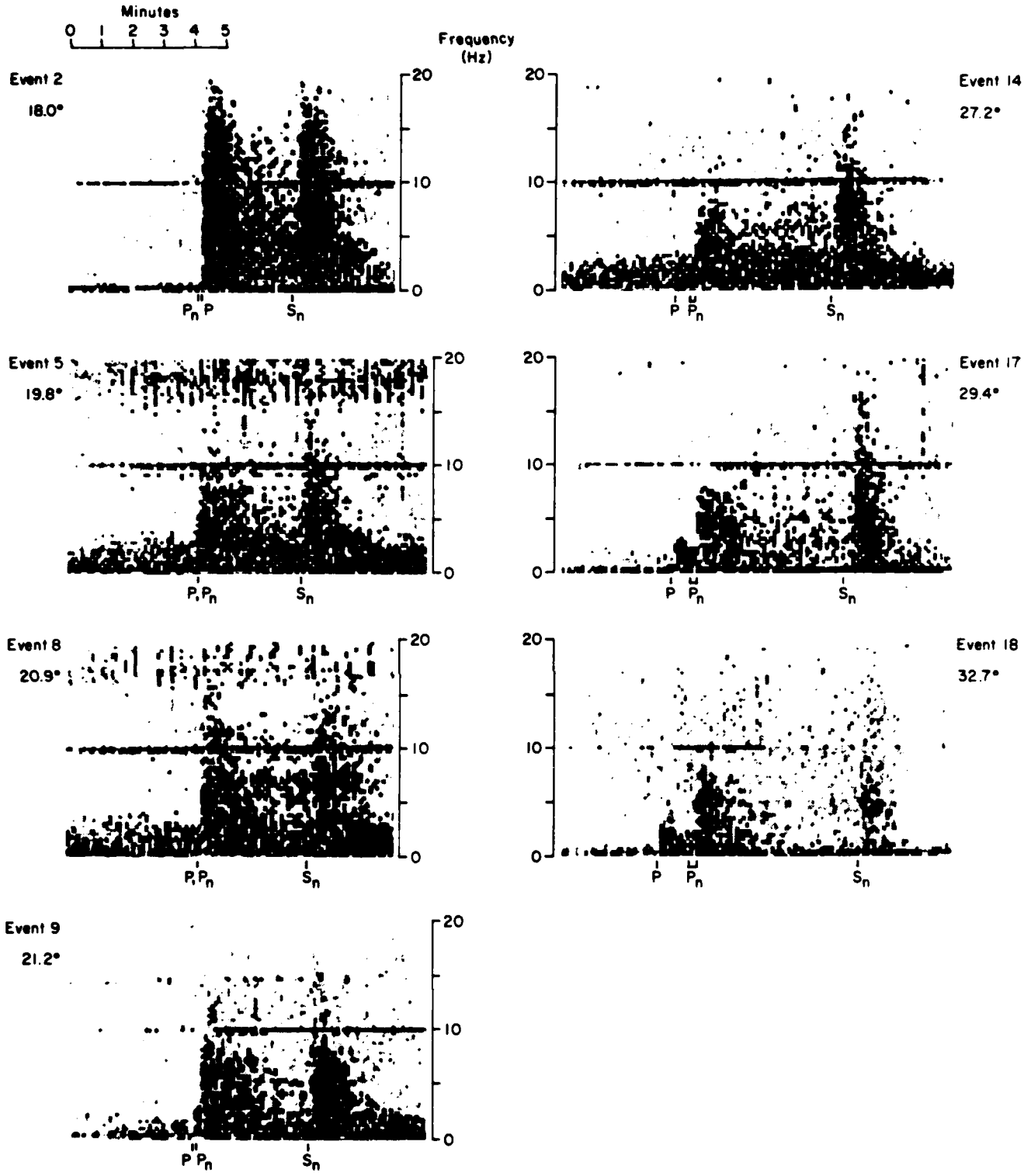

Fig. 1. Spectrograms for some earthquakes having travel paths to Wake under the Northwestern Pacific Basin. Expected times of arrivals are based on either the Jeffreys-Bullen tables (1958) for P or Pn/Sn travel time curves from Walker (1977a). The contour interval is 8 db. The line at 10 Hz is due to time code cross talk.

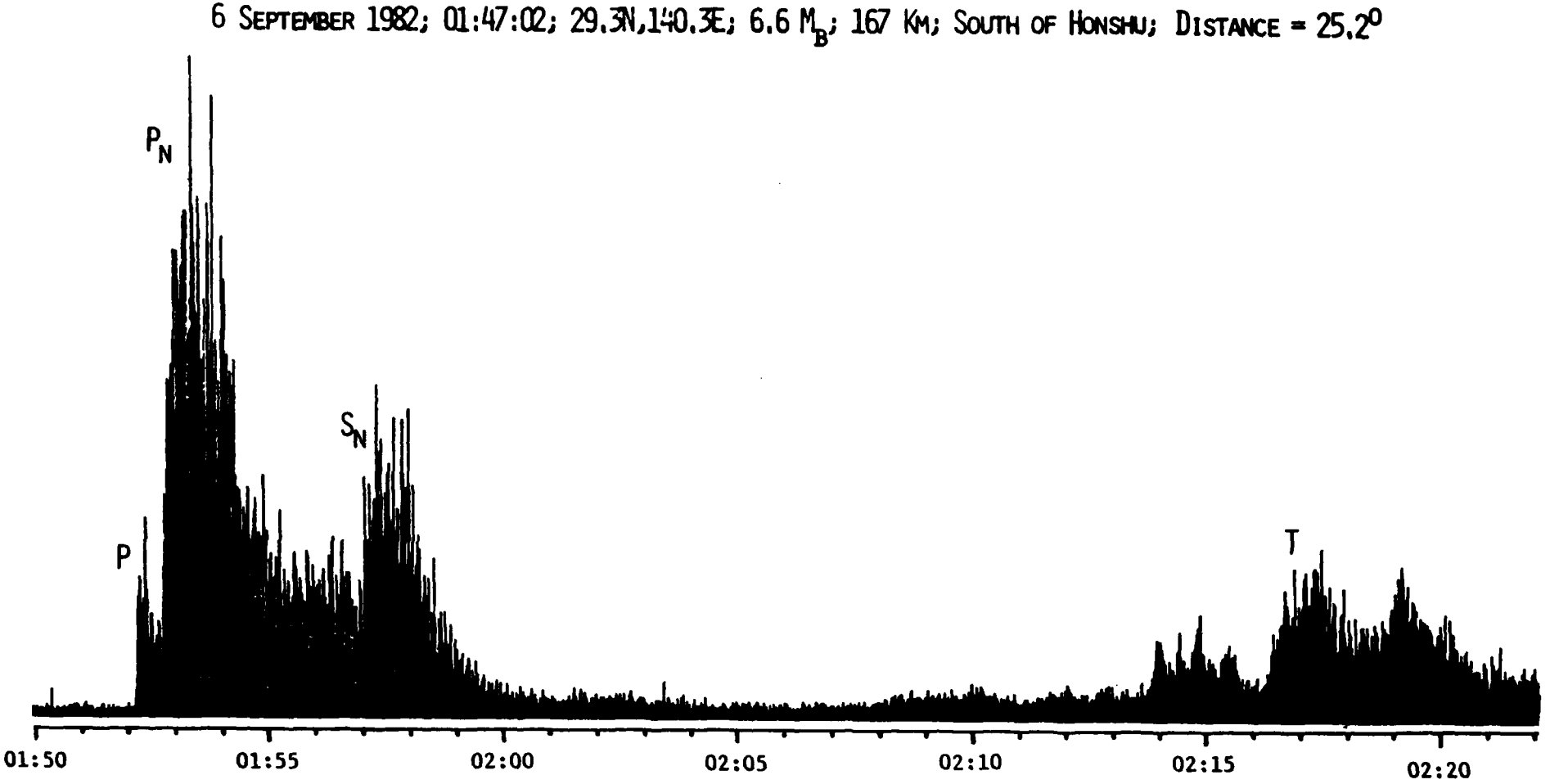

Fig. 2. Digitally rectified and compressed plot of P, Pn, Sn, and T phases for an earthquake south of Japan recorded by the Wake Island hydrophones.

OCEAN-SURFACE REFLECTIONS

Other potentially significant contributors to the Pn, as well as Sn, wavetrains are multiple ocean-surface reflections of all Pn/Sn variations observed on the ocean bottom that are capable of becoming compressional water waves at the sediment-water interface. Such reflections have already been proposed in synthetic Pn model studies (Gettrust and Frazier, 1981). An example of an ocean-surface reflection is shown in Figure 3.

PN/SN PHASES AT GREAT DISTANCES

Another puzzling aspect of Pn/Sn propagation is the frequent absence or weakness of Sn, yet presence of Pn, at great distances (often more than 4000 km) throughout the North Pacific (Walker, 1977a and b) and Central Pacific (Talandier and Bouchon, 1979), in spite of stronger Sn's than Pn's for relatively homogeneous travel paths across the deep Northwestern Pacific Basin.

A possible explanation is that paths other than those across the relatively homogeneous deep Northwestern Pacific Basin are likely to encounter relatively large lateral changes in the crust and upper mantle. These changes would have to be of such a nature so as to reduce Sn signal strength without seriously affecting the Pn phase. Large lateral changes could be produced by plateaus, rises, ridge systems, island and seamount chains, fracture zones, transform faults, fossil arcs and trenches, and rafted continental fragments.

Specific examples of Sn's severely attenuated by large lateral variations are found in recordings of earthquakes from the Solomon Islands area on the Wake hydrophones. Although these events are at distances comparable to events from Japan and the Kurils which have strong Pn/Sn phases (Fig. 1), only their Pn's are well recorded (Fig. 4). Furthermore, this effect cannot be attributed to differences in source mechanisms because Sn's from the area are well recorded at Ponape (examples of such recordings are shown in Fig. 5; refer to Fig. 6 for the location of Ponape). A reasonable explanation would appear to be the large structural changes associated with the transition from the shallow Ontong Java Plateau to the deeper Northwestern Pacific Basin (Figs. 6 and 7). An additional factor may be the extension of the Caroline Archipelago through this region.

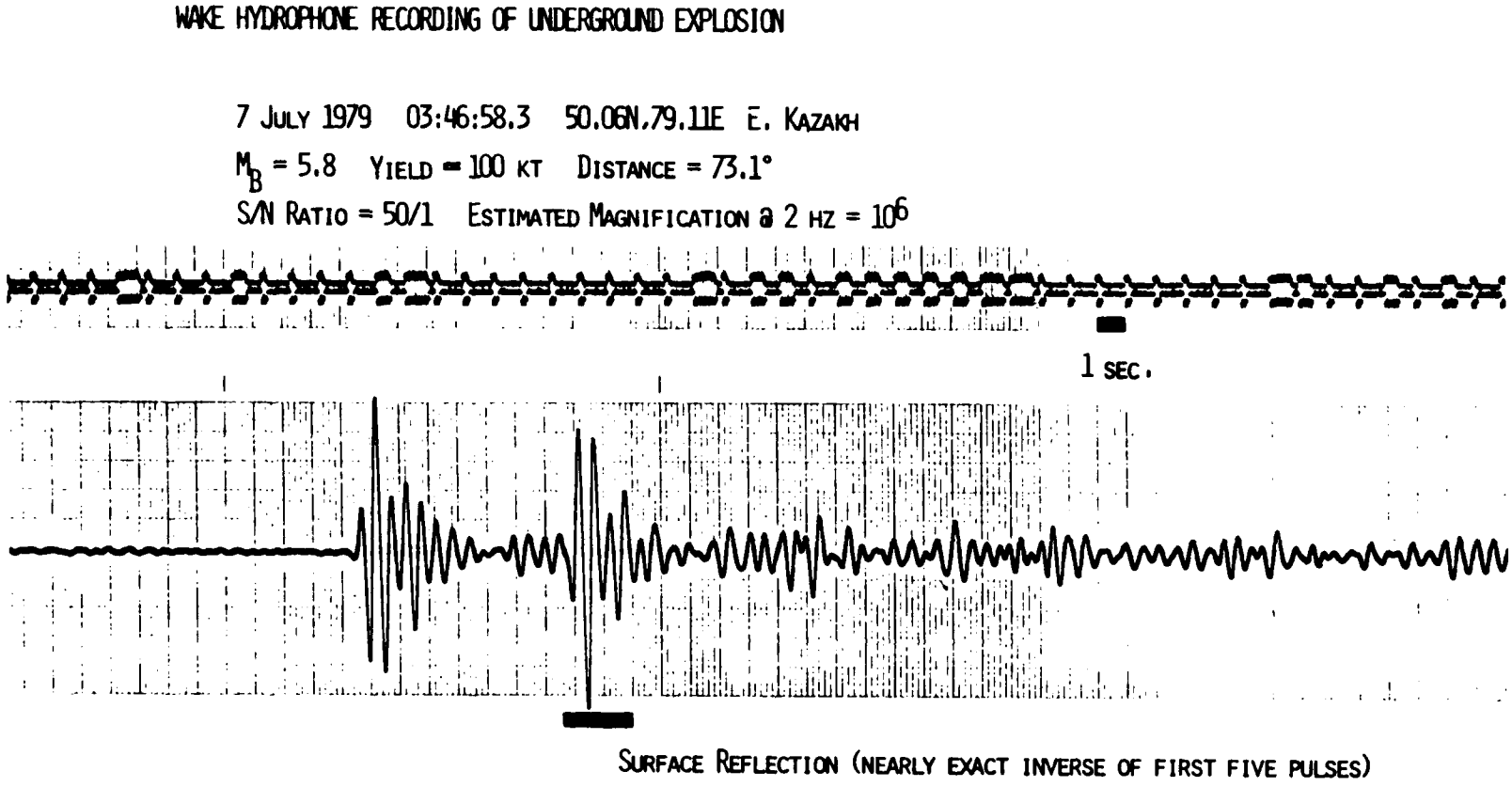

Fig. 3. An example of ocean-surface relfections.

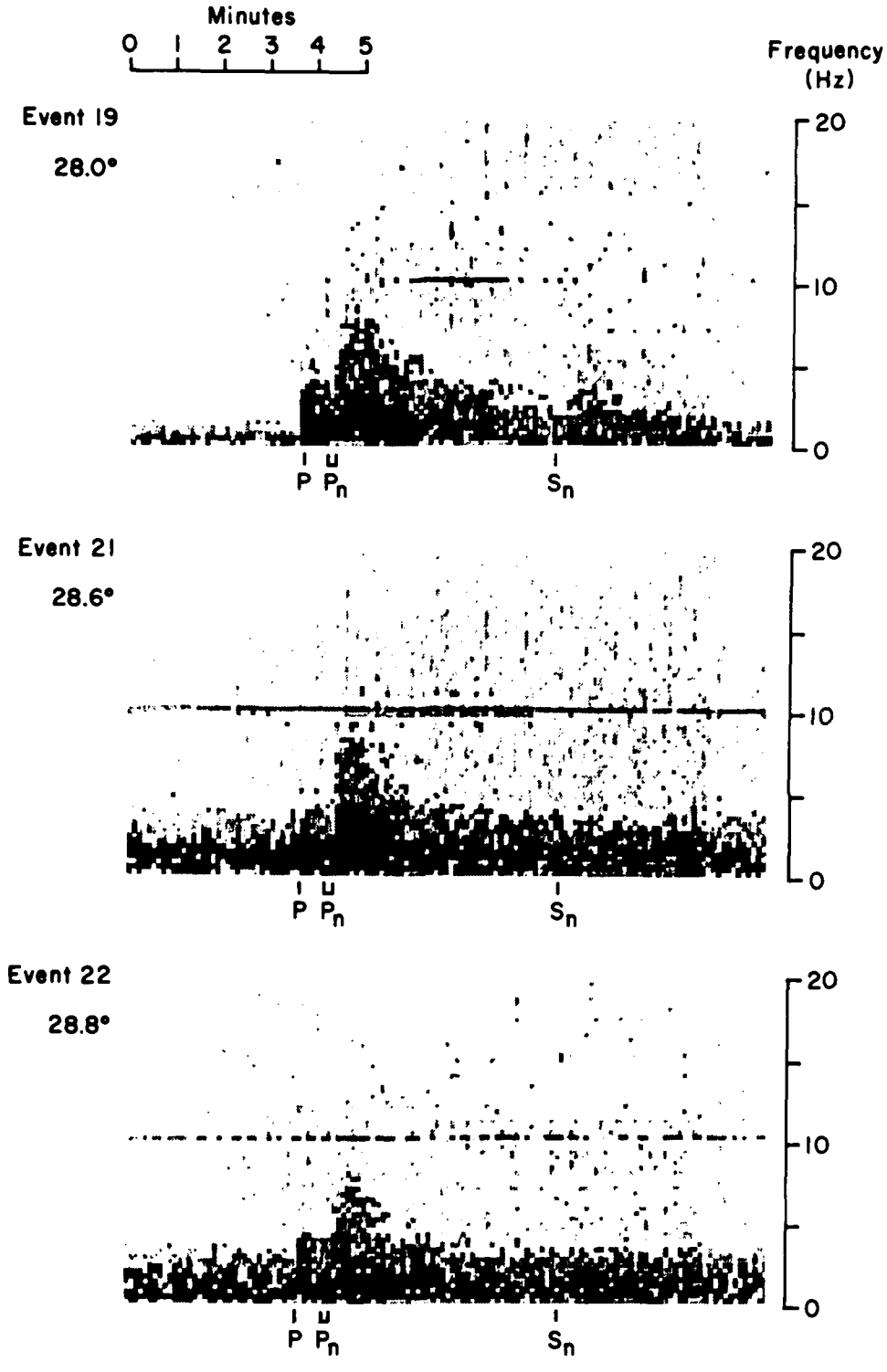

Fig. 4. Some spectrograms for earthquakes having portions of their travel paths to Wake under the Ontong-Java Plateau. Computational procedures are the same as used in Fig. 1.

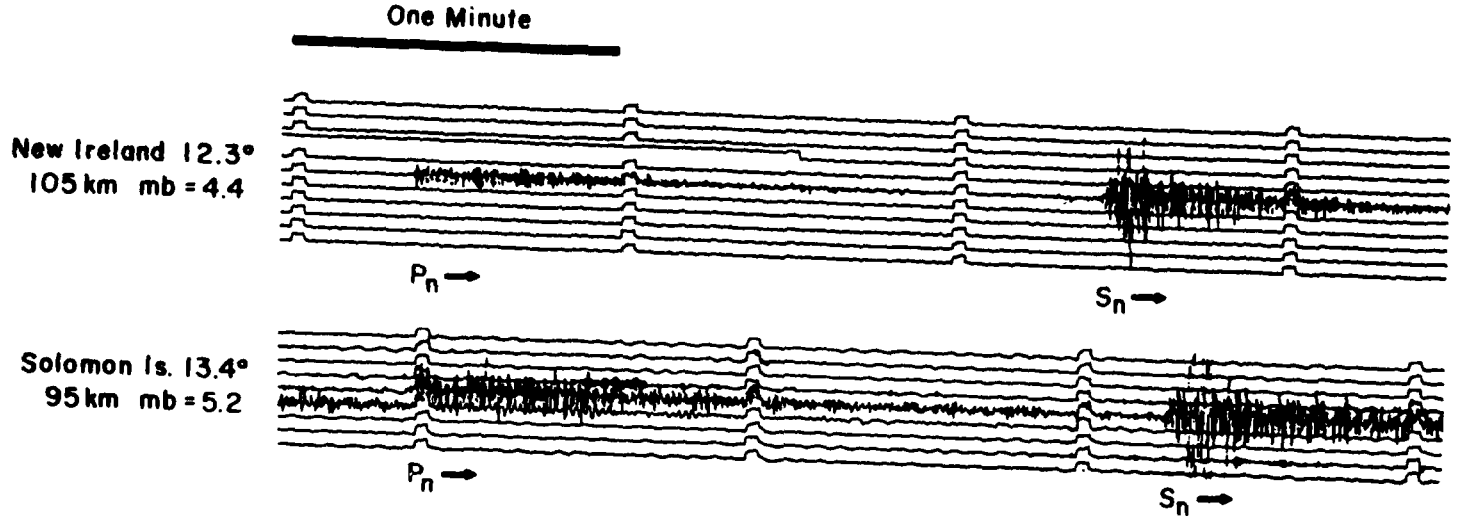

Fig. 5. Examples of Pn and Sn phases recorded at Ponape on the northern margin of the Ontong-Java Plateau. Of more than forty events from the New Ireland-Solomon Islands area, amplitudes of Sn phases are at least comparable to, and frequently larger than, those of their respective Pn phases.

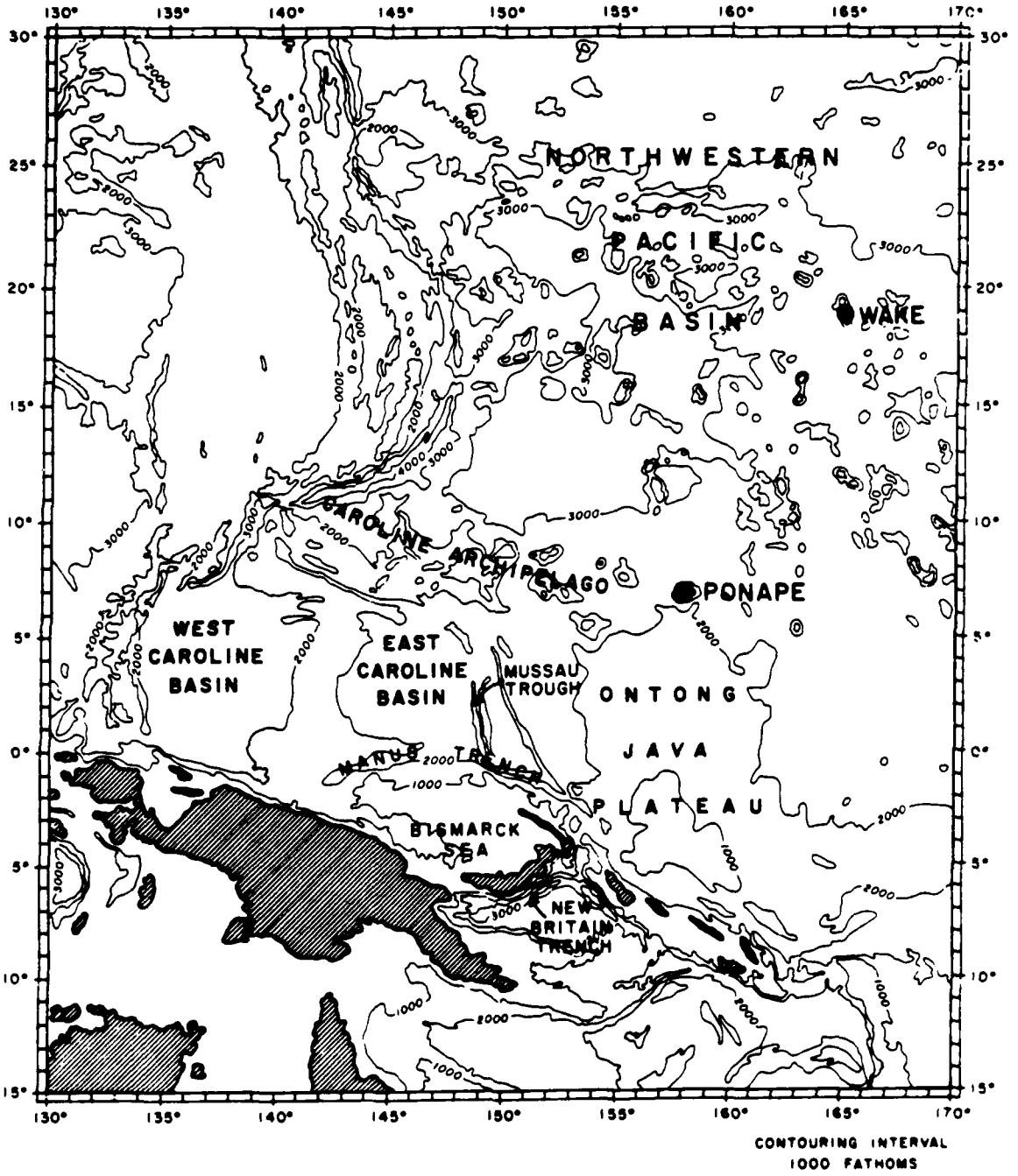

Fig. 6. Bathymetry map of the Northwestern Pacific area.

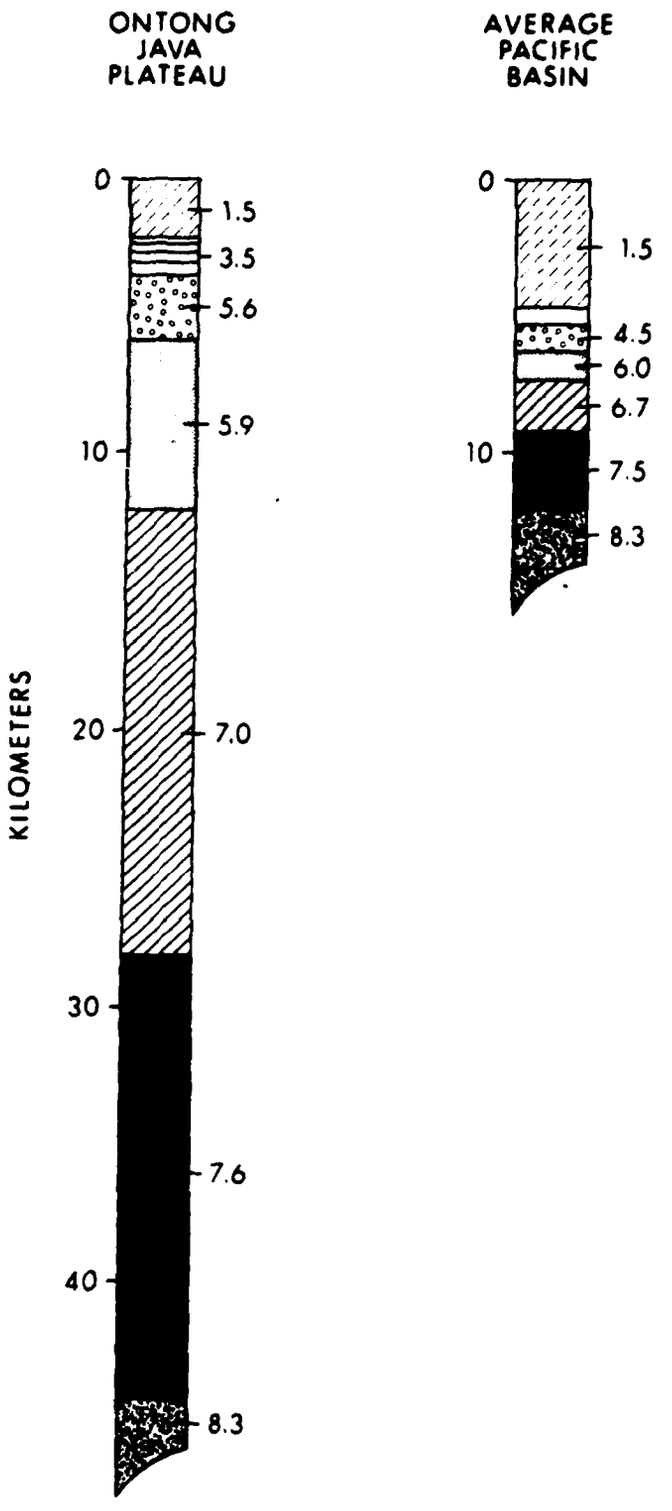

Fig. 7. Section profiles for the Ontong-Java Plateau and Pacific Basin (from Hussong et al. 1979).

T-PHASE MECHANISMS

Tolstoy and Ewing (1950) recognized the importance of a sloping bottom in the production of T-phases, and Milne (1959) provided a specific mechanism involving multiple reflections between the surface of the ocean and its downward sloping bottom. Although such a mechanism could be significant for T-phases originating in areas with the appropriate downward sloping bottom, many strong T-phases have been observed from regions where the ocean floor is level or at a greater depth than adjacent areas in the direction of the receiver (Johnson et al., 1968; Duennebier, 1968). Included among these regions are the deep ocean floor off the coast of California and Oregon, the deep ocean floor south of the subducting margins of the Northern Pacific and east of the Western Pacific, and the East Pacific Rise.

Because of these observations, a mechanism other than downslope propagation is required. Some suggestions included ocean surface scattering (Johnson et al., 1968), scattering from the sea floor by fault scarps near the source (Johnson and Norris, 1970), and coupling of Stoneley waves into the SOFAR channel (Biot, 1952; Duennebier, 1968). All of these proposed mechanisms, including downslope propagation, presume that the energy of the T-phase comes ultimately from P and, perhaps, S phases travelling upwards through the crust to the ocean bottom near the T-phase source location; however, with such a presumption, none of the proposed mechanisms is capable of explaining T-phase forerunners. In describing these forerunners, Johnson (1963) stated:

> "The time of earliest perceptible arrival is probably primarily a function of magnitude as the signal emerges slowly from the ocean background noise...Early, low-level arrivals, undetected in most T-phase recordings, must be normal-mode ground waves or, at least, must have followed a ground path for a significant portion of their travel."

He also states that in one instance (a 7.0-Ms earthquake from the Kurils) the forerunners were so early that "the transformation from P or S waves to sound channel waves would have to occur at a distance of about 1[illegible] to 21° from the source toward the receiver." In describing a P, S, and T phase (Fig. 8; actually the P and S phases are Pn and Sn phases) from a large (6.2 mb) earthquake in the Marianas recorded on hydrophones near Enewetok Atoll at a distance of about 18°, Duennebier (1968) notes that "the T phase does not have a definite onset and that energy was continuously received at the hydrophone after the arrival of the P wave."

Both authors suggest that the apparent coupling into the SOFAR channel was due to normal, mantle P or S waves or both refracted by the Emperor Seamount Chain (Johnson, 1963) and by several groups of seamounts in the Northwestern Pacific Basin (Duennebier, 1968). In terms of frequency content and strength of signal, however, the energy from the long-range, high-frequency, guided Pn and Sn phases seems more likely to be coupled into the SOFAR channel than the mantle-refracted P and S phases which are extremely weak at high frequencies. At teleseismic distances frequencies of P and S generally do not exceed 3 or 4 Hz, while Pn, Sn, and T frequencies may be as high as 20 Hz (Figs. 8 and 9).

For large earthquakes sufficient energy could be contained in the Pn/Sn phases for coupling into the SOFAR channel throughout the travel path to the receiver. This coupling could occur by any of the mechanisms proposed for the generation of the T-phase (i.e., scattering or Stoneley waves or both), with seamount enhancement remaining as an important consideration. In effect the Pn/Sn phases would serve as potential sources of energy at the sediment-basement (or water-sediment) interface. As Pn/Sn energy declines with increasing distance, the amount of energy coupled into the SOFAR channel would also decline, thus producing a T-phase signal which would slowly emerge from the ocean background noise. A recently recorded example of such an emergent T-phase is shown in Figure 2. Energy arriving at 02:08 corresponds to a Pn path of 9.6° at 8.0 km/sec and a T-phase path of only 15.6° at 1.5 km/sec.

Finally, an additional explanation for Sn appearing to have relatively more energy than Pn with increasing distance could be that Pn energy is coupled more efficiently into the SOFAR channel than Sn energy is.

SUMMARY

Vast regions of the world's oceans are characterized by thinly layered, homogeneous crustal and uppermost mantle structure. This report suggests that comprehensive observations of high-frequency phases, often referred to as Pn/Sn, throughout the Western, Northern, and Central Pacific may be explained by a waveguide which extends upward from the uppermost mantle through the crust and, to some extent, into the sedimentary layers and the entire water column. Pn energy is more efficiently propagated upward into the sedimentary column than

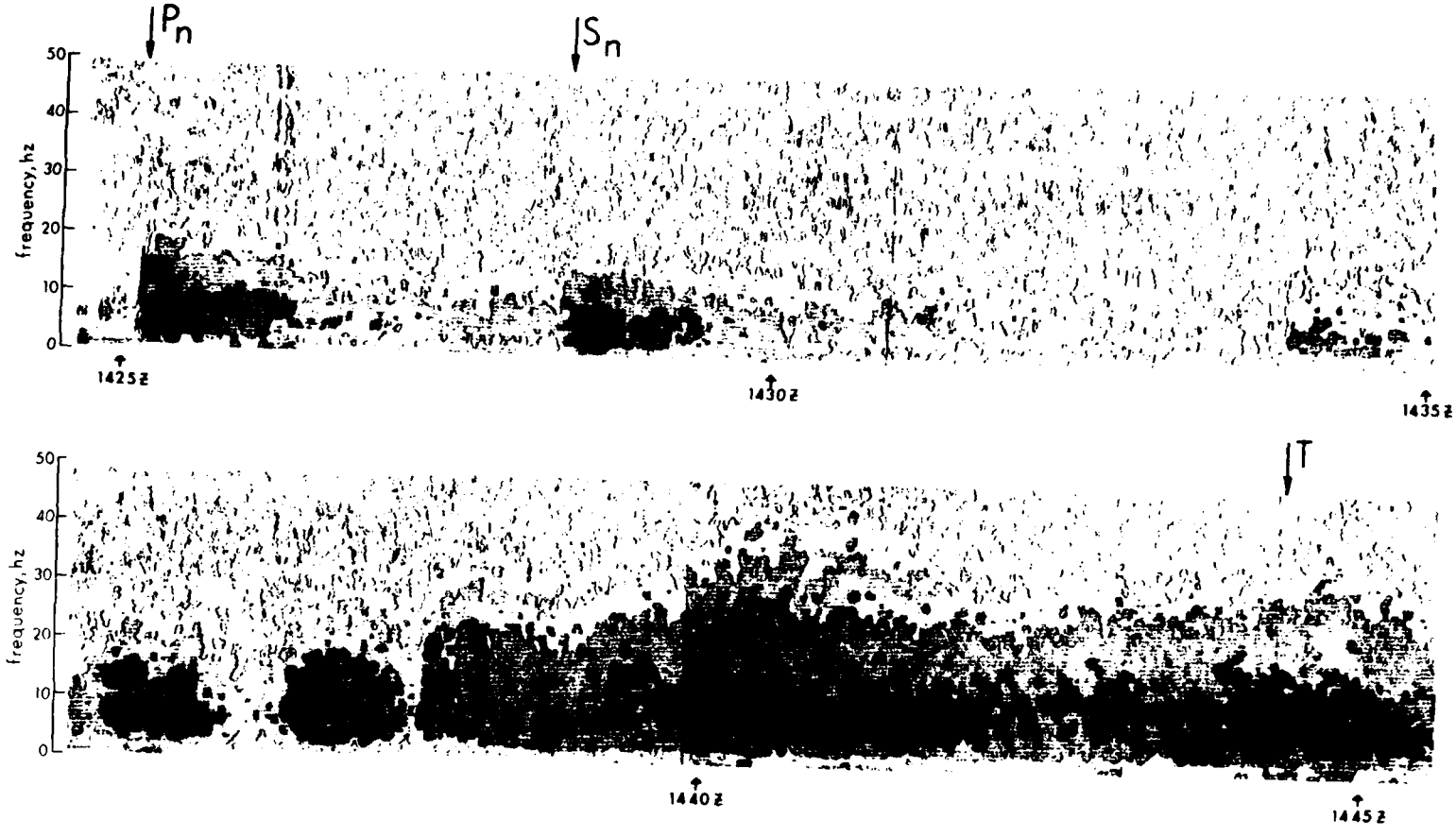

Fig. 8. Sonogram of Pn, Sn, and T phases (after Duennebier 1968). Note that the T-phase does not have a definite onset. Instead, energy appears to be continuously received at the hydrophone after the arrival of the P wave.

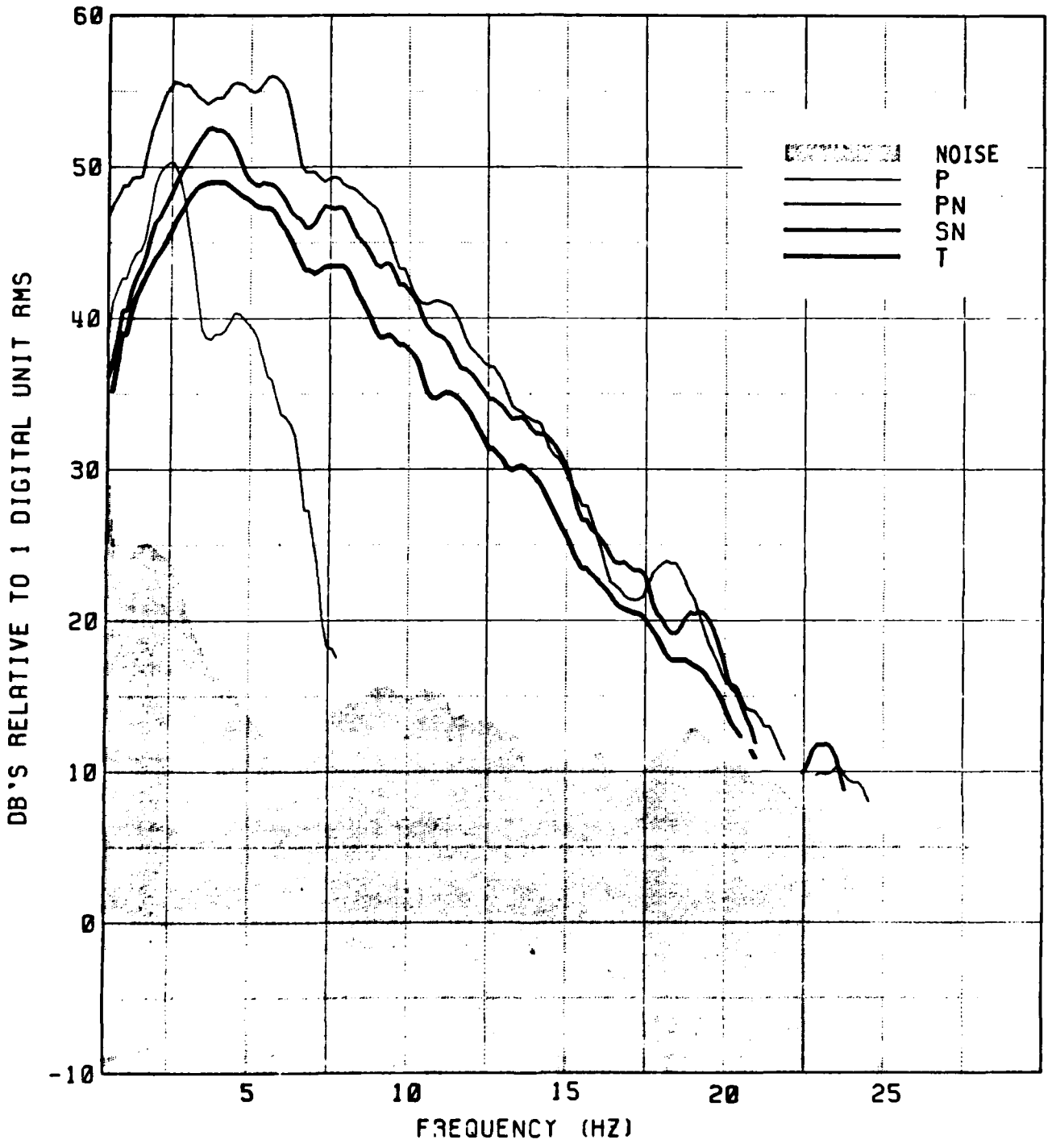

Fig. 9. Spectrums for the P, Pn, Sn, and T phases shown in Figure 2.

Sn energy, and, because of this, Pn is more rapidly attenuated than Sn. As distance increases, Pn's losses above the basement-sediment interface produce a relative strengthening of the Sn phase, such that Sn eventually has more energy than Pn.

The observed data also suggests that the long Pn/Sn wavetrains may, in part, be the result of multiple ocean-surface reflections near the receiver.

Pn to Sn and Sn to Pn conversions are suggested to explain Pn wavetrains consistently longer than the wavetrains of Sn. These conversions could occur when Pn or Sn energy passes through the basement-sediment interface and is returned to that interface by way of reflections from the ocean surface to continue in the waveguide, at least in part, as Sn or Pn phases. Such conversions might be produced at any of the interfaces encountered by Pn or Sn, or their converted phases.

In conjunction with the scattering mechanisms and Stoneley wave propagation already proposed to explain T-phase observations, Pn/Sn phases as sources of energy at the sediment-basement interface could explain: (1) the generation of T-phases in regions not having the downward sloping ocean bottom required by the classical downslope mechanism of Milne (1959) and (2) T-phase forerunners extending well ahead of the peak arrivals--occasionally beginning perhaps as early as the Pn and/or Sn phases. Also, another explanation for Sn having more energy than Pn is provided if Pn energy is more efficiently transmitted than Sn energy into the SOFAR channel.

Finally, the observed data suggest that large lateral variations in the crust and upper mantle may produce significant reductions in Sn signal strength without seriously affecting the Pn phase.

CONCLUSIONS

Although many puzzling observations of long-range oceanic Pn/Sn phases may be resolved by the suggestions presented in this report, many of these suggestions can, and should, be tested quantitatively. These analyses could include the re-examination of existing data, new experiments, and theoretical modeling efforts leading to the generation of complete synthetic seismograms. Furthermore, one should not forget that the mechanisms for the generation and propagation of the main Pn and Sn phases are still not generally agreed

upon, nor have proposed models been matched in a comprehensive manner with observations. Such tasks are of utmost importance if the phenomenon is to finally achieve the status it deserves as a major geophysical feature and tool for mapping the crust and uppermost mantle of the world's oceans--this after nearly fifty years of being little more than an obscure curiosity.

Regarding the T-phase, it seems appropriate that the earth's most efficient acoustical waveguides, the SOFAR channel and the Pn/Sn waveguide, finally should be related; and in the hypothesis formulated in this report, the SOFAR channel is energized by leakage from the Pn/Sn waveguide. The recognition of this relationship could be an important, and perhaps critical, factor in arriving at a comprehensive understanding of these oceanic phases.

> "In the bulletin of the Harvard Seismograph Station, under date of September 15, 1935 attention was directed to the unusual character of certain records from the vicinity of 17°N, 62°W. One of the novel features was a short-period phase about 23 minutes after P. It has become known as T, for third, with P and S constituting the first and second groups of short-period waves of similar general appearance...Actually, many features of P and S are abnormal on this and later records from certain areas at this distance range, and work on that part of the problem is in progress, but the investigation of T has been undertaken first." (Leet et al., 1951)

ACKNOWLEDGMENTS

This research was supported by the Office of Naval Research (Code 425GG). Supplementary funds were provided by the Air Force Office of Scientific Research and the U. S. Arms Control and Disarmament Agency. The Ponape Island Seismic Station which operated from May of 1972 through September of 1973 was supported by the National Science Foundation under grants GA-37118X1 and DES75-14814. The author thanks the U. S. Air Force (Detachment 4, 15th Air Base Wing) and Kentron International for assistance in installing and maintaining the recording stations at Wake.

Special appreciation goes to Charles McCreery, George Sutton, and Loren Kroenke for constructive comments and discussions. Editorial assistance was provided by Barbara Jones.

SUPPLEMENTARY NOTE

It may be appropriate at this time to suggest that a new name be given to the high-frequency compressional and shear phases often observed at great distances in the world's oceans. The difficulty with the nomenclature used to date is that: (1) an, as yet, unsubstantiated relationship to the well known and much studied longer-period Pn/Sn phases of continents is inferred; and (2) the environmental feature most strongly linked to the observations is not cited. Thus, a more logical term would be "Ocean P" or "Ocean S" with the abbreviations being "Po/So." With this change, those unfamiliar with the phenomenon would not be as likely to make the false assumption that the phases are similar to continental Pn and Sn. Such assumptions in the past have been a major stumbling block in stimulating interest and support for "Po/So" research.

REFERENCES

Auld, B., G. Latham, A. Nowroozi, and L. Seeber, 1969. Seismicity off the coast of northern California determined from ocean bottom seismic measurements, Bull. Seismol. Soc. Am., 59, p. 2001-2015.

Biot, M., 1952. The interaction of Rayleigh and Stoneley waves in the ocean bottom, Bull. Seismol. Soc. Am., 42, p. 81-93.

Duennebier, F., 1968. Spectral variation of the T phase, Hawaii Inst. of Geophysics Rept. HIG-68-22, 18 pp., 11 figs.

Gettrust, J. and L. Frazer, 1981. A computer model study of the propagation of long-range Pn phase, Geophys. Res. Lett., 8, p. 749-752.

Hussong, D., L. Wipperman, and L. Kroenke, 1979. The crustal structure of the Ontong-Java and Manihiki oceanic plateaus, J. Geophys. Res., 84, p. 6003-6010.

Jeffreys, H. and K. Bullen, 1958. Seismological Tables, Office of the British Association, Burlington House, W. 1., London, 50 pp.

Johnson, R., 1963. Spectrum and dispersion of Pacific T phases, Hawaii Inst. of Geophysics Rept. HIG-34, 12 pp.

Johnson, R. and R. Norris, 1970. T wave generation mechanisms, Hawaii Inst. of Geophysics Rept. HIG-70-7, 16 pp, 6 figs., + Appen., 34 figs.

Johnson, R., R. Norris, and F. Duennebier, 1968. Abyssally generated T phases, pp. 70-78 in L. Knopoff, C. Drake, and P. Hart (eds.), The Crust and Upper Mantle of the Pacific Area, Am. Geophys. Union Geophys. Mono. No. 12.

Leet, L., D. Linehan, and P. Berger, 1951. Investigation of the T phase, Bull. Seismol. Soc. Am., 41, p. 123-141.

McCreery, C., D. Walker, and G. Sutton, in press. Spectra of nuclear explosions, earthquakes, and noise from Wake Island bottom hydrophones, Geophys. Res. Lett.

Milne, A., 1959. Comparison of spectra of an earthquake T phase with similar signals from nuclear explosions, Bull. Seismol. Soc. Am., 49, p. 317-329.

Molnar, P. and J. Oliver, 1969. Lateral variations of attenuation in the upper mantle and discontinuities in the lithosphere, J. Geophys. Res., 74, p. 2648-2682.

Shimamura, H., Y. Tomoda, and T. Asada, 1975. Seismograph observation at the bottom of the Central Basin Fault of the Philippine Sea, Nature, 253, p. 177-179.

Talandier, J. and M. Bouchon, 1979. Propagation of high frequency Pn waves at great distances in the Central and South Pacific and its implications for the structure of the lower lithosphere, J. Geophys. Res., 84, p. 5613-5619.

Tolstoy, I., and M. Ewing, 1950. The T phase of shallow focus earthquakes, Bull. Seismol. Soc. Am., 40, p. 25-51.

Walker, D., 1977a. High frequency Pn and Sn phases recorded in the western Pacific, J. Geophys. Res., 82, p. 3350-3360.

Walker, D., 1977b. High frequency Pn phases observed in the Pacific at great distances, Science, 197, p. 257-259.

Walker, D., C. McCreery, G. Sutton, and F. Duennebier, 1978. Spectral analysis of high-frequency Pn and Sn phases observed at great distances in the Western Pacific, Science, 197, p. 1333-1335.

Walker, D., C. McCreery, and G. Sutton, in press. Spectral characteristics of high-frequency Pn,Sn phases in the Western Pacific, J. Geophys. Res.

Unclassified

SECURITY CLASSIFICATION OF THIS PAGE (When Data Entered)

REPORT DOCUMENTATION PAGE		READ INSTRUCTIONS BEFORE COMPLETING FORM
1. REPORT NUMBER HIG Technical Report No. 82-6	2. GOVT ACCESSION NO.	3. RECIPIENT'S CATALOG NUMBER
4. TITLE (and Subtitle) Oceanic Pn/Sn Phases: A Qualitative Explanation and Reinterpretation of the T-Phase		5. TYPE OF REPORT & PERIOD COVERED 6. PERFORMING ORG. REPORT NUMBER HIG Technical Report No. 82-6
7. AUTHOR(s) Daniel A. Walker		8. CONTRACT OR GRANT NUMBER(s) N00014-75-C-0209
9. PERFORMING ORGANIZATION NAME AND ADDRESS Hawaii Institute of Geophysics 2525 Correa Road Honolulu, Hawaii 96822		10. PROGRAM ELEMENT, PROJECT, TASK AREA & WORK UNIT NUMBERS Project No. 083 603
11. CONTROLLING OFFICE NAME AND ADDRESS Office of Naval Research Code 425 GG Ocean Sciences and Technology Division Bay St. Louis, MS 39520		12. REPORT DATE November 1982 13. NUMBER OF PAGES
14. MONITORING AGENCY NAME & ADDRESS(if different from Controlling Office) Office of Naval Research Branch Office 1030 East Green St. Pasadena, CA 91106		15. SECURITY CLASS. (of this report) Unclassified 15a. DECLASSIFICATION/DOWNGRADING SCHEDULE

16. DISTRIBUTION STATEMENT (of this Report)

Approved for public release; distribution unlimited.

17. DISTRIBUTION STATEMENT (of the abstract entered in Block 20, if different from Report)

18. SUPPLEMENTARY NOTES

Published as Hawaii Institute of Geophysics Technical Report 82-6

19. KEY WORDS (Continue on reverse side if necessary and identify by block number)

Marine geophysics
Seismic waves
Waveguide
SOFAR
Western Pacific

20. ABSTRACT (Continue on reverse side if necessary and identify by block number)

The combined effects of: (1) differing efficiencies between Pn and Sn energy transmission across the basement-sediment interface; (2) ocean surface reflections; (3) Pn to Sn conversions; and, (4) large lateral variations in the crust and upper mantle are used to formulate a working hypothesis which appears to explain, qualitatively, many observations of high frequency Pn/Sn phases throughout the western, northern, and central Pacific. Also, the concept of Pn/Sn phases as sources of energy at the basement-sediment interface is suggested as a possible mechanism for T-phase generation through scattering or Stoneley wave generation.

DD FORM 1 JAN 73 1473 EDITION OF 1 NOV 65 IS OBSOLETE
S/N 0102-014-6601

Unclassified
SECURITY CLASSIFICATION OF THIS PAGE (When Data Entered)

CORRECTIONS AND ADDITIONS

Pg. 12 line 5
after "... (Duennebier, 1968)."
add " Northrop (1972) also suggests a transformation from P to T at a distance of about 17° to explain the earliest perceptible T phase arrivals on Oahu hydrophones from the 28 March 1964 Alaskan earthquake."

Pg. 12 line 27 (last sentence of 2nd paragraph)
"... path of 9.6° at 8.0 km/sec and a T-phase path of only 15.6°..."
should read "... path of 10.1° at 8.0 km/sec and a T-phase path of only 15.1°..."

Pg. 12 line 32 (last sentence of 3rd paragraph)
after "... than Sn energy is."
add " Conversions of Pn or Sn to T near the receiver could also strengthen and extend the Pn and Sn wavetrains."

Pg. 15 line 28 (last sentence of 4th paragraph)
after "... the SOFAR channel."
add " Conversions of Pn or Sn to T near the receiver could strengthen and extend the Pn and Sn wavetrains."

Pg. 18 McCreery et al. has since been published in volume 10, p. 59-62, of Geophysical Research Letters, 1983.

Pg. 19 add " Northrop, J. 1972. T-phases, in The Great Alaskan Earthquake of 1964: Oceanography and Coastal Engineering, Nat. Acad. of Sci., Washington, D.C., p. 19-24."

Dan Walker

APPENDIX IV

A Preliminary Informal Comparison of Signal/Noise Capabilities Between The Wake Bottom Hydrophone Array, The Ocean Sub-Bottom Seismometer, And Ocean Bottom Seismometers

by
Charles S. McCreery and Daniel A. Walker

both at
Hawaii Institute of Geophysics
2525 Correa Road
Honolulu, Hawaii 96822
(808) 948-8767

Abstract. A comparison has been made between noise levels and signal/noise (S/N) ratios of the Wake Bottom Hydrophone Array (WBHA), the Ocean Sub-Bottom Seismometer (OSS), and Ocean Bottom Seismometers (OBS's) using data which has recently become available. The general purpose of this comparison is to evaluate WBHA as a possible alternative or complement to deep sea drillhole seismometers such as the Marine Seismic System (MSS) now being developed and tested for possible deployment in the Northwestern Pacific Basin. Absolute noise measurements show roughly comparable levels between WBHA and OSS, although the OSS data was scant. S/N ratios were found to be approximately 17 dB greater on the OSS than on a nearby OBS over the band 2-20 Hz, and 10 dB greater on WBHA than on a nearby OBS over the band 1-20 Hz. Improvements in WBHA S/N ratios of at least 3 dB and up to 11 dB, by stacking the water surface reflections and all 6 hydrophone signals, may be gained depending upon the level of coherence between signals. An evaluation of coherence levels has revealed apparent differences between the individual hydrophone/cable responses. Appropriate correction factors for these differences will have to be determined and then applied to the data before coherence levels are accurately known. The limited amount of data available for the noise and S/N ratio comparisons, and the indirect route by which the comparisons were made are arguments for attaching a certain amount of skepticism to the results. Additional OSS data which will become available after May 1983 should provide for a more direct and statistically stronger comparison.

Introduction. Considerable effort has been expended in recent years to develop a deep-sea borehole seismometer such as DARPA's Marine Seismic System (MSS) and the Hawaii Institute of Geophysics (HIG) Ocean Sub-Bottom Seismometer (OSS), which can be deployed down drillholes in the ocean bottom. Impetus for this effort has come from a desire to make high quality seismic observations on the vast portions of the earth covered by oceans. Although seismic observations in the oceans are capable of being made more or less routinely using Ocean Bottom Seismometers (OBS's) sitting on top ot the sediments, it has often been presumed that an instrument located below the sediment-basalt interface would have significantly greater signal/noise (S/N) ratios, at least for upwardly arriving signals. This is because such an instrument should receive more energy from seismic signals arriving from below, and less energy from noise propagating downward through the water column and sediments.

Since July of 1979, HIG has monitored on a nearly continuous basis, an array of hydrophones located near Wake Island in the Northwestern Pacific Ocean. This array consists of six hydrophones on the ocean bottom at 5.5 km water depth in a 40 km, 2-dimensional grouping, and 3 pairs of hydrophones at 1 km water depth (SOFAR channel) spread over 300 km. Recordings from only two or three of the hydrophones were made prior to September 1982; subsequently recordings from eight of the hydrophones have been made. The array was installed with the hydrophones hardwired to Wake Island more than 20 years ago for the purpose of recording transient, non-tectonic signals at frequencies above 10 Hz. Recordings made by HIG indicate that the hydrophones are also excellent seismic sensors in at least the band 0.5-20 Hz. The capability to evaluate the full potential of this array as a seismic tool has only been possible since the September

1982 upgrading. One aspect of this evaluation is to compare the noise levels and the S/N ratios between the Wake Bottom Hydrophone Array (WBHA), a sub-bottom seismometer (the OSS), and an OBS. Although data for a direct comparison does not yet exist, a somewhat indirect comparison has been made using data collected recently. That comparison is the subject of this report.

Absolute Background Noise Levels. In September 1982, during Leg 88 of the R/V Glomar Challenger, the OSS was successfully deployed off of the Kuril Islands, 378 m below the ocean floor and 20 m below the sediment-basalt interface. For a period of about 2.5 days, data was recorded from the OSS directly on the ship. Then a 2 month continuous recording package was dropped over the side for pickup sometime in May 1983. Briefly overlapping this 2.5 day period was the nearby deployment of several HIG OBS's. Noise levels measured at about the same time by the OSS vertical seismometer and a representative OBS vertical seismometer are shown in Figure 1. Although the general shape of the curves is similar, the difference in absolute levels is striking. Some of this difference is due to the impedance difference between the basalt and the top of the sediment. Smaller signals, as well as lower noise levels, would be associated with the higher impedance of the basalt. If normalized to the sediment impedance by a $\sqrt{\rho c}$ correction, where ρ is density and c is compressional velocity, the OSS noise curve moves up by about 9 dB to the position of the dashed curve. The remaining differences between these two noise curves may reflect the attenuation of downwardly propagating noise energy. Some of this noise is certainly generated by the research vessels which were operating overhead.

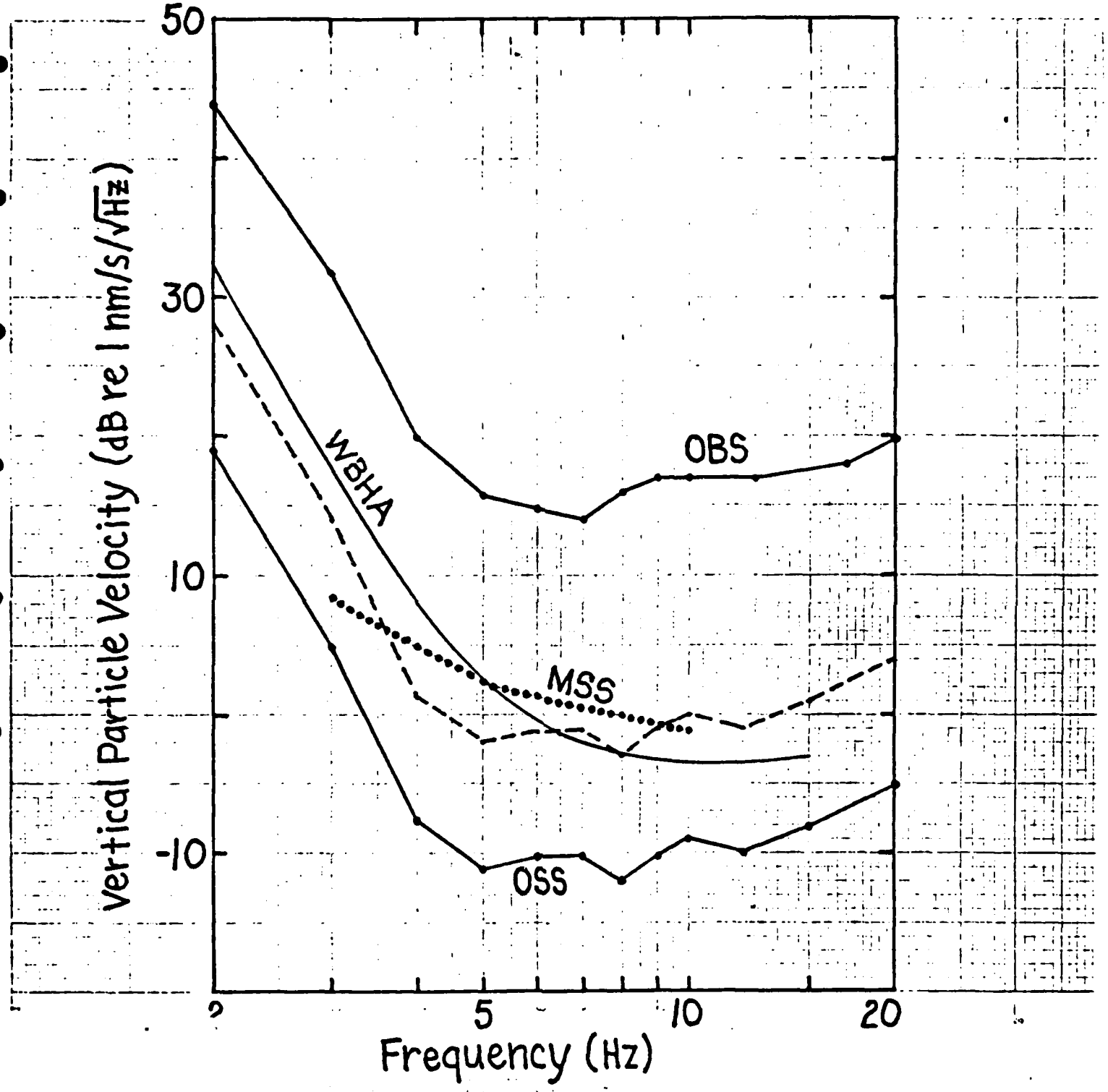

Figure 1. Background noise level measurements from WBHA (one hydrophone, 52 samples over 18 months), from an OBS and the OSS deployed in the NW Pacific Basin (vertical component-1 simultaneous sample) and the MSS in the Atlantic (vertical component-1 sample). The dashed curve is the OSS curve adjusted by 9 dB to normalize it to sediment impedance.

Also shown in Figure 1 is the average background noise for one of the Wake bottom hydrophones, determined from 52-2 minute random noise samples taken over a period of 18 months. Pressure has been converted to vertical particle velocity by the expression $\dot{x}=P/\rho c$, where $\dot{x}$ is vertical particle velocity, P is the pressure, ρ is seawater density, and c is the speed of sound in seawater. Although the hydrophone noise is certainly not generated entirely by vertically arriving pressure waves (thus vertical particle velocity), this conversion is useful to determine an equivalent noise level for comparison.

For reference purposes, the noise curve for MSS in the Atlantic has also been plotted. It is not known if an impedance correction need be applied to this curve and so none has been.

The OBS and OSS noise curves may not be representative of average noise levels because they are only 1 sample and because of the ship generated noise. The relationship between these two curves however, is probably significant, and illustrates the decrease in noise level which can be achieved by a downhole instrument. The average noise level of the Wake bottom hydrophone is similar to that of the normalized OSS curve. These two curves are also comparable to the MSS curve for frequencies between about 4 and 10 Hz.

Signal/Noise. Although absolute noise levels are important for evaluating the usefullness of a seismic sensor, a more important parameter is S/N. Ideally, a comparison should be made of an earthquake or explosion signal recorded simultaneously on the Wake hydrophones, an OBS, and a downhole instrument, all located in close proximity. Unfortunately, these data do

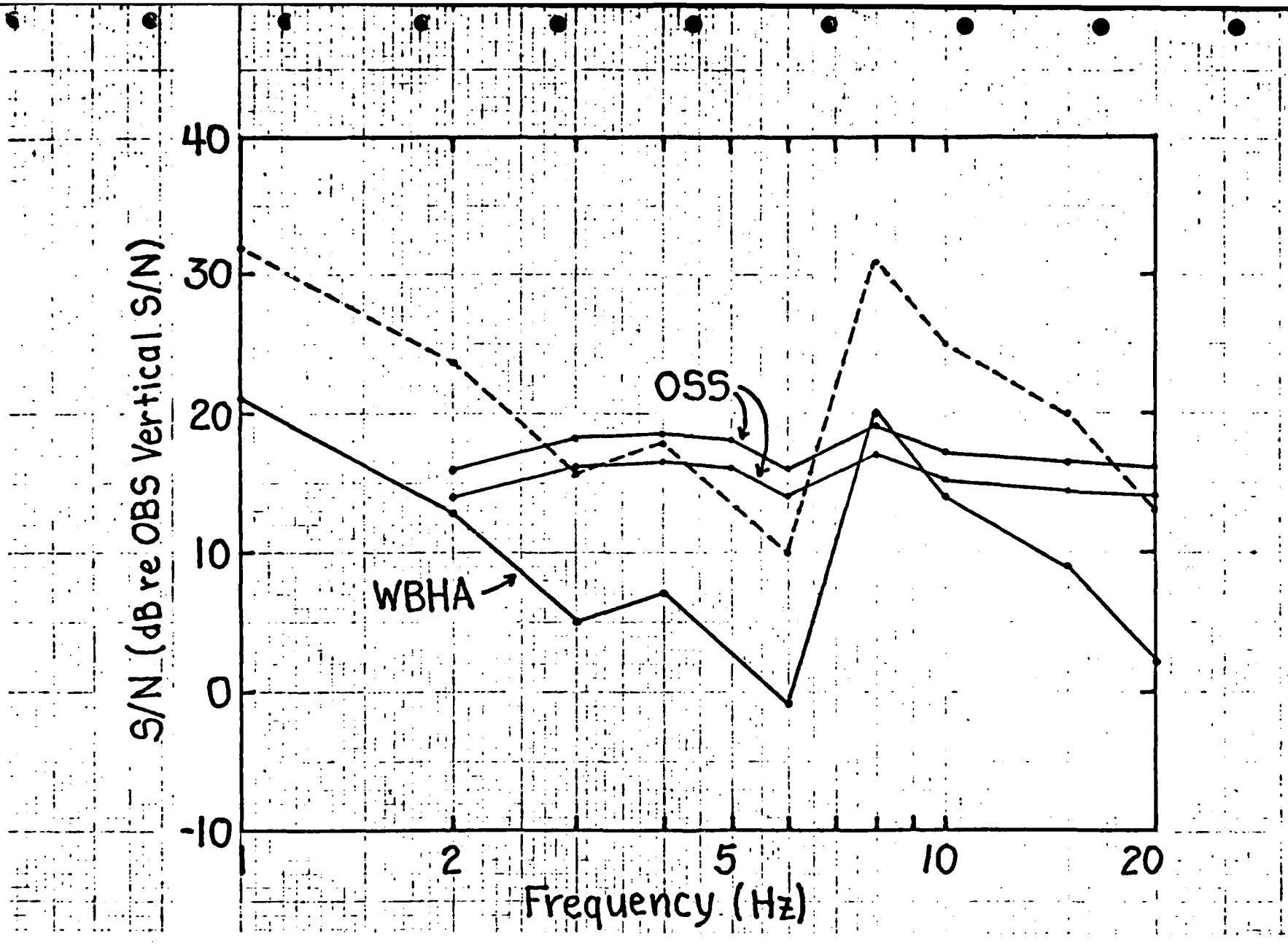

Figure 2. S/N measured on WBHA and on the OSS relative to S/N measured on nearby OBS's as described in the text. The lower OSS curve is based on shot S/N data, while the upper OSS curve is based strictly on noise data. The dashed curve is the WBHA curve raised by 11 dB to show the potential S/N by signal stacking.

not exist. With a few assumptions however, an indirect comparison can be made using data which do exist.

Within the 2.5 day period of OSS data previously mentioned is the record of a 126 pound shot at 80 km distance. It occurred, however, after the last of the nearby OBS's had been recovered. Fortunately, during the OBS deployment there was an 1800 pound shot also at 80 km distance from one of the OBS's. After making some assumptions and corrections, a comparison between ground arrivals on these records may yield information about the improvement in S/N between the OBS and OSS. The first correction is one for shot size, equal to the ratio of the shot weights to the power 0.66, or 15 dB. The spectral shape of the two shot records is very similar so a common shape was assumed. The second correction is for temporal changes in background noise which occured during the time between the shots. These effects were compensated for by assuming the same OBS/OSS noise ratios found for the simultaneous data discussed in the previous section. The resulting ratio of (OSS S/N)/(OBS S/N) is plotted in Figure 2.

Also shown is a curve which represents the possible gain in S/N of the OSS relative to the OBS based strictly on the simultaneous noise data. A correction for the impedance difference between the sediment and basalt has been applied. No assumptions were made about possible losses in upcoming signal levels between the OSS and OBS, and the effect of these would be to raise this curve by some amount. However, the near agreement in absolute level between this curve and the one based on the shot data may imply that these losses are not significant for the frequencies observed. (The parallel nature of the two curves is not significant but is due to having used the simultaneous noise data to correct for temporal differences in the

shot data.) On the average, these data support an improvement in S/N over the range 2-20 Hz of about 17 db.

A more direct comparison can be made between WBHA and an OBS. In August of 1981, HIG deployed an OBS array along a 1500 km line in the NW Pacific, and one of these OBS's was located within the bounds of WBHA. A strong Po (i.e.,"Ocean P"; formerly called high-frequency Pn) signal from a large earthquake in the Kuril Islands was recorded simultaneously by this OBS and by a recording system connected to 3 of the hydrophones of WBHA. A comparison between the OBS vertical geophone and WBHA could not be made because that sensor was not working properly on the OBS. Consequently, the OBS hydrophone signal has been used. To correct for any difference in S/N between the OBS vertical and OBS hydrophone, a factor equal to the actual measured difference in S/N between the vertical geophone and hydrophone for this same signal recorded on another OBS at a closer epicentral distance was added to the S/N of the hydrophone. This factor averaged 1 dB over the range 1-20 Hz. Plotted in Figure 2 is the ratio between the average S/N of the 3 Wake hydrophones and the S/N measured on the OBS hydrophone with the previously described correction added. The somewhat wild behavior of this curve, such as the jump from -1 dB at 6 Hz to 20 dB at 8 Hz, is not entirely understood. It may be related to resonances in the OBS package which contribute to the OBS noise level, or it may be due to other factors which could not be identified by the analysis of only this one signal. For most frequencies, however, the WBHA data show an improvement in S/N, and this improvement averages roughly 10 dB over the range 1-20 Hz.

A natural question to ask is: "Why should there be any difference at all in S/N between the OBS hydrophone and the nearby WBHA hydrophones, since they are both lying at the top of the sediment column?" One explanation

might be that the OBS used for comparison was particularly noisy due to noise sources in the water very close by or due to electrical noise in the amplification and recording system. Evidence which generally contradicts this hypothesis is that the noise levels measured on the other OBS's in the array were comparable. An alternate explanation may be related to the 20 year age of the array, and the possibility that the bottom hydrophones are now buried under a layer of sediment. Burial of the hydrophones would isolate them from noise generated by bottom water currents flowing around them, and also possibly from sediment surface phenomena such as Stonely waves. Although these explanations are not supported by direct evidence at this time, it would certainly be worthwhile to learn that shallow burial of a hydrophone under the sea floor sediment would greatly improve its S/N capabilities.

Coherence Across WBHA. An important aspect of current research at HIG is the investigation of coherence of teleseismic body waves across the 40 km aperture of WBHA. The impact of near receiver structure on these signals may be small due to the thin and relatively undisturbed nature of the oceanic lithosphere underlying WBHA. High coherency would have important implications for: (a) the planning of any future ocean seismic arrays; (b) studies of first arrivals requiring a great deal of timing precision; (c) studies requiring precise determination of seismic amplitudes (such as yield determination), and especially (d) studies of small signals where enhancement of S/N is desired (such as detection). Highly coherent signals may be added (with appropriate propagation delays) to yeild an increase in S/N equal to the square root of the number of sensors (for uncorrelated noise). At WBHA the theoretical increase in S/N would be equal to about 11

dB (3 dB of which comes from the first water surface reflection which is well established as having nearly perfect coherence with the initial arrival). Data from 3 WBHA hydrophones, collected prior to September 1982 on slow-speed cassettes, indicated high levels of coherence for a sampling of teleseismic P arrivals. Unfortunately, these data were not especially suited for this type of analysis because of timing inaccuracies and the suspect fidelity of the recording medium. Since September 1982, however, continuous data from 5 of the 6 bottom hydrophones have been collected digitally, essentially solving the timing and fidelity problem , and providing a format for a much speedier and more accurate analysis of the data. Software for the necessary quantitative analysis is still under development. However, "eyeball" checks for coherency have been made for a few of the digitally recorded teleseismic P phases with large S/N. The results are encouraging although not entirely conclusive.

Figure 3 illustrates the kind of broadband coherency which seems to be characteristic of the different P arrivals examined. Some features are "in phase" across the array while others are not. Certain pairs appear more coherent than other pairs. This relationship does not seem to be a function of epicentral distance or azimuth. Certainly a large improvement in S/N would not be expected from the stacking of these signals as they are.

Possible reasons for the observed difference in signals may be classified into the following categories: (a) major differences in the coda exist for very small changes in takeoff angle (for Figure 3, much less than 1°); (b) variations in lithospheric structure directly beneath the array have a significant impact on the signals; and (c) the hydrophone/cable responses differ significantly across the array. If the

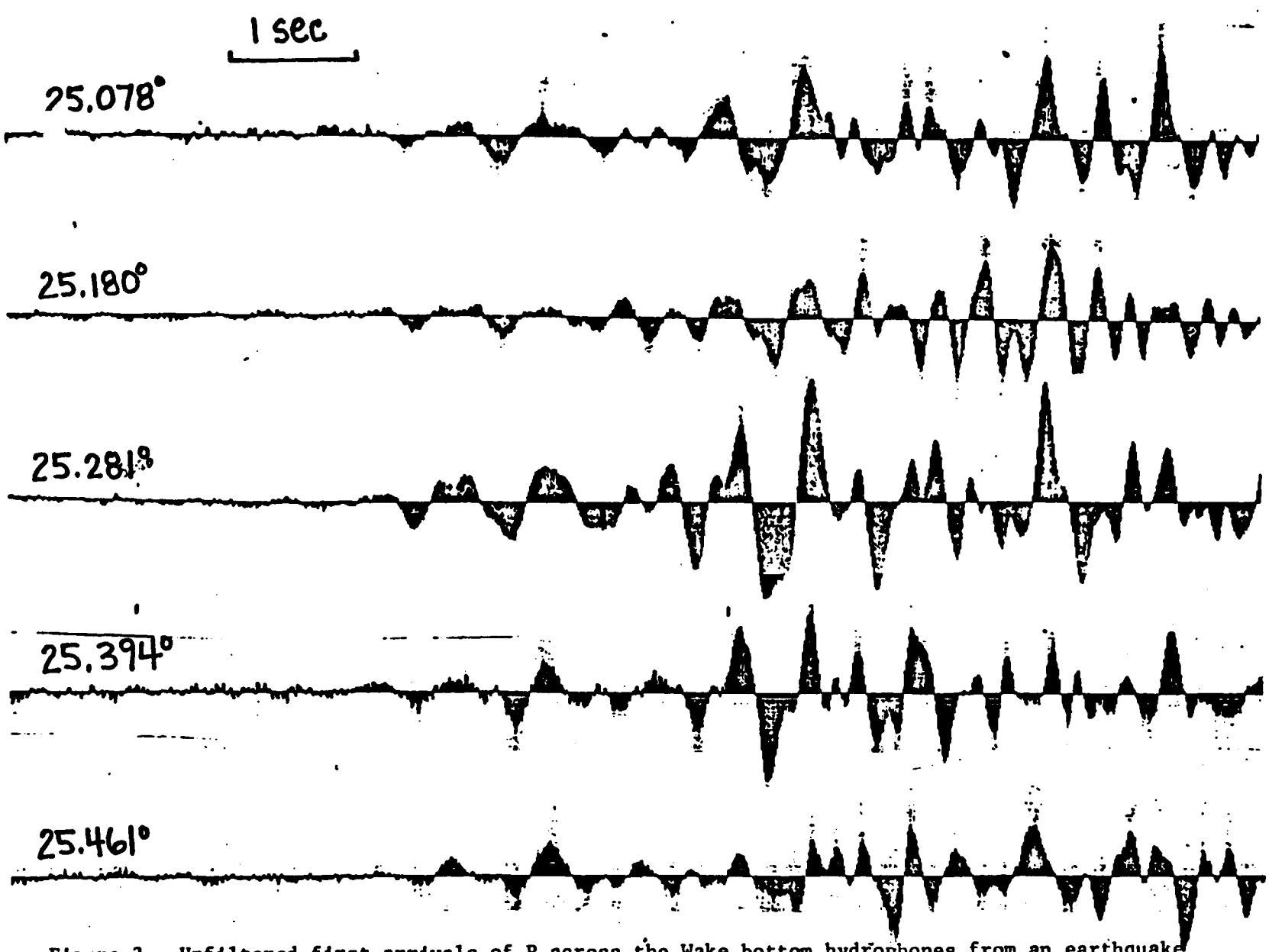

Figure 3. Unfiltered first arrivals of P across the Wake bottom hydrophones from an earthquake south of Honshu, Japan (6 Sept. 1981, h=167 km, m=6.6). Traces have been offset by travel time differences.

explanation is (a) then little, if any, improvement in coherence can be expected by massaging the data. If the explanation is (b) then significant improvements in coherence are possible, provided the lithospheric response does not vary greatly with small changes in azimuth or angle of incidence of incoming P arrivals. If the explanation is (c) then an even more significant improvement in coherence is possible. The technique which will be used to investigate (b) and (c) is basically a calculation of amplitude and phase differences between hydrophones for a given signal as a function of frequency. If (c) is true, then these differences should be consistent regardless of what kind of signal is being recorded - P, Po, So, T, or noise. If (b) is true, then the differences should be consistent for P and possibly Po and/or So. If both (b) and (c) are true, the effects should be seperable. These effects may then be removed by a deconvolution of the observed signals with the empirically determined impulse responses of the lithosphere and hydrophone/cable. Determination of these responses to a level of statistical signifigance will require the recording and analysis of a variety of signals at assorted azimuths and epicentral distances which have strong S/N. Evidence exists to suggest that at least (c) is true.

Figure 4 shows amplitude differences observed across WBHA for a 10 minute section of record which includes a P, Po, and So signal. The upper curve is the absolute value of the maximum difference in amplitude observed between the six hydrophone signals as a function of frequency. Energy below about 0.5 Hz is from microseisms while between 0.5 Hz and 20 Hz it is mostly an average of the P, Po, and So. The lower curve shows amplitude differences between two particular hydrophones. Although it may seem unusual to have combined energy from all of these different types of signals, the individual signals, P, Po, So, and noise, exhibit the same

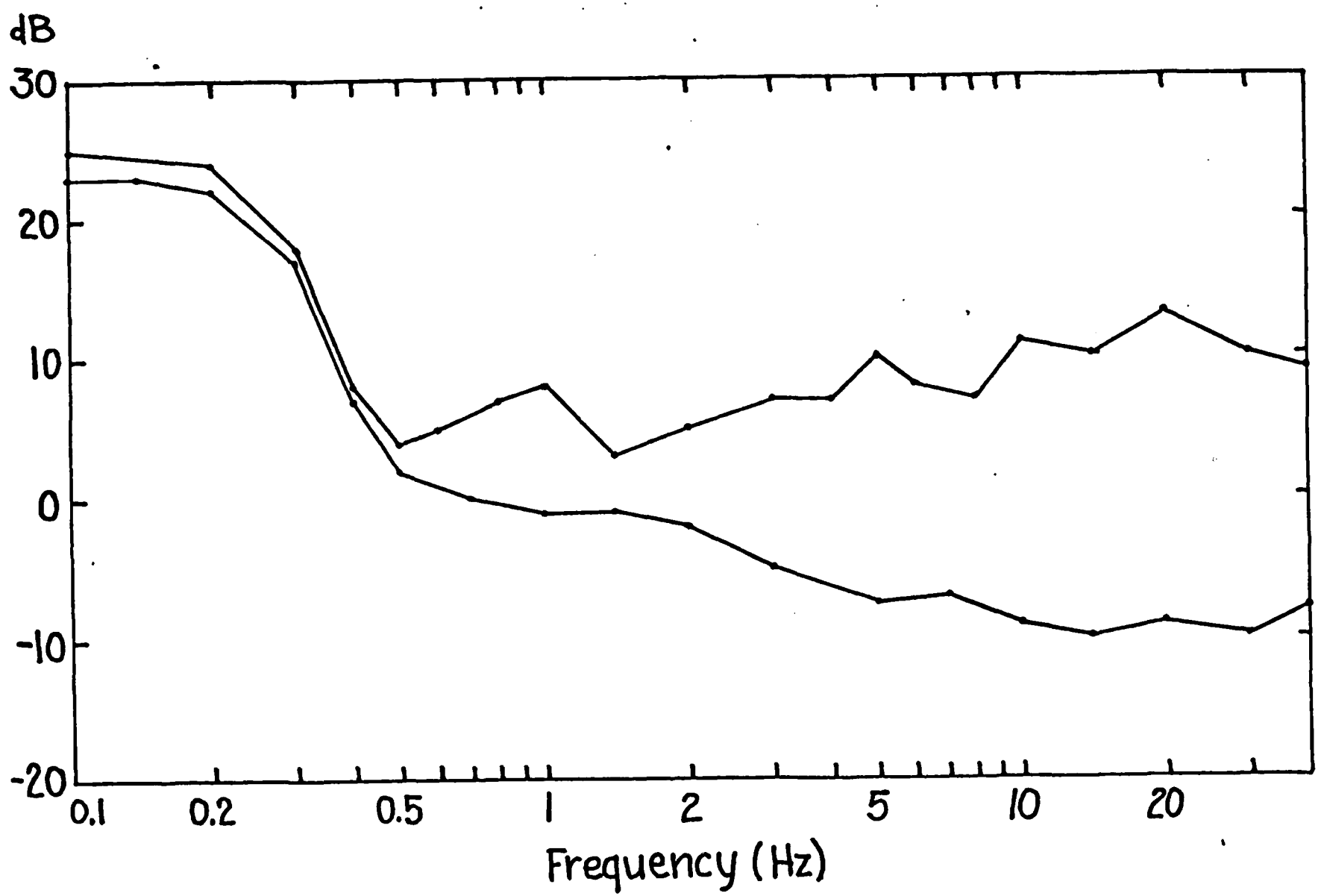

Figure 4. Plot of differences between spectra across the Wake bottom hydrophone array for a 10 minute section of record containing P, Po and So signal and noise. The upper curve shows the maximum value of variation in level between all of the hydrophones. The lower curve shows the difference in level between two of the hydrophones.

relationships although with a somewhat greater scatter. This strongly suggests that there are at least differences in the hydrophone/cable responses which are removable. These differences might easily produce the incoherencies seen in Figure 3. Further and more careful analysis of other events will necessary to precisely determine the differences in amplitude and especially phase. The reward may be stronger coherency and thus an increase in S/N.

Conclusions. The data presented in this report indicate that WBHA, the OSS, and, by inference, the MSS, are seismic tools of comparable quality. Noise levels measured were similar for all three although the data were somewhat limited. S/N ratios measured for OSS were greater than that for individual WBHA hydrophones by an average of about 7 dB. Gains in S/N levels, through stacking of the WBHA signals, will reduce, if not eliminate or reverse, that difference. Precise estimation of the coherence across WBHA will not be made until recently discovered differences in the hydrophone/cable responses have been more accurately determined so that their effects may be removed from the signals.

Many of the comparisons in this report were made via rather indirect routes due to the limited amount of data. Additional data should become available sometime this summer after the OSS recording package has been picked up and the data returned, reduced, and distributed. More data from the August 1981 Wake OBS Experiment will be in a reduced form soon. Also, data from OBS's deployed during the OSS experiment by Oregon State University should be available later this year. All of these future data should be examined and added or compared to those data presented here to

further understand these results.

Acknowledgements. This preliminary and informal report was sponsored by the Air Force Office of Scientific Research, with supplementary funds provided by the U.S. Arms Control and Disarmament Agency. Major upgrading of the Wake system in September of 1982, just prior to the Downhole Experiment, was made possible through the timely support of those agencies.

APPENDIX V

Po/So Phases: Propagation Velocity and Attenuation Across a 1600 Km Long Deep Ocean Hydrophone Array

by

Daniel A. Walker and Charles S. McCreery

both at

Hawaii Institute of Geophysics
2525 Correa Road
Honolulu, Hawaii 96822

Abstract. Po/So phases from numerous earthquakes along the margin of the Northwestern Pacific Basin were successfully recorded by a linear, 1500 km ocean bottom hydrophone (OBH) array deployed for two months near Wake Island. Data from ten shallow-focus (<100 km) events at 18° (2000 km) to 33° (3700 km) epicentral distance were used to compute propagation velocities for Po and So. The resulting travel-time equations T=X/(7.96 ± 0.05 km/sec) - (7.14 ± 2.38 sec) and T=X/(4.57 ± 0.04 km/sec) - (14.03 ± 5.31 sec) for Po and So, respectfully, successfully model all Northwestern Pacific Basin shallow-focus Po/So first arrival data collected by the Hawaii Institute of Geophysics since 1963 at epicentral distances greater than 12°. Also, arrivals from an event in the Kuril Islands (mb = 6.6, h = 45 km), which propagated down the axis of the array, were used to estimate the attenuation of Po and So between 25° (2800 km) and 33° (3700 km) epicentral distance. After a correction for cylindrical spreading, values for a frequency dependent Q are found to range from 625 ± 469 at 2 Hz to 2106 ± 473 at 13 Hz for Po and from 1401 ± 296 at 5 Hz to 3953 ± 863 at 15 Hz for So. These same data may be alternatively described as exhibiting an average attenuation of -21.5 ± 0.9 dB per 1000 km of travel path, which applies to both Po and So at all frequencies studied.

Introduction

Late in the summer of 1981, the Hawaii Institute of Geophysics (HIG) successfully deployed a 1500 km long linear array of twelve ocean bottom hydrophones (OBH's) near Wake Island (Fig. 1). Half of the instruments (indicated by open circles) started recording on 12 August and ended on 23 September. The remaining half started on 3 September and ended on 15 October. The total recording time was about 65 days, with all twelve instruments in operation from 3 September through 23 September. Of the twelve OBH's deployed, ten were successfully recovered, and nine of these had quality data throughout their operational period. Recorded concurrently were three bottom hydrophones of the Wake Hydrophone Array (WHA), a 40 km array of sensors located near, and cabled directly to, Wake Island. WHA data were used in the study of first arrivals, and were considered to be part of the OBH array data. All of the OBH and WHA instruments were in ocean depths between 5265 m and 5657 m. Of more than 130 events identified from seismic phases in the recordings, 108 were located by the National Earthquake Information Service (NEIS; Table 1 and Fig. 1). The primary purpose of the experiment was to acquire data of critical importance in understanding a phenomenon known as high-frequency Pn/Sn, long-range Pn/Sn, or Ph.f./Sh.f.; but referred to here as Po/So or Ocean P/Ocean S after Walker (1982).

Po/So phases were first observed in the North Atlantic and have been found throughout the North, Western, and Central Pacific. First arriving Po/So energy travels with a fairly constant apparent velocity (epicentral distance/travel time) of about 8.0 and 4.6 km/sec, respectively, while peak amplitude arrivals have apparent velocities of about 7.6 and 4.5 km/sec, respectively, which are comparable to basal crustal rates. At distances of about 18° ($\cong$ 2000 km), observed frequencies of Po/So are as high as 30 and 35 Hz, respectively; and at distances of of about 30° ($\cong$ 3300 km), as high as 15 and 20 Hz, respectively. The signal/noise ratios for Po/So phases are generally at least ten times greater than the ratios of their respective normal, mantle-refracted P and S phases; and in many instances no P's or S's can be found in spite of the presence of very strong Po's and So's. Aside from the SOFAR channel of the world's oceans, the Po/So waveguide appears the be the earth's most efficient acoustical waveguide. Also, it seems probable that the phenomenon is a dominant feature of all of the world's oceans and marginal seas.

Recent efforts have been made, using synthetics, to determine the mechanism of Po/So propagation (e.g., Stephens and Isacks, 1977; Menke and Richards, 1980; Sutton and Harvey, 1981; and Gettrust and Frazer, 1981), although many essential characteristics of these phases are still poorly known. Data collected before this experiment, composed almost entirely of events recorded at single stations and over an unevenly distributed range of epicentral distances, made difficult the precise determination of the travel-time curve between 0° and 40°, as well as the attenuation of these phases as a function of frequency and distance. These parameters need to be accurately determined so that a unique model can eventually be found.

To exemplify this point consider Fig. 2: a plot of apparent velocity versus epicentral distance for Po and So having Northwestern Pacific travel paths and source focal depths of 100 km or less which is based on data collected and published (Walker, 1981) by HIG before this experiment. Two

Table 1. Events Recorded by the OBH Array
(Data from NEIS Monthly Lists)

No.	Date		Time	Location	h	m	M	n	Po	So
1	Aug.	12	22:35	Solomon Is.	33	4.9	-	3	-	-
2		13	02:57	Tonga Is.	191	5.4	-	3	-	-
3		14	05:42	Volcano Is.	33	4.7	-	3	-	-
4		14	06:24	Molucca Passage	38	5.5	5.3	1	-	-
5		14	09:05	Honshu, Japan	58	-	-	2	-	-
6		15	10:30	Alaska	53	5.1	-	2	-	-
7		15	19:53	Philippine Is.	152	4.8	-	1	-	-
8		16	23:54	Kuril Is.	33	5.6	5.0	3	-	-
9		17	02:17	West Irian	34	5.7	5.8	3	-	-
10		17	17:07	Fiji Is.	383	5.5	-	2	-	-
11		18	05:29	Banda Sea	34	5.1	4.8	1	-	-
12		19	01:41	Kermadec Is.	185	5.1	-	1	-	-
13		19	03:01	Fiji Is.	507	4.8	-	1	-	-
14		19	06:06	Loyalty Is.	25	5.6	4.9	1	-	-
15		20	02:19	Santa Cruz Is.	71	5.0	-	3	-	-
16		20	12:53	Mariana Is.	193	3.8	-	4	-	-
17		20	15:10	Kermadec Is.	347	4.9	-	1	-	-
18		21	14:29	Bonin Is.	509	4.6	-	1	-	-
19		23	01:59	Loyalty Is.	100	5.8	-	1	-	-
20		23	12:00	Kuril Is.	40	6.0	5.8	4	3	3
21		24	15:46	Aleutian Is.	56	5.2	-	2	-	-
22		25	06:56	Honshu, Japan	325	4.8	-	4	-	-
23		25	07:16	Tonga Is.	33	5.9	5.7	1	-	-
24		25	07:22	Tonga Is.	33	5.7	-	1	-	-
25		25	20:07	Mariana Is.	33	4.9	4.4	1	-	-
26		26	04:51	Mariana Is.	40	5.2	5.1	5	-	-
27		26	16:32	New Britain	74	5.7	-	6	-	-
28		26	18:56	Honshu, Japan	230	4.4	-	3	-	-
29		28	09:04	Alaska	71	5.1	-	3	-	-
30		30	11:36	Fiji Is.	609	5.4	-	6	-	-
31		31	06:14	Komandorsky Is.	33	4.7	3.8	1	-	-
32	Sept.	1	07:23	Tonga Is.	33	5.8	5.7	4	-	-
33		1	09:29	Samoa Is.	25	7.0	7.7	6	-	-
34		1	18:38	Tonga Is.	33	5.7	5.3	3	-	-
35		1	23:55	Tonga Is.	33	5.6	5.4	3	-	-
36		2	08:44	Samoa Is.	33	5.3	5.5	1	-	-

Legend: h - event depth (km); m - body-wave magnitude; M - surface-wave magnitude; n - number of instruments in array which recorded body-wave phases P, Po, or So from this event; Po - number of Po arrivals from this event used in first-arrival study; So - number of So arrivals from this event used in first-arrival study.

No.	Date	Time	Location	h	m	M	n	Po	So
37	Sept. 2	09:24	Honshu, Japan	58	5.5	-	2	-	-
38	3	03:59	Hokkaido, Japan	52	4.7	-	4	-	-
39	3	04:29	Philippine Is.	93	5.8	-	4	-	-
40	3	05:35	Kuril Is.	45	6.6	6.6	10	6	8
41	3	19:39	Honshu, Japan	44	5.6	5.4	4	-	-
42	3	19:44	New Guinea	136	4.8	-	5	-	-
43	4	11:15	Philippine Is.	645	6.0	-	10	-	-
44	4	23:44	Solomon Is.	38	5.4	5.3	9	-	-
45	6	11:02	Loyalty Is.	31	5.9	6.2	1	-	-
46	7	15:11	Fiji Is.	231	5.2	-	3	-	-
47	7	16:20	Honshu, Japan	440	4.9	-	3	-	-
48	7	19:06	Honshu, Japan	33	5.8	5.5	7	6	5
49	7	20:07	Honshu, Japan	29	5.1	4.7	7	5	4
50	8	19:26	Kuril Is.	46	5.7	5.4	5	-	3
51	10	03:29	Solomon Is.	110	4.9	-	3	-	-
52	10	23:21	Mariana Is.	13	5.6	5.2	10	5	-
53	11	08:33	Fiji Is.	554	5.2	-	5	-	-
54	12	03:40	Fiji Is.	302	5.2	-	3	-	-
55	12	07:15	Kashmir	33	6.2	5.9	3	-	-
56	12	14:51	Hokkaido, Japan	111	4.9	-	7	-	-
57	12	16:14	Bonin Is.	33	4.6	-	2	-	-
58	13	01:20	Honshu, Japan	39	4.8	4.8	4	-	-
59	13	02:17	Eastern Kazakh	0	6.0	4.5	4	-	-
60	13	20:24	Honshu, Japan	87	4.9	-	3	-	-
61	14	15:08	Honshu, Japan	33	5.4	5.0	4	4	-
62	15	14:12	Banda Sea	102	5.9	-	2	-	-
63	15	20:43	Taiwan	167	4.9	-	3	-	-
64	17	06:19	Banda Sea	33	5.7	5.8	1	-	-
65	17	08:23	Loyalty Is.	30	5.7	6.6	2	-	-
66	17	12:42	Fiji Is.	356	5.2	-	10	-	-
67	17	21:12	Kamchatka	33	4.9	3.9	2	-	-
68	19	07:27	China	561	4.4	-	3	-	-
69	20	04:39	Honshu, Japan	33	4.4	-	2	-	-
70	22	06:55	Mariana Is.	33	4.2	-	6	-	-
71	24	17:20	Bonin Is.	33	5.7	5.3	5	3	2
72	25	03:25	New Guinea	116	4.8	-	1	-	-
73	25	10:21	Bonin Is.	33	4.4	-	2	-	-
74	25	14:30	Kermadec Is.	45	5.9	5.9	5	-	-
75	25	15:01	Honshu, Japan	25	5.5	6.1	2	-	-
76	28	03:36	Honshu, Japan	31	5.5	5.3	5	-	-
77	28	17:56	Kermadec Is.	323	6.0	-	5	-	-
78	29	23:02	Tonga Is.	226	5.1	-	5	-	-

Legend: h - event depth (km); m - body-wave magnitude; M - surface-wave magnitude; n - number of instruments in array which recorded body-wave phases P, Po, or So from this event; Po - number of Po arrivals from this event used in first-arrival study; So - number of So arrivals from this event used in first-arrival study.

No.	Date	Time	Location	h	m	M	n	Po	So
79	Sept. 30	07:04	New Guinea	123	5.4	-	4	-	-
80	30	23:03	Pacific Ocean	10	5.9	5.2	2	-	-
81	30	23:37	Hokkaido, Japan	52	4.9	4.9	2	-	-
82	Oct. 1	12:14	Novaya Zemlya	0	5.9	3.8	4	-	-
83	1	13:10	New Ireland	85	5.0	-	2	-	-
84	1	16:02	Kermadec Is.	33	5.6	5.1	5	-	-
85	1	17:04	Kuril Is.	33	5.9	5.7	5	4	4
86	1	19:00	S. Nevada	0	4.9	-	2	-	-
87	2	05:51	Savu Sea	109	4.6	-	4	-	-
88	2	15:13	Mariana Is.	113	5.0	-	5	-	-
89	3	07:21	Kuril Is.	75	5.1	-	4	-	-
90	3	08:26	Hokkaido, Japan	62	4.4	-	2	-	-
91	3	16:48	Philippine Is.	238	5.0	-	2	-	-
92	4	00:01	New Guinea	33	5.9	6.3	4	-	-
93	4	04:11	Honshu, Japan	38	5.2	5.0	4	-	2
94	4	10:18	Solomon Is.	58	5.1	-	2	-	-
95	4	10:27	Solomon Is.	24	5.7	5.4	5	-	-
96	5	04:28	China	534	4.7	-	2	-	-
97	6	07:40	Aleutian Is.	23	5.2	4.3	3	-	-
98	7	03:02	Fiji Is.	620	5.8	-	5	-	-
99	7	08:32	Solomon Is.	41	5.8	5.3	5	-	-
100	7	15:03	Samoa Is.	33	4.8	-	2	-	-
101	7	17:48	Philippine Is.	595	5.3	-	4	-	-
102	9	12:19	Solomon Is.	50	6.0	6.4	5	-	-
103	9	19:46	Mariana Is.	96	4.7	-	5	-	-
104	11	00:36	Minahassa Pen.	94	5.6	-	4	-	-
105	13	15:53	Kamchatka	112	5.3	-	3	-	-
106	14	12:29	Mariana Is.	205	5.0	-	5	-	-
107	14	20:09	Mariana Is.	131	4.9	-	5	-	-
108	15	01:47	Honshu, Japan	47	6.0	5.4	5	-	-

Legend: h - event depth (km); m - body-wave magnitude; M - surface-wave magnitude; n - number of instruments in array which recorded body-wave phases P, Po, or So from this event; Po - number of Po arrivals from this event used in first-arrival study; So - number of So arrivals from this event used in first-arrival study.

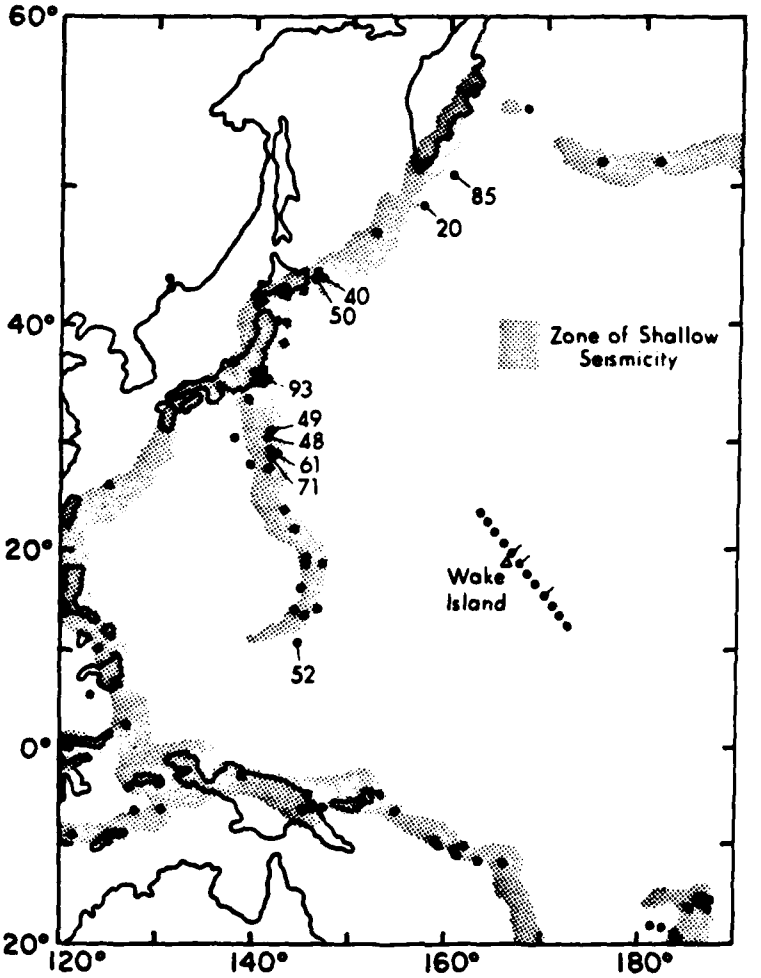

Figure 1. Map showing OBH locations and epicenters of earthquakes recorded by the array (see Table 1). Instruments operating from 12 August through 23 September are indicated by open circles. Those operating from 3 September through 15 October are indicated by closed circles. Three instruments which did not work properly are flagged. Event numbers (from Table 1) are indicated for epicenters of events specifically used in this study.

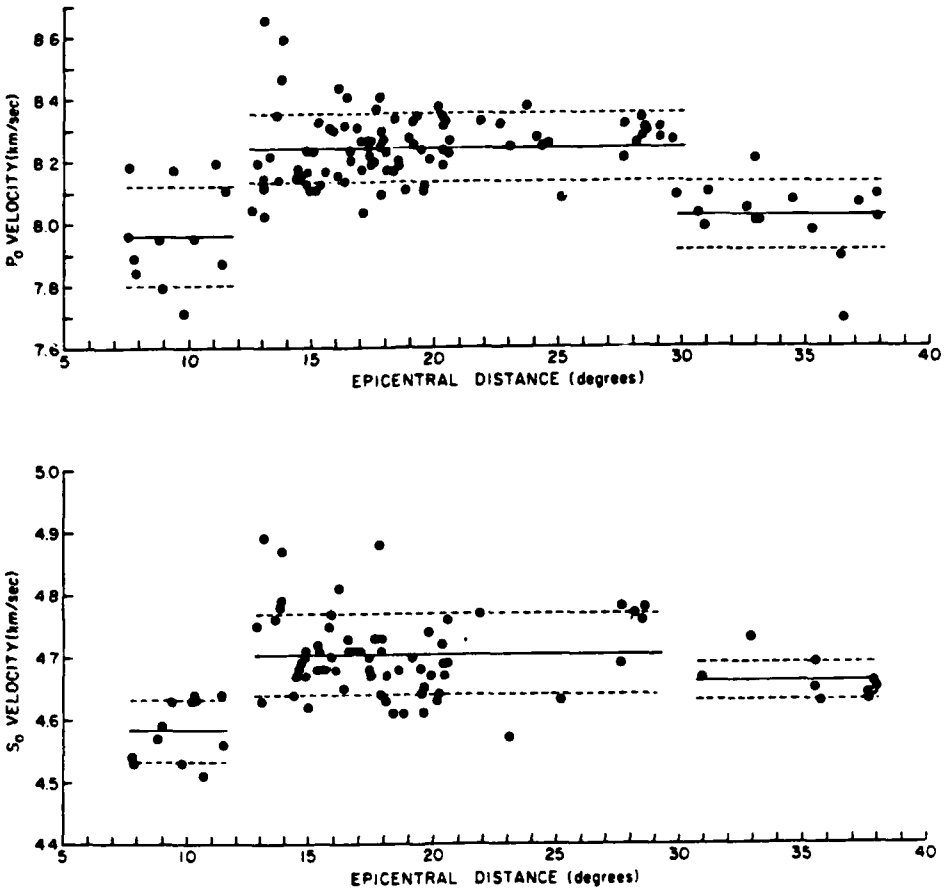

Figure 2. Apparent velocity (X/T) versus epicentral distance (X) for Po and So with Northwestern Pacific travel paths and focal depths of 100 km or less. Note the discontinuities at 12° and 30°. Solid and dashed lines represent the mean apparent velocity plus and minus one standard deviation over the three distance ranges. This plot is based on data compiled before the OBH experiment.

significant features of this plot are the lower apparent velocity values at distances less than 12° and greater than 30° in comparison to values within the 12° to 30° range. The large amount of scatter coupled with insufficient sampling near 12° and 30°, however, make the exact nature of these velocity transitions unknown. For the purpose of modeling, it is important to know if these transitions are smooth or abrupt, and might therefore represent a gradual increase in velocity with depth or a discontinuity in velocity at some depth.

Similar difficulties arise when attempting to use older data to estimate the attenuation of Po/So energy as a function of travel-time (or distance). The high frequencies and large signal/noise ratios observed would indicate that their attenuation must be significantly smaller than that of normal, mantle-refracted P or S phases at similar distances. However, these observations might also be due in part to a frequency-dependent Q combined with low noise levels at the higher frequencies (> 4 Hz) where Po/So are most prominent. Unfortunately, the mix of data (i.e., different earthquakes recorded at only single stations) make it hard to separate attenuation from other factors which influence the observed amplitudes such as magnitude, focal depth, epicentral distance, source orientation, and possibly azimuth.

To help clarify these uncertainties, an experiment was designed to record Po/So across a linear, 1500 km array consisting of 12 OBH's. The data provided by such an experiment would permit determination of Po and So phase velocities independent of the source parameters, thus hopefully eliminating the major source of scatter in velocity estimates. Data from the experiment would also facilitate a nearly direct measure of attenuation as a function of frequency and travel-time (only a spreading term would have to be assumed in order to determine the apparent Q). In addition, any other changes in the Po/So coda would for the first time be observed at several distances along approximately the same azimuth.

The array was aimed towards northern Japan and the southern-most islands of the Kuril chain (Fig. 1), and was positioned to provide data across the 30° transition zone previously described. This target was chosen because of its long history of moderate-to-large earthquakes and several successful recordings of Po/So phases from this region on the hydrophone installation at Wake Island. Of the events recorded by the OBH array in the Marianas through Kuril portion of the circum-Pacific arc, the largest (a 6.6 mb; event 40 in Table 1) occurred in the target area while all of the instruments were recording.

Po/So Propagation and Apparent Velocity

To confirm the assumption that much of the scatter in Fig. 2 can be attributed to errors in the epicenters and/or origin times of these single station data points (i.e., no more than one station recorded any given earthquake), a similar plot has been constructed for some of the OBH data (Fig. 3). Although this data as a whole exhibits scatter of about the same magnitude as that shown in Fig. 2, there is significantly less scatter within each subset of data representing individual events at several OBH's. Thus, the larger source of scatter may be attributed to apparent velocity differences between events; and a strong possibility is that these

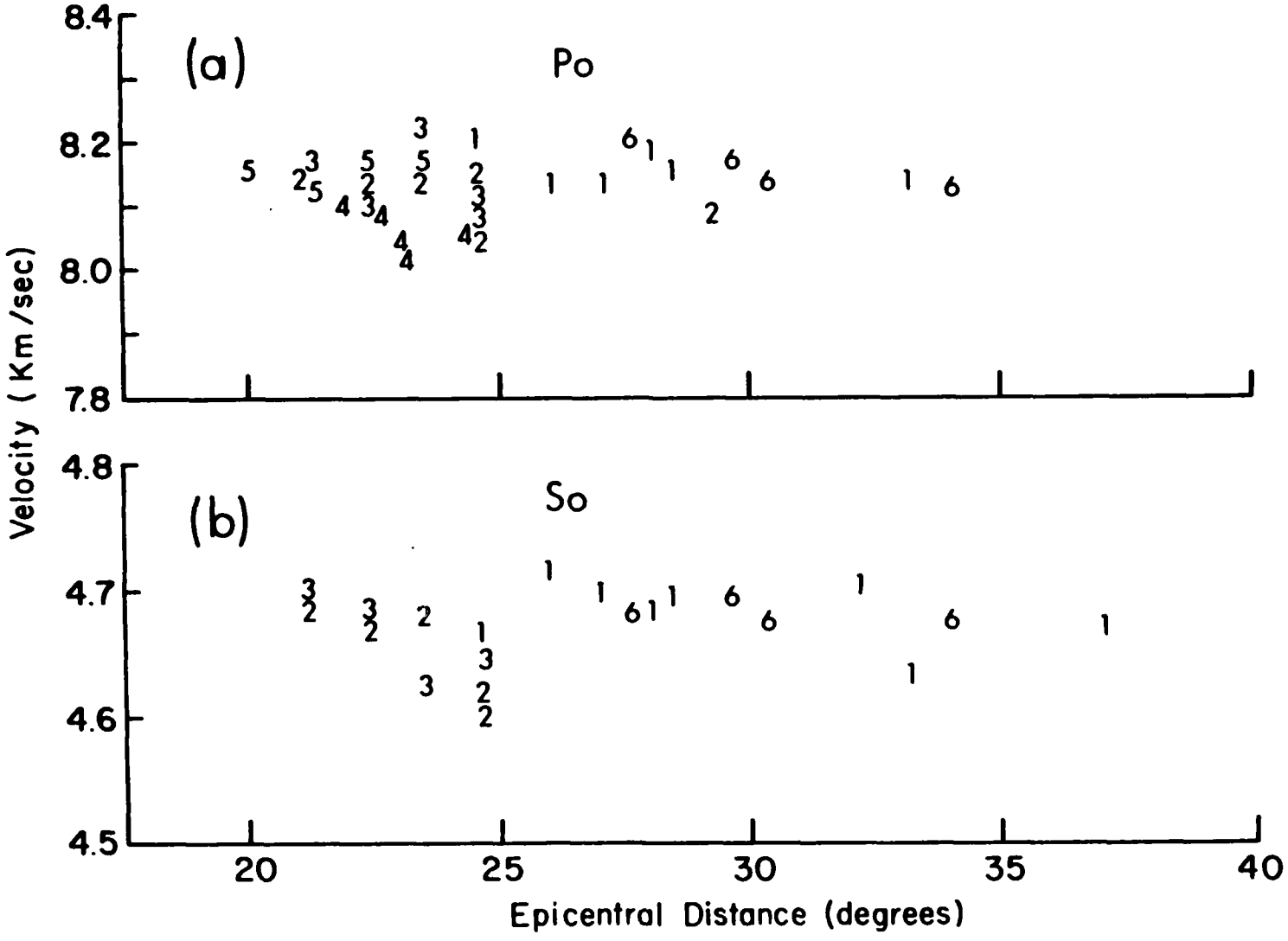

Figure 3. Apparent velocity (X/T) versus epicentral distance (X) for some of the Po and So data collected during the OBH experiment. Data points numbered 1 through 6 represent each set of first arrivals recorded across the OBH array from events 40. 48. 49. 52 61. and 85. respectively. Note that the scatter of each subset is less than the scatter of the combined data.

differences are a result of errors in NEIS origin times and hypocenter locations. The remaining scatter within each subset may be the result of: (1) uncertainty in the time of onset, (2) OBH location errors, (3) OBH clock correction errors, and/or (4) local differences in crustal and sediment structure between OBH's. Unfortunately, the magnitude of this remaining scatter is enough to cause an unacceptable level of uncertainty in the propagation velocity of Po or So for any given event. An uncertainty of 1 sec in travel-time over 500 km of the array at a phase velocity of 8.0 km/sec will produce an uncertainty of 0.13 km/sec in the determination of that phase velocity, as well as an uncertainty of 5.0 sec in the travel-time intercept for data taken at an average epicentral distance of 2500 km. To reduce this uncertainty, a method was sought to determine propagation velocity and travel-time intercept by combining the first arrival data of all the events in a way which would have the following important properties: (1) propagation velocity would be determined from the differences in travel time between OBH's for a given event and would be independent of the NEIS origin time published for the event; (2) events recorded on more instruments would be weighted more heavily; (3) events recorded over a larger range of epicentral distance would also be weighted more heavily; and (4) the travel-time - epicentral distance relationships within the data set of each individual event would be maintained. The following method satisfactorily meets those requirements.

Using only those events with focal depths of 100 km or less, having Northwestern Pacific Basin travel paths, and recorded with distinct onsets at two or more stations (see Table 1), the raw epicentral distance and travel time data were computed using NEIS epicenters. For each subset of data associated with a single event, the mean epicentral distance and travel time was computed and subtacted from the raw data for that event to yield zero-meaned data for each event, as well as for the data as a whole. From these combined data the slope of the travel-time line could be computed, but the intercept would be lost (it would be exactly zero). Consequently, the mean for all of the raw epicentral distance and travel-time data was computed and added to each point of the zero-meaned data set to restore the intercept. The travel-time lines computed from these data, and shown in Fig. 4, represent the best available estimates of Po/So velocities at distances between about 2400 and 3400 km. These values (i.e., inverse slopes) are 7.96 ± 0.05 km/sec and 4.57 ± 0.04 km/sec for Po and So, respectively. The large negative intercepts found, -7.14 ± 2.38 sec and -14.03 ± 5.31 sec for Po and So respectively, imply that the first arriving energy propagates at a higher velocity than indicated by the inverse slopes over some portion of the travel path nearer to the source than where the observations were made.

In Fig. 5, we have superimposed Po/So data from the Wake OBH experiment (solid triangles) on Fig. 2. It is obvious that these data do not support the discontinuity in apparent velocity at 30° which was a feature of the older data; but they appear, instead, to describe a smooth transition across this boundary. A re-examination of the older data, especially those data points near the offset, was made to determine if the cause of this discrepancy could be found. Consequently, the original computer cards used to calculate epicentral distances for data collected in 1963 and 1964 were found to contain systematic errors in the coordinates of some recording sites. The formerly classified status of these sites and

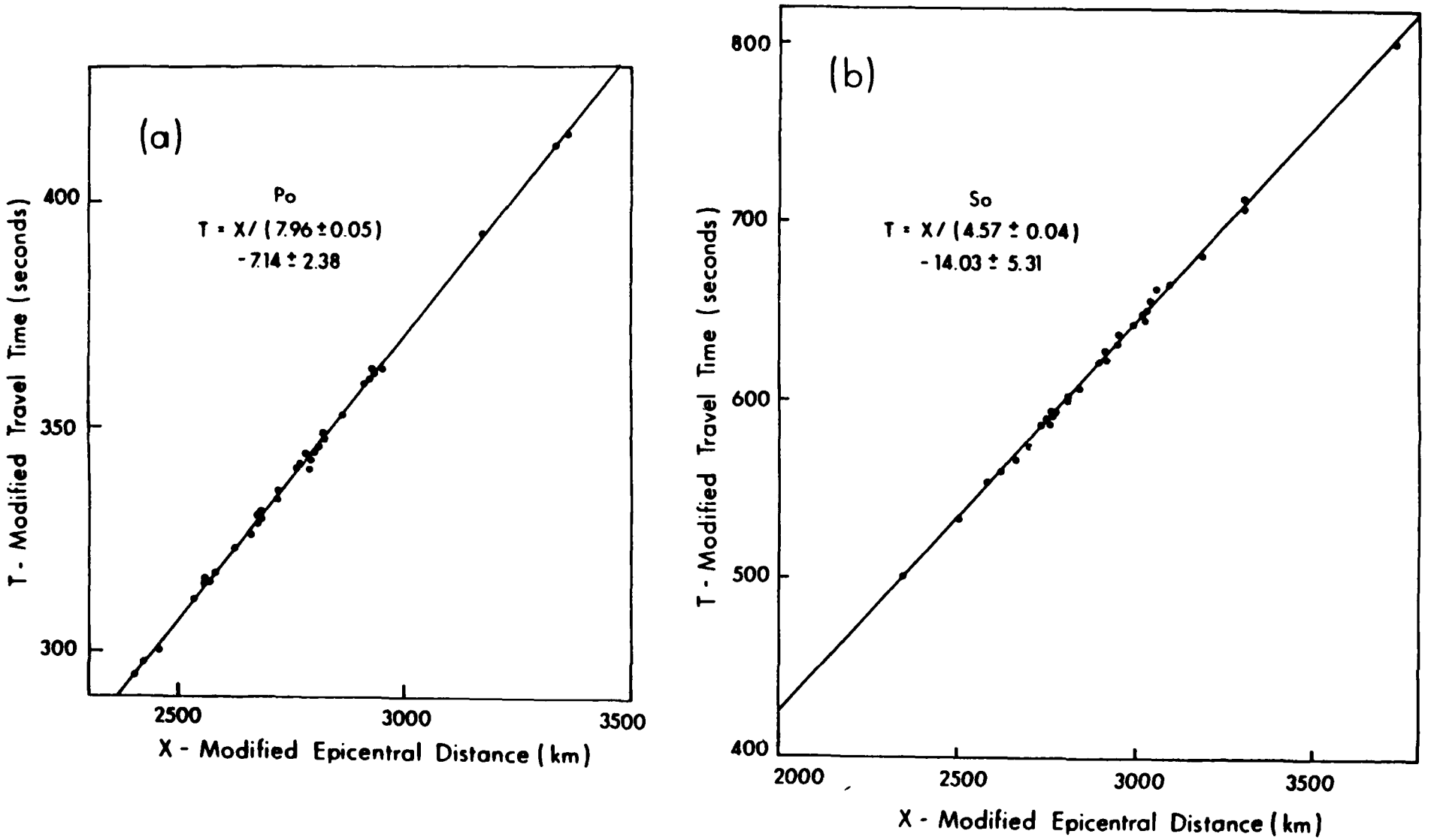

Figure 4. Modified travel-time plots for Po and So as described in the text.

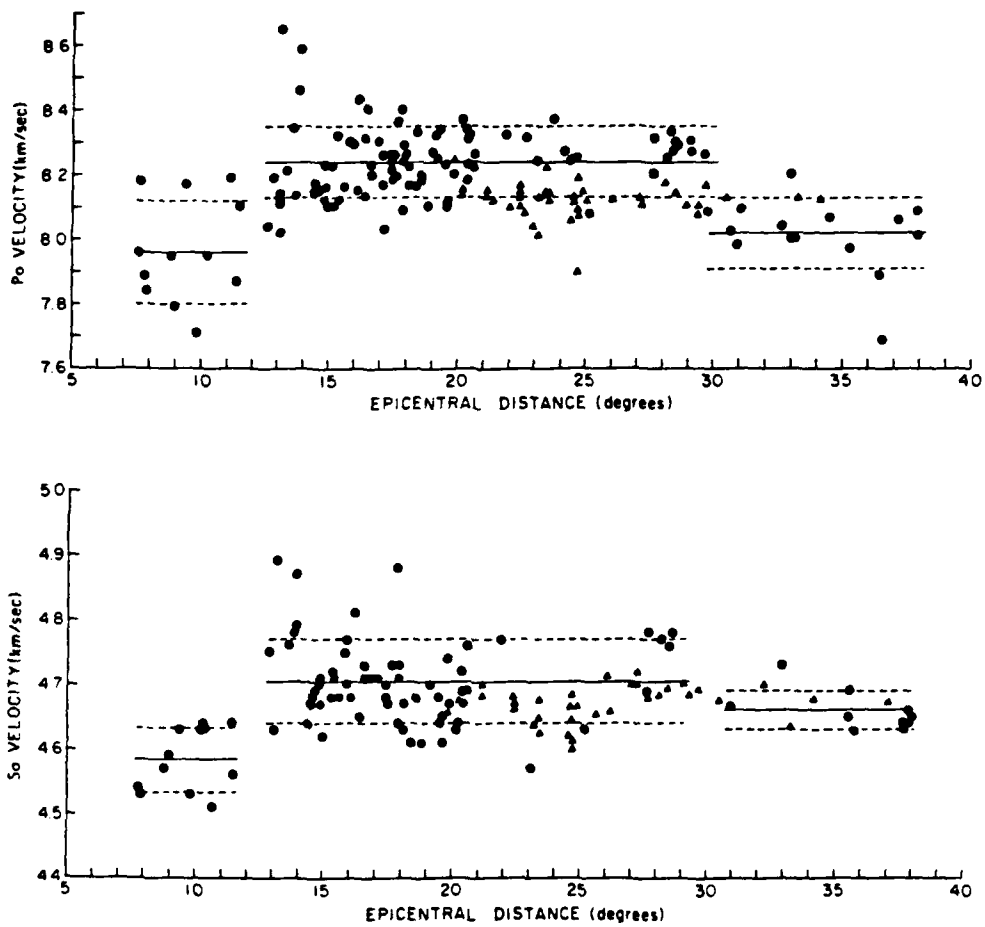

Figure 5. Po and So data from the OBH experiment (solid triangles) superimposed on Fig. 2a and Fig. 2b, respectively. Note that these data do not support a discontinuity in apparent velocity at 30°.

the circuitous route by which these coordinates had been previously obtained may be an explanation for these errors. The erroneous data have been plotted as open circles and the corrected data as solid circles (along with the rest of the older data) in Fig. 6. Also plotted in Fig. 6 (as open triangles) are some additional hydrophone data from the analog cassette recording system at Wake, collected since 1978. It is clear from this comprehensive data set that an apparent velocity discontinuity at 30° is no longer supported by the data. Instead, a gradual decrease of apparent velocity with distance is observed between about 12° and 38° for both Po and So. This characteristic of apparent velocity is entirely compatable with the inverse slope propagation velocity and intercept values computed from the OBH data and shown in Fig. 4.

To illustrate this compatability, the travel-time equations have been converted into relationships between apparent velocity and epicentral distance as follows:

$$T = X/V + I$$

Travel-time equation where T is travel-time, X is epicentral distance, V is propagation velocity, and I is the travel-time intercept.

$$A = X/T = X/(X/V + I)$$

Apparent velocity equation where A is the apparent velocity.

$$S_A^2 = \frac{(X/V+I)^2 V^4 S_X^2 + X^4 S_V^2 + X^2 V^4 (S_I^2+S_0^2)}{V^4 (X/V+I)^4}$$

Mean-squared error in apparent velocity, S_A^2, resulting from errors in: the propagation velocity, S_V; the travel-time intercept, S_I; the epicentral distance, S_X, due to epicenter errors; and the observed travel-time, S_0, due to errors in origin-time.

Plotted in Fig. 7 are A, and A $\pm$ S_A versus epicentral distance, X. Values for V, S_V, I, and S_I are those given in Fig. 4; S_X is 10 km; and S_0 is 1 sec. Values used for S_X and S_0 are reasonable for epicenter/origin-time data taken from the NEIS listings, and these lists have been used for all of the data in the figure. The figure shows that approximately one standard deviation of the data (ie. 68 percent for normally distributed

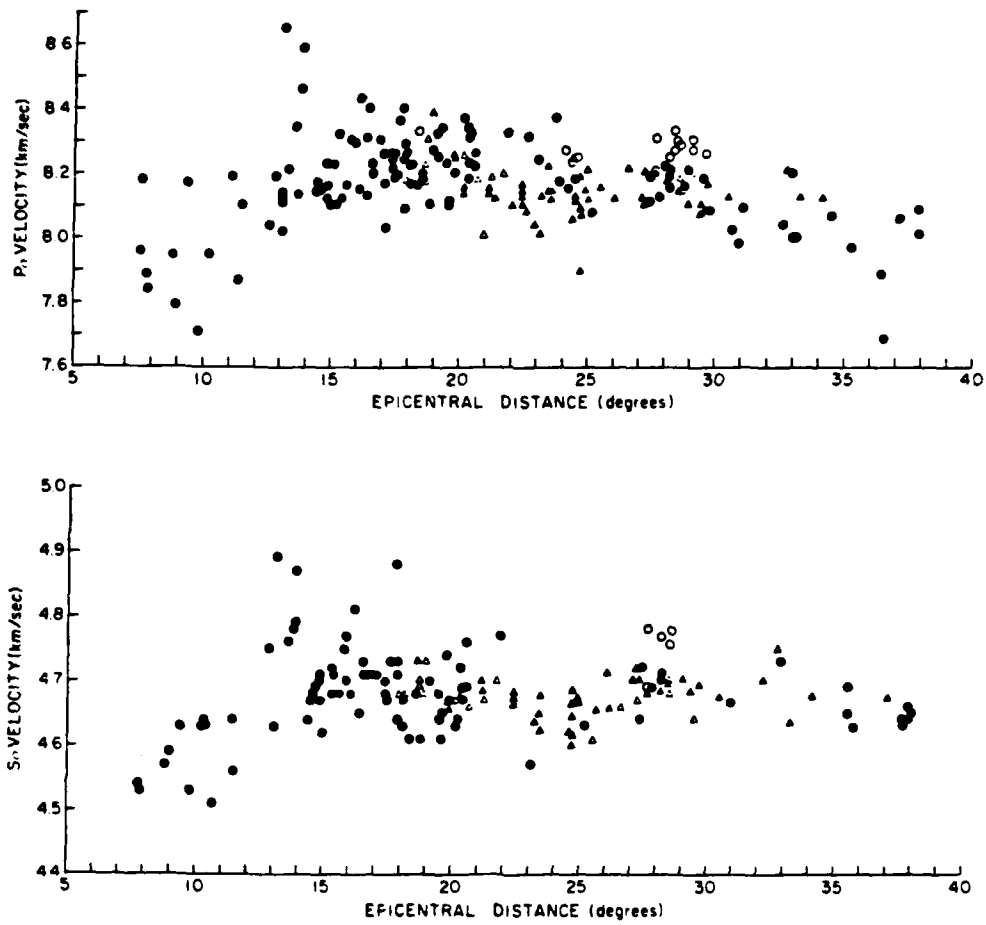

Figure 6. This figure is the same as Fig. 5 except that: (1) erroneous data from 1963 and 1964 (open circles) have been replotted as closed circles; and (2) addition hydrophone data from Wake. collected since 1978. are plotted as open triangles.

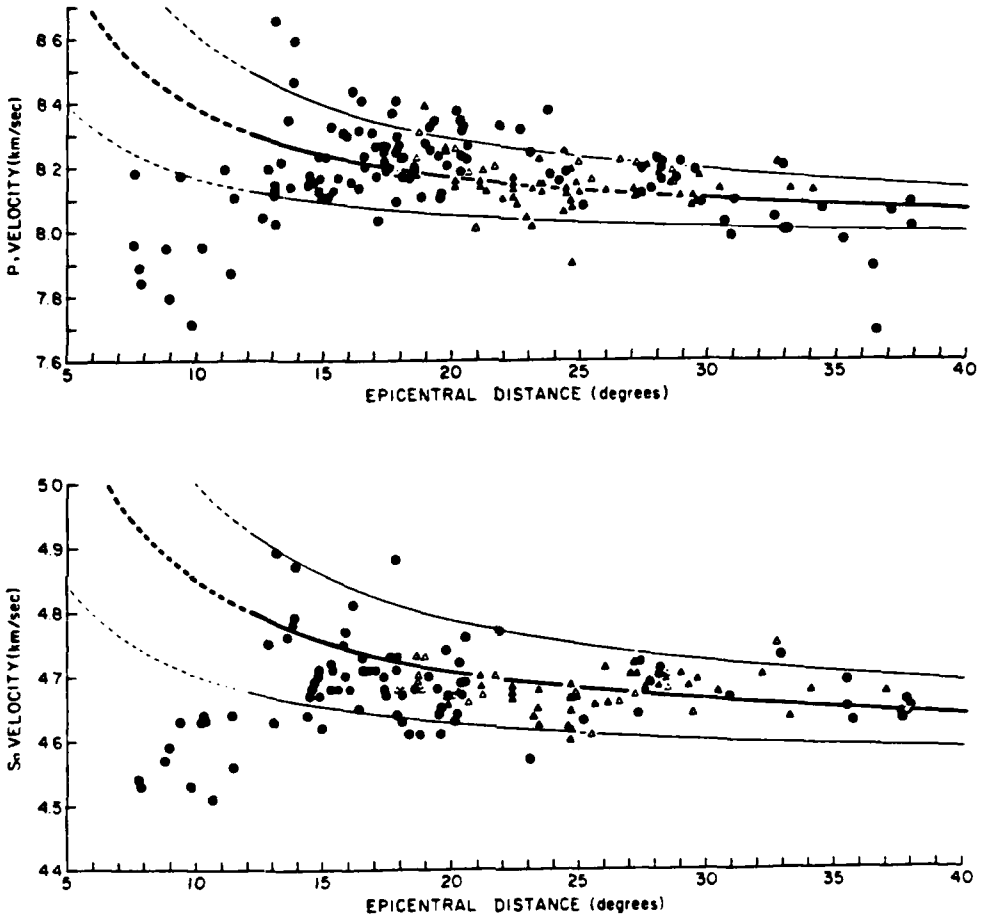

Figure 7. This figure contains the data from Fig. 6. representing all of the Po and So first arrival data from shallow-focus events with Northwestern Pacific Basin travel paths collected by HIG since 1963. Superimposed on these data are curves representing the Po and So travel-time equations (Fig. 4). with plus and minus one standard deviation. determined strictly from the OBH data.

Note that most of the data beyond 12^{o} epicentral distance falls within the bounds described by these curves.

data) falls within the bounds of A S_A. It is concluded, therefore, that the first arrival times of Po and So phases from shallow-focus (i.e., focal depths less than 100 km) earthquakes occuring along the margin of the Northwestern Pacific Basin with travel paths greater than 12° epicentral distance across the Northwestern Pacific Basin, may be successfully modeled by the travel-time equations given in Fig. 4.

An important question which remains to be answered is: By what methods of generation and propagation are the first arrivals on both sides of the 12° apparent velocity discontinuity produced? In spite of those modeling efforts mentioned previously, which have successfully reproduced certain aspects of Po/So travel-time and coda, no model as yet exists which addresses this question or reproduces the observations which led to this question. A hypothesis proposed here, which seems to contain some credibility, is that energy observed at less than 12° has propagated from near the source to near the receiver entirely within the waveguide (i.e., up the descending lithosphere and across the plate), while first-arriving energy observed at greater than 12° has propagated along a higher velocity, or deeper, P or S type path over distances less than 12° before coupling into the waveguide at a distance greater than 12°. (The term "waveguide" refers here to the structure within which Po/So energy propagates at the constant velocity value given in Fig. 4.) Evidence which supports this hypothesis is: (1) the apparent velocity data observed for Po and So at distances less than 12° could reasonably be fit by a zero-intercept linear travel-time equation with a propagation velocity equal to the propagation velocity found for the data beyond 12° (This would imply that the propagation velocity and thus the structure of the waveguide are continuous across 12° - an intuitively pleasing result.); and (2) the apparent velocities for shallow-focus P and S at 12° (from Jeffreys and Bullen, 1958) are near those required for P and S to couple into the Po/So waveguide and produce the observed arrival times beyond 12°. Although a propagation mechanism of this type might fit the data quite well, a velocity model of the oceanic crust and upper mantle which produces this phenomena has not been found. It is probable that such a velocity model would contain lateral heterogeneities associated with the downgoing slab in order to propagate energy between 0°and 12° with an average velocity greater than the waveguide velocity, and still couple this energy into the waveguide. This requirement is not easy to satisfy (and may be impossible to satisfy) with a radially symmetric velocity model.

One test of this proposed hypothesis could be made by examining Po/So arrivals from earthquakes with depths greater than 100 km. Po/So energy has been observed and recorded by HIG for many earthquakes with focal depths greater than 100 km and up to 600 km. Energy which has propagated along a P or S type path before coupling into the waveguide should contain a depth dependence in travel-time, coda, and/or frequency content. The precise nature of such a dependance would serve to either confirm or deny the hypothesis, or to generate a new one.

Attenuation of Po and So

As stated earlier, one of the more remarkable features of Po/So is their high-frequency content; therefore, a major goal of Po/So research in recent years has been to quantify those properties within the earth in terms of Q which permit the efficient transmission of these frequencies over great distances. When a frequency-independent model for Q was fit to some older Po/So data with frequencies between about 2 and 10 Hz, the resulting Q values were greater than 5000 in most cases (Walker et al., 1978 and Sutton et al., 1978). These values are much higher than those generally found for upper mantle travel paths using P and S data at frequencies below 2 or 3 Hz. A frequency-dependent Q, however, might satisfy both sets of observations. Sutton et al. (1983) found two methods for extracting a relationship between Q and frequency from single-station Po/So data. They found that Q was approximately proportional to frequency over the range 2-9 Hz and that the Q of So was higher than the Q of Po for any given frequency.

Data collected during the OBH experiment provided, for the first time, the opportunity to observe Po/So energy propagating across a large array of instruments. Although Po/So phases from numerous events were recorded, the magnitude 6.6, Kuril Is. event noted earlier (event 40, Table 1) was especially well suited for a study of attenuation. Its large magnitude and its location in the area targeted by the array produced Po/So phases which travelled down the axis of the 1500 km deployment line with sufficient energy to be observed with high signal/noise ratios on many of the instruments.

Fig. 8 shows the spectra of the Po and So coda from the Kuril event at five epicentral distances corresponding to the five OBH's that were used. These spectra have been computed from a series of contiguous 512 point FFT's taken on the time series data which was digitized at 80 samples per sec. The spectral energy has been summed over an apparent velocity window extending from 8.2-7.0 km/sec and from 4.7-4.0 km/sec for Po and So, respectively, and has also been summed over a 1 Hz band at any given frequency. Instrument response has not been removed; however, the response of each individual OBH is presumed to be identical so that intercomparison of the spectra is valid. Only signal levels which were at least 4 dB above background noise levels, at any given frequency, have been plotted. A correction for cylindrical spreading has also been applied to these spectra so that the losses observed in the figure represent attenuation due to anelasticity, scattering, tunneling, and/or any mechanism other than cylindrical spreading. Note that in general the energy level falls off at a constant rate with distance, regardless of frequency. Also note that the attenuation of So with distance is about the same as that for Po.

A general expression for the observed amplitude of seismic signals of this type is:

$$A(f) = A_0(f) r^{-b} e^{-\pi f p q(f)[r-1]}$$

where $A(f)$ is the observed signal amplitude at a given frequency,
$A_0(f)$ is the source amplitude ($r=1$) at a given frequency,
f is the given frequency,

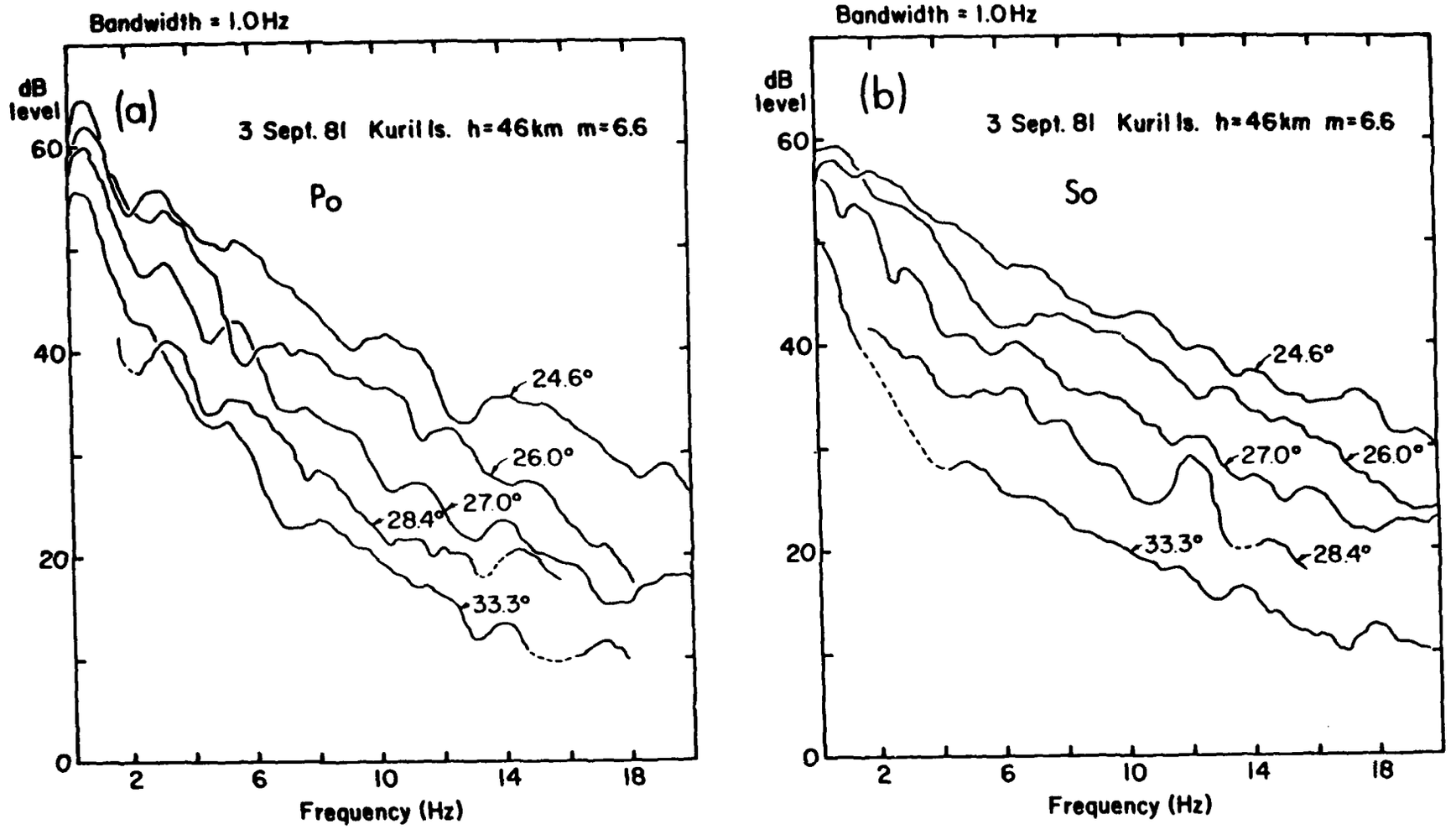

Figure 8. Spectra of Po and So from a large event in the Kuril Is. observed at five epicentral distances corresponding to five OBH's. Spectral energy has been summed over the apparent velocity ranges 8.0 - 7.2 km/sec and 4.7 - 4.0 km/sec for Po and So, respectively. The effect of cylindrical spreading, amounting to only 1.3 dB between 24.6° and 33.3°, has been removed from the data. Only signal levels at least 4 dB above ambient noise levels have been plotted. Dashed portions of the spectra are for continuity only, and do not represent actual data at those frequencies.

r is the epicentral distance,
b is the spreading parameter (0.5 for cylindrical spreading; 1.0 for spherical spreading),
p is slowness (i.e., travel-time/epicentral distance),
and $q(f) = Q(f)^{-1}$ is the apparent anelastic attenuation coefficient.

Conversion of the observed amplitude into decibels gives:

$$20\log_{10}A(f) = 20\log_{10}A_0(f) - 20b\log_{10}(r) - 20\pi fpq(f)[r-1]\log_{10}(e)$$

Rearranging terms and differentiating with respect to r gives:

$$\frac{d(20\log_{10}A(f) + 20b\log_{10}(r))}{dr} = -20\pi fpq(f)\log_{10}(e)$$

Therefore:

$$Q(f) = q(f)^{-1} = \frac{-20\pi fp\log_{10}(e)}{\frac{d(20\log_{10}(A(f)r^b))}{dr}}$$

Each curve plotted in Fig. 8 represents $20\log_{10}[A(f)r^{0.5}]$ at a given r for a range of frequencies. At any given frequency, we know $20\log_{10}[A(f)r^{0.5}]$ at several r's and can thus determine $\frac{d\{20\log_{10}[A(f)r^{0.5}]\}}{dr}$ by simple linear regression. All other quantities in the equation for Q(f) are known. Q(f) has thus been found for data sampled in one Hertz bands, and these values are plotted in Fig. 9. Although cylindrical spreading (b = 0.5) has been assumed, the spreading term plays only a minor role in these calculations. A choice of spherical spreading would raise the values of Q(f) by no more than about 10 percent. Only frequencies where data exist at all five distances have been used. The standard deviations shown include contributions from the error in the determination of $\frac{d\{20\log_{10}[A(f)r^{0.5}]\}}{dr}$, the error in slowness which is due to sampling the data over a range of slownesses, and the error in frequency due to sampling over a 1 Hz band. This method gives values for Q(f) roughly proportional to frequency, and gives higher values of Q(f) for So relative to those for Po at any given frequency. These results are consistent with those found by Sutton et al. (1983) mentioned earlier, although the absolute levels for Q(f) are lower at any given frequency in this study. The relationship between the Q(f) values of Po and So, $Q_\beta(f) >= 1.4Q_\alpha(f)$, is markedly different from the relationship $t^*_\beta = 4t^*_\alpha$, which implies $Q_\beta(f) = 0.44Q_\alpha(f)$, found by others (see for example Cormier, 1982).

The nature of the Q(f) values suggests that a simpler mathematical model might be used to describe the attenuation of Po/So. This is because

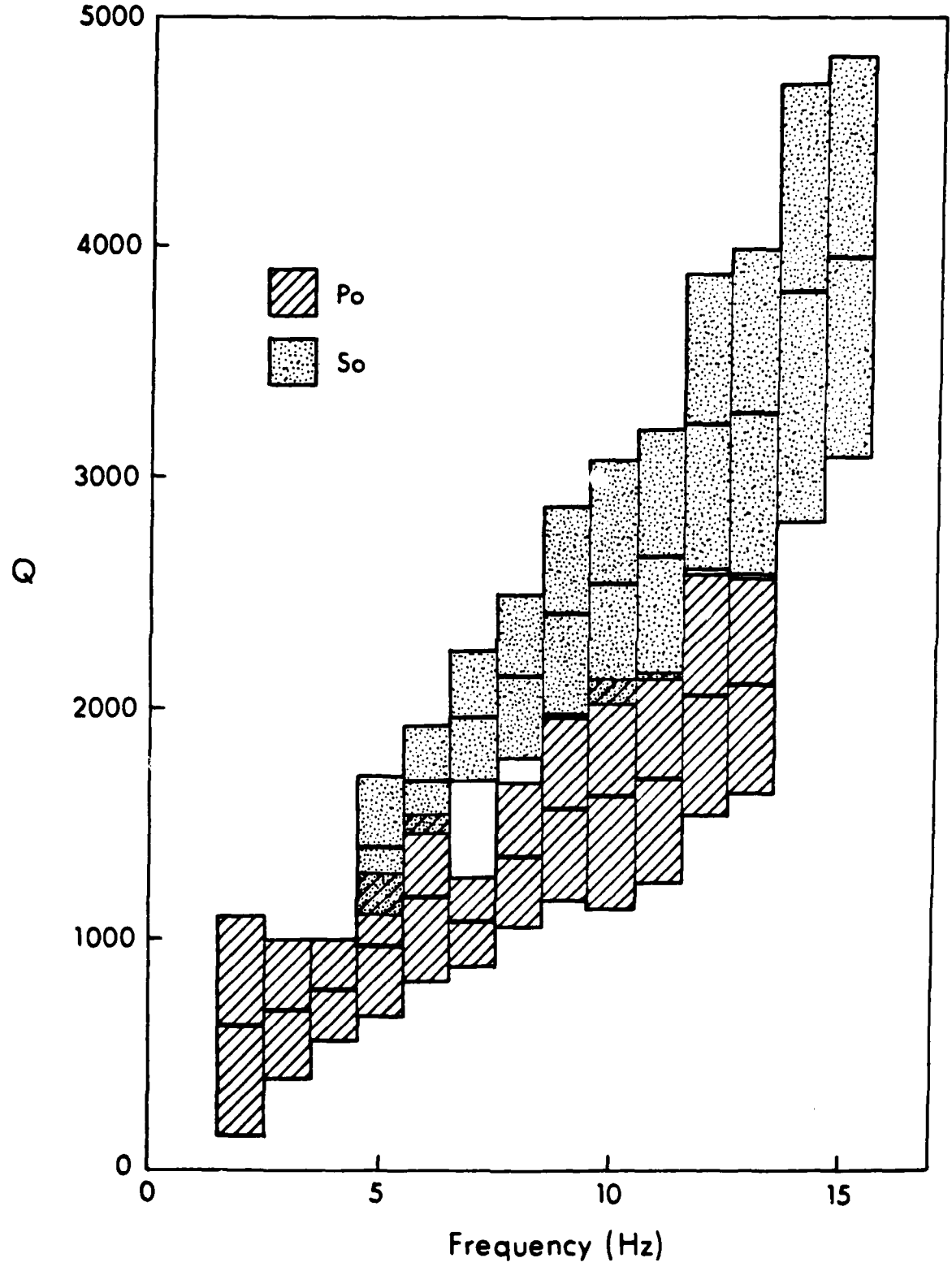

Figure 9. Values for Q(f) plus and minus one standard deviation as explained in the text are plotted versus frequency for both Po and So.

values for fpq(f) are approximately the same for any given frequency and slowness (ie., Po or So). Thus, the form of this model is: $A(f) = A_0(f)r^{-b}e^{-a(r-1)}$, where "a" is the coefficient of attenuation. In this expression, the change in signal amplitude over some propagation distance is not a function of frequency or slowness as in the previous expression containing "q". By a method similar to that described earlier it can be shown that: $-20a\log_{10}(e) = \frac{d\{20\log_{10}[A(f)r^{0.5}]\}}{dr}$, where $-20a\log_{10}(e)$ equals the decibel change in amplitude, after a cylindrical spreading correction, per unit propagation distance. The right-hand side of the above equation may be evaluated by linear regression, using the set of values for $20\log_{10}[A(f)r^{0.5}]$, which can be computed from the observed values for A at a given r (and for a given frequency band), versus r. Values for $-20a\log_{10}(e)$ have been computed and tabulated in Table 2. The same data set used to determine the Q(f) values discussed previously has been used to compute values in the table. With the exception of two lower values for Po at 2 Hz and 3 Hz and the slightly higher average values for Po relative to So, it could be said that the data generally support the assumption that "a" is nearly a constant value for both Po and So at any of the frequencies examined.

All of the data can be combined by a zero-meaning method, similar to that described for combining the *first arrival data*, to yield a single value for $-20a\log_{10}(e)$. These modified data are shown in Fig. 10, and the regression line fit to them has a slope of -21.5 ± 0.9 dB per 1000 km of travel path. Also shown are regression lines fit to the subsets of Po and So data which have slopes of -19.7 ± 1.4 and -23.6 ± 1.1 dB per 1000 km, respectively. Differences between the Po and So values reflect those differences observed in Table 2. Note that all of the data lie at five distances corresponding to the five OBH's. Also note that the data points at each distance do not cluster about the central regression line, but tend to cluster about some value away from the line. It is possible that these shifts, amounting to a few dB at most, are due to differences between individual OBH responses. These differences may exist because of complexities in processing the slow-speed cassette tapes, and uncertainties in the absolute calibration of the individual hydrophones. Computation of new regression lines, under the assumption that the data of each OBH contain a constant but unknown bias, and under the condition that the sum of the squares of the biases are minimized, results in exactly the same regression lines shown in the figure with somewhat smaller variances. This result is due to the mathematics, and not to any unique property of the data.

Conclusions

Data collected by a 1500 km OBH array deployed for two months in the Northwestern Pacific Basin near Wake Island has provided important new information about the propagation of Po/So phases. Using this array, propagation velocities of first arrivals from shallow-focus (<100 km)

Table 2. Attenuation of Po and So as a Function of Frequency and Propagation Distance

f	Attenuation (dB/1000 km)	
(Hz)	Po	So
2	-11.5 ± 8.4	- -
3	-15.4 ± 6.1	- -
4	-18.5 ± 4.7	- -
5	-18.4 ± 5.6	-22.4 ± 4.3
6	-18.3 ± 5.4	-22.3 ± 2.6
7	-23.4 ± 3.8	-22.3 ± 2.8
8	-21.1 ± 4.6	-23.4 ± 3.4
9	-20.6 ± 5.1	-23.4 ± 4.1
10	-22.1 ± 6.7	-24.7 ± 4.8
11	-23.4 ± 6.0	-25.9 ± 4.9
12	-21.0 ± 5.2	-23.3 ± 4.3
13	-22.2 ± 4.8	-24.8 ± 5.1
14	- -	-23.1 ± 5.2
15	- -	-23.8 ± 5.0

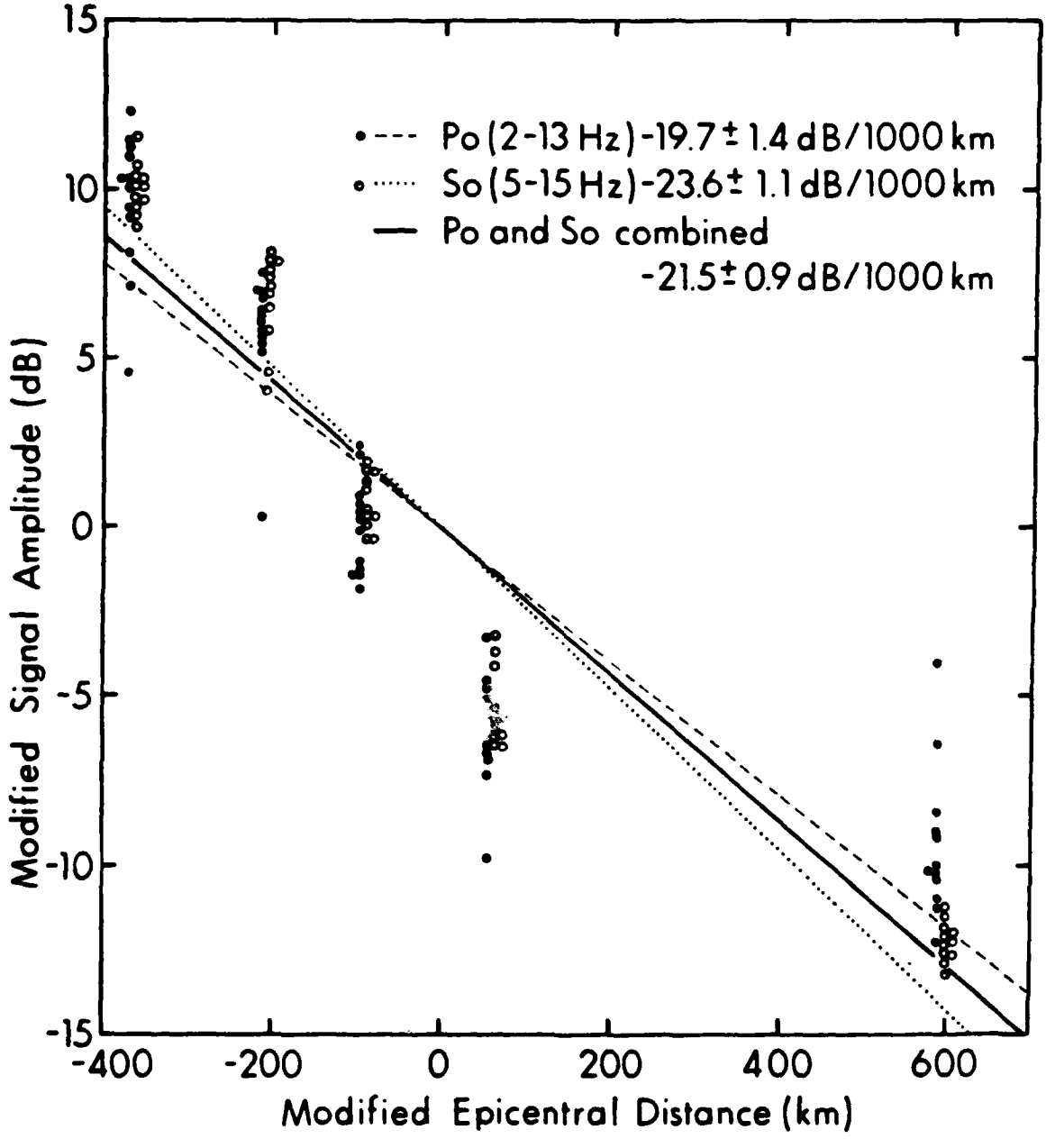

Figure 10. Spectral amplitudes at each frequency studied (Po: 2-13 Hz and So: 5-15 Hz) are plotted versus epicentral distance after modification by zero-meaning as explained in the text. The five data clusters represent the five OBH's used. Note that the data of both Po and So, at all frequencies, follow the same general trend, which is attenuation as a function of distance. For reference, attenuation as a function of distance at each individual frequency in Po and So is listed in Table 2.

events have been measured by a more accurate method than was previously possible using single station data. The velocities found are 7.96 ± 0.05 km/sec and 4.57 ± 0.04 km/sec for Po and So, respectively.

measured at epicentral distances between 18°(2000 km) and 33°(3700 km). Associated with these propagation velocities in the linear travel-time equation are intercepts equal to -7.14 ± 2.38 sec and -14.03 ± 5.31 sec for Po and So, respectively. These large negative intercepts imply higher propagation velocities over some part of the travel path nearer to the source than where the data were recorded. Travel times of all Po/So first arrivals collected by HIG since 1963, from shallow-focus events with

Northwestern Pacific Basin travel paths greater than 12° epicentral distance, are successfully modeled by the linear travel-time equation: $T=X/V + I$, using those values for V (propagation velocity) and I (travel-time intercept) reported here. Data at epicentral distances less

than 12° (collected prior to this experiment) appear to follow a different Po/So travel-time branch than the one described by the OBH data. The exact nature of this branch is not clear due to deficiencies in the quantity and quality of this data. Additional insight into this transition may be found through the examination of Po/So arrivals from numerous deeper-focus events (up to 600 km focal depth) which have been recorded but not yet studied. The OBH data have also been used to directly measure the attenuation of Po and So. An event which occured in the Kuril Islands (mb=6.6, h=45 km) and generated Po and So arrivals which propagated almost exactly down the axis of the array, was used to quantify attenuation in terms of a frequency-dependent Q. Values found for Q(f) range from 625 ± 469 at 2 Hz to 2106 ± 473 at 13 Hz for Po, and from 1401 ± 296 at 5 Hz to 3953 ± 863 at 15 Hz for So. This attenuation may be more simply described in terms of the single value -21.5 ± 0.9 decibels per 1000 km of travel path, which in general applies to all the frequencies studied in both Po and So.

AD-A137 778 SPECTRAL ANALYSES OF HIGH-FREQUENCY PN SN PHASES FROM VERY SHALLOW FOCUS EARTHQUAKES(U) HAWAII INST OF GEOPHYSICS HONOLULU D A WALKER SEP 83 AFOSR-TR-84-0059 2/2

UNCLASSIFIED F49620-81-C-0065 F/G 8/11 NL

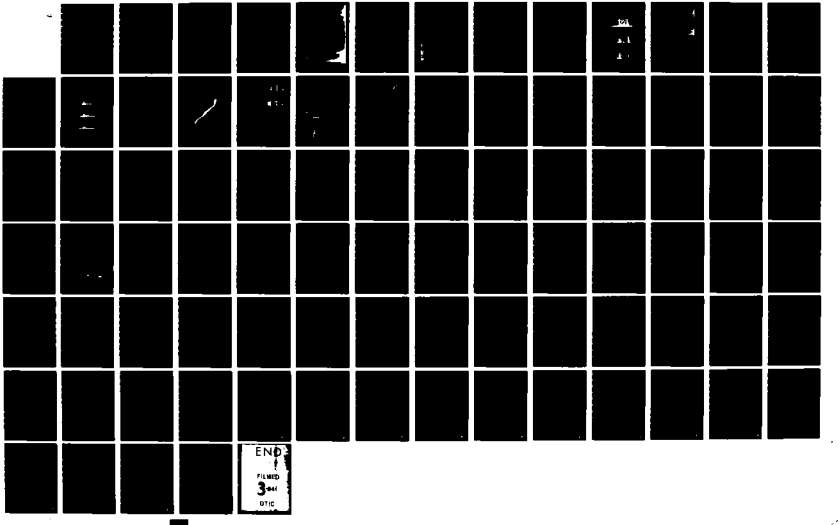

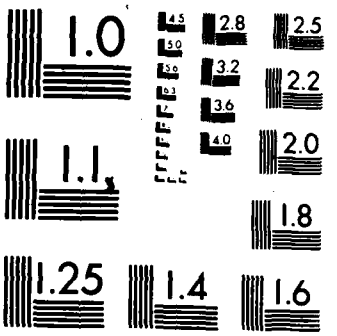

MICROCOPY RESOLUTION TEST CHART
NATIONAL BUREAU OF STANDARDS-1963-A

Acknowledgements. This research was supported by the Office of Naval Research (code 425GG). Funds for support of the hydrophone station at Wake Island were provided primarily by the Air Force Office of Scientific Research under Contract No. F-49620-81-C-0065. with supplementary support from the U.S. Arms Control and Disarmament Agency. The authors express thanks to Dave Byrne. Grant Blackinton. Bob Mitiguy. Dave Barrett. and Fred Duennebier for their help in modifying, testing. launching, and recovering the OBH's. Appreciation is also expressed to Al David and Kentron Corporation for their part in maintaining the recording station at Wake. The authors also thank George Sutton for reviewing this manuscript. and Rita Pujalet for editorial assistance. Hawaii Institute of Geophysics Contribution No. 0000.

References

Cormier, V., The effect of attenuation on seismic body waves. Bull. Seismol. Soc. Am., 72. S169-S200. 1982.

Gettrust, J., and L. Frazer. A computer model study of the propagation of the long-range Pn phase. Geophy. Res. Lett., 8, 749-752. 1981.

Jeffreys. H., and K. Bullen. Seismological Tables. Office of the British Association, Burlington House. London. 1958.

Menke. W., and P. Richards. Crust-mantle whispering gallery phases: a deterministic model of teleseismic Pn wave propagation. J. Geophys. Res., 85. 5416-5422. 1980.

Stephens. C., and B. Isacks. Toward an understanding of Sn: normal modes of Love waves in an oceanic structure. Bull. Seismol. Soc. Am., 67. 69-78, 1977.

Sutton. G., and D. Harvey. Complete synthetic seismograms to 2 Hz and 1000 km for an oceanic lithosphere (abstract), EOS Trans. AGU. 62. 327. 1981.

Sutton. G., C. McCreery. F. Duennebier. and D. Walker. Spectral analyses of high-frequency Pn, Sn phases recorded on ocean bottom seismographs. Geophys. Res. Lett., 5. 745-747. 1978.

Sutton. G., P. Pomeroy, J. Carter. and C. McCreery. Short period guided waves over oceanic and continental paths. DARPA Annual Program Review. 1983.

Walker, D., High-frequency Pn, Sn velocities: some comparisons for the Western. Central, and South Pacific, Geophys. Res. Lett., 8, 207-209, 1981.

Walker. D., Oceanic Pn/Sn phases: a qualitative explanation and reinterpretation of the T-Phase. Hawaii Inst. of Geophysics Rept. HIG-82-6. 1982.

Walker. D., C. McCreery. G. Sutton. and F. Duennebier. Spectral analyses of high-frequency Pn and Sn phases observed at great distances in the Western Pacific, Science. 199, 1333-1335, 1978.

APPENDIX VI

OPA

Newsletter of the Ocean P Alliance
Number 1 September 15, 1982

6 SEPTEMBER 1982; 01:47:02; 29.3N,140.3E; 6.6 M_B; 167 KM; SOUTH OF HONSHU; DISTANCE = 25.2°

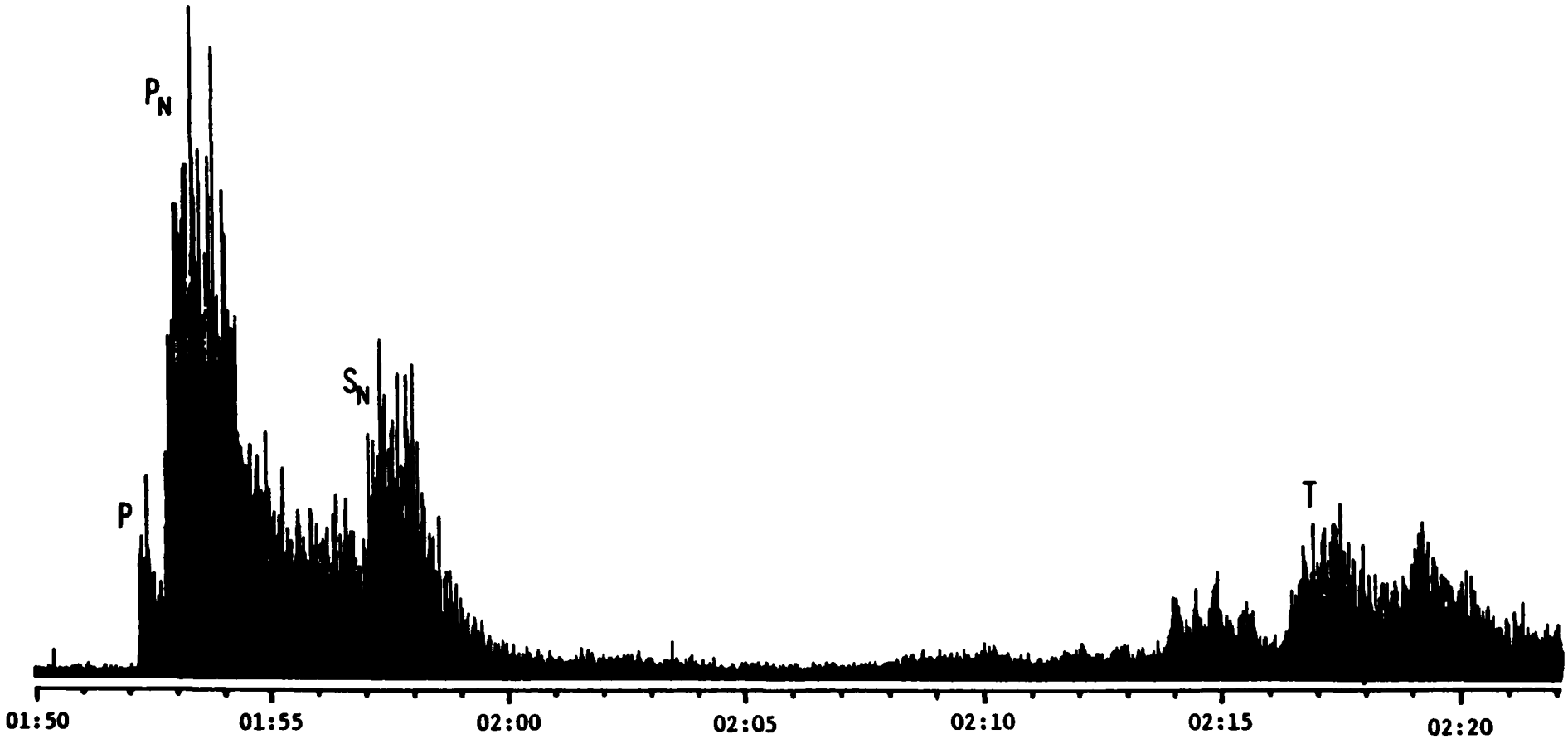

OPA

NEWSLETTER OF THE OCEAN P ALLIANCE

The purpose of OPA, the newsletter of the "Ocean P Alliance," is to stimulate interest in a seismic phase known as "Ocean P." This phase, Po, and its associated S phase, So, were first observed in the North Atlantic and have since been found throughout the North, Western, and Central Pacific. First arriving Po/So phases travel with fairly constant apparent velocities of about 8.0 and 4.6 km/sec, respectively, while peak arrivals have velocities (about 7.6 and 4.5 km/sec) comparable to basal crustal rates. At distances of about 18° (~ 2000 km), observed frequencies of Po and So are as high as 30 and 35 Hz, respectively; and at distances of about 30°, as high as 15 and 20 Hz, respectively. The signal-to-noise ratios for Po/So phases are generally at least ten times greater than the ratios of their respective normal, mantle-refracted P and S phases; and, in many instances no P's and S's can be found in spite of the presence of very strong Po's and So's.

Aside from the SOFAR channel of the world's oceans, the Po/So waveguide appears to be the earth's most efficient acoustical waveguide (estimates of Q are as high as 20,000). Also it seems probable that the phenomenon is a dominant feature of all of the world's oceans and marginal seas.

In spite of these remarkable and extensive observations, Po/So research has not yet received the general recognition, interest, and support that it deserves. Recent observations indicate the phenomenon is not just of interest in terms of basic science, but applied science as well. The applied aspects include the detection and discrimination of underground nuclear explosions along subduction zones and/or continental margins, large-scale mapping of the crust and uppermost mantle of the world's oceans and marginal seas, and acoustical studies of ocean sediments and crust at high frequencies.

In view of the foregoing discussions, the intent of this newsletter is to promote interest in Po/So research by providing an additional, and more effective, forum for the exchange of observations and ideas. Contributions or correspondence should be addressed to:

Dan Walker, OPA
Rm. 432, HIG, U. of H.
2525 Correa Rd.
Honolulu, HI 96822

Views expressed in this publication are those of the authors only and do not reflect official positions of the Ocean P Alliance unless expressly stated.

Acknowledgments. The concept of a newsletter to improve communications among those interested in Po/So research grew directly out of responses to my 30 March letter. I thank all of those who provided this encouragement. I would also like to express my appreciation to a few visionary program managers at the National Science Foundation, the Office of Naval Research, the Air Force Office of Scientific Research, and the U.S. Arms Control and Disarmanent Agency .

Dear Potential Ocean P Alliance Members:

On 30 March 1982, I wrote a rather lengthy letter to some of you concerning seismic phases variously referred to as high-frequency Pn/Sn, long-range Pn/Sn, or Ph.f./Sh.f. It was, and is, my opinion that the level of interest in, and support for, research on these phases was far less than commensurate with their potential importance to geophysics. [In the event that your may have misplaced the 30 March letter, some of the more significant observations are summarized in the masthead.] To share this concern and to obtain an objective assessment, I requested that you reciprocate and express your views to me.

As you may have guessed, the response has been very encouraging—so much so that you have before you a new means for the exchange of observations and ideas on the phenomenon of "high-frequency Pn/Sn" propagation.

Rationale. The history of research on these phases since they were first recognized nearly fifty years ago could best be described as sporadic--with only a small number (often zero) of researchers actively studying the phenomenon at any given time. Such efforts for those early years are understandable. Unfortunately, even with the advent of ocean-bottom hydrophones, digital systems which greatly facilitate spectral analyses, and rapidly evolving computer techniques for modeling complex seismic phases, the number of researchers actively studying the phenomenon is still small. As a result much of what we publish is given little attention, or is totally ignored; and this situation is exacerbated by the large number of journals ("haystacks") in which these studies ("needles") can be published.

Thus, the timing now seems appropritate for building a larger constituency and pushing for a solution. Legitimate means are increased communications, as well as continuing quality research. Without such an effort at this time, I am fearful that research on the phenomenon will still be dangerously close to the "sporadic mode," making hard times and additional periods of dormancy very real possibilities.

I believe the assessment that high-frequency Pn/Sn propagation is "a challenge remaining to the theoretician," (Richards, 1979, Rev. Geophys. Space Phys., 17, 312-328) and is "the challenge to both explosion and earthquake seismology for the coming decade" (Hirn et al., 1973, Z. Geophys., 39, 363-384). I also believe that the opportunities for widespread participation in the solution of major geophysical problems are increasingly rare and that such opportunities should be seized.

Name Change. It may be advantageous at this time to suggest that a new name be given to the high-frequency compressional and shear phases observed at great distances in the world's oceans. The

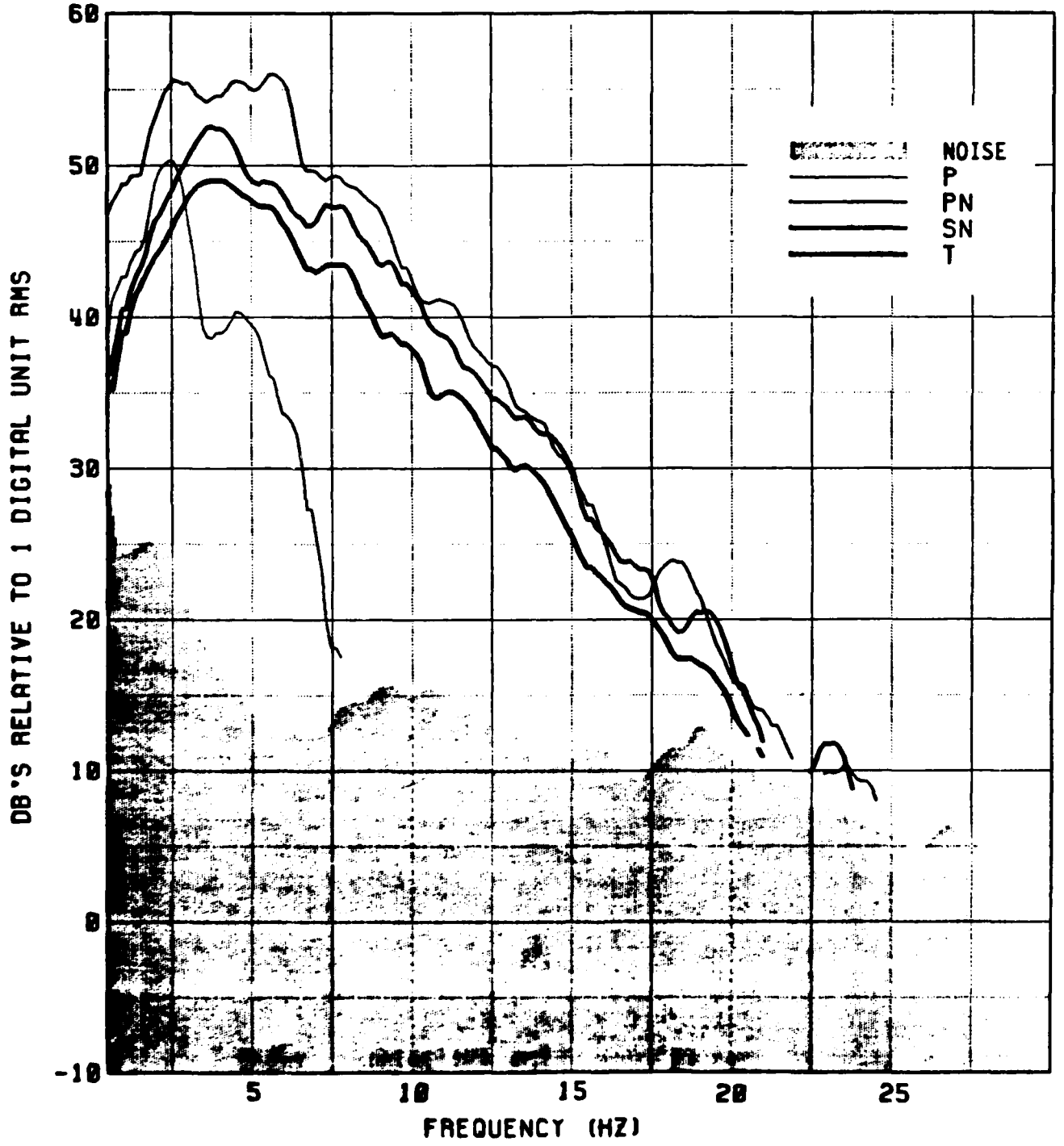
60
50
40
30
20
10
0
-10
5
10
15
20
25
NOISE
P
PN
SN
T
DB'S RELATIVE TO 1 DIGITAL UNIT RMS
FREQUENCY (HZ)

difficulty with the nomenclature used to date is that: (1) an, as yet, unsubstantiated relationship to the well known longer-period Pn/Sn phases of continents is inferred; and (2) the environmental feature most strongly linked to the observations is not cited. Thus, a more logical term would be "Ocean P" or "Ocean S" with the abbreviations being "Po/So." With this change, those unfamiliar with the phenomenon would not be as likely to make the false assumption that the phases are similar to continental Pn and Sn. Such assumptions in the past have been a major stumbling block in stimulating interest and support for "Po/So" research.

Our Birthday. You may have noticed something special about the date of this inaugural newsletter--15 September 1982 commemorates the 47th anniversary of the first known published report of Po/So phases.

"In the bulletin of the Harvard Seismograph Station, under date of September 15, 1935, attention was directed to the unusual character of certain records from the vicinity of 17°N, 62°W. One of the novel features was a short-period phase about 23 minutes after P. It has become known as T, for third, with P and S constituting the first and second groups of short-period waves of similar general appearance. The problem was discussed with Weston, and since that time those two stations have been working on it. Linehan published in 1940 the first description outside station bulletins." [Leet et al., 1951, Bull. Seismol. Soc. Am., 41, 123-141].

"At the 1939 meeting of the Eastern Section of the Seismological Society of America, the author presented a paper on earthquakes occurring about 15° to 30° distance from Weston, Massachusetts. The difficulty of locating these quakes was stressed in the paper, due to the strange characteristics of the recordings. Observers of many stations thought of them as a series of locals. As has been mentioned, the records from this area are quite different from those we have recorded from other locations. The predominant characteristic is the multiplicity of their extremely short period. The so-called P-group may last as long as three or four minutes due to the multiplicity mentioned and frequently runs into the S-group: The second group lasts about the same length of time as the former. About 20 minutes after the P-group is a third unidentified group which we have labelled as T." [Linehan, 1940, EOS Trans. AGU, 21, 229-232].

"Actually, many features of P and S are abnormal on this and later records from certain areas at this distance range, and work on that part of the problem is in progress, but the investigation of T has been undertaken first." [Leet et al., op. cit.]

As I stated in my 30 March letter, although the T-phase was accurately identified in a relatively short time as compressional energy traveling in the sound channel of the world's oceans, one could best describe work on the other "part of the problem" (i.e., the "abnormal" P and S phases), 47 years later, as still being "in progress."

It is my hope that on the 50th anniversary of the first reported observations of Po and So, the need for a special newsletter would no longer exist.

Success. The minimum objective of the newsletter is nothing more than the stimulation of deserved interest in Po/So research. Achievements beyond the minimum objective will be strongly dependent on contributions and correspondence from members and their "lobbying efforts" with program managers.

Membership. The "Ocean P Alliance" is not at the moment a formal organization. If no useful purpose would be achieved by "formalization" then this current status should remain unchanged. Anyone wishing to be considered as a member of the Alliance is automatically "in." Anyone wishing to remain skeptical, but nonetheless interested, could consider themselves, if they wish as non-members and still receive the newsletter. I may at some later date directly ask you for your opinions on the newsletter.

I would hope that those receiving the newsletter would provide: (1) The names and addresses of individuals who should be added to our mailing list, and (2) Po/So publications which should be added to our Po/So bibliography, as well as news of forthcoming publications. If you have some other newsworthy items or comments on topics discussed in OPA, please send them to me. I would also like to know if you have been mistakenly placed on the mailing list.

Format. We hope that you will save all issues of OPA for future reference. To that end we have a format conducive to storage in a 3-hole binder.

Future Topics. Items for future issues include the OPA mailing list, correspondence from members, a bibliography of Po/So research, more amazing Po/So recordings, news of upcoming publications, and interesting questions for debate.

Our Covers. To further commemorate the first reported observation of Po, So, and T phases in September of 1935 across the North Atlantic Basin, we have covered our newsletter with Po, So, and T phases which were generated in September of 1982 across the Northwestern Pacific Basin. In addition, the normal, mantle-refracted P is also shown. These phases were recorded on a twelve channel hydrophone array located near Wake Island. Do you see any similarities between these Pacific phases and those from the Atlantic discussed by Leet et al. (op.cit) and Linehan (op. cit.)? What significant observations can be made from these plots? For answers, "tune in" to the next issue of OPA!

Dan Walker

APPENDIX VII

OPA
Newsletter of the Ocean P Alliance
Number 2 January 15, 1983

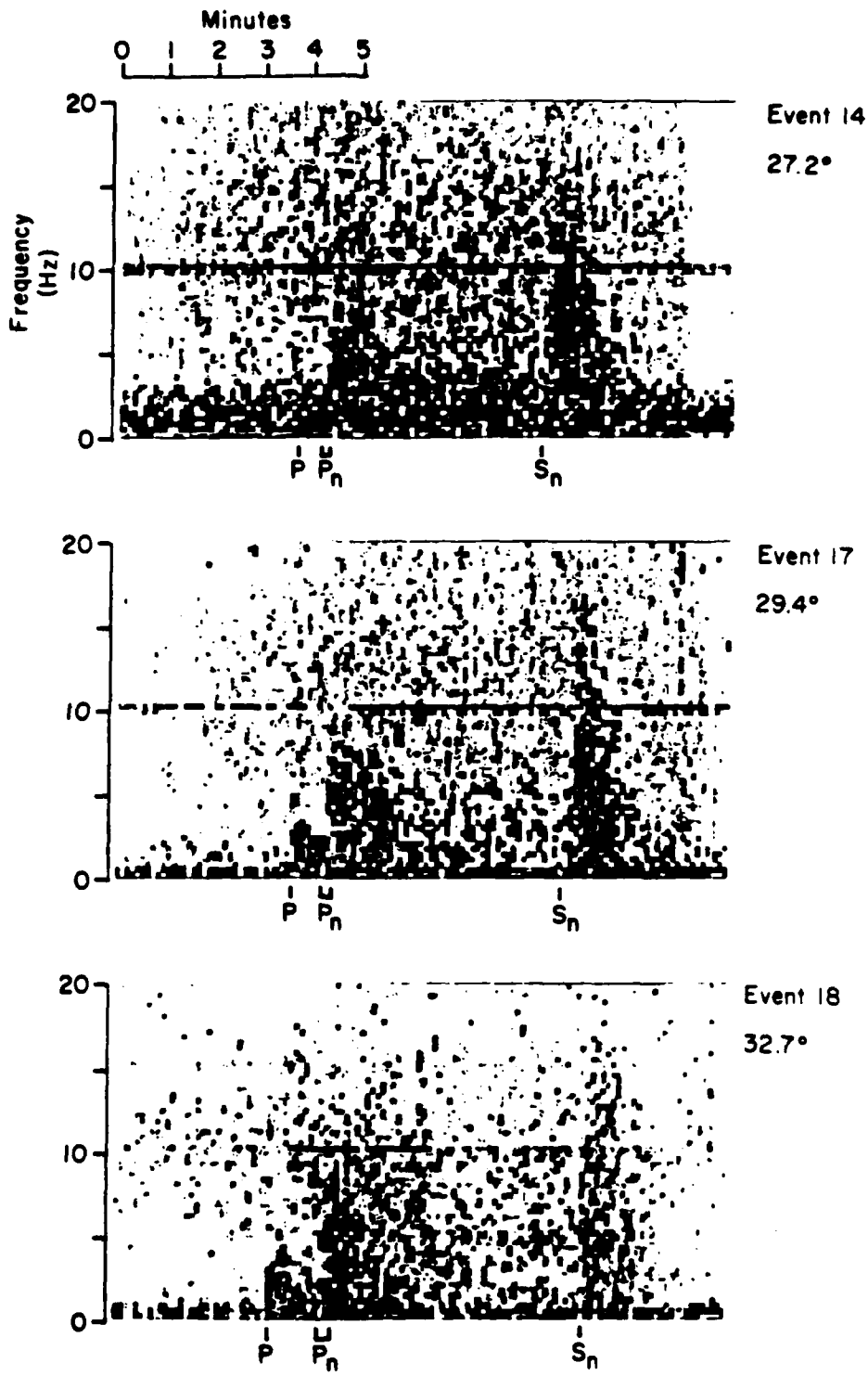

OPA

NEWSLETTER OF THE OCEAN P ALLIANCE

The purpose of OPA, the newsletter of the "Ocean P Alliance," is to stimulate interest in a seismic phase known as "Ocean P." This phase, Po, and its associated S phase, So, were first observed in the North Atlantic and have since been found throughout the North, Western, and Central Pacific. First arriving Po/So phases travel with fairly constant apparent velocities of about 8.0 and 4.6 km/sec, respectively, while peak arrivals have velocities (about 7.6 and 4.5 km/sec) comparable to basal crustal rates. At distances of about 18° (~ 2000 km), observed frequencies of Po and So are as high as 30 and 35 Hz, respectively; and at distances of about 30°, as high as 15 and 20 Hz, respectively. The signal-to-noise ratios for Po/So phases are generally at least ten times greater than the ratios of their respective normal, mantle-refracted P and S phases; and, in many instances no P's and S's can be found in spite of the presence of very strong Po's and So's.

Aside from the SOFAR channel of the world's oceans, the Po/So waveguide appears to be the earth's most efficient acoustical waveguide (estimates of Q are as high as 20,000). Also it seems probable that the phenomenon is a dominant feature of all of the world's oceans and marginal seas.

In spite of these remarkable and extensive observations, Po/So research has not yet received the general recognition, interest, and support that it deserves. Recent observations indicate the phenomenon is not just of interest in terms of basic science, but applied science as well. The applied aspects include the detection and discrimination of underground nuclear explosions along subduction zones and/or continental margins, large-scale mapping of the crust and uppermost mantle of the world's oceans and marginal seas, and acoustical studies of ocean sediments and crust at high frequencies.

In view of the foregoing discussions, the intent of this newsletter is to promote interest in Po/So research by providing an additional, and more effective, forum for the exchange of observations and ideas. Contributions or correspondence should be addressed to:

Dan Walker, OPA
Rm. 432, HIG, U. of H.
2525 Correa Rd.
Honolulu, HI 96822

Dear Colleague:

As you may recall, the covers for our inaugural issue consisted of a digitally rectified and compressed plot of P, Po, So, and T phases for an earthquake south of Japan recorded by the Wake hydrophones (front cover) and spectrums for these same phases (back cover). For purposes of the discussion which will follow these figures are repeated here in a severely reduced form. In closing the inaugural issue, I asked whether you could see any similarities between these Pacific phases and those from the Atlantic discussed by Leet, Linehan, and Berger (1951) and Linehan (1940). The unusual characteristics mentioned by these authors are the similar general appearance of their so-called P (primary) and S (secondary) groups to the later arriving T (tertiary) group, the multiplicity of their extremely short period with the P frequently running into the S group, and S about as long as P.

Certainly all of these characteristics have been seen in the Pacific as exemplified in the figures shown here. The P, S, and T groups are of the same general appearance, the P group runs into the S group, in some respects the S group may be about as long as P, and the phases are of extremely short period. The striking and remarkable similarities of these phases are most evident in the spectrums, which also serve to quantify their short period content.

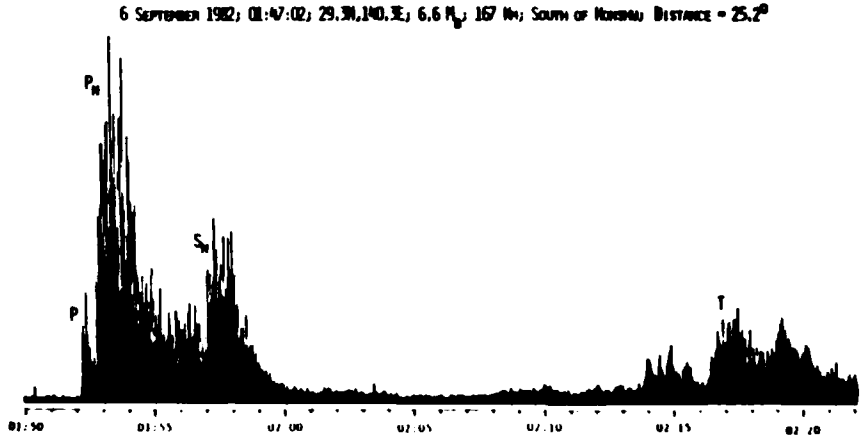

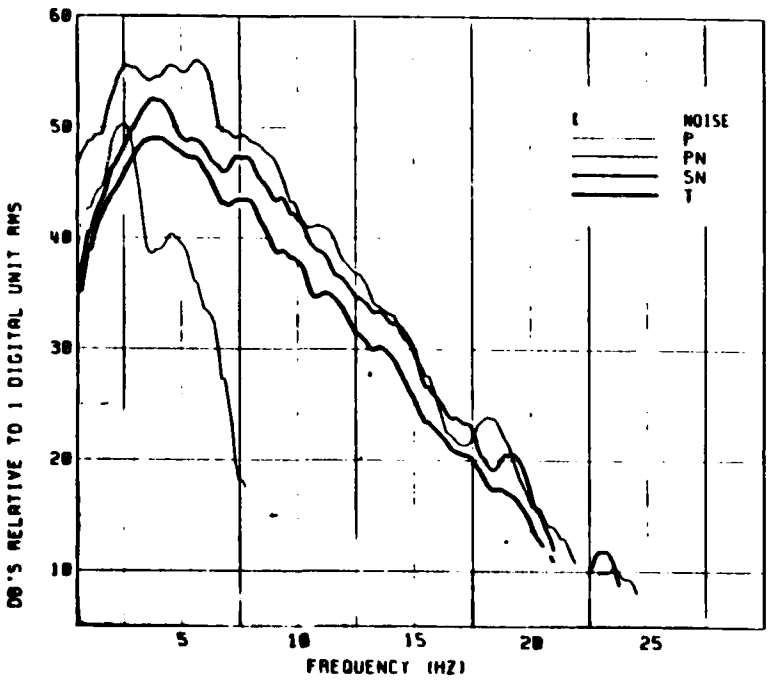

The T Phase: A New Approach to Po/So Research. Especially intriguing is the detailed correlation of the T spectrum to the So spectrum. This and the general correlation of the T and Po spectrums suggests a possible new approach to Po/So research. In the future it would seem appropriate to consider the possible relationship of Po and So to T. [Other evidence suggesting a possible relationship of Po and So to T is contained in the report "Oceanic Pn/Sn Phases: A Qualitative Explanation and Reinterpretation of the T-Phase" (D. Walker, HIG Report 82-6, 1982). [Topics from this report are discussed in this newletter].

Spectrums for Atlantic Po, So, and T Phases: A Challenge for East and Gulf Coast Seismologists. I believe that Leet, Linehan, and Berger would be surprised at just how short the periods were for the phases they observed. Unfortunately, the recordings and instrumentation which they had (in all probability 60 mm/minute analog recordings from standard 1 Hz instrumentation) did not permit them to see just how high the frequencies were. In the deep ocean near Wake, forty years later, we have the advantages of lower noise in the 3 Hz to 15 Hz range than most continental stations, a better system response to those frequencies than conventional 1 Hz instrumentation, digital recordings, and computers which facilitate the derivation of spectrums. It is nonetheless surprising that spectrums of Atlantic Po, So, and T phases have not been published. (If I am mistaken, I hope someone will write and provide references.) It would be interesting to compare these spectrums to those from the Pacific. I hope that some east or gulf coast seismologists will take the challenge and be the first to quantify the frequency content of Atlantic Po/So phases.

Continuing Japanese Research on Po/So. I was pleased to meet recently with Drs. Nagumo and Kasahara and to review a preprint of their new paper, with Drs. Ouchi and Koresawa, on OBS observations of Po/So phases. The report contains important information on Po/So velocities. I wish them every success in efforts to publish this important paper.

Po/So Bibliography. One of the major objectives of the OPA Newsletter is to acquire a comprehensive and up-to-date bibliography of Po/So research. A preliminary attempt to achieve this objective follows. I hope that readers aware of omissions will bring them to my attention so that they can be added to the listings.

Our Covers: Now you see "it". Now you don't! The covers are spectrograms from the Wake Island hydrophones. Expected times of arrivals are based on either the Jeffreys-Bullen tables for P or Po/So travel time curves. The contour interval is 8 db. The line at 10 Hz is due to time code cross talk.

What's "it"? The So - very strong on the front cover, but weak or absent on the back cover. Phases shown on the front cover are typical of events from the Japan, Kuril, Kamchatka portion of the circum-Pacific arc; and, therefore, these phases have travel paths to Wake under the deep Northwestern Pacific Basin. Phases shown on the back cover are typical of events from the New Ireland and Solomon Islands area; and, therefore, these phases have travel paths to Wake under the shallow Ontong-Java Plateau as well as portions of the deep Northwestern Pacific Basin.

An obvious explanation is differences in source characteristics. Unfortunately, this seemingly reasonable explanation cannot be correct, since So phases from the New Ireland and Solomon Islands area are well recorded at Ponape on the northern margin of the Ontong-Java Plateau (roughly mid-way between the source locations and the receivers at Wake). [Of the more than forty events from the New Ireland and Solomon Island area recorded at Ponape during an approximate seventeen month experiment, amplitudes of So phases are at least comparable to, and frequently larger than, those of their respective Po phases.]

What, then, could be the explanation? Possible clues are: (1) the transition [illegible] shallower Ontong-Java Plateau to the deeper Northwestern [illegible]; and (2) the frequent absence or weakness of So, [illegible] presence of Po, at great distances (often more

than 4000 km) throughout the North Pacific (Walker, 1977a and b) and Central Pacific (Talandier and Bouchon, 1979), in spite of stronger So's than Po's for relatively homogeneous travel paths across the deep Northwestern Pacific Basin.

A possible explanation will be given in the next issue of OPA. Please send any comments or suggestions on this or other items.

Po/So Bibliography

Asada, T. and H. Shimamura, 1976, Observation of earthquakes and explosions at the bottom of the Western Pacific: Structure of the oceanic lithosphere revealed by longshot experiment, in The Geophysics of the Pacific Ocean Basin and Its Margin, Geophys. Monogr. Ser., ed. G. Sutton, M. Manghnani, and R. Moberly, Vol. 19, Am. Geophys. Union, Washington, D.C., 135-153.

Auld, B., G. Latham, A. Nowroozi, and L. Seeber, 1969, Seismicity off the coast of northern California determined from ocean bottom seismic measurements, Bull. Seismol. Soc. Am., 59, 2001-2015.

Barazangi, M., B. Isacks, and J. Oliver, 1972, Propagation of seismic waves through and beneath the lithosphere that descends under the Tonga Island arc, J. Geophys. Res., 77, 952-958.

Bath, M., 1966, Propagation of Sn and Pn to teleseismic distances, Pure Appl. Geophys., 64, 19-30.

Brune, J., and J. Dorman, 1963, Seismic waves and earth structure in the Canadian shield, Bull. Seismol. Soc. Amer., 53, 167-210.

Fuchs, K., and K. Schulz, 1976, Tunneling of low-frequency waves through the subcrustal lithosphere, J. Geophys., 42, 175-190.

Gettrust, J., and L. Frazer, 1981, A computer model study of the propagation of the long-range Pn phase, Geophys. Res. Lett., 8, 749-752.

Hales, A., C. Helsley, and J. Nation 1970, P travel times for an oceanic path, J. Geophys. Res., 75, 7362-7381.

Hart, R., and F. Press, 1973, Sn velocities and the composition of the lithosphere in the regionalized Atlantic, J. Geophys. Res., 78, 407-411.

Hirn, A., L. Steinmetz, R. Kind, and K. Fuchs, 1973, Long range profiles in western Europe, II, Fine structure of the lower lithosphere in France (southern Bretagne), Z. Geophys., 39, 363-384.

Isacks, B., and J. Oliver, 1964, Seismic waves with frequencies from 1 to 100 cycles per second recorded in a deep mine in northern New Jersey, Bull. Seismol. Soc. Amer., 54, 1941-1979.

Kasahara, J., and R. Harvey, 1977, Seismological evidence for the high-velocity zone in the Kuril trench area from ocean bottom seismometer observations, J. Geophys. Res., 82, 3805-3814.

Khalturin, V., T. Rautian, and P. Molnar, 1977, The spectral content of Pamir-Hindu Kush intermediate depth earthquakes: Evidence for a high-Q zone in the upper mantle, J. Geophys. Res., 82, 2931-2943.

Kind, R., 1974, Long range propagation of seismic energy in the lower lithosphere, J. Geophys., 40, 189-202.

Latham, G., and G. Sutton, 1966, Seismic measurements of the ocean floor, J. Geophys. Res., 71, 2545-2573.

Leet, L., D. Linehan, and P. Berger, 1951, Investigation of the T phase, Bull. Seismol. Soc. Amer., 41, 123-141.

Linehan, D., 1940, Earthquakes in the West Indian region, EOS Trans. AGU, 21, 229-232.

Mantovani, E., F. Schwab, H. Liso, and L. Knopoff, 1977, Teleseismic Sn: A guided wave in the mantle, Geophys. J. R. Astron. Soc., 51, 709-726.

McCreery, C., 1981, High-frequency Pn, Sn phases recorded by ocean bottom seismometers on the Cocos Plate, Geophys. Res. Lett., 8, 489-492.

McCreery, C. and G. Sutton, 1980, Wave train characteristics of long-range, high-frequency Pn, Sn crossing an ocean bottom hydrophone array, Bull. Seismol. Soc. Amer., 70, 437-446.

Menke, W., and P. Richards, 1980, Crust-mantle whispering gallery phases: a deterministic model of teleseismic Pn wave propagation, J. Geophys. Res., 85, 5416-5422.

Mitronovas, W., B. Isacks, and L. Seeber, 1969, Earthquake locations and seismic wave propagation in the upper 250 km of the Tonga Island arc, Bull. Seismol. Soc. Amer., 59, 1115-1135.

Molnar, P., and J. Oliver, 1969, Lateral variations of attenuation in the upper mantle and discontinuities in the lithosphere, J. Geophys. Res., 74, 2648-2682.

Nagumo, S., and J. Kasahara, 1976, Ocean-bottom seismograph study of the western margin of the Pacific, in The Geophysics of the Pacific Ocean Basin and Its Margin, Geophys. Monogr. Ser., ed. G. Sutton, M. Manghnani, and R. Moberly, Vol. 19, Am. Geophys. Union, Washington, D.C., 155-167.

Odegard, M., 1975, Upper mantle structure of the North Pacific, Ph.D. thesis, Univ. of Hawaii, Honolulu.

Oliver, J., and B. Isacks, 1967, Deep earthquake zones, anomalous structures in the upper mantle, and the lithosphere, J. Geophys. Res., 72, 4259-4275.

Ouchi, T., 1981, Spectral structure of high frequency P and S phases observed by OBS's in the Mariana Basin, J. Phys. Earth., 29, 305-326.

Ouchi, T., S. Nagumo, and S. Koresawa, 1981, Ocean bottom seismometer study on the seismic activity in the Mariana Island arc region, Bull. Earthq. Res. Inst., 56, 43-65.

Press, F., and M. Ewing, 1955, Waves with Pn and Sn velocity at great distances, Proc. Nat. Acad. of Sci., 41, 24-27.

Richards, P., 1979, Theoretical seismic wave propagation, Rev. Geophys. Space Phys., 17, 312-328.

Shimamura, H., and T. Asada, 1975, T waves from deep earthquakes generated exactly at the bottom of deep-sea trenches, Earth and Planet. Sci. Lett., 27, 137-142.

Shimamura, H., and T. Asada, 1976, Apparent velocity measurements on an oceanic lithosphere, Phys. Earth Planet. Int., 13, 15-22.

Shimamura, H., T. Asada, and M. Kumazawa, 1977, High shear velocity layer in the upper mantle of the western Pacific, Nature, 269, 680-682.

Shimamura, H., Y. Tomoda, and T. Asada, 1975, Seismographic observations at the bottom of the Central Basin Fault of the Philippine Sea, Nature, 253, 177-179.

Shurbet, D., 1962, The high-frequency P and S phases from the West Indies, Bull. Seismol. Soc. Amer., 52, 957-962.

Shurbet, D., 1964, The high-frequency S phase and structure of the upper mantle, J. Geophys. Res., 69, 2065-2070.

Stephens, C., and B. Isacks, 1977, Toward an understanding of Sn: Normal modes of Love waves in an oceanic structure, Bull. Seismol. Soc. Amer., 67, 69-78.

Sutton, G., C. McCreery, F. Duennebier, and D. Walker, 1978, Spectral analyses of high-frequency Pn,Sn phases recorded on ocean bottom seismographs, Geophys. Res. Lett., 5, 745-747.

Sutton, G., and D. Harvey, 1981, Complete synthetic seismograms to 2 Hz and 1000 km for an oceanic lithosphere, EOS Trans. AGU., 62, p. 327.

Sutton, G., and D. Walker, 1972, Oceanic mantle phases recorded on seismographs in the Northwestern Pacific at distances between 7° and 40°, Bull. Seismol. Soc. Amer., 62, 631-655.

Talandier, J., and M. Bouchon, 1979, Propagation of high frequency Pn waves at great distances in the Central and South Pacific and its implications for the structure of the lower lithosphere, J. Geophys. Res., 84, 5613-5619.

Utsu, T., 1967, Anomalies in a seismic wave velocity and attenuation associated with a deep earthquake zone (I), J. Fac. Sci. Hokkaido Univ., Ser. 7, Geophysics, 3, 1-25.

Walker, D., 1977, High-frequency Pn and Sn phases recorded in the Western Pacific, J. Geophys. Res., 82, 3350-3360.

Walker, D., 1977, High-frequency Pn phases observed in the Pacific at great distances, Science, 197, 257-259.

Walker, D., 1981, High-frequency Pn,Sn velocities: some comparisons for the Western, Central, and South Pacific, Geophys. Res. Lett., 8, 207-209.

Walker, D., 1982, Oceanic Pn/Sn phases: a qualitative explanation and reinterpretation of the T-phase, Hawaii Inst. of Geophysics Rept. HIG-82-6, 19 pp.

Walker, D., C. McCreery, G. Sutton, and F. Duennebier, 1978, Spectral analyses of high-frequency Pn and Sn phases observed at great distances in the Western Pacific, Science, 199, 1333-1335.

Walker, D., and G. Sutton, 1971, Oceanic mantle phases recorded on hydrophones in the Northwestern Pacific at distances between 9° and 40°, Bull Seismol. Soc. Amer., 61, 65-78.

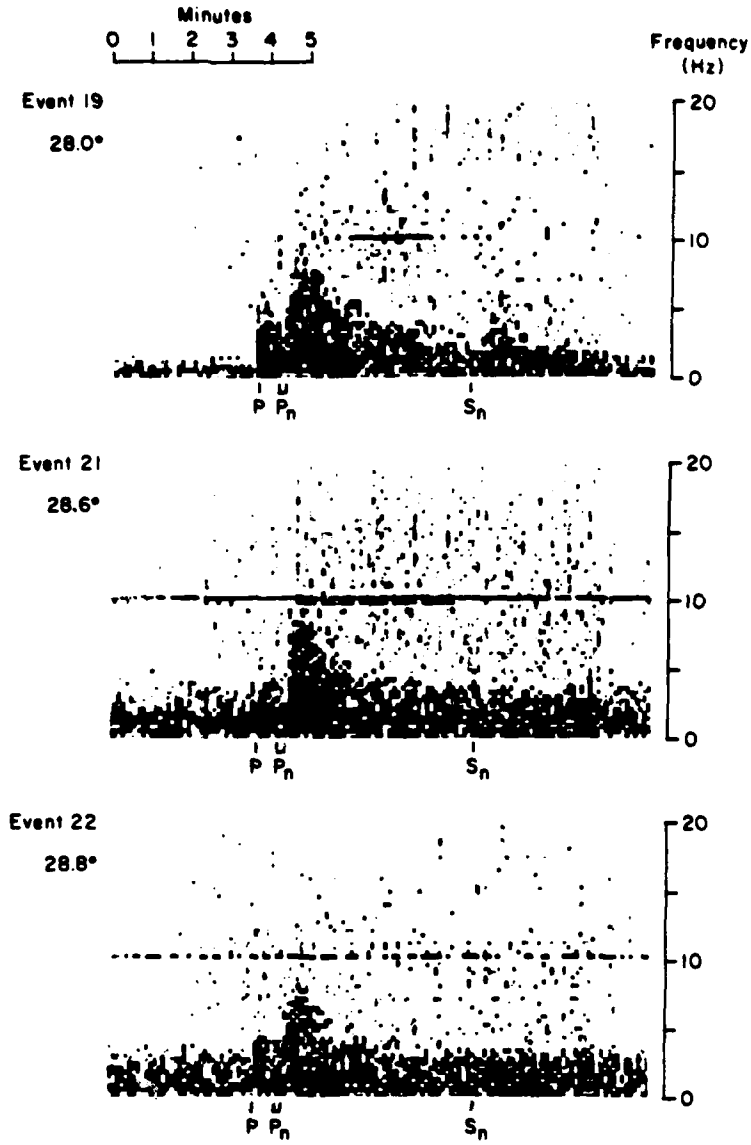
Minutes
0 1 2 3 4 5
Frequency (Hz)
Event 19
28.0°
20
10
0
P
Pn
Sn
Event 21
28.6°
20
10
0
P
Pn
Sn
Event 22
28.8°
20
10
0
P
Pn
Sn

APPENDIX VIII

OPA Newsletter of the Ocean P Alliance
Number 3 May 15, 1983

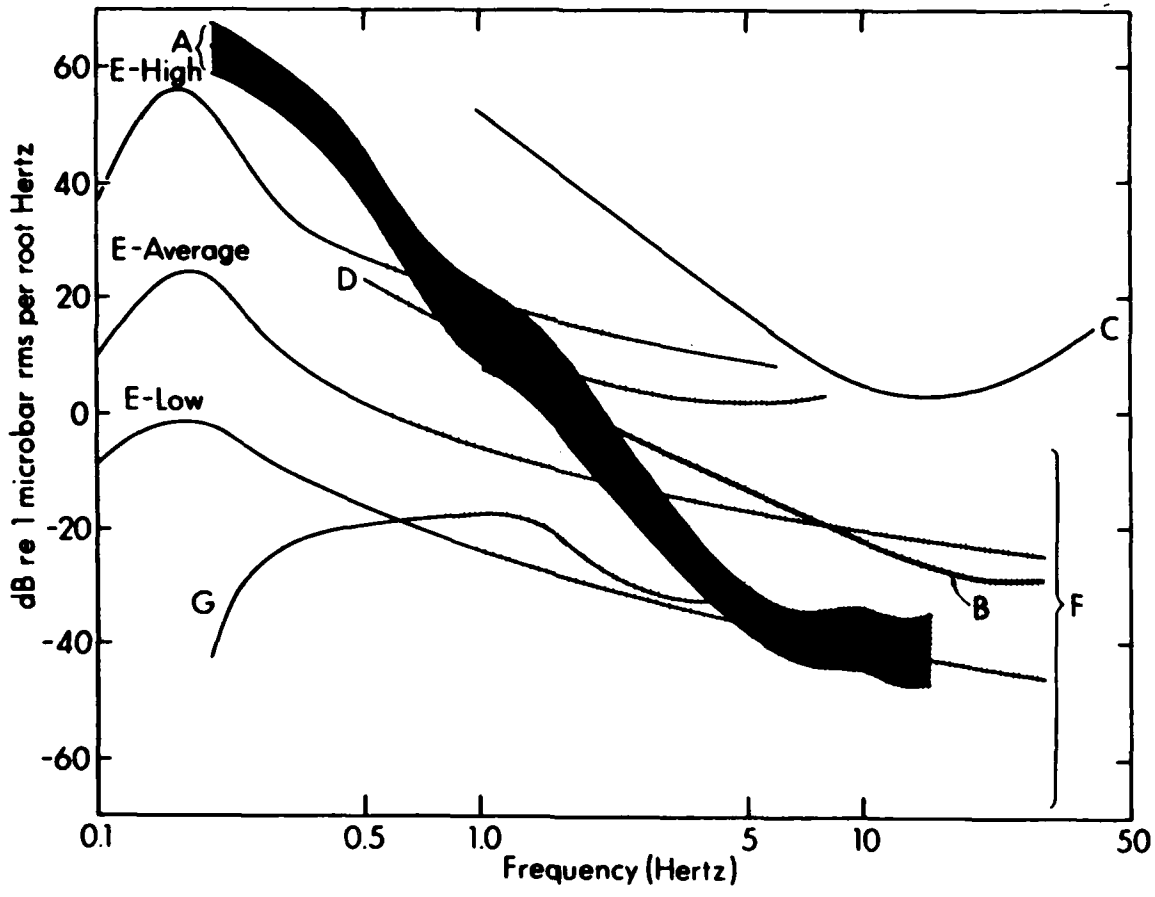

OPA

NEWSLETTER OF THE OCEAN P ALLIANCE

The purpose of OPA, the newsletter of the "Ocean P Alliance," is to stimulate interest in a seismic phase known as "Ocean P." This phase, Po, and its associated S phase, So, were first observed in the North Atlantic and have since been found throughout the North, Western, and Central Pacific. First arriving Po/So phases travel with fairly constant apparent velocities of about 8.0 and 4.6 km/sec, respectively, while peak arrivals have velocities (about 7.6 and 4.5 km/sec) comparable to basal crustal rates. At distances of about 18° (≃ 2000 km), observed frequencies of Po and So are as high as 30 and 35 Hz, respectively; and at distances of about 30°, as high as 15 and 20 Hz, respectively. The signal-to-noise ratios for Po/So phases are generally at least ten times greater than the ratios of their respective normal, mantle-refracted P and S phases; and, in many instances no P's and S's can be found in spite of the presence of very strong Po's and So's.

Aside from the SOFAR channel of the world's oceans, the Po/So waveguide appears to be the earth's most efficient acoustical waveguide (estimates of Q are as high as 20,000). Also it seems probable that the phenomenon is a dominant feature of all of the world's oceans and marginal seas.

In spite of these remarkable and extensive observations, Po/So research has not yet received the general recognition, interest, and support that it deserves. Recent observations indicate the phenomenon is not just of interest in terms of basic science, but applied science as well. The applied aspects include the detection and discrimination of underground nuclear explosions along subduction zones and/or continental margins, large-scale mapping of the crust and uppermost mantle of the world's oceans and marginal seas, and acoustical studies of ocean sediments and crust at high frequencies.

In view of the foregoing discussions, the intent of this newsletter is to promote interest in Po/So research by providing an additional, and more effective, forum for the exchange of observations and ideas. Contributions or correspondence should be addressed to:

Dan Walker, OPA
Rm. 432, HIG, U. of H.
2525 Correa Rd.
Honolulu, HI 96822

Dear Colleague:

The covers of our last issue, shown here in reduced form, are spectrograms for phases with travel paths to the Wake Island hydrophones under the deep Northwestern Pacific Basin (front cover) and under the shallow Ontong Java Plateau (back cover). An obvious explanation for the absence, or weakness, of So (labeled Sn) on the back cover is differences in source characteristics. However, recordings made during an earlier experiment at Ponape, roughly midway between the receivers at Wake and the source locations of earthquakes in the New Ireland and Solomon Island area (see accompanying map), indicate that this explanation can not be correct. Over an approximate seventeen month recording period, more than forty events from the New Ireland and Solomon Island area were recorded, with the amplitudes of So at least comparable to, and frequently larger than, those of their respective Po phases.

An observation which contributes to a possible explanation is the frequent absence or weakness of So, yet presence of Po, at great distances (often more than 4000 km) throughout the North Pacific (Walker, 1977a and b) and Central Pacific (Talandier and Bouchon, 1979), in spite of stronger So's than Po's for relatively homogeneous travel paths across the deep Northwestern Pacific Basin.

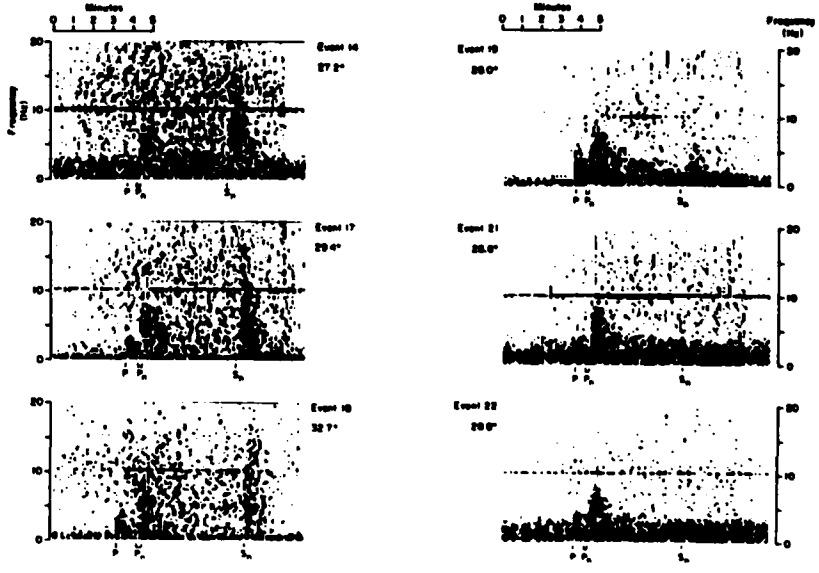

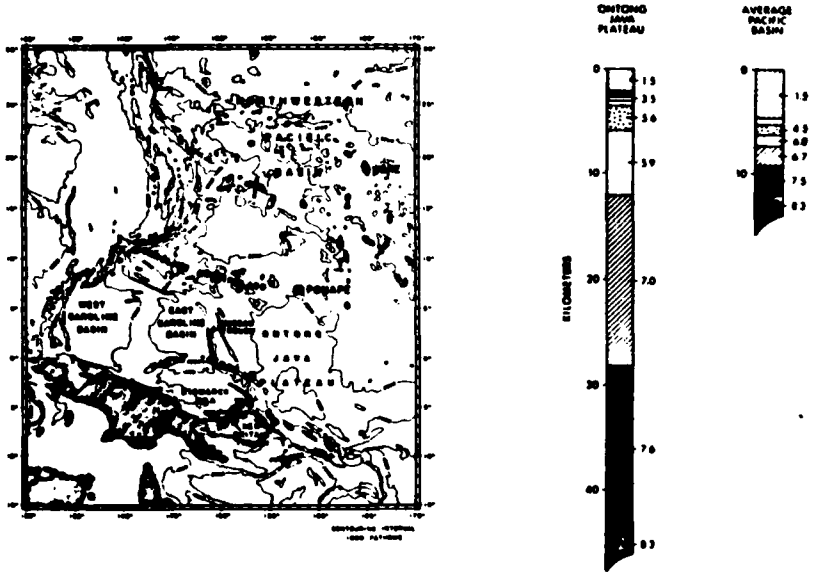

The explanation arising from these observations, then, is that paths other than those across relatively homogeneous ocean basins are likely to encounter large lateral changes in the crust and upper mantle. Observations require that the changes be such that So signal strength is reduced without seriously affecting the Po phase. Large lateral changes could be produced by plateaus, rises, ridge systems, island and seamount chains, fracture zones, transform faults, fossil arcs and trenches, and rafted continental fragments. The transition from the shallow Ontong Java Plateau to the deeper Northwestern Pacific Basin (see accompanying figures), as well as the extension of the Caroline Archipelago through this region, could be features responsible for the weak, or absent, So's at Wake from events in the New Ireland and Solomon Island area. [This interpretation has been taken from a recent attempt (Walker, 1982) to provide a qualitative framework consistent with all of the diverse observational aspects of Po/So - hoping that this would eventually lead to comprehensive and detailed quantitative analyses and, ultimately, a generally acceptable model for the generation and propagation of Po/So.]

Nuclear Connections. In the masthead of this newsletter, reference is made to Po/So being of interest in terms of the detection and discrimination of underground nuclear explosions. It may be worthwhile at this time to be more explicit as to possible reasons for such interest.

A. Obvious - Large S/N Ratios for Po/So. An examination of the covers of previous OPA newsletters is all that is needed to suggest that S/N ratios for Po/So may be larger than the ratios for mantle refracted P (S is not generally apparent for distances of up to about 20°). Indeed, numerous observations from the deep ocean, as well as hard rock island sites, in the Western Pacific indicate the S/N ratios for Po/So at their dominant frequencies (about 4 to 8 Hz) are generally from 5 to 10X greater than the S/N ratios for P at its dominant frequencies (about 1.5 to 2.5 Hz). This dominance may extend out to distances of 3000 km, with P increasing in strength relative to Po/So beyond this range. Also, at distances less than about 20°, the travel times of Po phases are such that they may arrive ahead of the mantle refracted P, thus masking whatever P energy may be present.

Although some of the most extensive observations of Po/So phases have been in the Western Pacific, these phases have also been observed in other portions of the Pacific and the North Atlantic. The nature and extent of those observations suggest that the phenomenon could be a dominant feature of all the world's oceans and marginal seas.

Thus regional detection and discrimination of underground explosions with seismic instrumentation in an ocean environment (islands, the water column, bottom, or sub-bottom) may in large part be based on Po/So recordings.

As to why detection and discrimination in an ocean environment should be important, one has only to look at a globe. As to whether, in fact, detection and discrimination in an ocean environment is important, one has only to consider recent investments in ocean sub-bottom seismometers.

B. Less Obvious - Lg/Pg Comparisons. Just as Po/So are the most prominent phases recorded at regional distances for oceanic travel paths, Lg and Pg are prominent phases recorded at regional distances for continental travel paths. Certainly Lg/Pg are of great importance in regional detection using continental stations (just as Po/So should be of great importance in regional detection using oceanic stations). Surprisingly, the much studied phenomenon of Lg/Pg suffers problems of understanding not unlike those associated with Po/So. In a recent publication (1983) Gupta and Blandford state:

"The mechanism for the generation of transverse component motion from explosions is still not clearly understood in spite of the large number of studies on the subject." [p. 571] and "... no convincing explanation has so far been offered for the generation of short-period (about 1 sec or less) transverse motion from explosions." [p. 572.]

[In their report they propose a scattering mechanism for the generation of short period transverse motion (including Lg) from explosions.]

Regarding the utility of Lg/Pg in the discrimination of nuclear explosions, several theoretical studies suggest a strong dependence of Lg/Pg signal character on focal depth. Also, Gupta and Blandford note that "the observed differences in the spectra of shear waves

(i.e., Lg) from explosions and earthquakes seem to be large enough to be useful for source discrimination". [p. 589].

Could it be that Lg/Pg investigators might better understand certain aspects of Lg/Pg by turning their attention to Po/So? Or, conversely, might Po/So investigators better understand Po/So by turning their attention to Lg/Pg? Because of the thinness and uniformity of the oceanic crust and upper mantle under the deep ocean basins relative to that under large portions of continents, could Po/So be viewed as less adulterated (and, therefore, less complex) forms of Lg/Pg? And, finally, could comparative studies of Lg/Pg and Po/So lead to important breakthroughs in detection and discrimination capabilities on continents and in the oceans?

In my opinion all of these questions are very important. If you share this view, I hope that you will bring the phenomenon of Po/So to the attention of your associates who may be working on Lg/Pg. I am happy to report that at least one organization (Rondout Associates Incorporated) has recognized the potential of comparative studies between Po/So and Lg/Pg in the form of a research proposal submitted to AFOSR. [Indeed, most of my views on this topic were based on discussions presented in that proposal.]

C. Indirect - Mantle Refracted Explosion P's. Our front cover is a plot of estimated ocean bottom background noise (shaded region "A") near Wake Island compared to other measurements. [A detailed description of this figure is given at the end of the newsletter.] It is apparent from this plot that the noise levels near Wake for frequencies from about 3 to 15 Hz are comparable to, or better than, levels for some of the best continental sites. This would be of little significance if there were no signals at these frequencies. However, by some fortuitous accident of nature (my apologies to those of you who may be new to the field), Po/So phases (as has already been mentioned) have strong signals in the 4 to 8 Hz range. Further compounding this accident, (a) mantle-refracted P phases from underground nuclear explosions recorded at great distances (i.e., at distances from about 60° to 90°) have suprisingly large amounts of energy at frequencies above 3 Hz, with higher corner frequencies than earthquakes at comparable distances;(b) explosions with smaller yields are believed to be relatively richer at higher frequencies;(c) the Wake hydrophones are ideally located in the 60° to 90° distance range from most of the known nuclear test sites (see accompanying figure: the shaded area represents the 60° to 90° distance range; solid circles represent underground nuclear test sites; the 90° boundary is firm since no P energy is observed beyond this distance; the 60° boundary is not firm since high frequency P energy has been observed at shorter distances); and, (d) ocean suface reflections can be used in signal enhancement (see back cover; a thorough description of this figure is given at the end of the newsletter).

The connection, then, is that sites ideal for the study of Po/So may also be of great value in recording underground explosions at great distances. [More detailed discussions of hydrophone recorded explosion P's may be found in a recent publication by McCreery et al. (1983).]

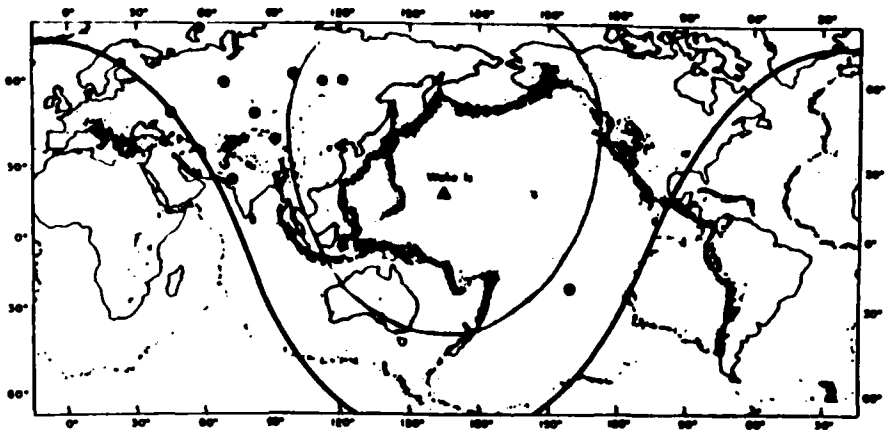

Challenge Answered. Although Po/So phases were first observed nearly fifty years ago on the east coast from an earthquake in the West Indies, I noted in the last newsletter that I had never seen spectrums for Po/So phases from an Atlantic event. Therefore, in the last newsletter, east and gulf coast seismologists were "challenged" to spectrally analyze Po/So phases for Atlantic travel paths.

Suprisingly, that challenge has already been met by Rondout Associates Incorporated (RAI), and they have generously permitted the publication of their spectrums in this newsletter (see accompanying figure). The event occurred near Puerto Rico (h = 189km; mb = 5.7) and was recorded on RAI's Catskill (New York) Seismic Array (CSA) at a distance of 27.8°. Shown are the ground velocity spectra for Po (solid line), So (dotted line), and background noise (dot-dash line).

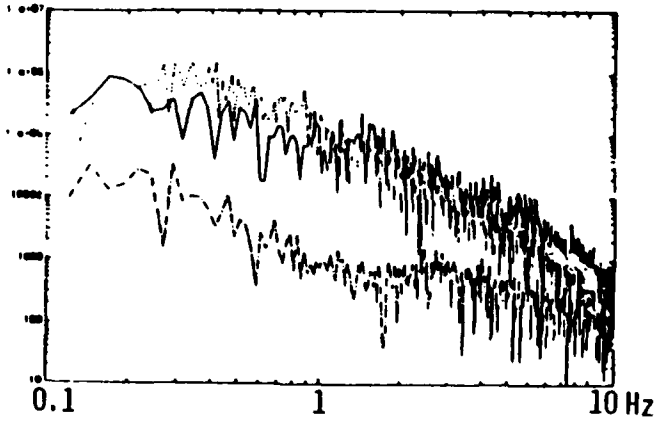

Comparisons of these spectrums, those on the back cover of OPA No.1 (shown here in reduced form), and the front cover of this newsletter are most interesting. For both sets of spectrums, Po's and So's are well above background noise out to about 10 Hz. The greater S/N ratios recorded on the ocean bottom (Wake hydrophone) at frequencies above 10 Hz may be the result of stronger signals, the lower noise levels of the ocean bottom at those frequencies, and/or greater attenuation of high frequencies by the continental portion of the Puerto Rico to CSA path. The greater S/N ratios recorded on the continent (CSA) at frequencies below 1 Hz is almost certainly a result of the lower noise levels of continents at those values. Therefore, the S/N ratios indicated in the spectrums do appear to be consistent with the noise curves for continents and oceans shown on the front cover of this newsletter.

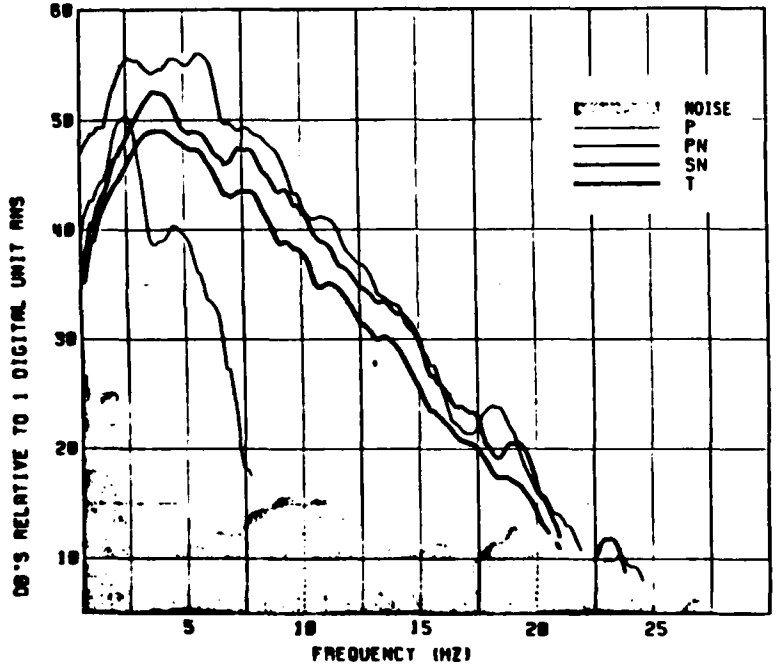

It is hoped that the publication of the Atlantic Po/So spectrums is just the beginning of many comparative studies with Pacific Po/So phases (e.g.; velocities, spectra, Q's, effects of continental paths, structural interpretations, etc.).

Po/So Bibliography. Some additions to the bibliography published in the last issue of OPA can already be made. Item #1 is a tentative addition since this modeling effort is appliclable only down to periods of 5 seconds and no direct references are made to the "Pn/Sn" phases observed at much higher frequencies for oceanic travel paths (i.e. Po/So). Item #3 was mistakenly omitted from the original list.

1. Menke, W., and P. Richards, 1983, The horizontal propagation of P waves through scattering media: analog model studies relevant to long-range Pn propagation, Bull. Seismol. Soc. Amer., 73, 125-142.

2. Walker, D., C. McCeery, and G. Sutton, 1983, Spectral characteristics of high-frequency Pn, Sn phases in the Western Pacific, J. Geophys. Res., 88, 4289-4298.

3. Walker, D., C. McCreery, G. Sutton, and F. Duennebier, 1978, Spectral analyses of high-frequency Pn and Sn phases observed at great distances in the Western Pacific, Science, 199, 1333-1335.

Our Covers. The front cover shows the average spectrum ± 1 standard deviation of 52 samples of background noise over 18 months from the Wake bottom hydrophones (A). Also shown are some published noise curves for both ocean-bottom (B, C, D, and H) and continental (E, F, and G) environments, which have been converted from an assortment of units to the scale shown. B is a hypothetical "sample spectrum of deep-sea noise" (Urick, 1975; p. 188). C is a vertical seismometer measurement made in the Mariana Basin (Asada and Shimamura, 1976). D is a vertical seismometer measurement made at 4.6-km depth between Hawaii and California (Bradner and Dodds, 1964). H is a noise curve for a hydrophone bottomed off Eleuthera Island at 1200-m depth (Nichols, 1981). E represents low, average, and high noise levels estimated from curves compiled by Brune and Oliver (1959). F is an area bounded by the limits of noise curves measured on vertical seismometers for 16 locations within the United States and Germany (Frantti et al., 1962). G is the noise curve for the Oyer subarray of the Norwegian seismic array measured during a period "when most of the North Atlantic Ocean was very quite" (Bungum et al., 1971). The back cover shows a sample time series of P, filtered to maximize signal/noise, from two nuclear explosions recorded on the Wake bottom hydrophones. The upper trace is from a single hydrophone and shows the direct arrival and its first water surface reflection. The lower trace is a composite of signals from two hydrophones with 40-km separation, obtained as follows: the filtered (1.5-5.0 Hz) time series from each hydrophone was inverted, shifted in time by the water surface reflection time, weighted to maximize the increase in signal/noise, and added to itself; the two resulting time series were then added with the appropriate propagation delay, and weighted to maximize the increase in signal/noise. Signal/noise was increased by 90% of the theoretical maximum with this method, indicating a high level of coherence between the signals added.

Both covers are discussed elsewhere in the newsletter. An interesting question posed by the front cover is this:

"Would instruments with responses comparable to those of the short period components of the World-Wide Seismograph Network (WWSSN) be appropriate for the studies of regional and teleseismic body phases recorded on, or in, the ocean bottom?"

Reminder: You are invited to comment on topics presented in the newsletter and to provide other items of interest. Also, since it is difficult to be aware of all papers published in the many differing geophysical journals, advice on any omissions in the Po/So bibliography would be appreciated. Again, special thanks to RAI for sharing their Po/So spectrums with us.

References

Asada, T., and H. Shimamura, 1976, Observations of earthquakes and explosions at the bottom of the western Pacific: Structure of oceanic lithosphere revealed by Longshot experiment, The Geophysics of the Pacific Ocean Basin and Its Margins, edited by G. H. Sutton, M. H. Manghnani, and R. Moberly, Am. Geophys. Union Monograph 19, p. 135-153.

Bradner, H., and J. Dodds, 1964, Comparative seismic noise on the ocean bottom and land, J. Geophys. Res., 69, 4339-4348.

Bruns, J., and J. Oliver, 1959, The seismic noise of the earth's surface, Bull. Seismol. Soc. Amer., 49, 349-353.

Bungum, H., E. Rygg, and L. Bruland, 1971, Short-period seismic noise structure at Norwegian seismic array, Bull. Seismol. Soc. Amer., 61, 357-373.

Frantti, G., D. Willis, and J. Wilson, 1962, The spectrum of seismic noise, Bull. Seismol. Soc. Amer., 52, 113-121.

Gupta, I., and R. Blandford, 1983, A mechanism for generation of short-period transverse motion from explosions, Bull. Seismol. Soc. Amer., 73, 571-591.

McCreery, C., D. Walker, and G. Sutton, 1983, Spectra of nuclear explosions, earthquakes, and noise from Wake Island bottom hydrophones, Geophys. Res. Lett., 10, 59-62.

Nichols, R., 1981, Infrasonic ambient ocean noise measurements: Eleuthera, J. Acoustic. Soc. Am., 69, 974-981.

Talandier, J., and M. Bouchon, 1979, Propagation of high frequency Pn waves at great distances in the Central and South Pacific and its implications for the structure of the lower lithosphere, J. Geophys. Res., 84, 5613-5619.

Urick, R., Principles of Underwater Sound, McGraw-Hill, 1975.

Walker, D., 1977a, High-frequency Pn and Sn phases recorded in the Western Pacific, J. Geophys. Res., 82. 3350-3360.

Walker, D., 1977b, High-frequency Pn phases observed in the Pacific at great distances, Science, 197, 257-259.

Walker, D., 1982, Oceanic Pn/Sn phases: a qualitative explanation and reinterpretation of the T-phases, Hawaii Inst. of Geophysics Rept. HIG-82-6, 19 pp.

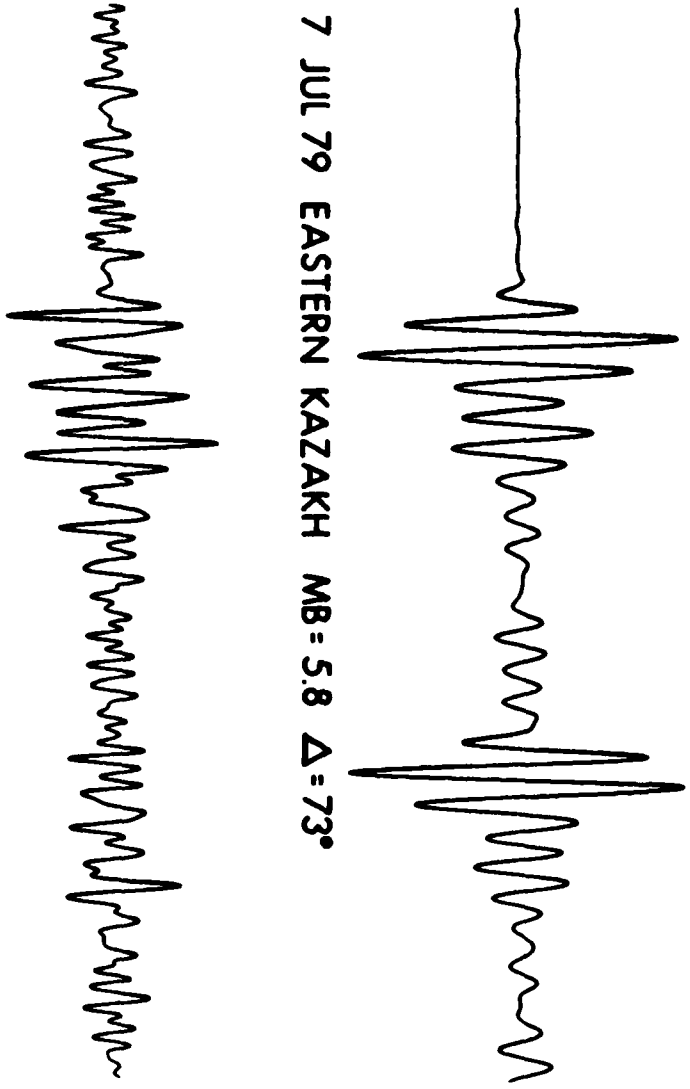

APPENDIX IX

The Continuous Digital Data Collection System for the Wake Island Hydrophones

by

Charles S. McCreery

at

Hawaii Institute of Geophysics

2525 Correa Road

Honolulu, Hawaii 96822

(808) 948-8767

ABSTRACT

A continuous digital data collection system was installed on Wake Island in August, 1982, to record seismic signals from an array of nearby hydrophones. Most of the hardware has been purchased "off-the-shelf" from various nationally known vendors. A few components have been built at the Hawaii Institute of Geophysics (HIG). Software for both the data collection and data reduction has been written at HIG. Some key features of the data collection system are: 1) 96 dB dynamic range (i.e., 16 bits), 2) up to 16 data channels, 3) accurate absolute timing ($\pm$ 1 msec, generally), 4) accurate interchannel timing, 5) power-failure recoverability, 6) up to 80 samples per second per channel (variable), 7) ease of operation (only four operator commands necessary), 8) operator intervention only once per day (to change up to 4 full reels of 9 track tape), and 9) common tape format (blocked data, 2 bytes per word, 2's complement notation). The preliminary data reduction consists of: 1) stripping off intervals of data for which seismic phases from known events are suspected of being present; and 2) stripping off randomly spaced 3-minute intervals (1 per hour on the average) as ambient noise samples. These tasks are accomplished by a series of programs run at HIG on a Harris H800 computer. This paper is primarily intended for the reader who wants to build a digital data acquisition system, or who wants to use the data collected by this particular system at Wake.

TABLE OF CONTENTS

INTRODUCTION

In June, 1979, HIG began operation of a four-channel (3 data, 1 time-code), slow-speed, cassette recording system for continuous monitoring of hydrophones located near Wake Island. The seismic data collected from this system have provided much needed information about ambient noise in the deep ocean, Po/So propagation, and the spectra at high frequencies (i.e., > 2 Hz) of deep mantle P phases from earthquakes and explosions recorded at great distances. However, the recording system itself had limitations which prevented more quantitative types of data analysis. These limitations included: 1) a dynamic recording range of only about 40 dB - this caused many signals to be clipped; 2) poor timing due to clock drift - absolute timing was accurate to only $\pm$0.3 sec.; 3) poor interchannel timing - differences in skew between the recording and playback heads could easily result in a 0.1 sec. timing error between channels; 4) analog format - a sophisticated, time consuming and data degenerating process was necessary to convert the analog signals to digital time series for further processing; and 5) only three of at least eleven working hydrophones could be recorded.

To eliminate these problems, a system was sought with the following general capabilities and constraints: 1) a large dynamic range to record, without distortion, events ranging from at least mb = 4.0 to mb = 8.0 (i.e., at least 80 dB); 2) Absolute timing accurate to less than 0.1 sec (for ease in processing, no time correction should need to be applied to acheive this accuracy); 3) Interchannel timing accurate to within only a small change in phase of the highest frequency of interest (e.g., 0.002 sec for a $\pi/8$ phase change at 30 Hz); 4) a digital recording format such that only a minimal amount of processing is necessary to convert the data to a widely

useable format; 5) the capability to record all eleven available hydrophones; 6) the recording of frequencies at least as high as those already observed at Wake in Po and So (i.e., 30 Hz); 7) operation of the system so simple that it can be accomplished by personnel untrained in computer hardware and software; 8) required servicing (i.e., changing tapes) no more than once per day; and 9) the capability of restarting automatically after power failures (which occur frequently at Wake). After exploring numerous options, a design was chosen which met the specifications outlined above, and also appeared to have the best chance for success in terms of the reliability and intercompatability of its components and the feasibility of writing the necessary data acquisition software. This system was purchased, assembled, softwared and tested between March and August, 1982, and was installed at Wake during the last week of August, 1982.

Because of the large volume of raw data which would be collected by this system (i.e., up to 1460 full reel, 9-track, computer tapes per year) a scheme was desired for compressing the data. Data types which were considered the highest priority for saving are: 1) seismic phases applicable to ongoing research topics, 2) ambient noise samples, and 3) seismic phases for future research topics. A system of programs was written to extract and save those intervals in the raw data which contain these priority events. These programs also manage the data for easy accessibility and transmission to other scientists.

RECORDING SYSTEM HARDWARE

The hardware used for the digital recording system is outlined in the flow chart of Fig. 1. The hydrophone signals are first amplified and shaped by the preamps and pre-whitening filters. Two of these signals are filtered further and used to create a helicorder-style seismogram. All of the signals from the preamps are converted to discrete time series by the A/D (analog to digital) convertor. The digitized data is then assembled into blocks and output to the tape drives by the LSI-11/2 computer. The satellite clock provides a time code for the helicorder, a synchronization signal for the A/D sampling pulse generator, and the date and time in digital format for inclusion with the data blocks written to tape. A more detailed description of the function of each component in Fig. 1 is given below:

Wake Hydrophones

The hydrophones are passive, moving-coil type, which are connected via cable to Wake Island. The estimated response is shown in Fig. 2. The hydrophones are located in two arrays. One array contains six sensors on the ocean floor at 5.5 km depth, and has an aperture of 40 km. The other array consists of five hydrophone pairs at SOFAR depth (1 km) and has an aperture of 300 km. Of the ten hydrophones in the SOFAR array, at least five of them at three sites appear to be working.

Preamp/Pre-Whitening Filters (HIG built)

The preamps are designed to have very low intrinsic noise levels because the hydrophone outputs are very small [as small as 10 nVolts/$(Hz)^{1/2}$ at 10 Hz]. The pre-whitening filters are designed to flatten the ambient

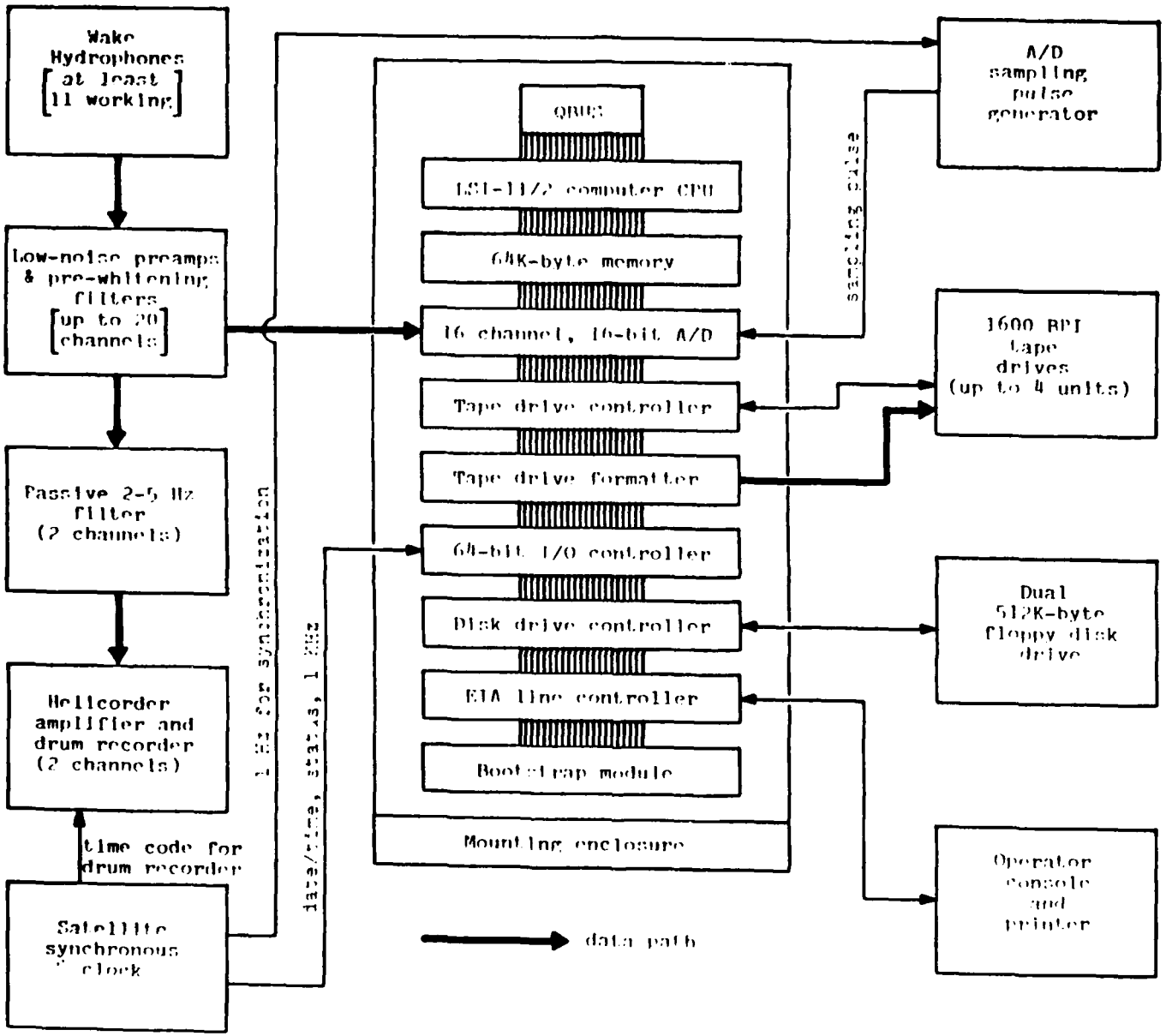

Figure 1. A general diagram of the hardware used for the Wake data acquisition system. Each device on QBUS represents a single printed circuit board, and these boards are mounted in the enclosure from top to bottom as shown.

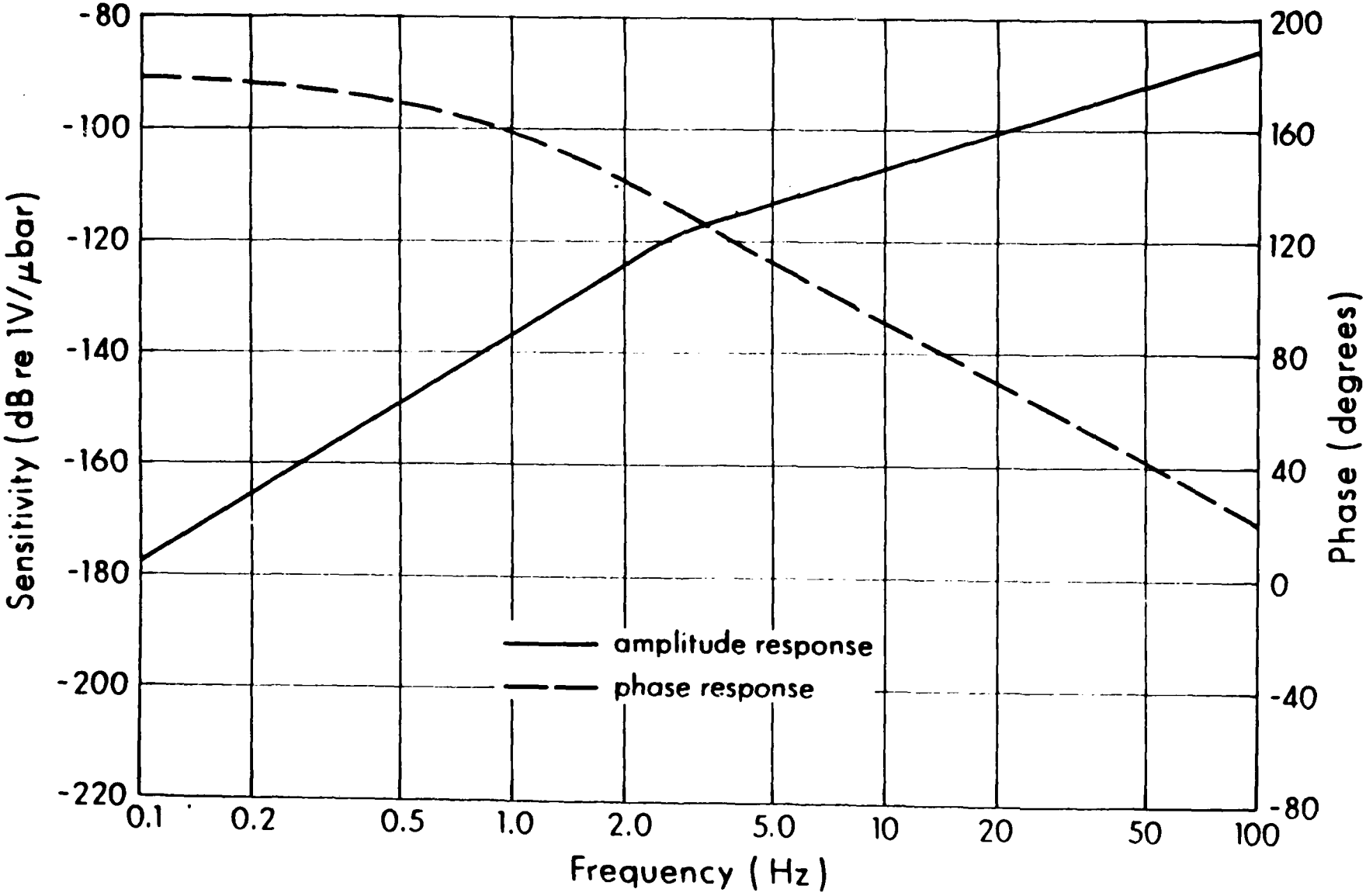

Figure 2. The estimated response of the Wake hydrophones (taken from the Columbia University's OBS Calibration Manual by S. N. Thanos, 1966).

ocean-bottom noise spectrum out of the hydrophone (measured previously using analog data), for the purpose of maximizing the dynamic recording range at all frequencies. Anti-aliasing filters and a 60 Hz notch filter are also included. The output amplifier stage has 10 gain steps (0-9), each 3 dB apart, which can be manually set. The response of the preamp/pre-whitening filters is shown in Fig. 3 (for gain step 9).

A/D Convertor (Data Translation Model DT2784SE/DT5716-B

The A/D convertor is designed to fit into the backplane of the LSI-11/2 computer (i.e., into. QBUS), with a cable and connector for receiving the signals to be digitized. The resolution is 16 bits, giving decimal values between -32,768 and +32,767 for inputs between -10.0 and +10.0 Volts, respectively. Up to 16 single ended inputs are acceptable, and the maximum throughput rate is 2.5 kHz (i.e., a minimum of 0.4 msec between samples). Simultaneous sample and hold of all channels is not available on this board, so the 16 channels are sampled sequentially. Furthermore, the design of this device actually requires that all 16 channels be sampled sequentially; the data of unwanted channels being discarded by the software. The trigger which causes a sample to be taken is provided externally by the A/D sampling pulse generator. An example of the temporal spacing between data points which is created by this scheme is shown in Fig. 4. Digital output from the A/D convertor is loaded directly into the LSI-11/2 core memory via direct memory access (DMA).

Satellite Clock (Kinemetrics model 468 DC)

The satellite clock provides inexpensive accurate time at a remote site by monitoring signals from the GOES satellites (East or West). Accuracy is

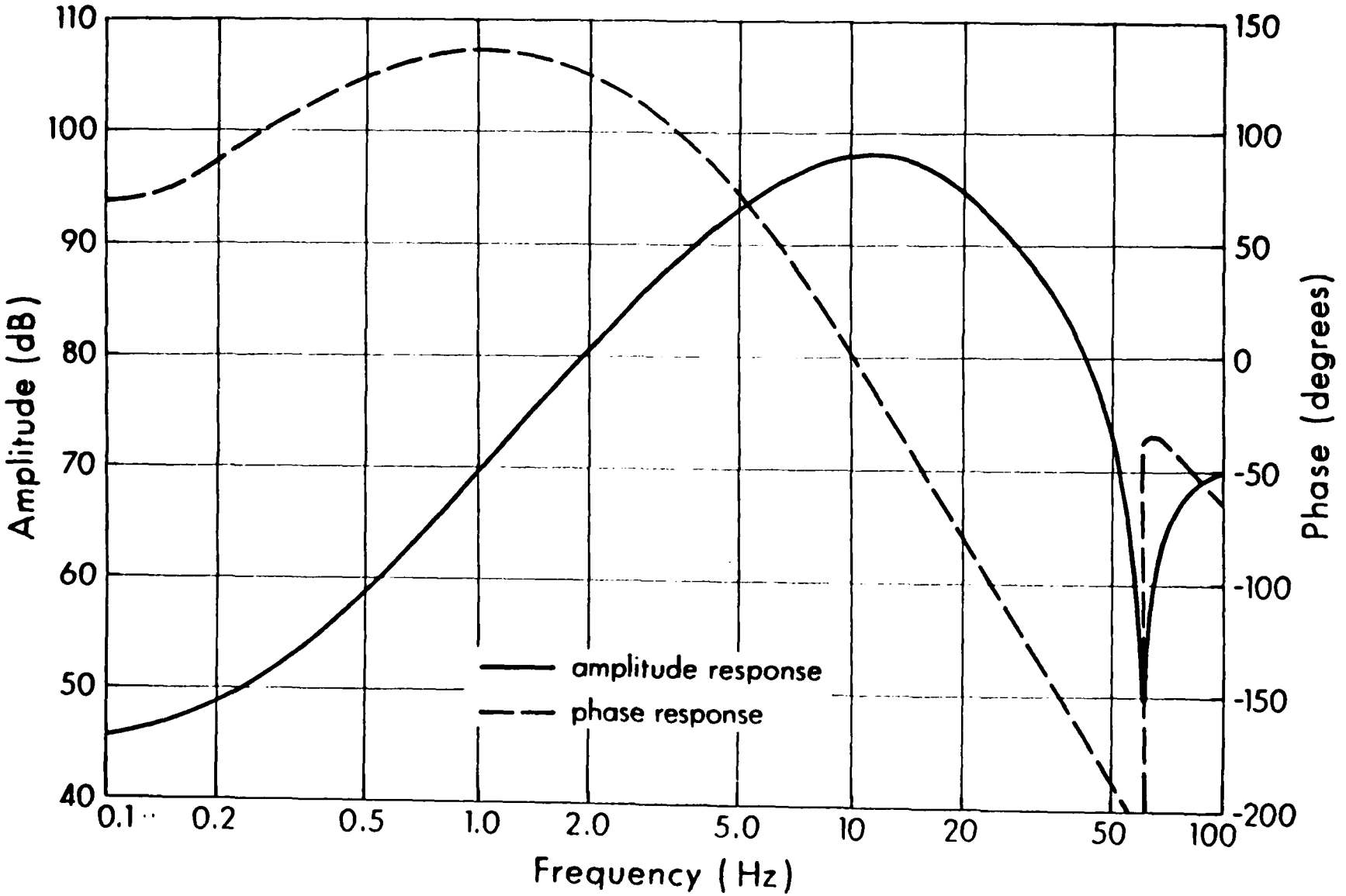

Figure 3. The response of the preamp/pre-whitening filters at gain step 9 (of 0-9). Subtract 3 dB from the amplitude response for each gain step down from 9.

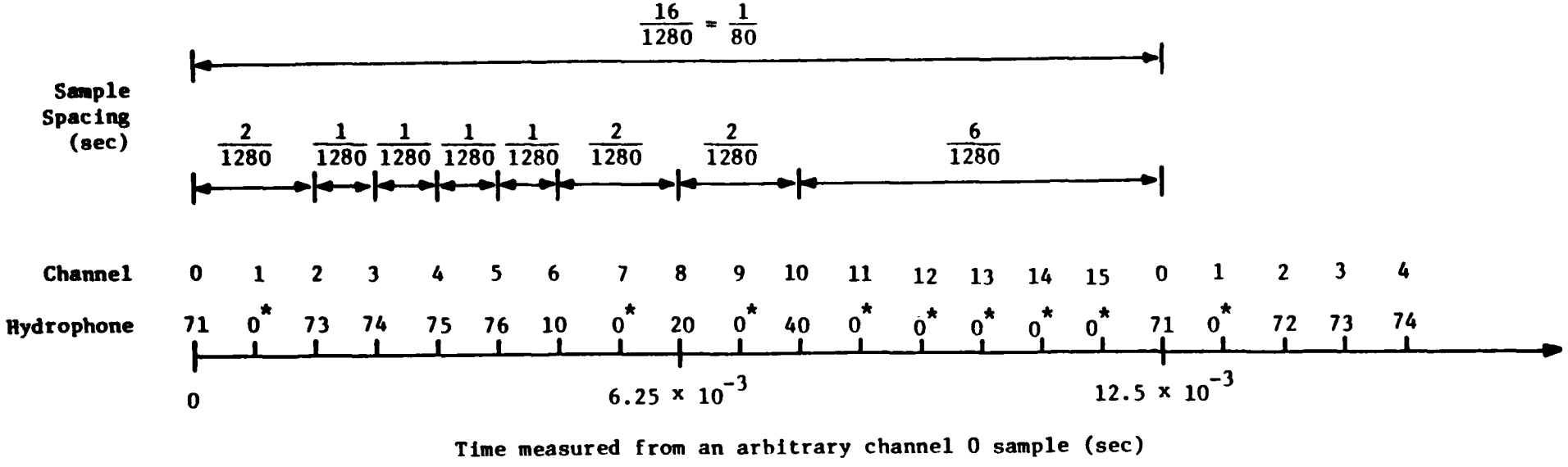

Figure 4. An example of the temporal spacing between data channels created by the data acquisition hardware and software for a sampling rate of 80 samples/second/channel. Hydrophones numbered 0 (also starred, *) are for unwanted data channels which are sampled by the A/D convertor but later discarded by the WAKEUP software. This channel/hydrophone information is written into the header part of each data block. The configuration shown is one which has been in use since the system was installed.

better than ±1 msec when the satellite signal is being received. The time, in Julian days through milliseconds, is output in parallel BCD format through 45 pins of a 50 pin connector. This connector also contains 4 pins for the clock status (i.e., the worst case clock accuracy based on the amount of time since satellite synchronization was lost), and 1 pin with a 1 kHz square-wave used to determine when the other pins can be read (i.e., are not changing states). Also output (on BNC connectors) are a 1 Hz square-wave used to synchronize A/D sampling with the clock, and a slow code used for marking time on the helicorder record.

A/D Sampling Pulse Generator (HIG built)

This device is used to create precisely timed pulses (downward zero-crossings) which are synchronized with the satellite clock and trigger A/D conversions. The front panel has thumbwheel selectors for setting the number of channels of data to be sampled (always 16 in this system due to the A/D convertor; software discards unwanted channels), and the sampling rate (in samples/sec/channel). For 16 channels of data, sampled at 80 samples/sec/channel, the pulse generator produces a 1280 Hz square-wave. A/D synchronization with the clock is necessary so that the starting times of output data blocks, which are assembled for a constant number of A/D conversions, will also remain synchronized over long periods of time.

Mounting Enclosure (DEC model BA11-NE)

The mounting enclosure contains the power supply, backplane (QBUS), and cooling fan for the LSI-11/2 computer. The backplane has quad connectors for nine boards, all of which are occupied in this system configuration.

These nine boards, and the order in which they are placed from top to bottom in the enclosure, are noted in Fig. 1.

LSI-11/2 Computer (DEC model KD11-HA)

This is the central processing unit of the computer.

64 K-byte memory (DEC model MSV11-DD)

This is the core memory for the computer, consisting of 32K 2-byte words.

Bootstrap module (DEC model BDV11-AA)

This module brings up the computer from a down or power fail status, and causes the RT-11 operating system to be loaded from the disk.

64 Bit I/O Controller (DEC model DRV11-J)

This board is necessary to interface the LSI-11/2 with the 50 pin output of the satellite clock. The 64 bits of I/O correspond to four two-byte words which may be accessed by the software to read the clock.

Floppy Disk Drive Controller (DEC model RXV21-BA)

This board interfaces the disk drive to the computer.

Dual 512K Byte Floppy Disk Drive (DEC model RXV21-BA)

The floppy disks contain all of the software necessary for performing data acquisition with the hardware. Under the present configuration, one disk contains the DEC RT-11 operating system software, while the other disk contains the programs written at HIG for collecting the data and a

parameters file which describes the exact configuration to be run (i.e., number of channels of data, blocksize, etc.). It is possible, should one disk drive become faulty, to combine all of the programs and data on one disk, and run from a single drive. A special function of the disk drive is to record the number of the current tape drive to which the data are being written. In the case of a power failure, which causes the core memory of the LSI-11/2 to be lost, the current tape drive number is necessary to safely and efficiently resume recording.

EIA Line Controller (DEC model DLV11-J)

This device provides four ports (0 to 3) for serial I/O (RS-232C, RS-422, or RS-423) to the LSI-11/2. Port 3 is the only one in use under the current operating configuration and interfaces to the DEC LA38-GA which is serving as both a line printer and operator console at 300 baud. Separate ports for the line printer and a CRT operator console were used during program development to facilitate higher baud rates.

Console and Printer (DEC model LA38-GA)

This device is used for all operator input and output (I/O) with the system, and for all program messages. Since there is actually very little I/O to this device, its slow speed is not a problem. Also, there is a distinct advantage in having a hardcopy record of certain essential I/O, especially since the system is at a remote site. Sample I/O is shown in Fig. 5.

Tape Controller and Formatter (DATUM model 15221)

```
WAKE HYDROPHONE ARRAY CONTINUOUS DIGITAL SEISMIC RECORDING SYSTEM

USING DRIVE 2              DATE 1983:153   TIME/08:06:00:000   CLOCK/00
USING TAPE 10781
DRIVE 2 END OF TAPE REACHED
        05820 BLOCKS WRITTEN
USING DRIVE 3              DATE/1983:153   TIME/18:10:59:999   CLOCK/00
USING TAPE 10782
DRIVE 3 END OF TAPE REACHED
        05824 BLOCKS WRITTEN
DRIVE 0 OFFLINE
USING DRIVE 1              DATE/1983:154   TIME/00:16:19:999   CLOCK/00
USING TAPE 10783
SWITCH DRIVES
DRIVE 1 05217 BLOCKS WRITTEN

WAKE HYDROPHONE ARRAY CONTINUOUS DIGITAL SEISMIC RECORDING SYSTEM

USING DRIVE 2              DATE 1983:154   TIME/07:31:04:999   CLOCK/00
USING TAPE 10784
DRIVE 2 END OF TAPE REACHED
        05824 BLOCKS WRITTEN
USING DRIVE 3              DATE/1983:154   TIME/15:36:24:999   CLOCK/00
USING TAPE 10785
DRIVE 3 END OF TAPE REACHED
        05804 BLOCKS WRITTEN
DRIVE 0 OFFLINE
USING DRIVE 1              DATE/1983:154   TIME/23:40:04:999   CLOCK/00
USING TAPE 10786
RESET-WAIT FOR MINUTE
DRIVE 1 06065 BLOCKS WRITTEN

WAKE HYDROPHONE ARRAY CONTINUOUS DIGITAL SEISMIC RECORDING SYSTEM

USING DRIVE 2              DATE 1983:155   TIME/08:11:00:000   CLOCK/00
USING TAPE 10787
DRIVE 2 END OF TAPE REACHED
        05822 BLOCKS WRITTEN
USING DRIVE 3              DATE/1983:155   TIME/16:16:10:000   CLOCK/00
USING TAPE 10788
DRIVE 3 END OF TAPE REACHED
        05807 BLOCKS WRITTEN
DRIVE 0 OFFLINE
USING DRIVE 1              DATE/1983:156   TIME/00:20:05:000   CLOCK/00
USING TAPE 10789
SWITCH DRIVES
DRIVE 1 05063 BLOCKS WRITTEN
```

Figure 5. A sample of 3 consecutive days of I/O through the console at Wake. Operator input has been underlined (S, R, and S). The operator writes-in the WAKEUP tape identification numbers.

The tape controller interfaces the tape drives with the LSI-11/2. Only one controller is necessary for the four tape drives used. The formatter encodes the blocks of data written to tape, and decodes the blocks read from the tape. Only one formatter is necessary for the four tape drives.

Tape Drives (DATUM model D451)

Four 1600 bpi tape drives (0-3) are available for writing out the digitized data. Data is written to one drive until its tape is full (or until a specified number of blocks have been written), then data is written to the next drive in the sequence until its tape is full, and so on. Four tape drives are required if tapes are changed only once per day, since one day's data (11 channels at 80 samples/sec/channel) fills four tapes. An important feature which these tape drives have, is that they re-tension the tape, advance the tape several inches for safety, and put themselves "on line" after a power failure. This is an important factor which allows the system to start collecting data again without operator intervention or the unnecessary loss of data.

2-5 Hz Filter (HIG built)

The two-channel 2-5 Hz bandpass filter is for filtering the two signals going to the drum recorder in a way which enhances signal to noise ratios of teleseismic P from underground nuclear tests. The filters are a two-pole passive RC design with the response shown in Fig. 6

Helicorder Amplifier and Drum Recorder (Teledyne Geotech models AR-311 and RV-301)

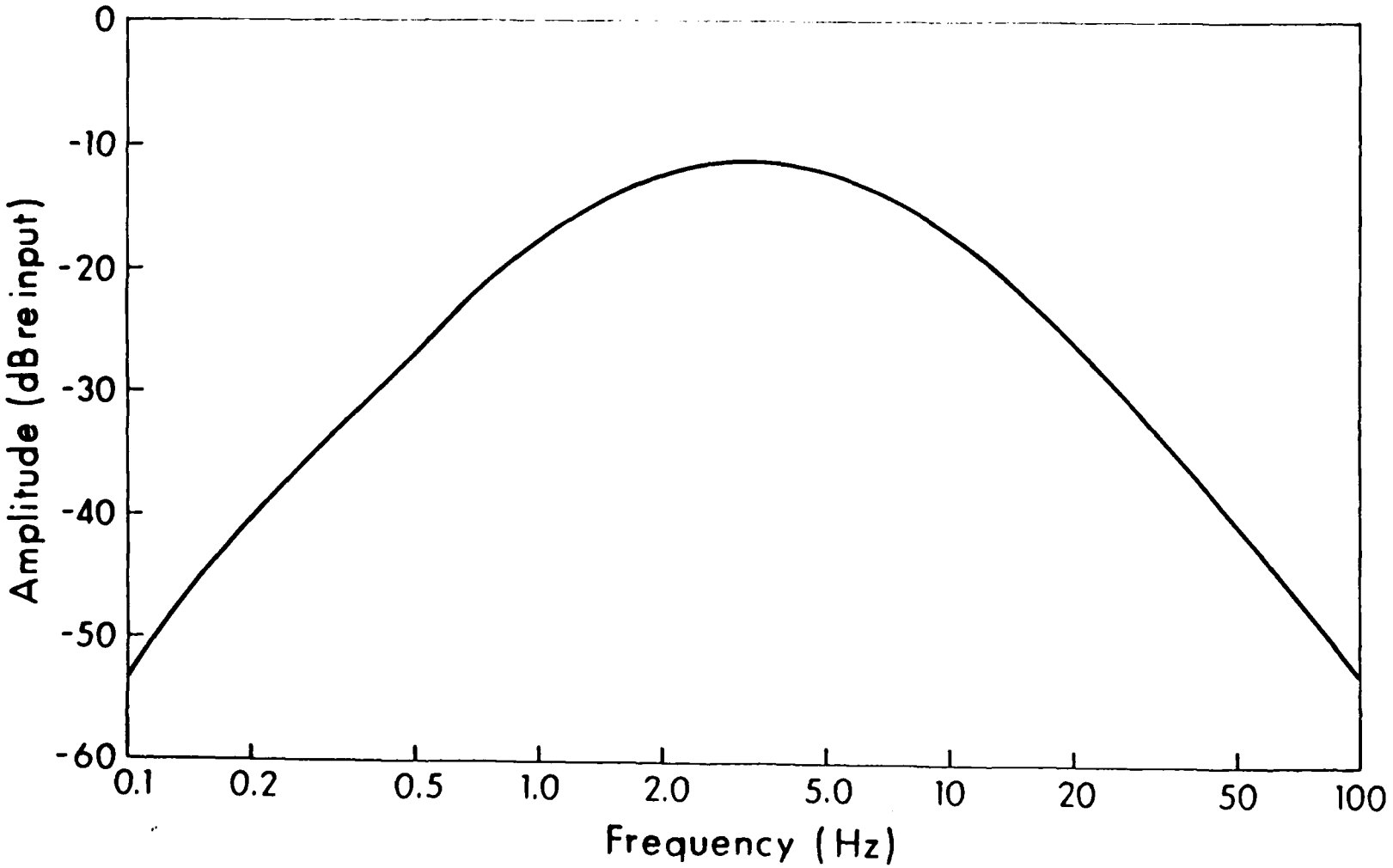

Figure 6. Response curve for the 2-5 Hz filter which precede.. the helicorder.

This equipment is used to provide easily scanable visible records of the continuous seismic data. The recorder has two pens for the two input signals, and is geared so that one recording sheet lasts 24 hours. Additionally, the amplifiers and drum recorder are powered by a trickle charged, automobile battery backup system to provide continuous operation through power failures. Time code is input from the satellite clock. A sample helicorder record is shown in Fig. 7.

CONTINUOUS DATA ACQUISITION SOFTWARE

The data acquisition program, titled WAKEUP, is written in assembler code and executed under the RT-11 operating system. A simplified flow chart of this software is shown in Fig. 8. Some key features of program WAKEUP are: 1) it is controlled by an input parameters file which can be changed to satisfy differing data collection requirements; 2) it is extremely simple to run - only four, one-letter, operator commands (to be discussed later) are recognized; 3) it can restart itself after a power failure; and 4) it makes a hardcopy log of important program events.

WAKEUP Parameters

The WAKEUP running parameters can be displayed and changed by an interactive fortran program called PARAMS. A sample run of PARAMS is shown in Fig. 9. The parameters and their meanings are described below:

Digitization Rate. The value set here should be the same as the value set on the A/D sampling pulse generator for samples/sec/channel.

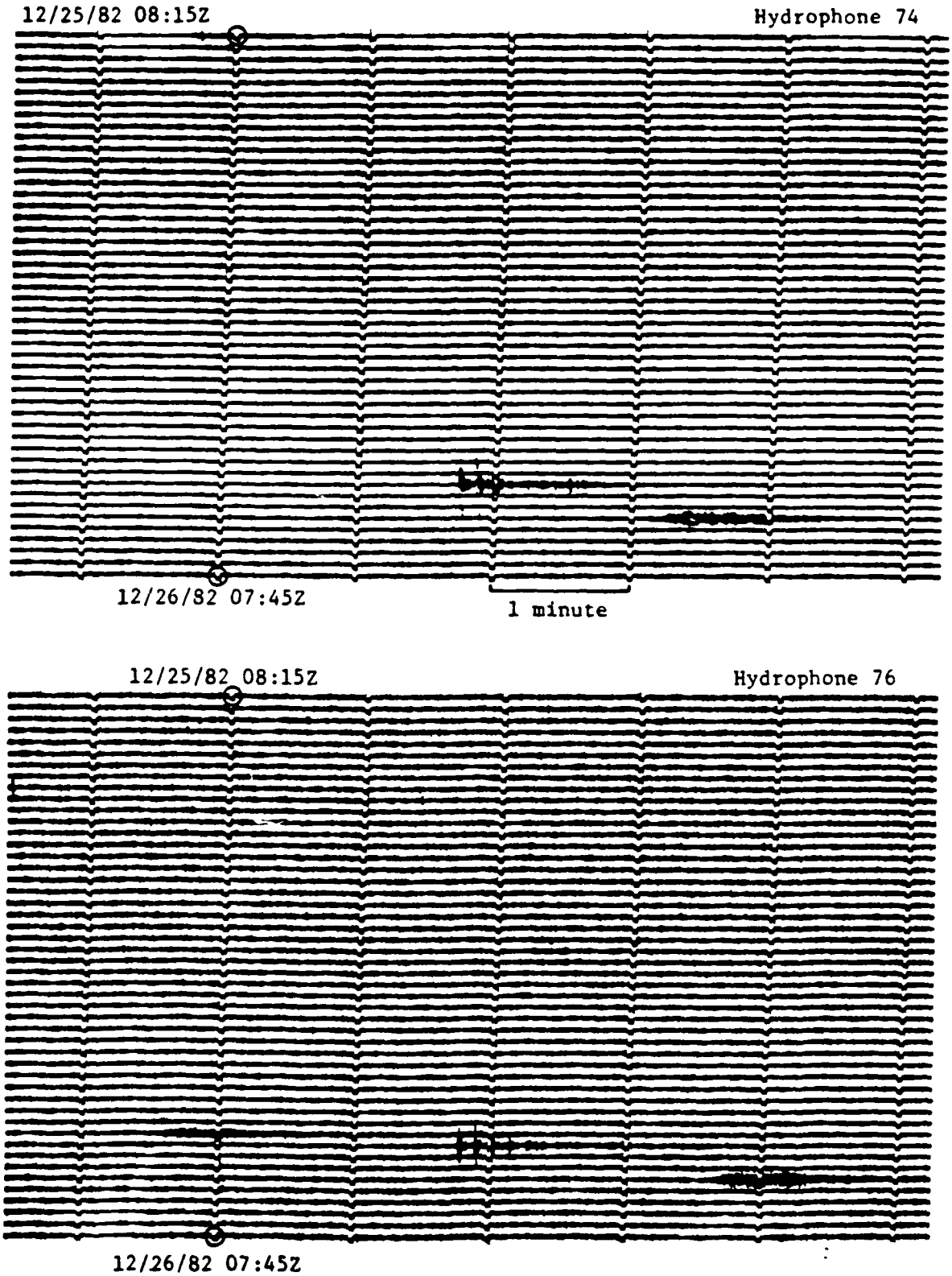

Figure 7. A section of helicorder record from Wake showing the P arrival from an Eastern Kazakh explosion (the impulsive arrival) and some other unidentified arrivals which are probably T-phases. There are 30 minutes between each trace.

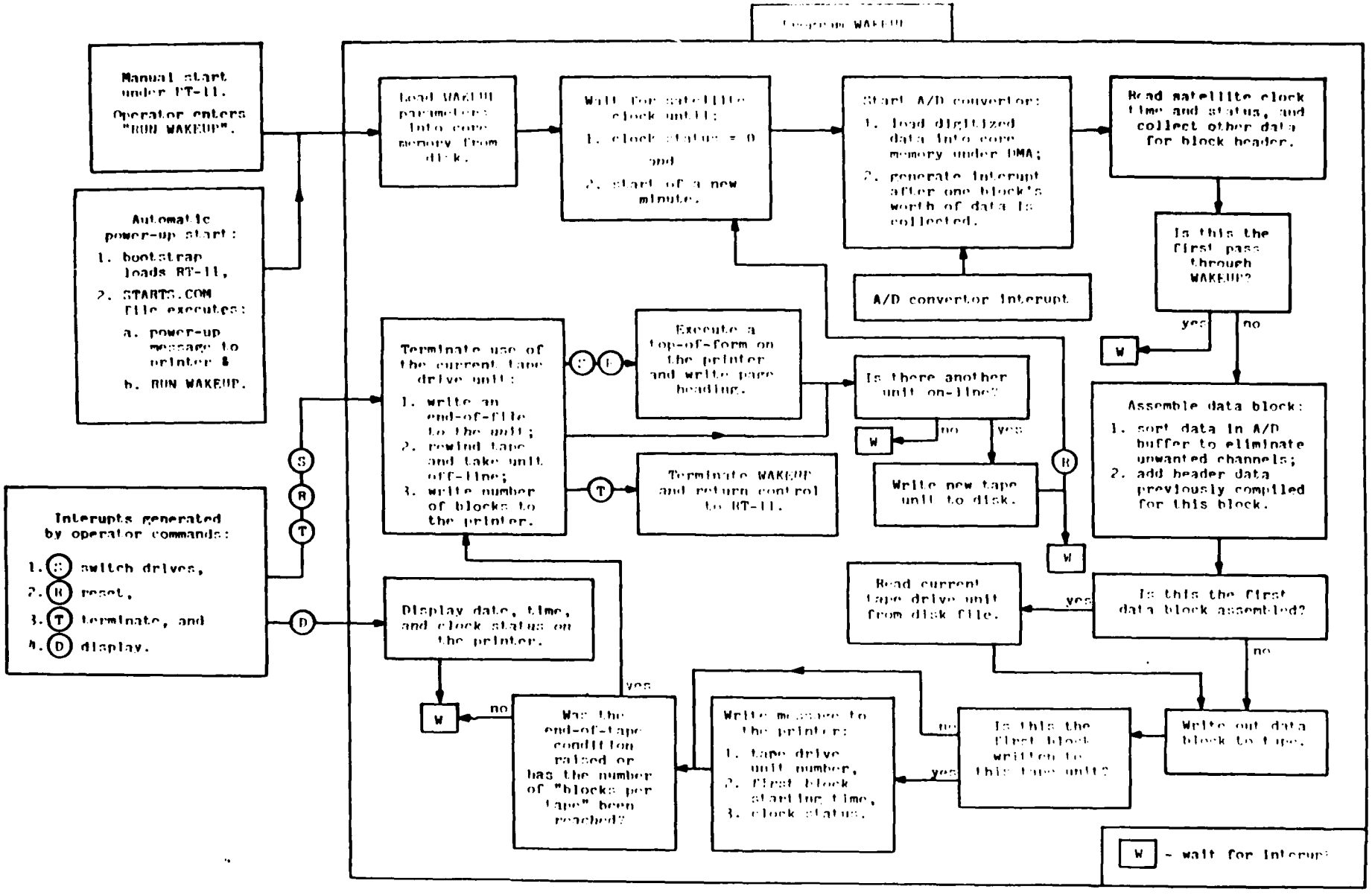

Figure 8. Generalized logic flow-chart of program WAKEUP which controls the data acquisition. The program is started either manually, or automatically after a power failure. The A/D convertor interupt has a high priority and is serviced immediately. The operator command interupts are low-priority and are serviced when the CPU is in the wait (W) condition. Paths marked S, R, T, or D are followed (only once) after the corresponding operator interupt is serviced. Three data buffers are used; two of them provide a double buffer for DMA output from the A/D convertor, and the third is used for assembling the data block to be output to tape.

```
.RUN PARAMS

PARAMS - SETTING WAKEUP PARAMETERS

CURRENT PARAMETER VALUES
DIGITIZATION RATE:  80 SAMPLES/CHANNEL/SEC
SECONDS PER TAPE BLACK:  5
CH  HYD  AMP  GN  CH  HYD  AMP  GN  CH  HYD  AMP  GN  CH  HYD  AMP  GN
 0   71    6   9   1   72    8   9   2   73    9   9   3   74    0   9
 4   75   19   9   5   76    1   9   6   10   13   9   7   11   16   9
 8   20   11   9   9   21    3   9  10   40   18   9  11    0    0   0
12    0    0   0  13    0    0   0  14    0    0   0  15    0    0   0
BLOCKS PER TAPE:  32000
UNIT - DRIVE SERIAL NUMBER:  0-318  1-319  2-322  3-326
STARTING TAPE UNIT NUMBER:  0
YEAR:  1982   JULIAN DAY:  250

ENTER COMMAND (8 TO DISPLAY COMMANDS).  8

COMMAND - FUNCTION
 0 - CHANGE DIGITIZATION RATE.
 1 - CHANGE SECONDS PER BLOCK.
 2 - CHANGE A/D CHANNEL ASSIGNMENTS.
 3 - CHANGE BLOCKS PER TAPE.
 4 - CHANGE TAPE UNIT SERIAL NUMBER.
 5 - CHANGE STARTING UNIT NUMBER.
 6 - CHANGE YEAR/JULIAN DAY.
 7 - DISPLAY CURRENT PARAMETER VALUES.
 8 - DISPLAY COMMAND FUNCTIONS.
 9 - UPDATE AND DISPLAY WKPARM AND RCOVRY.
10 - CHANGES COMPLETE.  UPDATE AND EXIT.

ENTER COMMAND (8 TO DISPLAY COMMANDS).  10

DK:WKPARM.BIN
 80      400      4400       71        69       72       89       73
 99       74         9       75       199       76       19       10
139       11       169       20       119       21       39       40
189        0         0        0         0        0        0        0
  0        0         0     6400     32000      318      319      322
326        5         0        0         0        0        0        0
DK:RCOVRY.BIN
  0     1982       250        0         0        0        0        0
  0        0         0        0         0        0        0        0
  0        0         0        0         0        0        0        0
  0        0         0        0         0        0        0        0
  0        0         0        0         0        0        0        0
  0        0         0        0         0        0        0        0
DK:WKPARM.BIN AND DK:RCOVRY.BIN UPDATED.

STOP --

.
```

Figure 9. A sample run of program PARAMS which is used to change (or view) the running parameters of program WAKEUP. These parameters are stored on disk files DK:WKPARM.BIN and DK:RCOVRY.BIN. Operator commands have been underlined.

Seconds Per Tape Block. This value, multiplied by the sampling rate and by the number of active data channels, will determine the total number of samples per block. The number of samples per block should not exceed 5000 due to size limitations in the core memory containing the buffers. Very small blocksizes should also be avoided, since the time to write a very small block to tape may exceed the time necessary to collect the data block.

Channel Number (CH). This is not a changeable parameter, but merely indicates which channel (0-15), of the A/D convertor, is being referred to.

Hydrophone (HYD). This parameter indicates which hydrophone (71-76 for the bottom array, and 10, 11, 20, 21, 40, and 41 for the SOFAR array) is connected to the A/D channel. If 0 is specified, then the channel is considered inactive. To compute the number of active channels, simply count the number of channels with non-zero values for this parameter (11 for the example in the figure). It is not necessary that the active channels be contiguous as shown in the figure.

Amplifier (AMP). This parameter indicates which of the preamp/pre-whitening filters (1-20) the hydrophone signal is connected to.

Gain (GN) . This parameter indicates the gain step (0-9) manually set on the final stage of the preamp/pre-whitening filters.

Blocks Per Tape. This parameter will set the number of blocks written to any tape drive before the next tape drive is used. When the value is set to a large number, as shown in the example, the program will write to a drive until the end-of-tape mark is sensed before switching drives. Estimates of how many blocks may fit on a tape can be computed by dividing the block length in bytes by 1600 bytes per inch, adding the length of the preamble, postamble and inter-record gap (~0.6 inches), and dividing into the tape length (28800 inches for a full-reel).

Unit-Drive Serial Number. This information is used to indicate which physical tape drive is connected to the tape drive unit (0-3) recognized by the computer.

Starting Tape Unit Number. This parameter is used to determine which tape drive to write to at the start of program WAKEUP. It is continually updated by WAKEUP to facilitate a smooth recovery after a power failure.

Year and Julian Day - These parameters are necessary because the satellite clock does not output the year. WAKEUP continually reads the Julian day from the parameters file and then updates it with the value ouput by the satellite clock. When the satellite clock Julian day is less than the Julian day in the parameters file (i.e., at the beginning of a new year), then the year is incremented by one.

Next in the example shown in Fig. 9, the user has typed 8 to display all the commands. No changes were necessary so a 10 was then typed to exit PARAMS.

The values in the parameters file (actually two files, DK:WKPARM.BIN and DK:RCOVRY.BIN) are displayed and control returned to the system.

Current WAKEUP Configuration

The WAKEUP configuration, set up by PARAMS, which has been in operation from 8 September 82 to the present (16 June 83) has the following key features: 1) data is digitized at a rate of 80 samples/sec/channel; 2) there are 8 active channels which are (given in the order in which they are multiplexed) 71, 73, 74, 75, 76, 10, 20, and 40 as previously described in Fig. 4; 3) each block contains 5 seconds of data which produces a block size of 3300 2-byte words (i.e., 3200 words of data plus a 100 word block header) and 4) the number of blocks per tape is large so that tapes are always written to their end-of-tape marks. Although it had been intended to digitize and record 11 hydrophones, which would produce 4 tapes per day, assorted problems with the tape drives have made it necessary to only record 8 hydrophones, which produces 3 tapes per day.

WAKEUP Operator Commands

Because Wake Island is such a remote place, and because those who must operate the system are untrained in computer hardware or software, program WAKEUP has been designed to handle many unusual situations without operator intervention. Only four operator commands are necessary during continuous data collection under WAKEUP, and these are described below:

Switch Drives(S). This command is used to force WAKEUP to write to the next available tape drive. This command is normally executed once per day when the operator comes in to change tapes. First he changes tapes on

those drives which have tapes full of data, and allows WAKEUP to continue writing onto the current drive. When fresh tapes are mounted, he executes the S, which causes WAKEUP to start writing to a fresh tape, and then he changes tapes on that last drive. A sample of S is shown in Fig. 5.

Reset(R). The reset command is nearly identical to the switch drives command, except that WAKEUP will wait for the satellite clock to indicate a change in the minute before it starts the A/D convertor collecting data for the next block. It is desirable to have data blocks which start on an integral second, (or integral minute) because it makes the measurement of time on plots, made later on during data reduction, somewhat simpler. Under ideal conditions, once the block beginnings are synchronized with the minute (i.e., if the number of seconds per block is 5, then all blocks should begin at 0, 5, 10, 15, 20, 25, 30, 35, 40, 45, 50, or 55 seconds after the minute) they should stay that way forever. Unfortunately, the satellite clock sometimes loses synchronization with the satellite for a while and begins to drift. When resynchronization occurs, the accumulated error gets propagated into the starting times of the blocks. When the operator notices this condition, he can correct it by using reset instead of switch drives. A sample of R is shown in Fig. 5.

Terminate (T). This command is used to terminate WAKEUP and return control to the RT-11 operating system.

Display (D). This command is used to display the date, time, and clock status at the beginning of the last data block collected.

Power Fail Recovery

Probably the most harmful abnormal condition, in terms of potential loss of data, from which WAKEUP can recover without operator intervention is a power failure. Temporary periods without power are fairly common on Wake and can be due to storms, construction, and generator problems. Since an operator is only present once per day, an irrecoverable system crash due to a short power failure could cause the loss of the entire day's data. Fortunately, with the help of some unique features in the Datum tape drives (described previously), the DEC LSI-11/2 hardware, and the RT-11 operating system, it was possible to write the WAKEUP program with the capability to resume collecting data after a power failure, without wasting tape (which could cause the system to run out of tape before the operator arrived) and without writing over old data. An essential element of this recovery capability is that the particular tape drive being written to is stored on a disk file. When power comes back after a failure, WAKEUP reads this file and then resumes writing to the proper drive.

WAKEUP Log

All operator input as well as RT-11 and WAKEUP messages and operator prompts go through the printer/console to create a log of events. A sample of this log is shown in Fig. 5, and has already been referred to several times. This log is essential for keeping track of normal system operations as well as problems which occur from time to time. The operator is

responsible for filling in the identification numbers of tapes mounted on each drive.

WAKEUP Tape Format

The WAKEUP tapes are numbered sequentially beginning with 10001. A detailed description of the format of the tapes and the blocks contained within the tapes is given in Fig. 10. The date and time given in the header are for the first data point in the block.

PRELIMINARY DATA REDUCTION SOFTWARE - WAKE HYDROPHONE INFORMATION PROCESSING SYSTEM (WHIPS)

Because of the large amount of data which is collected by this system (i.e., 50 billion bytes per year or 1500 tapes per year for 11 channels at 80 samples/sec/channel) it was realized that some sort of data compression scheme would have to be implemented in order to efficiently store, manage, retrieve, and distribute those data of current and future interest. These data have been defined in two general categories: 1) seismic phases such as P. S, Po, So, and T, and 2) ambient background noise. Software to sample these categories has been written and its structure is diagramed in the flow chart of Fig. 11. Intervals of data are saved when seismic phases from particular events are suspected of being present; and, in addition, 3-minute intervals of data selected at random times, with an average of one interval per hour, are also saved in order to sample the ambient noise. Three minutes of data is long enough to view several cycles at the longest periods thus far observed on the hydrophones - 20 seconds, and also long enough to provide reasonable statistics on the higher frequencies (1-20 Hz) where most of the oceanic, short-period seismic data are present. By sampling at

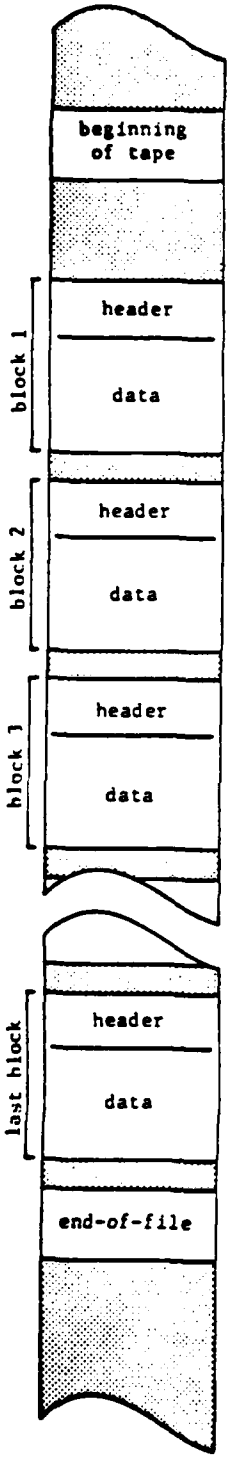

WAKEUP Tape Description

General Format: 1600 BPI
2 bytes per word
IBM format
2's complement notation

All Blocks	
header: words 1-100 data: words 101-end	
Word(s)	**Description**
1	Year (e.g., 1983)
2	Julian day (1-366)
3	Hour
4	Minute
5	Second
6	Millisecond
7	Digitization rate (samples/sec/channel)
8	Number of samples/channel/block
9	Total number of samples/block
10-41	A/D channel information - 16 channels, 2 words per channel 1st word - hydrophone I.D. number (0 if channel not used) 2nd word - hundreds and tens digit is the amplifier I.D. number, units digit is the amplifier gain step
42	Tape unit (0-3)
43	Tape drive serial number
44	Clock status
45	A/D buffer size
46-100	Not used
101-end	Digitized hydrophone data (multiplexed-order of hydrophones is the same as the order of the active channels described in words 10-41)

Figure 10. The WAKEUP tape format.

Wake Hydrophone Information Processing System (WHIPS)

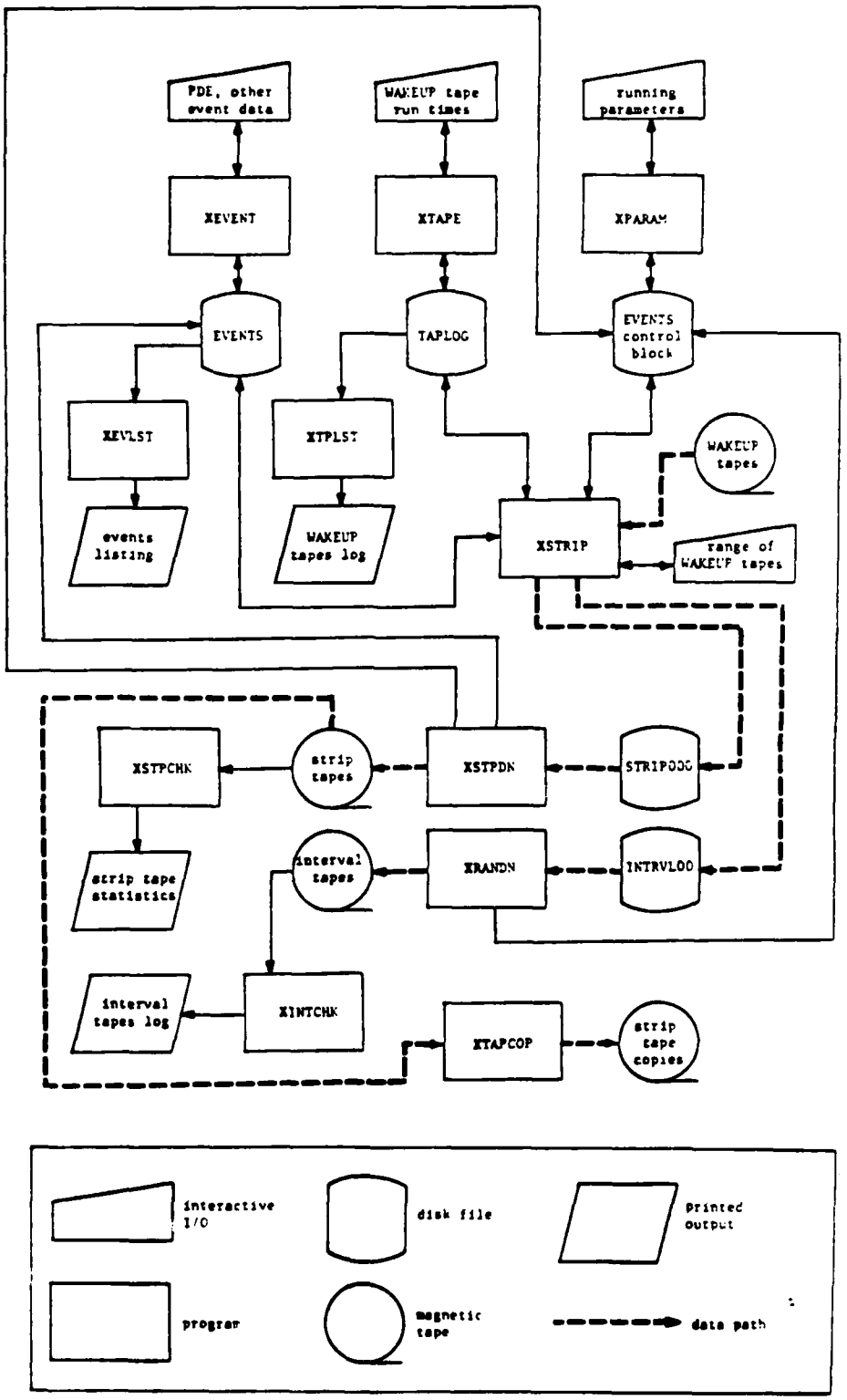

Figure 11. Generalized flow chart of the programs and files used in the preliminary reduction of the Wake digital data.

random time intervals, periodic noise of artificial nature is hopefully avoided. This system of programs and files which performs processing of the WAKEUP data is called WHIPS for Wake Hydrophone Information Processing System, and is run on a Harris model H800 computer.

WAKEUP Log Entry (XTAPE)

An initial step in the WHIPS procedure is to create or update file TAPLOG, which contains an identification number, starting time, block count, and status of each tape created by WAKEUP. This information is entered from the WAKEUP log (Fig. 5), using interactive program XTAPE. The data is necessary, as input to program STRIP, for calculating the time window to be processed for the compression of a given range of WAKEUP tape. Some sample data contained in TAPLOG, and printed out using program XTPLST is shown in Fig. 12. The total time represented on an individual tape can be found by multiplying the number of blocks by the number of seconds per block (which is 5 seconds per block for the tapes shown). The tape status indicates whether the tape is available for current or further processing (ACTIVE), or has been recycled (RECYCL).

Event Data Entry (XEVENT)

Another initial step in the WHIPS procedure is to create or update file EVENTS, which contains data about each earthquake for which an interval of data is to be saved. A sample of data contained in this file has been listed using program XEVLST and is shown in Fig. 13. Hypocenter/origin-time data are taken mostly from the Preliminary Determination of Epicenter (PDE) lists, published by the National Earthquake Information Service (NEIS), although other sources of data are used to complement the PDE's when

PAGE 001
5 JUL 83

WAKE HYDROPHONE INFORMATION PROCESSING SYSTEM

WAKEUP TAPE LOG LIST

TAPE#	----START TIME---- YR	JLN	HR	MN	SC	MIL	#BLKS	STATUS
10561	83	076	05	27	25	000	5783	ACTIVE
10562	83	076	13	29	20	000	5791	ACTIVE
10563	83	077	05	12	40	000	5766	ACTIVE
10564	83	077	13	13	10	000	5824	ACTIVE
10565	83	078	05	15	15	000	5922	ACTIVE
10566	83	078	13	28	45	000	5829	ACTIVE
10567	83	079	04	34	45	000	5862	ACTIVE
10568	83	079	12	43	15	000	5796	ACTIVE
10569	83	080	05	17	25	000	5857	ACTIVE
10570	83	080	13	25	30	000	5805	ACTIVE
10571	83	081	06	15	50	000	5874	ACTIVE
10572	83	081	14	25	20	000	5827	ACTIVE
10573	83	081	22	30	55	000	4895	ACTIVE
10574	83	082	05	18	50	000	5860	ACTIVE
10575	83	082	13	27	10	000	5787	ACTIVE
10576	83	082	21	29	25	000	5605	ACTIVE
10577	83	083	05	16	30	000	5755	ACTIVE
10578	83	083	13	16	05	000	5805	ACTIVE
10579	83	083	21	19	50	000	5696	ACTIVE
10580	83	084	05	14	30	000	5856	ACTIVE

Figure 12. A sample of the WAKEUP tape information contained within WHIPS file TAPLOG which has been printed using program XTPLST. A detailed description of this printout is contained in the text.

WAKE HYDROPHONE INFORMATION PROCESSING SYSTEM (WHIPS) EVENT LISTING 22 JUN 83

KEY: INFORMATION SOURCES - PDE=NEIS PDECARD, MON=NEIS MONTHLY LIST, ICS=ICS LIST, HEL=HELICORDER, OTH=OTHER
EVENT TYPE - EQ=EARTHQUAKE, NX=NUCLEAR EXPLOSION, SX=SCIENTIFIC EXPLOSION, OT=OTHER, UN=UNKNOWN
PHASES - A=P, B=PO, C=S, D=SO, E=T, F=OTHER

EVNT	******ORIGIN TIME******	**COORDINATES***	**********LOCATION**********	DEP	*MAGNI*	INF	EV	********SAVED********	**STRIP**
NO	YR*MO*DA*JUL*HR*MN*SECS	**LAT*****LON***	**********DESCRIPTION*********	*M*	BDY*SRF	SRC	TP	PHASES**INTERVAL***HRS	TAPE/FILE
0001	83 03 19 078 22:59:47.1	4.826S	151.812E	NEW IRELAND REGION	119	4.8	0.0	PDE	EQ	ABD	23:00-23:15	15	2000427-11
0002	83 03 20 079 11:24:48.4	2.37 N	126.800E	MOLUCCA PASSAGE	50	5.5	4.0	PDE	EQ	A	11:20-11:39	12	2000427-12
0003	83 03 20 079 13:45:49.8	4.72 S	153.12 E	NEW IRELAND REGION	80	5.9	0.0	PDE	EQ	ABDE	13:46-14:27	42	2000427-13
0004	83 03 20 079 16:24:13.3	18.82 S	177.76 W	FIJI ISLANDS REGION	633	5.0	0.0	PDE	EQ	A	16:26-16:37	12	2000427-14
0005	83 03 20 079 17:44:07.1	18.80 S	177.67 W	FIJI ISLANDS REGION	614	4.9	0.0	PDE	EQ	A	17:46-17:57	12	2000427-15
0006	83 03 21 080 04:06:24.8	5.83 S	153.69 E	NEW IRELAND REGION	40	5.5	0.0	PDE	EQ	ABDE	04:07-04:48	42	2000427-16
0007	83 03 21 080 07:44:17.6	21.66 S	175.32 W	TONGA ISLANDS	33	6.3	0.0	PDE	EQ	A	07:47-07:59	13	2000427-17
0008	83 03 21 080 07:57:18.4	7.34 S	129.9 E	BANDA SEA	143	5.6	0.0	PDE	EQ	A	08:00-08:12	13	2000427-17
0009	83 03 21 080 15:23:40.7	36.58 N	70.59 E	HINDU KUSH REGION	166	4.2	0.0	PDE	EQ	A	15:31-15:42	12	2000427-18
0010	83 03 21 080 15:49:52.8	21.39 S	175.45 W	TONGA ISLANDS	70	5.4	0.0	PDE	EQ	A	15:53-16:04	12	2000427-19
0011	83 03 22 081 01:32:28.6	51.29 N	176.48 W	ANDREANOF ISL. ALEUTIAN ISL.	33	4.9	0.0	PDE	EQ	ABD	01:34-01:50	17	2000427-20
0012	83 03 22 081 20:17:07.5	53.21 N	162.25 E	OFF EAST COAST OF KAMCHATKA	33	4.7	0.0	PDE	EQ	ABD	20:19-20:35	17	2000427-21
0013	83 03 23 082 06:09:29.6	6.61 S	154.61 E	SOLOMON ISLANDS	41	5.7	6.2	PDE	EQ	ABDE	06:10-06:52	43	2000427-22
0014	83 03 23 082 06:48:32.1	6.66 S	154.55 E	SOLOMON ISLANDS	59	5.2	0.0	PDE	EQ	ABDE	06:41-07:23	43	2000427-22
0015	83 03 23 082 08:26:55.2	6.62 S	154.58 E	SOLOMON ISLANDS	33	5.4	5.6	PDE	EQ	ABDE	08:28-09:09	42	2000427-23
0016	83 03 23 082 12:11:23.9	37.81 N	71.40 E	AFGHANISTAN U.S.S.R. BORDER REGION	127	5.2	0.0	PDE	EQ	A	12:18-12:30	13	2000427-24
0017	83 03 23 082 14:04:50.1	6.78 S	154.52 E	SOLOMON ISLANDS	61	5.2	0.0	PDE	EQ	ABDE	14:06-14:47	42	2000430-01
0018	83 03 23 082 15:07:01.2	3.37 S	177.49 E	GILBERT ISLANDS REGION	22	4.8	0.0	PDE	EQ	ABD	15:07-15:21	15	2000430-02
0019	83 03 23 082 21:54:36.3	37.22 N	138.12 E	NEAR W COAST OF HONSHU JAPAN	54	4.6	0.0	PDE	EQ	ABD	21:56-22:11	16	2000430-03
0020	00 00 00 000 00:00:00.0	0.00 N	0.00 E	LOCAL PO, SO, T	0	0.0	0.0	HEL	EQ	BDE	00:22-00:51	30	2000430-04
0021	83 03 24 083 07:01:40.9	10.55 S	159.82 E	SOLOMON ISLANDS	151	4.9	0.0	PDE	EQ	ABD	07:03-07:18	16	2000430-05
0022	83 03 24 083 07:24:12.5	7.61 S	107.17 E	JAVA	57	4.9	0.0	PDE	EQ	A	07:30-07:41	12	2000430-06
0023	83 03 24 083 09:44:53.9	6.68 S	154.56 E	SOLOMON ISLANDS	53	5.1	0.0	PDE	EQ	ABDE	08:46-09:27	42	2000430-07
0024	83 03 24 083 10:47:40.5	4.72 S	153.33 E	NEW IRELAND REGION	83	5.2	0.0	PDE	EQ	ABDE	10:48-11:29	42	2000430-08
0025	83 03 24 083 12:24:35.2	10.81 S	161.99 E	SOLOMON ISLANDS	74	4.9	0.0	PDE	EQ	ABD	12:25-12:41	17	2000430-09
0026	00 00 00 000 00:00:00.0	0.00 N	0.00 E	PROBABLE MARIANAS PO, SO, T	0	0.0	0.0	HEL	EQ	BDE	20:10-20:39	30	2000430-10
0027	83 03 25 084 07:44:01.2	6.55 S	130.00 E	BANDA SEA	164	5.4	0.0	PDE	EQ	A	07:47-07:58	12	2000430-11
0028	83 03 25 084 13:00:14.2	6.49 S	151.72 E	NEW BRITAIN REGION	45	5.3	0.0	PDE	EQ	ABDE	13:01-13:44	44	2000430-12
0029	83 03 25 084 19:33:54.1	8.39 S	124.68 E	TIMOR	169	4.8	0.0	PDE	EQ	A	19:37-19:49	13	2000430-13
0030	83 03 25 084 21:41:54.8	6.49 S	155.11 E	SOLOMON ISLANDS	121	5.1	0.0	PDE	EQ	ABDE	21:42-22:24	43	2000430-14
0031	83 03 26 085 10:51:48.4	39.13 N	44.58 E	N.W. IRAN-USSR BORDER REGION	33	4.6	0.0	PDE	EQ	A	11:00-11:20	21	2000430-15
0032	83 03 26 085 12:46:47.7	5.10 S	153.59 E	NEW IRELAND REGION	78	4.9	0.0	PDE	EQ	ABD	12:47-13:02	16	2000430-16
0033	83 03 26 085 14:57:49.3	1.16 N	126.58 E	MOLUCCA PASSAGE	7	5.2	0.0	PDE	EQ	A	15:01-15:12	12	2000430-17
0034	83 03 26 085 17:19:37.5	4.63 S	141.8 E	PAPUA NEW GUINEA	101	4.5	0.0	PDE	EQ	ABD	17:21-17:37	17	2000430-18
0035	83 03 26 085 18:42:46.8	42.84 N	141.79 E	HOKKAIDO JAPAN REGION	80	4.4	0.0	PDE	EQ	ABD	18:44-19:00	17	2000430-19
0036	83 03 26 085 20:20:00.0	37.38 N	116.46 W	SOUTHERN NEVADA	0	5.1	0.0	NEIS	MN	A	20:26-20:37	12	2000441-01
0037	83 03 27 086 02:42:41.4	34.26 N	92.64 E	QINGHAI PROVINCE CHINA	3	4.5	0.0	PDE	EQ	A	02:48-03:00	13	2000441-02
0038	83 03 27 086 09:04:33.5	27.51 N	141.17 E	BONIN ISLANDS REGION	33	4.8	0.0	PDE	EQ	ABD	09:05-09:19	15	2000441-03
0039	83 03 27 086 10:32:00.1	4.83 S	153.56 E	NEW IRELAND REGION	95	4.9	0.0	PDE	EQ	ABD	10:33-10:47	15	2000441-04
0040	83 03 27 086 20:05:07.6	6.89 S	149.45 E	NEW BRITAIN REGION	33	5.0	0.0	PDE	EQ	ABDE	20:06-20:51	46	2000441-05
0041	83 03 28 087 19:17:58.8	26.30 N	127.31 E	RYUKYU ISLANDS	62	5.1	0.0	PDE	EQ	A	19:20-19:31	12	2000441-06
0042	83 03 28 087 23:38:27.2	12.98 N	146.35 E	SOUTH OF MARIANA ISLANDS	33	4.7	0.0	PDE	EQ	ABD	23:38-23:51	14	2000441-07
0043	83 03 29 088 04:53:09.4	30.44 N	131.50 E	KYUSHU JAPAN	33	4.9	0.0	PDE	EQ	ABD	04:55-05:11	17	2000441-08
0044	83 03 29 088 22:55:47.8	6.98 S	154.80 E	SOLOMON ISLANDS	33	5.1	0.0	PDE	EQ	ABDE	22:57-23:38	42	2000441-09
0045	83 03 30 089 00:49:09.9	1.57 N	122.56 E	MINDANAO PENINSULA	49	5.1	5.1	PDE	EQ	A	00:53-01:04	12	2000441-10
0046	83 03 30 089 06:46:22.5	40.00 N	75.00 E	KIRGHIZ-SINKIANG BORDER REGION	33	4.9	4.9	PDE	EQ	A	06:53-07:05	13	2000441-11
0047	83 03 30 089 12:02:57.3	6.63 S	154.56 E	SOLOMON ISLANDS	33	4.8	0.0	PDE	EQ	ABD	12:04-12:18	15	2000441-12
0048	83 03 30 089 16:13:35.2	39.88 N	75.46 E	SOUTHERN XINJIANG CHINA	3	4.6	0.0	PDE	EQ	A	16:21-16:32	12	2000441-13
0049	83 03 30 089 18:55:49.1	5.91 S	147.20 E	PAPUA NEW GUINEA	33	5.2	0.0	PDE	EQ	ABDE	18:58-19:46	49	2000441-14
0050	83 03 31 090 14:24:45.6	34.28 N	135.81 E	NEAR S COAST OF SOUTH HONSHU	380	4.9	0.0	PDE	EQ	ABDE	14:25-14:11	47	0/ 00

Figure 13. A sample of event information contained within WHIPS file EVENTS, which has been printed using program XEVLST. A detailed description of this printout is contained in the text.

necessary. A general procedure has been formulated for determining which events from the PDE lists might produce seismic energy observable at Wake, based on experience gained from scanning the analog data collected since 1979. An outline of event types and their corresponding phases is presented in Fig. 14. Intervals to save for these events and phases are computed automatically by program XEVENT, at the time the hypocenter data are entered, and may be altered manually if necessary. The only seismic energy from events which is deliberately discarded is that of T-phases from smaller magnitude and unknown events. T-phase energy is generally so abundant (it is estimated that at least 10 times as many circum-Pacific events may be detected using T-phases than may be detected using other seismic phases) that very little data compression would be possible if all of these T-phase data were saved. This procedure is weighted towards saving more data than necessary (i.e., many of these events may not have observable energy at Wake, but this is hard to determine without scanning all the channels in particular frequency bands) so that a) unusual events are not discarded, b) data from small events may be enhanced with array processing, and c) data from events which are not of current interest but may be of future interest are saved. The helicorder records from Wake are also scanned for seismic phases such as P, Po, S, and So which do not correspond to known events, and intervals are saved to capture these phases. Two such intervals, corresponding to events 820 and 826, appear in Fig. 13. The final column of the listing shown in Fig. 13 gives the strip tape and file number which contains the corresponding interval of data. Some data intervals are contiguous or overlap and have therefore been saved in a single file (for example: events 807 and 808, and events 813 and 814). Other events have not yet been extracted from the WAKEUP tapes and are noted

Source Region(s)	Magnitude	Depth(km)	$\sim\Delta$	Phases
1. Nuclear Explosions Anywhere	all	all	0°-35°	P.Po.So.T
	all	all	$> 35^{\circ}$	P
2. Mariana Is., Bonin Is., Volcano Is., Honshu, and Gilbert Islands	$m_b < 5.0$	<100	18°-25°	P.Po.So
	$m_b > 5.0$	<100	18°-25°	P.Po.So.T
	all	>100	18°-25°	P.Po.So.T
3. Kuril Is., Kamchatka, Aleutian Is., New Guinea, New Britain, Solomon Is., and Santa Cruz Islands	$m_b > 5.0$	<100	25°-35°	P.Po.So.T
	all	>100	25°-35°	P.Po.So.T
4. Asian Continent	$m_b > 4.5$	all	30°-90°	P
5. Mid Pacific Plate Events	all	all	0°-35°	P.Po.So.T
	$m_b > 4.5$	all	$>35^{\circ}$	P.Po.So.T
6. Not Regions 2, 3, 4, or 5.	$m_b > 5.0$	all	$<90^{\circ}$	P
7. Mid Atlantic Antipode	all	all	340°-360°	P
8. Anywhere	M > 6.0	all	all	P
	$m_b > 6.5$	all	340°-360°	P

Figure 14. The general criteria used for deciding which phases (if any) to save for a known event. Time intervals which contain those phases are computed automatically by XEVENT or may be entered manually.

by a tape and file number of 0 (such as event 850). Some events, such as 801, 806, and 811, could not be extracted because there was no WAKEUP data available (in this case, due to a tape drive failure at WAKE). A file for these events, containing only header and trailer records, exists on the strip tape indicated, and the file number has been flagged as negative on the XEVLST listing.

XSTRIP Parameters (XPARAM)

The last initial step in the WHIPS procedure is to set up the running parameters for program XSTRIP which are stored in the header block of the EVENTS file. These parameters may be viewed and changed using program XPARAM, and a sample output from this program is shown in Fig. 15. Many of these parameters (D, E, F, G, H, and I) are continually updated by programs XSTRIP, XSTPDN, and XRANDN; and these parameters may be changed manually when necessary. Other parameters (A, B, and C) must always be entered and changed manually as the situation warrants. The "WAKEUP tape record length" (A) is equal to the WAKEUP sampling rate times the number of channels, times the number of seconds per block, plus 100 words for the block header (i.e., [80 x 8 x 5] + 100 = 3300). The "strip/interval disk record length" (A) is the block length used for disk files STRIP000 and INTRVL00; and it must be a multiple of 112 words (Harris sector size = 112 words) which is greater than or equal to the WAKEUP tape record length. The "maximum records ..." (B) is a conservative estimate of how many blocks of data (in this case, 3300 word blocks), will fit onto a tape created by XSTPDN or XRANDN. This parameter is necessary for XSTPDN to organize its output data so that individual intervals which are saved do not cross XSTPDN tape boundaries. The "seconds per WAKEUP tape block" (C) is used to convert terms which refer to a

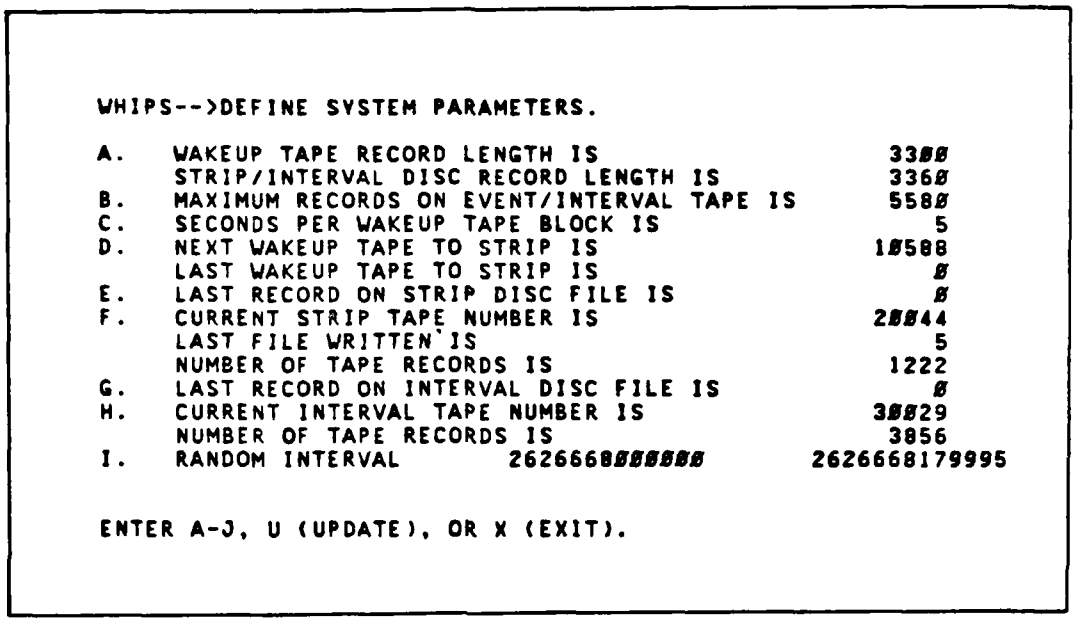

Figure 1. A part of the interactive I/O generated by WHIPS program XPARAM which is used to view or change the running parameters of program XSTRIP. More detailed explanation of these parameters is given in the text.

particular block on a WAKEUP tape into absolute times (for example - to calculated the ending time of a WAKEUP tape, given its starting time and total number of blocks). The "next" and "last WAKEUP tape to strip" (D) refers to the range of WAKEUP tapes which are to be processed during a particular run of XSTRIP. These parameters are continually updated during the XSTRIP run to facilitate recovery in case of a system crash. At the completion of the run, the last tape which was processed becomes the "next WAKEUP tape to strip", and the "last WAKEUP tape to strip" is set to 0, as shown in the figure. The "last record on the strip disk file" (E) allows XSTRIP to begin writing into STRIP000 where it last left off. This parameter is set to 0 after a successful downloading of the data using XSTPDN, as is shown in the figure. The "current strip tape", "last file", and "number of tape records" (F), allows XSTPDN to download the data onto tape from the point on the tape at which it left off after the last run. G and H serve the same function for the random interval data as did E and F for the stripped events data. The "random interval" (I) gives the 3 minute time range, in century-milliseconds, of the next random interval to be stripped.

Extracting the data (XSTRIP)

XSTRIP is the program which extracts and stores data of events and of random intervals on disk for later downloading. The only operator input required is specification of the range of WAKEUP tapes to be processed. Normally, this processing takes place in contiguous chronological order. After the total time interval represented by the WAKEUP tapes has been computed from the TAPLOG file, a search of the EVENTS file is made to determine which event intervals, not yet extracted, lie entirely within the

total time interval. From these individual event intervals, grand intervals are computed which combine the times of overlapping event intervals. As the WAKEUP tapes are read one by one (the operator is prompted to mount each tape), the grand intervals are extracted and stored on disk file STRIP000. Concurrently, the random, three-minute intervals are being extracted and stored on disk file INTRVL00. The timing of these intervals is computed "on the fly" and the number of minutes of data between the beginnings of one 3-minute interval and the next is computed using a random variable with a uniform distribution between 3 (i.e., no overlap) and 117, giving an average separation of 60 minutes. The parameters list at the beginning of the EVENTS file is updated after the extraction of each grand interval and each random interval. This facilitates a smooth and efficient recovery after an XSTRIP abortion of any kind and provides information for later downloading of the data to tape. XSTRIP is complete after the last WAKEUP tape has been run. It should be noted that a typical XSTRIP run at HIG processes from 10 to 20 WAKEUP tapes, and requires approximately 20 million words of disk storage for the STRIP000 and INTRVL00 files.

Events Download to Strip Tapes (XSTPDN)

The STRIP000 disk file containing the event data is downloaded to tape using program XSTPDN. This program first accesses the running parameters in the EVENT file to find out which tape to download to, and how many files to advance into that tape before writing. As each grand interval in the STRIP000 file is downloaded to tape, the running parameters are updated, and the EVENTS file is updated with the strip tape number and file for those events contained in the grand interval. If the grand interval contains too many records to completely fit on the strip tape (based on "B" in the

running parameters), then an end-of-file is written to the strip tape and a new strip tape is mounted following a prompt to the operator. Strip tapes are numbered sequentially beginning with 20001. The XSTPDN run is complete when all the grand intervals have been downloaded, and at that time the "last record on strip disk file" (E) in the running parameters is set to 0 as shown in Fig. 15. The format of the strip tape, and format of the blocks contained on the strip tape is given in Fig. 16.

Random Interval Download to Interval Tapes (XRANDN)

The INTRVL00 disk file, containing the 3-minute randomly spaced ambient noise samples, is downloaded to tape using program XRANDN. This program first accesses the running parameters to determine which interval tape to download to, and how many records from the INTRVL00 file to tape until the maximum number of records on tape ("B" in the running parameters) is reached. There are no end-of-files between the 3-minute intervals, however, an end-of-file is written after the last record on the interval tape. Interval tapes are numbered sequentially beginning with 30001. The XRANDN run is complete when all of the records in INTRVL00 have been downloaded, at which time item "G" in the running partameters is set to 0 as shown in Fig. 15. The format of the interval tape, and the format of the blocks contained on the interval tape is given in Fig. 17.

Checking Procedures (XSTPCHK and XINTCHK)

As a safety measure, and as a way of accumulating some preliminary statistics on the data, all strip and interval tapes are checked using programs XSTPCHK and XINTCHK, respectively. The outputs from these programs are viewed before the STRIP000 and INTRVL00 files are eliminated from disk

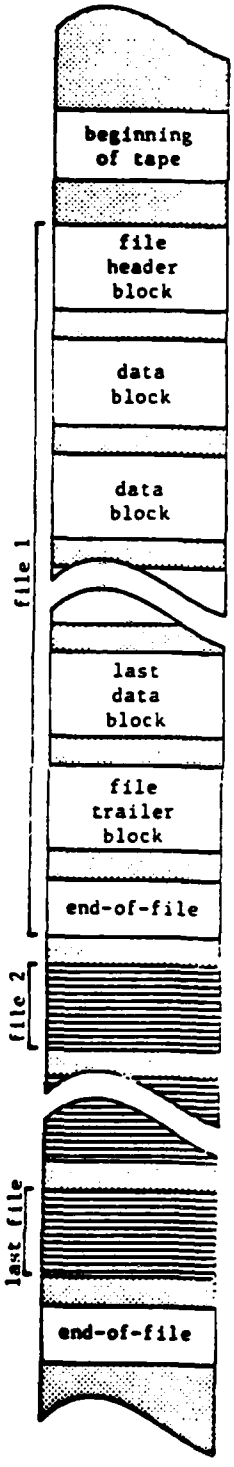

WHIPS Strip Tape Description

General Format: 1600 BPI
2 bytes per word
IBM format
2's complement notation

File Header Block	
Word(s)	Description
1	Always 0 to identify block as a header/trailer
2	Strip tape I.D. number
3	Strip file number
4-56	Not used
57	Estimated number of data block in this file
58-62	Not used
63	Total number of events (n) represented in this file
64-100	Not used
101-(101+n)	Event number(s)
(102+n)-end	Not used
Note: header block is the same size as the data block	

Data Block
The format of the strip tape data blocks is exactly the same as the format of the WAKEUP tape blocks.

File Trailer Block	
Word(s)	Description
1-3	Same as header block words 1-3
4-56	Not used
57	Actual number of data blocks in file
58	Number of words per block
59-63	Same as header block words 59-63
64-65	WAKEUP tape I.D. number(s)
66	Number of WAKEUP tape read errors
67-86	Block numbers with WAKEUP tape read errors
87-end	Same as header block words 87-end
Note: trailer block is the same size as the data block.	

Figure 16. Format for the WHIPS strip tapes which contain the event data.

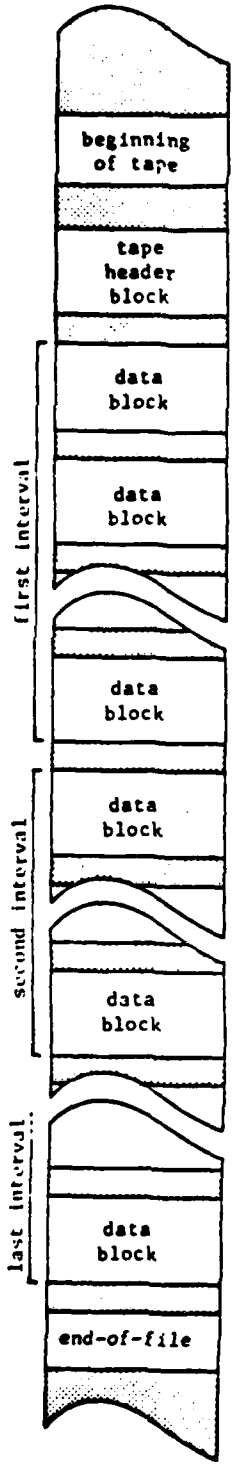

WHIPS Interval Tape Description

General Format: 1600 BPI
2 bytes per word
IBM format
2's complement notation

Tape Header Block	
Word(s)	Description
1	Always 0 to identify block as a tape header
2	Interval tape I.D. number
3-end	Not used
Note: tape header block is the same size as the data block	

Data Block
The format of the interval tape data blocks is exactly the same as the format of the WAKEUP tape blocks.

Figure 17. Format for the WHIPS interval tapes which contain randomly spaced 3-minute intervals of data (1 per hour on the average) which are collected as noise samples.

and the WAKEUP tapes recycled. A sample output from XSTPCHK is shown in Fig. 18. Most of the lines of output are self-explanatory. The "error blocks" are for blocks of data which had tape read errors coming off of the WAKEUP tapes during XSTRIP. The "clipped data" lines show the number of data points in a particular block, and for a particular channel, which are equal to -32,768 or 32,767, the maximum and minimum values output by the A/D convertor at Wake. The clipped data in this file is on two SOFAR hydrophones and corresponds to the T-phase arrival from event 824 (see Fig. 11 for event 824). The table of values gives information about each multiplexed in the file which is described as follows: 1) "ch" - multiplexed channel number; 2) "hydr" - hydrophone number; 3) "amp" - preamp/pre-whitening filter identification number; 4) "gain" - gain step of the final stage of the preamp/pre-whitening filter (see previous section on the recording system); 5) "avgval" - the average value of this channel (non-zero due to small but constant DC biases in the amplifiers); 6) "stddev" - the standard deviation of each channel (note the much higher values for the noisier SOFAR hydrophones); 7) "0/blk" - average number of zeros per block (note that channel 3 has most zeros due to its near zero average value and small standard deviation); 8) "0/blk/std" - the standard deviation of the number of zeros per block; and 9) "# clips" - the total number of clipped data points for this channel in this file. The "worst case clock error code" indicates the maximum error between the satellite clock time written in each block header and the actual coordinated Universal Time. The codes are as follows:

0 - less than ± 1 msec

1 - less than ± 5 msec

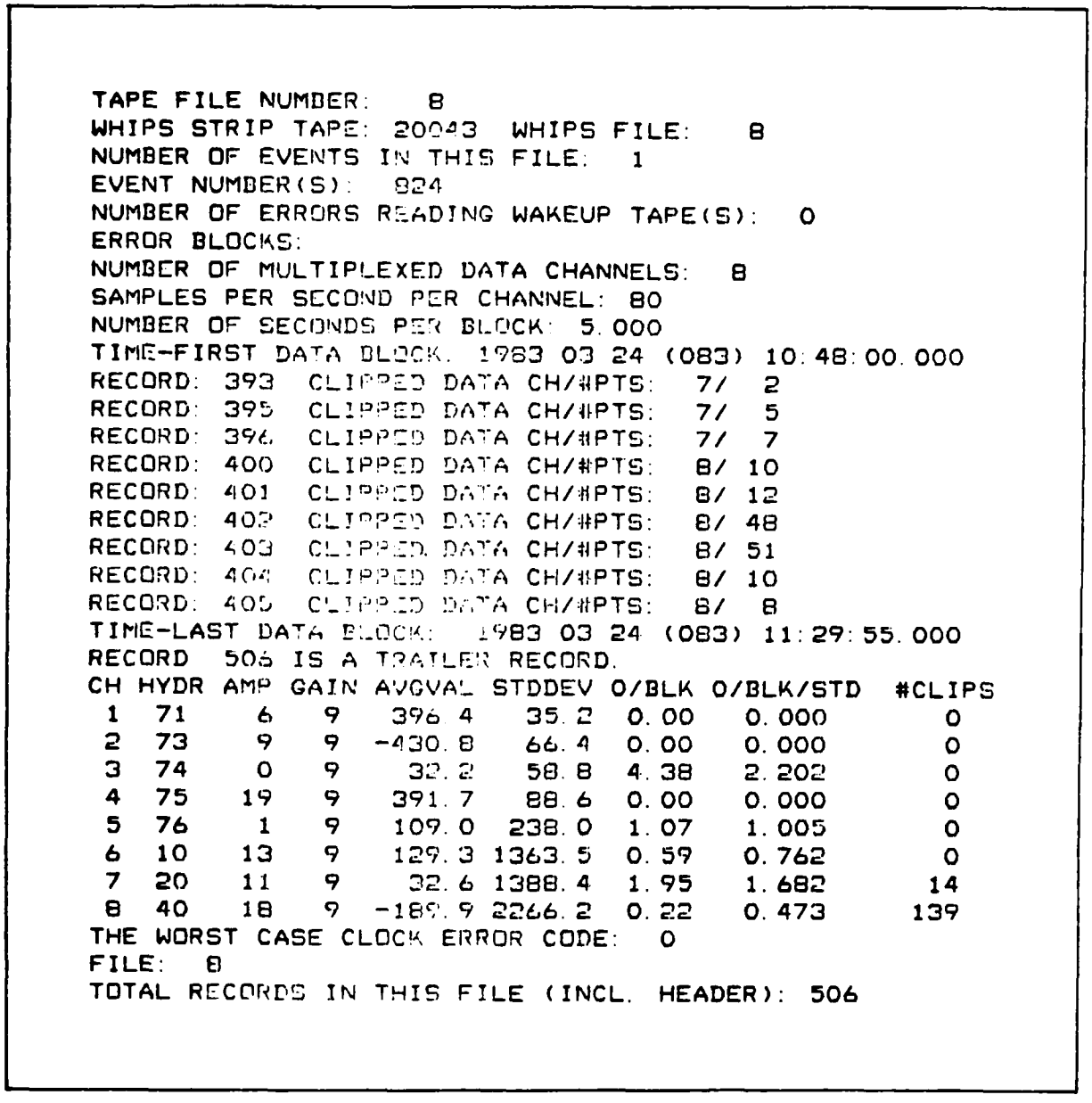

```
TAPE FILE NUMBER:    8
WHIPS STRIP TAPE: 20043  WHIPS FILE:    8
NUMBER OF EVENTS IN THIS FILE:  1
EVENT NUMBER(S):  824
NUMBER OF ERRORS READING WAKEUP TAPE(S):  0
ERROR BLOCKS:
NUMBER OF MULTIPLEXED DATA CHANNELS:  8
SAMPLES PER SECOND PER CHANNEL: 80
NUMBER OF SECONDS PER BLOCK: 5.000
TIME-FIRST DATA BLOCK:  1983 03 24 (083) 10:48:00.000
RECORD:  393  CLIPPED DATA CH/#PTS:  7/  2
RECORD:  395  CLIPPED DATA CH/#PTS:  7/  5
RECORD:  396  CLIPPED DATA CH/#PTS:  7/  7
RECORD:  400  CLIPPED DATA CH/#PTS:  8/ 10
RECORD:  401  CLIPPED DATA CH/#PTS:  8/ 12
RECORD:  402  CLIPPED DATA CH/#PTS:  8/ 48
RECORD:  403  CLIPPED DATA CH/#PTS:  8/ 51
RECORD:  404  CLIPPED DATA CH/#PTS:  8/ 10
RECORD:  405  CLIPPED DATA CH/#PTS:  8/  8
TIME-LAST DATA BLOCK:  1983 03 24 (083) 11:29:55.000
RECORD  506 IS A TRAILER RECORD.
CH HYDR AMP GAIN AVGVAL STDDEV O/BLK O/BLK/STD  #CLIPS
 1  71   6   9   396.4   35.2  0.00    0.000       0
 2  73   9   9  -430.8   66.4  0.00    0.000       0
 3  74   0   9    32.2   58.8  4.38    2.202       0
 4  75  19   9   391.7   88.6  0.00    0.000       0
 5  76   1   9   109.0  238.0  1.07    1.005       0
 6  10  13   9   129.3 1363.5  0.59    0.762       0
 7  20  11   9    32.6 1388.4  1.95    1.682      14
 8  40  18   9  -189.9 2266.2  0.22    0.473     139
THE WORST CASE CLOCK ERROR CODE:  0
FILE:  8
TOTAL RECORDS IN THIS FILE (INCL. HEADER): 506
```

Figure 18. Sample output from program XSTPCHK. Detailed explanation of this figure is given in the text.

3 - less than ± 50 msec

7 - less than ± 500 msec

15 - more than ± 500 msec

A sample output from XINTCHK is shown in Fig. 19. Much less computation is done on the interval data, and the XINTCHK output serves more as a simple log of what has been saved.

Strip Tape Copies (XTAPCOP)

As a final step in the preliminary processing, the strip tapes are copied using program XTAPCOP, and the copies are sent to the DARPA Center for Seismic Studies (CSS) in Rosslyn, Virginia. Copies of interval tapes are not currently sent to CSS but may be at some time in the future.

```
RECORD     1 IS A HEADER RECORD.
#BLKS: 21     2-   22 INT: 1983 04 20 (110) 02:18:15-02:20:00 #SEC:  105.000
#BLKS: 36    23-   58 INT: 1983 04 20 (110) 03:38:00-03:41:00 #SEC:  180.000
#BLKS: 36    59-   94 INT: 1983 04 20 (110) 05:20:00-05:23:00 #SEC:  180.000
#BLKS: 36    95-  130 INT: 1983 04 20 (110) 06:47:00-06:50:00 #SEC:  180.000
#BLKS: 36   131-  166 INT: 1983 04 20 (110) 07:03:00-07:06:00 #SEC:  180.000
#BLKS: 36   167-  202 INT: 1983 04 20 (110) 08:07:00-08:10:00 #SEC:  180.000
#BLKS: 36   203-  238 INT: 1983 04 20 (110) 09:57:00-10:00:00 #SEC:  180.000
#BLKS: 36   239-  274 INT: 1983 04 20 (110) 11:18:00-11:21:00 #SEC:  180.000
#BLKS: 36   275-  310 INT: 1983 04 20 (110) 11:41:00-11:44:00 #SEC:  180.000
#BLKS: 36   311-  346 INT: 1983 04 20 (110) 12:28:00-12:31:00 #SEC:  180.000
#BLKS: 36   347-  382 INT: 1983 04 20 (110) 13:13:00-13:16:00 #SEC:  180.000
#BLKS: 36   383-  418 INT: 1983 04 20 (110) 15:03:00-15:06:00 #SEC:  180.000
#BLKS: 36   419-  454 INT: 1983 04 20 (110) 15:54:00-15:57:00 #SEC:  180.000
#BLKS: 36   455-  490 INT: 1983 04 20 (110) 16:22:00-16:25:00 #SEC:  180.000
#BLKS: 36   491-  526 INT: 1983 04 20 (110) 18:23:00-18:26:00 #SEC:  180.000
#BLKS: 36   527-  562 INT: 1983 04 20 (110) 19:30:00-19:33:00 #SEC:  180.000
#BLKS: 36   563-  598 INT: 1983 04 20 (110) 20:48:00-20:51:00 #SEC:  180.000
#BLKS: 36   599-  634 INT: 1983 04 20 (110) 21:40:00-21:43:00 #SEC:  180.000
#BLKS: 36   635-  670 INT: 1983 04 20 (110) 22:29:00-22:32:00 #SEC:  180.000
#BLKS: 36   671-  706 INT: 1983 04 20 (110) 23:10:00-23:13:00 #SEC:  180.000
#BLKS: 36   707-  742 INT: 1983 04 20 (110) 23:55:00-23:58:00 #SEC:  180.000
#BLKS: 36   743-  778 INT: 1983 04 21 (111) 01:07:00-01:10:00 #SEC:  180.000
#BLKS: 36   779-  814 INT: 1983 04 21 (111) 01:33:00-01:36:00 #SEC:  180.000
#BLKS: 36   815-  850 INT: 1983 04 21 (111) 02:26:00-02:29:00 #SEC:  180.000
#BLKS: 36   851-  886 INT: 1983 04 21 (111) 04:15:00-04:18:00 #SEC:  180.000
#BLKS: 36   887-  922 INT: 1983 04 21 (111) 05:04:00-05:07:00 #SEC:  180.000
#BLKS: 36   923-  958 INT: 1983 04 21 (111) 06:13:00-06:16:00 #SEC:  180.000
#BLKS: 36   959-  994 INT: 1983 04 21 (111) 07:27:00-07:30:00 #SEC:  180.000
#BLKS: 36   995-1030 INT: 1983 04 21 (111) 08:13:00-08:16:00 #SEC:  180.000
#BLKS: 36  1031-1066 INT: 1983 04 21 (111) 10:04:00-10:07:00 #SEC:  180.000
#BLKS: 36  1067-1102 INT: 1983 04 21 (111) 12:04:00-12:07:00 #SEC:  180.000
#BLKS: 36  1103-1138 INT: 1983 04 21 (111) 12:22:00-12:25:00 #SEC:  180.000
#BLKS: 36  1139-1174 INT: 1983 04 21 (111) 12:27:00-12:30:00 #SEC:  180.000
#BLKS: 36  1175-1210 INT: 1983 04 21 (111) 13:15:00-13:18:00 #SEC:  180.000
#BLKS: 36  1211-1246 INT: 1983 04 21 (111) 13:48:00-13:51:00 #SEC:  180.000
#BLKS: 72  1247-1318 INT: 1983 04 21 (111) 14:47:00-14:53:00 #SEC:  360.000
#BLKS: 36  1319-1354 INT: 1983 04 21 (111) 15:19:00-15:22:00 #SEC:  180.000
#BLKS: 36  1355-1390 INT: 1983 04 21 (111) 16:41:00-16:44:00 #SEC:  180.000
#BLKS: 36  1391-1426 INT: 1983 04 21 (111) 18:07:00-18:10:00 #SEC:  180.000
#BLKS: 36  1427-1462 INT: 1983 04 21 (111) 18:53:00-18:56:00 #SEC:  180.000
#BLKS: 36  1463-1498 INT: 1983 04 21 (111) 19:27:00-19:30:00 #SEC:  180.000
#BLKS: 36  1499-1534 INT: 1983 04 21 (111) 19:38:00-19:41:00 #SEC:  180.000
#BLKS: 36  1535-1570 INT: 1983 04 21 (111) 21:02:00-21:05:00 #SEC:  180.000
#BLKS: 36  1571-1606 INT: 1983 04 21 (111) 22:03:00-22:06:00 #SEC:  180.000
#BLKS: 36  1607-1642 INT: 1983 04 21 (111) 22:18:00-22:21:00 #SEC:  180.000
#BLKS: 36  1643-1678 INT: 1983 04 22 (112) 00:08:00-00:11:00 #SEC:  180.000
#BLKS: 36  1679-1714 INT: 1983 04 22 (112) 00:18:00-00:21:00 #SEC:  180.000
```

Figure 19. Sample output from program XINTCHK showing some of the 3-minute intervals saved on a WHIPS interval tape. The first interval shown, blocks 2-22, contains only 105 seconds because part of that interval was written to the previous interval tape. Another interval, blocks 1247-1318, contains 360 seconds and represents two contiguous 3-minute intervals.

ACKNOWLEDGEMENTS

This system has been sponsored primarily by the Air Force Office of Scientific Research with supplemental funds provided by the U.S. Arms Control and Disarmament Agency. Appreciation is expressed to Dan Walker, George Sutton, Paul Jubinski, Grant Blackinton and Joe Gettrust for their respective contributions towards the design and implementation of this system. Firmin Oliveira successfully programmed most of the WAKEUP and WHIPS software in less time than seemed possible. Al David, Bonnie Jose, and Kentron Corporation have provided excellent day to day operation of the system at Wake.

APPENDIX X

WAKE HYDROPHONE INFORMATION PROCESSING SYSTEM (WHIPS) EVENT LISTING 6 JUL 83

KEY: INFORMATION SOURCES - PDE=NEIS PDECARD, MON=NEIS MONTHLY LIST, ICS=ICS LIST, HEL=HELICORDER, OTH=OTHER
EVENT TYPE - EQ=EARTHQUAKE, NX=NUCLEAR EXPLOSION, SX=SCIENTIFIC EXPLOSION, OT=OTHER, UN=UNKNOWN
PHASES - A=P, B=PO, C=S, D=SO, E=T, F=OTHER

EVNT NO	ORIGIN TIME YR MO DA JUL HR MN SECS	COORDINATES LAT LON	LOCATION DESCRIPTION	DEP KM	MAGNI BDY	MAGNI SRF	INF SRC	EV TP	SAVED PHASES	INTERVAL	STRIP MNS	STRIP TAPE/FILE
0001	82 09 09 252 03:06:44.0	30.299N 137.670E	SOUTH OF HONSHU, JAPAN	481	5.0	0.0	PDE	EQ	ABDE	03:00-03:50	43	20001/ 06
0002	82 09 09 252 05:43:52.1	3.306S 177.566E	GILBERT ISLANDS REGION	33	5.4	0.0	PDE	EQ	ABDE	05:44-06:22	39	20001/ 07
0003	82 09 09 252 06:40:21.2	35.597S 102.453W	SOUTHERN PACIFIC OCEAN.	10	5.1	0.0	PDE	EQ	A	06:49-07:09	21	20001/ 08
0004	82 09 09 252 12:49:00.4	43.563N 146.606E	KURIL ISLANDS	33	4.7	0.0	PDE	EQ	ABD	12:50-13:17	28	20001/ 09
0005	82 09 09 252 15:42:22.0	15.493N 147.571E	MARIANA ISLANDS REGION	33	5.4	5.2	PDE	EQ	ABDE	15:41-16:12	32	20001/ 10
0006	82 09 09 252 16:09:30.3	15.518N 147.593E	MARIANA ISLANDS REGION	33	5.2	0.0	PDE	EQ	ABDE	16:09-16:39	31	20001/ 10
0007	82 09 09 252 16:13:59.7	15.638N 147.648E	MARIANA ISLANDS	33	5.1	0.0	PDE	EQ	ABDE	16:13-16:44	32	20001/ 10
0008	82 09 09 252 16:40:13.1	22.103S 169.446E	LOYALTY ISLANDS	33	5.5	4.9	PDE	EQ	A	16:43-16:54	12	20001/ 10
0009	82 09 10 253 01:43:15.2	3.437S 177.650E	GILBERT ISLANDS	33	5.1	0.0	PDE	EQ	ABDE	01:43-02:22	40	20001/ 11
0010	82 09 10 253 10:20:37.5	55.161N 161.673E	NEAR EAST COAST OF KAMCHATKA	33	5.0	4.3	PDE	EQ	ABDE	10:23-11:13	51	20002/ 01
0011	82 09 10 253 13:41:42.2	2.447N 126.910E	MOLUCCA PASSAGE 46 DEGS.	45	4.8	0.0	PDE	EQ	A	13:45-13:56	12	20002/ 02
0012	82 09 11 254 06:31:48.6	26.620S 176.644W	SOUTH OF FIJI ISLANDS 49 DEGS.	33	5.2	4.9	PDE	EQ	A	06:41-07:00	20	20002/ 03
0013	82 09 11 254 06:57:44.6	26.803S 176.210W	SOUTH OF FIJI ISLANDS 49 DEGS.	33	5.0	4.9	PDE	EQ	A	07:01-07:13	13	20002/ 03
0014	82 09 11 254 13:59:07.0	15.611N 147.818E	MARIANA ISLANDS	38	4.2	0.0	PDE	EQ	ABD	13:58-14:27	30	20002/ 04
0015	82 09 12 255 03:42:43.1	42.031N 142.702E	HOKKAIDO, JAPAN	66	4.8	0.0	PDE	EQ	ABD	03:44-03:59	16	20002/ 05
0016	82 09 12 255 07:22:39.3	19.727S 177.914W	FIJI ISLANDS	577	5.1	0.0	PDE	EQ	A	07:25-07:37	13	20002/ 06
0017	82 09 12 255 08:46:06.0	26.952S 176.475W	SOUTH OF FIJI	33	5.1	5.2	PDE	EQ	A	08:50-09:01	12	20002/ 07
0018	82 09 12 255 09:22:23.2	52.671N 166.937W	FOX ISLANDS, ALEUTIAN ISLANDS.	33	5.7	5.8	PDE	EQ	ABDE	09:26-10:18	53	20002/ 08
0019	82 09 12 255 11:59:52.6	52.783N 166.772W	FOX ISLANDS, ALEUTIAN ISLANDS.	33	5.2	4.9	PDE	EQ	ABDE	12:03-12:56	54	20002/ 09
0020	82 09 12 255 13:03:10.2	0.820N 126.037E	MOLLACA PASSAGE	70	4.9	0.0	PDE	EQ	A	13:12-13:31	20	20002/ 10
0021	82 09 12 255 16:50:38.0	52.847N 166.977W	FOX ISLANDS, ALEUTIAN ISLANDS.	33	5.5	5.1	PDE	EQ	ABDE	16:53-17:46	54	20002/ 11
0022	82 09 13 256 16:46:57.7	17.992S 178.496W	FIJI ISLANDS.	597	4.3	0.0	PDE	EQ	A	16:49-17:01	13	20003/ 02
0023	82 09 13 256 18:03:36.3	37.526N 141.306E	NEAR COAST OF HONSHU, JAPAN.	62	5.0	0.0	PDE	EQ	ABDE	18:04-18:47	44	20003/ 03
0024	82 09 13 256 19:00:51.6	3.520S 177.622E	GILBERT ISLANDS.	33	5.2	5.1	PDE	EQ	ABDE	19:09-19:47	39	20003/ 04
0025	82 09 14 257 00:26:04.9	15.495N 147.722E	MARIANA ISLANDS.	38	4.8	0.0	PDE	EQ	ABD	00:25-00:38	14	20003/ 05
0026	82 09 14 257 03:53:42.6	3.442S 177.667E	GILBERT ISLANDS.	33	5.4	0.0	PDE	EQ	ABDE	03:54-04:32	39	20003/ 06
0027	82 09 14 257 05:11:49.4	31.077S 179.615W	KERMADEC ISLANDS.	78	5.4	0.0	PDE	EQ	A	05:21-05:40	20	20003/ 07
0028	82 09 14 257 11:37:18.6	43.729N 140.130E	HOKKAIDO, JAPAN.	161	5.2	0.0	PDE	EQ	ABDE	11:39-12:26	48	20003/ 08
0029	82 09 14 257 12:42:23.8	27.017S 176.480W	KERMADEC ISLANDS.	33	5.0	4.6	PDE	EQ	A	12:46-12:57	12	20003/ 09
0030	82 09 14 257 18:17:02.4	7.247S 149.056E	EAST PAPUA NEW GUINEA.	33	5.0	6.3	PDE	EQ	ABDE	18:18-19:04	47	20003/ 10
0031	82 09 14 257 21:18:38.5	7.360S 13.499W	ASCENSION ISLAND.	10	4.9	0.0	PDE	EQ	A	21:20-21:47	20	20003/ 11
0032	82 09 15 258 20:22:57.5	14.515S 70.842W	PERU. MB 6.3 (BRK).	152	5.9	0.0	PDE	EQ	A	20:32-20:51	20	20004/ 01
0033	82 09 15 258 22:34:09.2	21.510S 169.300E	LOYALTY ISLANDS.	67	5.6	0.0	PDE	EQ	A	22:37-22:48	12	20004/ 02
0034	82 09 15 258 23:31:54.1	12.022N 143.743E	SOUTH OF MARIANA ISLANDS	33	4.9	0.0	PDE	EQ	ABD	23:32-00:00	29	20004/ 03
0035	82 09 16 259 02:20:30.5	30.103N 138.966E	SOUTH OF HONSHU, JAPAN.	370	5.1	0.0	PDE	EQ	ABDE	02:21-03:02	42	20004/ 04
0036	82 09 16 259 03:07:50.5	3.568S 177.684E	GILBERT ISLANDS.	33	4.8	0.0	PDE	EQ	ABD	03:00-03:22	15	20004/ 05
0037	82 09 16 259 08:23:23.2	15.335S 173.283W	TONGA ISLANDS.	129	5.5	0.0	PDE	EQ	A	08:26-08:37	12	20004/ 06
0038	82 09 16 259 09:21:11.0	5.261S 152.059E	NEW BRITAIN.	63	5.2	0.0	PDE	EQ	ABDE	09:22-10:03	42	20004/ 07
0039	82 09 16 259 11:41:00.9	3.351S 177.602E	GILBERT ISLANDS.	33	5.2	4.7	PDE	EQ	ABDE	11:41-12:19	39	20004/ 08
0040	82 09 16 259 12:27:38.7	7.294S 127.056E	BANDA SEA.	389	5.0	0.0	PDE	EQ	A	12:31-12:42	12	20004/ 09
0041	82 09 16 259 13:28:39.3	6.070N 125.882E	MINDANAO, PHILIPPINE ISLANDS.	169	5.1	0.0	PDE	EQ	A	13:31-13:43	13	20004/ 10
0042	82 09 16 259 16:46:02.2	3.397S 177.557E	GILBERT ISLANDS.	33	4.7	0.0	PDE	EQ	ABD	16:46-17:14	29	20004/ 11
0043	82 09 00 251 06:07:53.3	41.411N 160.095E	DOWNHOLE NEAR KURIL IS.	0	0.0	0.0	OTH	SX	AE	06:00-06:44	37	0/ 00
0044	82 09 00 251 09:00:35.0	41.715N 160.077E	DOWNHOLE NEAR KURIL IS.	0	0.0	0.0	OTH	SX	AE	09:01-09:37	37	0/ 00
0045	82 09 00 251 12:00:24.7	42.017N 160.033E	DOWNHOLE NEAR KURIL IS.	0	0.0	0.0	OTH	SX	AE	12:00-12:37	38	20001/ 01
0046	82 09 00 251 15:01:23.3	42.317N 160.010E	DOWNHOLE NEAR KURIL IS.	0	0.0	0.0	OTH	SX	AE	15:01-15:38	38	20001/ 02
0047	82 09 00 251 18:01:00.5	42.605N 159.971E	DOWNHOLE NEAR KURIL IS.	0	0.0	0.0	OTH	SX	AE	18:01-18:38	38	20001/ 03
0048	82 09 00 251 21:00:23.5	42.883N 159.906E	DOWNHOLE NEAR KURIL IS.	0	0.0	0.0	OTH	SX	AE	21:00-21:38	39	20001/ 04
0049	82 09 00 252 00:00:57.9	43.203N 159.793E	DOWNHOLE NEAR KURIL IS.	0	0.0	0.0	OTH	SX	AE	00:01-00:39	39	20001/ 05
0050	82 09 12 255 22:45:04.2	44.252N 160.776E	KURILS DOWNHOLE - 240# SHOT	0	0.0	0.0	OTH	SX	AE	22:45-23:24	40	20002/ 12
0051	82 09 12 255 23:01:00.5	44.276N 160.826E	KURILS DOWNHOLE - 240# SHOT	0	0.0	0.0	OTH	SX	AE	23:01-23:40	40	20003/ 01
0052	82 09 12 255 23:16:58.0	44.296N 160.881E	KURILS DOWNHOLE - 240# SHOT	0	0.0	0.0	OTH	SX	AE	23:17-23:56	40	20003/ 01
0053	82 09 12 255 23:33:02.3	44.316N 160.936E	KURILS DOWNHOLE - 240# SHOT	0	0.0	0.0	OTH	SX	AE	23:33-00:12	40	20003/ 01
0054	82 09 12 255 23:49:05.4	44.338N 160.982E	KURILS DOWNHOLE - 240# SHOT	0	0.0	0.0	OTH	SX	AE	23:49-00:28	40	20003/ 01
0055	82 09 13 256 00:05:07.1	44.359N 161.037E	KURILS DOWNHOLE - 240# SHOT	0	0.0	0.0	OTH	SX	AE	00:05-00:44	40	20003/ 01
0056	82 09 17 260 02:57:48.1	11.151S 162.212E	SOLOMON ISLANDS	69	5.2	0.0	PDE	EQ	ABDE	02:59-03:43	45	20005/ 01
0057	82 09 17 260 04:15:21.7	17.725S 172.756W	TONGA IS. REG.	33	5.2	5.4	PDE	EQ	A	04:24-04:44	21	20005/ 02
0058	82 09 17 260 09:40:41.2	3.400S 177.608E	GILBERT IS. REG.	33	4.7	0.0	PDE	EQ	ABD	09:41-10:09	29	20005/ 03
0059	82 09 17 260 13:28:25.6	23.446S 179.947W	S. OF FIJI IS.	555	5.9	0.0	PDE	EQ	A	13:37-13:57	21	20005/ 04
0060	82 09 17 260 15:38:16.6	11.857S 117.188E	S. OF SUMBAWA IS.	33	5.1	0.0	PDE	EQ	A	15:43-15:54	12	20005/ 05
0061	82 09 17 260 20:21:03.1	23.426S 179.611W	S. OF FIJI IS.	33	5.3	0.0	PDE	EQ	A	20:24-20:35	12	20005/ 06
0062	82 09 18 261 14:25:03.0	3.488S 177.679E	GILBERT IS. REG.	33	5.0	0.0	PDE	EQ	ABDE	14:25-15:04	40	20005/ 07
0063	82 09 18 261 15:00:41.3	7.676S 127.477E	BANDA SEA	165	5.4	0.0	PDE	EQ	A	15:04-15:15	12	20000/ 06
0064	82 09 18 261 18:19:35.9	36.118N 141.454E	NR. E. COAST HONSHU, JAPAN	33	4.7	0.0	PDE	EQ	ABD	18:21-18:48	28	20005/ 09
0065	82 09 18 261 21:20:19.2	26.950S 176.461W	S. OF. FIJI IS.	116	5.2	0.0	PDE	EQ	A	21:24-21:35	12	20000/ 07
0066	82 09 20 263 12:57:45.3	26.924S 175.814W	S. OF TONGA IS.	33	5.5	6.0	PDE	EQ	ABDE	13:01-14:06	66	20005/ 11
0067	82 09 20 263 13:48:32.5	26.870S 175.934W	S. OF TONGA IS.	33	5.1	0.0	PDE	EQ	A	13:52-14:04	13	20005/ 11
0068	82 09 20 263 13:56:06.6	54.612S 143.723E	W. OF MACQUARIE IS.	10	5.7	5.8	PDE	EQ	A	14:05-14:24	20	20005/ 11
0069	82 09 20 263 17:05:06.3	26.858S 176.406W	S. OF FIJI IS.	67	5.3	0.0	PDE	EQ	A	17:09-17:20	12	20005/ 12
0070	82 09 20 263 19:30:28.6	27.116S 176.633W	KERMADEC IS. REG.	33	5.0	0.0	PDE	EQ	A	19:34-19:45	12	20005/ 13
0071	82 09 21 264 00:46:31.7	9.581S 151.972E	DENTRECASTEAUX IS. REG.	33	5.6	5.9	PDE	EQ	A	00:48-00:59	12	20005/ 14
0072	82 09 21 264 01:28:19.6	9.584S 152.252E	DENTRECASTEAUX IS. REG.	33	5.0	6.1	PDE	EQ	A	01:30-01:41	12	20005/ 15
0073	82 09 21 264 02:02:31.7	9.331S 152.320E	DENTRECASTEAUX IS. REG.	33	5.5	0.0	PDE	EQ	A	02:04-02:15	12	20005/ 16
0074	82 09 21 264 02:57:01.1	49.989N 78.229E	EASTERN KAZAKH SSR	0	5.2	0.0	PDE	NX	A	03:04-03:15	12	20000/ 00
0075	82 09 21 264 17:54:00.4	4.461S 126.569E	BANDA SEA	33	5.0	0.0	PDE	EQ	A	17:57-18:00	12	20005/ 18
0076	82 09 22 265 04:12:31.6	3.681S 177.756E	GILBERT IS. REG.	33	4.7	0.0	PDE	EQ	ABD	04:13-04:27	15	20005/ 19
0077	82 09 22 265 08:17:32.3	33.512N 143.144E	OFF E. COAST OF HONSHU	33	4.4	0.0	PDE	EQ	ABD	08:18-08:32	15	20005/ 20
0078	82 09 22 265 10:39:13.3	42.193N 142.559E	HOKKAIDO, JAPAN REG.	33	4.8	0.0	PDE	EQ	ABD	10:40-10:56	17	20006/ 01
0079	82 09 22 265 12:01:26.9	36.300N 71.310E	AFGHANISTAN-USSR BORDER REGION	185	4.7	0.0	PDE	EQ	A	12:00-12:20	13	20006/ 02
0080	82 09 22 265 21:25:51.9	26.864S 176.145W	SOUTH OF FIJI IS.	33	5.2	0.0	PDE	EQ	A	21:29-21:41	13	20006/ 03
0081	82 09 23 266 04:20:06.7	21.701N 143.000E	MARIANA ISLANDS REGION.	321	5.0	0.0	PDE	EQ	ABDE	04:20-04:55	36	20006/ 04
0082	82 09 23 266 16:00:00.0	37.212N 116.207W	SOUTHERN NEVADA.	0	4.9	0.0	PDE	NX	A	16:06-16:17	12	20006/ 05
0083	82 09 23 266 17:00:00.0	37.175N 116.000W	SOUTHERN NEVADA.	0	4.9	0.0	PDE	NX	A	17:06-17:17	12	20006/ 06
0084	82 09 24 267 07:40:24.3	37.852N 118.123W	CALIFORNIA-NEVADA BORDERREG.	5	5.0	4.6	PDE	EQ	A	07:46-07:57	12	20006/ 07
0085	82 09 24 267 18:57:55.5	15.737N 147.583E	MARIANA IS. REGION.	49	5.1	4.3	PDE	EQ	ABDE	18:57-19:20	32	20006/ 08
0086	82 09 24 267 19:47:18.0	0.268N 120.753E	MINAHASSA PENINSULA.	123	5.5	0.0	PDE	EQ	A	19:51-20:02	12	20006/ 09
0087	82 09 24 267 21:11:27.9	3.367S 177.604E	GILBERT IS. REGION.	20	5.1	0.0	PDE	EQ	ABDE	21:12-21:50	39	20006/ 10
0088	82 09 24 267 22:34:47.8	6.002N 126.711E	MINDANAO, PHILIPPINE IS.	50	5.0	5.3	PDE	EQ	A	22:37-22:49	13	20006/ 11
0089	82 09 24 267 22:51:50.9	5.900N 126.671E	MINDANAO, PHILIPPINE IS.	35	5.5	5.6	PDE	EQ	A	22:54-23:06	13	20006/ 12
0090	82 09 25 268 03:11:41.4	4.426S 102.132E	SOUTHERN SUMATERA	51	5.1	0.0	PDE	EQ	A	03:10-03:29	12	20006/ 13
0091	82 09 25 268 08:48:43.6	15.736N 147.606E	MARIANA IS. REGION.	55	5.2	0.0	PDE	EQ	ABDE	08:48-09:18	31	20006/ 14
0092	82 09 25 268 09:03:43.5	17.557S 179.075W	FIJI IS.	543	5.0	0.0	PDE	EQ	A	09:05-09:17	13	20006/ 14
0093	82 09 25 268 16:04:01.8	11.361S 166.287E	SANTA CRUZ ISL.	47	5.5	5.3	PDE	EQ	A	16:05-16:16	12	20006/ 15
0094	82 09 25 268 17:59:57.0	64.311N 91.859E	CENTRAL SIBERIA.	0	5.1	0.0	PDE	NX	A	18:06-18:17	12	20006/ 16
0095	82 09 25 268 18:08:06.8	7.099S 129.795E	BANDA SEA.	94	5.5	0.0	PDE	EQ	A	18:11-18:22	12	20006/ 16
0096	82 09 26 269 01:09:38.4	50.040N 158.888E	KURIL IS. REGION.	42	5.5	4.5	PDE	EQ	ABDE	01:11-01:56	46	20006/ 17
0097	82 09 26 269 04:46:37.9	47.013N 152.320E	KURIL IS.	112	5.6	0.0	PDE	EQ	ABDE	04:47-05:32	46	20006/ 18
0098	82 09 26 269 04:32:31.7	6.619N 126.772E	MINDANAO, PHILIPPINE IS.	192	5.4	0.0	PDE	EQ	A	04:35-04:46	12	20006/ 19
0099	82 09 26 269 14:00:49.8	3.392S 177.612E	GILBERT IS. REGION.	25	5.4	4.9	PDE	EQ	ABDE	14:01-14:39	39	20006/ 20
0100	82 09 27 270 00:55:33.5	1.261N 126.325E	MOLUCCA PASSAGE.	56	5.5	0.0	PDE	EQ	A	00:58-01:10	13	20006/ 21

WAKE HYDROPHONE INFORMATION PROCESSING SYSTEM (WHIPS) EVENT LISTING 6 JUL 83

KEY: INFORMATION SOURCES - PDE=NEIS PDECARD, MON=NEIS MONTHLY LIST, ICS=ICS LIST, HEL=HELICORDER, OTH=OTHER
EVENT TYPE - EQ=EARTHQUAKE, NX=NUCLEAR EXPLOSION, SX=SCIENTIFIC EXPLOSION, OT=OTHER, UN=UNKNOWN
PHASES - A=P, B=PO, C=S, D=SO, E=T, F=OTHER

EVNT NO	ORIGIN TIME YR MO DA JUL HR MN SECS	COORDINATES LAT	LON	LOCATION DESCRIPTION	DEP KM	MAGNI BDY	SRF	INF SRC	EV TP	SAVED PHASES	INTERVAL	MNS	STRIP TAPE/FILE
#101	82 #9 27 278 12:37:38.4	39.278N	73.7#4E	TAJIK-SINKIANG BORDER REGION.	33	4.8	4.#	PDE	EQ	A	12:45-12:56	12	28887/ #1
#102	82 #9 27 278 21:37:12.7	1#.327N	126.158E	PHILIPPINE IS. REGION.	54	5.#	#.#	PDE	EQ	A	21:4#-21:51	12	2#227/ #2
#103	82 #9 28 271 #5:#7:15.7	3.#29S	177.554E	GILBERT IS. REGION.	33	4.9	#.#	PDE	EQ	ABD	#5:#7-#5:21	15	28227/ #3
#104	82 #9 28 271 15:14:36.#	24.173S	176.754W	SOUTH OF FIJI IS.	4#	6.#	6.1	PDE	EQ	AE	15:18-16:19	62	28287/ #4
#105	82 #9 28 271 22:42:2#.6	15.685N	147.658E	MARIANA IS. REGION.	33	5.1	#.#	PDE	EQ	ABDE	22:41-23:12	32	28#27/ #5
#106	82 #9 28 271 22:48:#5.4	15.72#N	147.761E	MARIANA IS. REGION.	33	4.7	#.#	PDE	EQ	ABD	22:47-23:##	14	28##7/ #5
#107	82 #9 29 272 #4:24:16.1	37.346N	72.942E	TAJIK SSR	33	5.4	4.9	PDE	EQ	A	#4:31-#4:43	13	28#27/ #6
#108	82 #9 29 272 #5:53:33.5	37.297N	73.258E	TAJIK SSR	33	4.8	#.#	PDE	EQ	A	#6:#1-#6:12	12	28#27/ #7
#109	82 #9 29 272 #9:29:47.2	25.139N	141.751E	VOLCANO ISLANDS REGION.	1#3	4.9	#.#	PDE	EQ	ABD	#9:3#-#9:44	15	28#27/ #8
#11#	82 #9 29 272 13:3#:##.1	37.#91N	116.#45W	SOUTHERN NEVADA	#	#.#	#.#	PDE	NX	A	13:36-13:47	12	28#27/ #9
#111	82 #9 29 272 19:#3:37.3	7.268S	155.723E	SOLOMON IS.	55	5.#	4.5	PDE	EQ	ABDE	19:#4-19:46	43	28#27/ 1#
#112	82 #9 29 272 20:46:49.9	7.275S	155.894E	SOLOMON IS.	33	6.1	4.4	PDE	EQ	ABDE	2#:48-21:29	42	28#27/ 11
#113	82 #9 3# 273 #1:44:#6.#	6.981S	155.758E	SOLOMON IS.	42	5.#	#.#	PDE	EQ	ABDE	#1:45-#2:26	42	28#27/ 12
#114	82 #9 3# 273 #2:28:3#.#	21.528S	177.98#W	FIJI IS. REG.	4##	4.4	#.#	PDE	EQ	A	#2:31-#2:42	12	28#27/ 13
#115	82 #9 3# 273 #5:44:49.1	3#.#51N	73.996E	TAJIK-SINKIANG BORDER REGION.	1#4	4.#	#.#	PDE	EQ	A	#5:52-#6:#3	12	28#27/ 14
#116	82 #9 3# 273 14:23:58.5	14.658S	173.2#4W	SAMOA IS. REGION.	2#	5.6	5.5	PDE	EQ	A	14:26-14:38	13	28#27/ 15
#117	82 1# #1 274 16:53:51.6	37.79#N	139.476E	HONSHU, JAPAN	15#	5.1	#.#	PDE	EQ	ABDE	16:55-17:39	45	28#27/ 16
#118	82 1# #2 275 #3:29:13.#	27.72#N	139.852E	BONIN ISLANDS REGION	485	4.2	#.#	PDE	EQ	ABD	##:29-##:44	16	28#27/ 17
#119	82 1# #2 275 #4:54:#7.5	8.883S	118.827E	SUMBAWA ISLAND REGION	33	4.9	#.#	PDE	EQ	A	#4:59-#5:1#	12	28#27/ 18
#12#	82 1# #2 275 #8:26:25.5	14.738S	167.284E	VANUATU ISLANDS	152	5.5	#.#	PDE	EQ	A	##:29-##:39	12	28#27/ 19
#121	82 1# #3 276 #1:12:58.#	5.646S	129.899E	BANDA SEA	228	5.#	#.#	PDE	EQ	A	#1:16-#1:27	12	28##7/ 2#
#122	82 1# #3 276 #8:41:29.4	3.372S	177.553E	GILBERT ISLANDS REGION	33	5.#	4.7	PDE	EQ	ABDE	##:42-#9:2#	39	28#28/ #1
#123	82 1# #3 276 11:#2:#4.3	9.377S	152.347E	DENTRECASTEAUX ISLANDS REGION	39	5.1	#.#	PDE	EQ	A	11:#3-11:15	13	28#28/ #9
#124	82 1# #3 276 16:1#:#9.3	55.963N	149.967W	GULF OF ALASKA	33	4.2	#.#	PDE	EQ	A	16:22-16:33	12	28#29/ #2
#125	82 1# #3 276 19:59:34.#	6.468S	15#.#38E	NEW BRITAIN REGION	42	5.2	#.#	PDE	EQ	ABDE	2#:#1-2#:44	44	28#28/ #3
#126	82 1# #3 276 22:26:34.#	8.142S	118.#87E	SUMBAWA ISLAND REGION	33	4.7	#.#	PDE	EQ	A	22:31-22:42	12	28#28/ #4
#127	82 1# #3 276 23:29:31.2	42.#64N	14#.761E	HOKKAIDO, JAPAN REGION.	152	4.7	#.#	PDE	EQ	ABD	23:31-23:47	17	28#28/ #5
#128	82 1# #4 277 #7:46:53.2	51.771N	176.#89W	ANDREANOF ISL., ALEUTION ISL.	62	5.4	#.#	PDE	EQ	ABDE	#7:49-#8:37	49	28#28/ 1#
#129	82 1# #4 277 #3:52:28.4	5.842N	126.744E	MINDANAO, PHILIPPINE ISL.	94	5.4	#.#	PDE	EQ	A	#8:55-#9:#6	12	28#28/ 11
#13#	82 1# #4 277 15:23:26.9	22.684S	171.192E	LOYALTY ISLAND REGION	33	5.1	5.#	PDE	EQ	A	15:26-15:37	12	28#29/ 12
#131	82 1# #4 277 16:2#:4#.#	22.685S	171.153E	LOYALTY ISLAND REGION	33	4.9	#.#	PDE	EQ	A	16:23-16:35	13	28#29/ 13
#132	82 1# #5 278 #3:18:53.#	#.217N	122.244E	MINAHASSA PENINSULA	221	4.#	#.#	PDE	EQ	A	##:22-##:33	12	28#28/ 14
#133	82 1# #5 278 #4:#9:16.7	3.41#S	177.591E	GILBERT ISL. REGION	33	5.3	#.#	PDE	EQ	ABDE	#4:#9-#4:48	4#	28#29/ 15
#134	82 1# #5 278 #9:14:41.3	15.642S	167.93#E	VANUATU ISL	91	5.9	#.#	PDE	EQ	ABDE	#9:16-1#:#5	5#	28#29/ 16
#135	82 1# #5 278 1#:15:15.4	3#.229S	178.#56W	KERMADEC ISL	146	5.5	#.#	PDE	EQ	A	1#:19-1#:3#	12	28#29/ 17
#136	82 1# #5 278 12:#4:13.2	4.239N	126.657E	TALAUD ISLANDS	95	5.3	#.#	PDE	EQ	A	12:#7-12:18	12	28#29/ 18
#137	82 1# #5 278 19:46:27.6	33.149N	136.9##E	NEAR S. COAST OF SOUTH HONSHU	391	4.7	#.#	PDE	EQ	ABD	19:47-2#:#3	17	28#28/ 19
#138	82 1# #5 278 22:17:19.9	3#.161S	179.3#4W	KERMADEC ISL. REGION	325	4.9	#.#	PDE	EQ	A	2#:21-2#:32	12	28#29/ 2#
#139	82 1# #5 278 22:25:56.#	22.817S	171.187E	LOYALTY ISL. REGION	45	5.6	5.4	PDE	EQ	A	2#:29-2#:4#	12	28#29/ 21
#14#	82 1# #6 279 21:13:12.#	22.##1S	171.241E	LOYALTY IS. REGION	33	5.5	5.1	PDE	EQ	A	21:16-21:27	12	28#29/ 22
#141	82 1# #7 28# #1:52:29.3	23.376N	94.349E	BURMA-INDIA BORDER REGION	98	4.7	#.#	PDE	EQ	A	#1:58-#2:#9	12	28#28/ #2
#142	82 1# #7 28# #7:15:56.9	7.163S	125.91#E	BANDA SEA	518	6.2	#.#	PDE	EQ	A	#7:19-#7:31	13	28#29/ #1
#143	82 1# #7 28# #9:26:#1.4	3.496S	177.516E	GILBERT IS. REGION	26	4.7	#.#	PDE	EQ	ABD	#9:26-#9:4#	15	28#29/ #2
#144	82 1# #7 28# 11:#2:17.4	32.34#N	137.455E	SOUTH OF HONSHU, JAPAN.	388	5.1	#.#	PDE	EQ	ABDE	11:#3-11:46	44	28#29/ #3
#145	82 1# #7 28# 13:4#:19.2	3.546S	177.678E	GILBERT IS. REGION	29	4.9	4.4	PDE	EQ	ABD	13:4#-13:55	16	28#29/ #4
#146	82 1# #7 28# 21:57:#3.3	32.143N	142.381E	SOUTH OF HONSHU, JAPAN.	33	4.8	#.#	PDE	EQ	ABD	21:57-22:12	16	28#29/ #5
#147	82 1# #8 281 13:34:57.2	26.356N	99.849E	YUNNAN PROVINCE, CHINA	4#	5.#	4.5	PDE	EQ	A	13:4#-13:51	12	28#29/ #6
#148	82 1# #8 281 18:45:39.4	23.314S	179.85#E	SOUTH OF FIJI IS.	65#	5.1	#.#	PDE	EQ	A	18:48-18:59	12	28#29/ #7
#149	82 1# #8 281 18:59:11.#	37.584N	72.#95E	TAJIK SSR	33	5.2	#.#	PDE	EQ	A	19:#6-19:18	12	28#29/ #8
#15#	82 1# #9 282 #8:53:15.2	4#.147N	143.742E	OFF EAST COAST OF HONSHU, JAPA	33	4.#	4.5	PDE	EQ	ABD	##:54-#1:#9	16	28#29/ #9
#151	82 1# #9 282 18:53:#2.1	3.519S	177.788E	GILBERT IS. REGION	33	5.3	4.7	PDE	EQ	ABDE	18:53-19:32	4#	28#39/ 1#
#152	82 1# #9 282 19:4#:23.#	3.478S	177.675E	GILBERT IS. REGION	33	5.3	4.4	PDE	EQ	ABDE	19:41-2#:19	35	28#39/ 11
#153	82 1# #9 282 22:#9:11.7	16.565S	167.479E	VANUATU IS.	33	5.1	4.7	PDE	EQ	A	22:11-22:22	12	28#29/ 12
#154	82 1# 1# 283 #4:59:56.#	61.555N	112.833E	CENTRAL SIBERIA	#	5.3	#.#	PDE	NX	A	#5:#5-#5:16	12	28#29/ 13
#155	82 1# 1# 283 12:41:#8.2	17.762S	178.573W	FIJI IS. REGION	596	4.1	#.#	PDE	EQ	A	12:43-12:54	12	28#29/ 14
#156	82 1# 1# 283 17:23:#3.#	4#.171N	143.882E	OFF EAST COAST OF HONSHU, JAPA	28	5.4	5.2	PDE	EQ	ABDE	17:24-18:#6	43	28#29/ 15
#157	82 1# 1# 283 2#:36:28.6	7.222S	129.621E	BANDA SEA	149	4.#	#.#	PDE	EQ	A	2#:39-2#:51	13	28#29/ 16
#158	82 1# 11 284 #7:14:58.1	73.368N	54.532E	NOVAYA ZEMLYA	#	5.6	3.6	PDE	NX	A	#7:22-#7:33	12	28#29/ 17
#159	82 1# 11 284 1#:25:35.2	62.551S	166.866E	BALENNY IS. REGION	1#	5.#	4.9	PDE	EQ	A	1#:33-1#:44	12	28#29/ 18
#16#	82 1# 11 284 16:34:47.#	27.43#S	176.441W	KERMADEC IS. REGION	45	5.2	#.#	PDE	EQ	A	16:38-16:5#	13	28#29/ 19
#161	82 1# 12 285 #4:49:38.9	37.28#N	69.7#4E	AFGHANISTAN-USSR BORDER REGION	33	4.#	#.#	PDE	EQ	A	#4:57-#5:##	12	28#29/ 2#
#162	82 1# 12 285 #8:39:57.3	21.186S	175.637W	TONGA IS.	198	4.7	#.#	PDE	EQ	A	##:43-##:54	12	28#29/ 21
#163	82 1# 13 286 18:52:49.3	14.156N	124.467E	LUZON, PHILIPPINE IS.	33	5.1	#.#	PDE	EQ	A	18:55-19:#7	13	28#29/ 22
#164	82 1# 14 287 21:4#:19.5	27.485N	139.837E	BONIN IS. REGION	495	5.1	#.#	PDE	EQ	ABDE	21:4#-22:2#	41	28#25/ 23
#165	82 1# 14 287 21:59:44.4	3#.449N	133.581E	SEA OF JAPAN	416	4.3	#.#	PDE	EQ	ABD	22:#1-22:18	1#	28#25/ 23
#166	82 1# 15 288 ##:54:#9.9	5.#49N	126.242E	MINDANAO, PHILIPPINE IS.	94	5.3	#.#	PDE	EQ	A	##:57-#1:##	12	28#1#/ #1
#167	82 1# 15 288 1#:58:39.#	32.871N	125.756W	NORTH PACIFIC OCEAN.	1#	5.1	4.4	PDE	EQ	A	11:#4-11:15	12	28#1#/ #2
#168	82 1# 16 289 #1:53:3#.9	5.544S	146.247E	EAST PAPUA NEW GUINEA REGION	76	5.3	#.#	PDE	EQ	ABDE	#1:55-#2:4#	46	28#1#/ #3
#169	82 1# 16 289 #3:#2:58.3	34.681N	139.411E	NEAR S. COAST OF HONSHU, JAPAN	133	4.7	#.#	PDE	EQ	ABD	#3:#4-#3:19	16	28#1#/ #4
#17#	82 1# 16 289 #5:59:57.2	46.727N	48.162E	SOUTHWESTERN USSR	#	5.2	3.#	PDE	NX	A	#6:#6-#6:19	12	28#1#/ #5
#171	82 1# 16 289 #6:#4:57.1	46.723N	48.222E	SOUTHWESTERN USSR	#	5.3	3.#	PDE	NX	A	#6:13-#6:24	12	28#1#/ #5
#172	82 1# 16 289 #6:#9:57.1	46.748N	46.258E	SOUTHWESTERN USSR	#	5.2	3.1	PDE	NX	A	#6:18-#6:29	12	28#1#/ #5
#173	82 1# 16 289 #6:14:57.1	46.787N	48.238E	SOUTHWESTERN USSR	#	5.4	3.1	PDE	NX	A	#6:23-#6:34	12	28#1#/ #5
#174	82 1# 16 289 #6:#2:54.3	23.321S	171.684E	LOYALTY IS. REGION	33	5.#	4.2	PDE	EQ	A	##:#6-##:17	12	28#1#/ #6
#175	82 1# 16 289 #3:46:56.#	36.486N	71.228E	AFGHANISTAN-USSR BORDER REGION	23#	4.6	#.#	PDE	EQ	A	##:54-#9:#5	12	28#1#/ #7
#176	82 1# 17 29# 1#:12:#9.#	49.623N	155.919E	KURIL IS.	47	5.5	4.9	PDE	EQ	ABDE	1#:13-1#:59	47	28#1#/ #8
#177	82 1# 1# 291 12:12:5#.#	12.826N	143.427E	SOUTH OF MARIANA IS.	11#	5.#	#.#	PDE	EQ	ABDE	12:13-12:48	36	28#1#/ #9
#178	82 1# 19 292 #3:34:36.2	17.##4S	173.233W	TONGA IS.	9#	5.4	#.#	PDE	EQ	A	#3:37-#3:4#	12	28#1#/ 1#
#179	82 1# 19 292 #3:43:#5.9	15.565S	174.985W	TONGA IS.	282	5.2	#.#	PDE	EQ	A	#3:45-#3:56	12	28#1#/ 1#
#18#	82 1# 19 292 12:46:#3.#	39.931N	118.#82E	NORTHEASTERN CHINA.	33	5.#	#.#	PDE	EQ	A	12:49-13:#1	13	28#1#/ 11
#181	82 1# 19 292 16:19:#5.5	11.394S	163.149E	SOLOMON IS.	46	5.6	5.9	PDE	EQ	ABDE	16:2#-17:#5	46	28#1#/ 12
#182	82 1# 19 292 22:2#:#9.6	3.114S	129.846E	CERAM	33	5.1	#.#	PDE	EQ	A	22:31-22:42	12	28#1#/ 13
#183	82 1# 2# 293 #2:29:49.7	9.112N	125.#82E	MINDANAO, PHILIPPINE IS.	144	4.9	#.#	PDE	EQ	A	#2:32-#2:43	12	28#1#/ 14
#184	82 1# 2# 293 #5:36:#6.2	41.158N	142.941E	HOKKAIDO, JAPAN REGION	33	5.1	4.7	PDE	EQ	ABDE	#5:37-#6:21	45	28#1#/ 15
#185	## ## ## ### ##:##:##.#	#.###N	#.###E		#	#.#	#.#	HEL	EQ	BDE	16:45-17:14	3#	28#1#/ 16
#186	82 1# 2# 293 19:23:#9.#	33.589N	14#.916E	SOUTH OF HONSHU, JAPAN	54	4.9	#.#	PDE	EQ	ABD	19:24-19:38	15	28#1#/ 17
#187	82 1# 2# 293 2#:#1:56.3	23.837N	121.981E	TAIWAN	2#	5.4	5.9	PDE	EQ	A	2#:#5-2#:16	12	28#1#/ 18
#188	82 1# 21 294 #9:47:#1.#	19.##6S	169.#52E	VANUATU IS.	181	5.2	#.#	PDE	EQ	A	#9:49-1#:##	12	28#1#/ 19
#189	82 1# 22 295 #1:##:3#.7	6.323S	13#.51#E	BANDA SEA	128	5.2	#.#	PDE	EQ	A	#1:11-#1:22	12	28#1#/ 2#
#19#	82 1# 22 295 #2:2#:37.7	43.496N	146.822E	KURIL IS.	33	5.#	#.#	PDE	EQ	ABDE	#2:29-#3:13	45	28#1#/ #1
#191	82 1# 22 295 #2:2#:58.9	3.45#S	177.69#E	GILBERT IS. REG.	33	4.#	#.#	PDE	EQ	ABD	##:21-##:35	15	28#11/ #2
#192	82 1# 22 295 ##:5#:3#.9	3.552S	177.##4E	GILBERT IS. REG.	33	5.#	#.#	PDE	EQ	ABDE	##:51-#9:29	39	28#1#/ #3
#193	82 1# 22 295 1#:17:37.5	18.7#5N	125.484E	LEYTE, PHILIPPINE IS.	45	5.3	4.6	PDE	EQ	A	1#:2#-1#:31	12	28#1#/ #4
#194	82 1# 22 295 11:32:47.#	48.191N	139.335E	NEAR W. COAST HONSHU, JAPAN	33	4.9	#.#	PDE	EQ	ABD	11:34-11:5#	17	28#11/ #5
#195	82 1# 23 296 #7:#8:25.9	1.965S	126.572E	MOLUCCA SEA	33	5.4	4.9	PDE	EQ	A	##:11-##:22	12	28#1#/ #6
#196	82 1# 23 296 #8:##:#3.6	7.#9#S	1#3.265E	SOUTHWEST OF SUMATERA	33	5.#	#.#	PDE	EQ	A	##:14-#9:25	12	28#1#/ #7
#197	82 1# 23 296 #3:26:37.#	5.272N	126.7#6E	MINDINAO, PHILIPPINE IS.	63	4.#	#.#	PDE	EQ	A	#9:29-#9:4#	12	28#1#/ #8
#198	82 1# 24 297 #1:1#:25.3	8.472N	126.953E	MINDINAO, PHILIPPINE IS.	33	5.#	#.#	PDE	EQ	A	#1:13-#1:24	12	28#1#/ #9
#199	82 1# 24 297 #5:45:54.6	3.28#S	177.494E	GILBERT IS. REG.	33	4.7	#.#	PDE	EQ	ABD	#5:46-#6:##	15	28#1#/ 1#
#2##	82 1# 24 297 15:35:25.6	3.7#1S	131.179E	WEST IRIAN REG.	33	5.3	#.#	PDE	EQ	A	15:3#-15:49	12	28#1#/ 11

WAKE HYDROPHONE INFORMATION PROCESSING SYSTEM (WHIPS) EVENT LISTING 6 JUL 83

KEY: INFORMATION SOURCES - PDE=NEIS PDECARD, MON=NEIS MONTHLY LIST, ICS=ICS LIST, HEL=HELICORDER, OTH=OTHER
EVENT TYPE - EQ=EARTHQUAKE, NX=NUCLEAR EXPLOSION, SX=SCIENTIFIC EXPLOSION, OT=OTHER, UN=UNKNOWN
PHASES - A=P, B=PO, C=S, D=SO, E=T, F=OTHER

EVNT NO	YR	MO	DA	JUL	ORIGIN TIME HR	MN	SECS	COORDINATES LAT	LON	LOCATION DESCRIPTION	DEP KM	MAGNI BDY	SRF	INF SRC	EV TP	PHASES	SAVED INTERVAL	HNS	STRIP TAPE/FILE
0201	82	10	24	297	16	09	05.5	3.739S	131.194E	WEST IRIAN REG.	33	4.9	0.0	PDE	EQ	A	16:12-16:23	12	200:1/ 12
0202	82	10	24	297	22	28	20.5	53.752S	141.746E	W. OF MACQUARIE IS.	10	4.8	5.3	PDE	EQ	A	22:35-22:46	12	200:1/ 13
0203	82	10	25	298	12	30	04.5	18.198S	173.920W	TONGA ISLANDS	142	4.6	0.0	PDE	EQ	A	12:33-12:44	12	200:1/ 14
0204	00	00	00	000	00	00	00.0	0.000N	0.000E		0	0.0	0.0	HEL	EQ	ABDE	12:51-13:29	39	200:1/ 15
0205	82	10	25	298	14	26	49.5	4.802S	152.327E	NEW BRITAIN REG.	86	5.4	0.0	PDE	EQ	ABDE	14:27-14:38	42	200:1/ 16
0206	82	10	25	298	19	23	52.0	23.684S	179.251E	S. OF FIJI ISLANDS	573	4.8	0.0	PDE	EQ	A	19:26-19:37	12	200:1/ 17
0207	82	10	25	298	22	26	04.4	36.322N	120.528W	CENTRAL CALIFORNIA	11	5.4	5.2	PDE	EQ	ABD	22:32-22:56	25	200:1/ 18
0208	82	10	26	299	07	33	07.6	85.992N	84.821E	NORTH OF SEVERNAYA ZEMLYA	10	4.6	0.0	PDE	EQ	A	07:39-07:51	13	200:1/ 19
0209	82	10	26	299	12	44	18.1	7.446S	105.653E	JAVA	119	5.6	0.0	PDE	EQ	A	12:58-13:01	12	200:1/ 20
0210	82	10	27	300	05	45	32.3	46.896N	152.478E	KURIL IS.	33	4.9	0.0	PDE	EQ	ABD	05:46-06:02	17	200:1/ 21
0211	82	10	27	300	10	30	13.9	20.484N	121.596E	PHILIPPINE IS. REGION	47	5.5	4.5	PDE	EQ	A	10:33-10:44	12	200:1/ 22
0212	82	10	27	300	15	36	36.3	23.838N	105.887E	YUNNAN PROVINCE, CHINA	33	5.2	5.1	PDE	EQ	A	15:41-15:52	12	200:1/ 23
0213	82	10	27	300	17	49	15.0	36.389N	69.465E	HINDU KUSH	51	4.8	0.0	PDE	EQ	A	17:57-18:08	12	200:1/ 24
0214	82	10	28	301	03	28	36.5	37.335N	134.887E	SEA OF JAPAN	351	4.8	0.0	PDE	EQ	ABDE	03:38-04:17	40	200:2/ 01
0215	82	10	28	301	15	30	15.2	7.992S	109.144E	JAVA	98	5.1	0.0	PDE	EQ	A	15:35-15:47	13	200:2/ 02
0216	82	10	28	301	18	30	29.2	46.447N	144.867E	SEA OF OKHOTSK	284	4.4	0.0	PDE	EQ	ABD	18:31-18:48	18	200:2/ 03
0217	82	10	29	302	02	42	15.5	4.569S	152.462E	NEW BRITAIN REGION	100	5.1	0.0	PDE	EQ	ABDE	02:43-02:24	42	200:2/ 04
0218	82	10	29	302	01	04	44.9	16.998S	173.768W	TONGA ISLANDS	124	4.8	0.0	PDE	EQ	A	01:07-01:18	12	200:2/ 04
0219	82	10	29	302	03	47	25.4	6.851S	132.426E	BANDA SEA	198	5.6	0.0	PDE	EQ	A	03:58-04:01	12	200:2/ 05
0220	82	10	29	302	20	13	06.0	8.114S	107.172E	JAVA	33	5.1	4.8	PDE	EQ	A	20:19-20:30	12	200:2/ 06
0221	82	10	30	303	16	30	00.1	12.176S	167.432E	SANTA CRUZ ISLANDS	327	5.3	0.0	PDE	EQ	ABDE	16:31-17:16	46	200:2/ 07
0222	82	10	31	304	02	36	58.6	11.630S	117.722E	SOUTH OF SUMBAWA ISLAND	33	5.1	0.0	PDE	EQ	A	02:42-02:53	12	200:2/ 08
0223	82	10	31	304	02	40	26.6	18.662S	169.068E	VANUATU ISLANDS	209	4.7	0.0	PDE	EQ	ABD	02:52-03:08	19	200:2/ 08
0224	82	10	31	304	01	30	41.2	6.642S	130.508E	BANDA SEA	100	5.0	0.0	PDE	EQ	A	01:34-01:45	12	200:2/ 09
0225	82	10	31	304	02	48	13.5	2.944N	96.126E	NORTHERN SUMATERA	61	5.5	0.0	PDE	EQ	A	02:54-03:05	12	200:2/ 10
0226	82	10	31	304	10	40	52.0	35.921N	82.516E	TIBET	33	6.2	6.1	PDE	EQ	A	10:47-10:59	13	200:2/ 11
0227	82	10	31	304	19	12	46.2	9.672N	126.895E	MINDANAO, PHILIPPINE IS.	68	4.7	0.0	PDE	EQ	A	19:15-19:26	12	200:2/ 12
0228	82	10	31	304	22	17	38.2	6.857S	105.540E	SUNDA STRAIT	69	5.0	0.0	PDE	EQ	A	22:23-22:34	12	200:2/ 13
0229	82	11	01	305	00	47	55.2	31.397N	141.755E	SOUTH OF HONSHU, JAPAN	33	4.2	0.0	PDE	EQ	ABD	00:46-00:02	15	200:2/ 14
0230	82	11	01	305	23	31	56.2	25.823S	179.751E	SOUTH OF FIJI IS.	543	4.9	0.0	PDE	EQ	A	23:34-23:46	13	200:2/ 15
0231	82	11	02	306	07	48	27.7	12.397N	125.666E	SAMAR, PHILIPPINE IS.	33	5.1	4.2	PDE	EQ	A	07:43-07:54	12	200:2/ 16
0232	82	11	02	306	18	38	04.6	55.494S	124.485W	EASTER IS. CORDILLERA	10	5.4	5.1	PDE	EQ	ABDE	18:46-19:42	117	200:2/ 17
0233	82	11	03	307	14	48	04.5	3.234S	139.692E	WEST IRIAN	33	5.3	0.0	PDE	EQ	A	14:58-15:01	12	200:2/ 18
0234	82	11	03	307	18	07	47.9	25.167S	179.724E	SOUTH OF FIJI IS.	486	5.3	0.0	PDE	EQ	A	18:18-18:22	13	200:2/ 19
0235	82	11	04	308	03	08	32.1	22.705N	121.643E	TAIWAN REGION	143	5.0	0.0	PDE	EQ	A	03:11-03:22	12	200:3/ 01
0236	82	11	04	308	09	29	53.3	44.888N	147.982E	KURIL IS.	38	5.7	5.1	PDE	EQ	ABDE	09:31-10:14	44	200:3/ 02
0237	82	11	04	308	15	54	13.1	38.548N	143.424E	OFF EAST COAST OF HONSHU, JAPA	33	5.4	4.9	PDE	EQ	ABDE	15:55-16:37	43	200:3/ 03
0238	82	11	04	308	10	49	17.3	15.260S	167.469E	VANUATU IS.	115	5.2	0.0	PDE	EQ	A	10:51-10:02	12	200:3/ 04
0239	82	11	05	309	03	50	32.1	3.598S	177.708E	GILBERT IS. REGION	33	5.0	0.0	PDE	EQ	ABDE	03:51-04:29	39	200:3/ 05
0240	82	11	05	309	04	52	02.3	3.633S	128.671E	CERAM	114	5.3	0.0	PDE	EQ	A	04:55-05:06	12	200:3/ 06
0241	82	11	05	309	06	31	53.0	26.185S	178.216E	NORFOLK IS. REGION	33	5.7	0.0	PDE	EQ	A	06:35-06:46	12	200:3/ 07
0242	00	00	00	000	00	00	00.0	0.000N	0.000E	POSSIBLY MARIANAS	0	0.0	0.0	HEL	EQ	BD	16:26-16:39	15	200:3/ 08
0243	82	11	05	309	16	59	36.0	7.155S	129.622E	BANDA SEA	143	5.2	0.0	PDE	EQ	A	19:03-19:14	12	200:3/ 09
0244	82	11	06	310	07	45	49.2	3.556N	126.631E	TALAUD IS.	63	5.2	0.0	PDE	EQ	A	07:49-08:00	12	200:3/ 10
0245	82	11	07	311	07	21	35.6	20.216S	173.000W	TONGA IS. REGION	33	5.1	5.1	PDE	EQ	A	07:24-07:36	13	200:3/ 11
0246	82	11	07	311	08	38	38.5	6.482S	132.262E	BANDA SEA	107	5.0	0.0	PDE	EQ	A	08:41-08:53	13	200:3/ 12
0247	82	11	07	311	15	31	56.4	3.985S	154.479E	NORTH OF SOLOMON IS.	488	4.6	0.0	PDE	EQ	ABD	15:32-15:47	16	200:3/ 13
0248	82	11	08	312	07	56	08.2	25.375S	177.167W	SOUTH OF FIJI IS.	150	5.2	0.0	PDE	EQ	A	07:59-08:10	12	200:3/ 14
0249	82	11	08	312	09	44	06.9	55.789S	27.861W	SOUTH OF SANDWICH IS. REGION	33	5.4	5.3	PDE	EQ	A	09:53-10:12	20	200:3/ 15
0250	82	11	08	312	11	35	42.1	8.855S	119.268E	FLORES IS. REGION	103	5.1	0.0	PDE	EQ	A	11:48-11:51	12	200:3/ 16
0251	82	11	08	312	16	48	07.4	55.048N	165.687E	KOMANDORSKY IS. REGION	33	5.2	0.0	PDE	EQ	ABDE	16:42-17:32	51	200:3/ 17
0252	82	11	08	312	16	48	26.2	3.616S	177.768E	GILBERT IS. REGION	33	5.0	0.0	PDE	EQ	ABDE	16:49-17:27	39	200:3/ 17
0253	82	11	08	312	18	35	34.8	4.827N	127.035E	TALAUD IS.	161	5.4	0.0	PDE	EQ	A	18:38-18:49	12	200:3/ 18
0254	82	11	09	313	00	46	56.1	21.303S	178.734W	FIJI IS. REGION	556	5.2	0.0	PDE	EQ	A	00:49-01:00	12	200:3/ 19
0255	82	11	09	313	01	36	35.4	7.236N	94.437E	NICOBAR IS. REGION	33	5.2	4.7	PDE	EQ	A	01:43-01:54	12	200:3/ 20
0256	82	11	09	313	09	25	20.4	3.447S	177.728E	GILBERT IS. REGION	33	5.2	0.0	PDE	EQ	ABDE	09:25-10:04	40	200:3/ 21
0257	82	11	10	314	07	36	23.0	44.171N	149.532E	KURIL IS.	33	6.1	0.0	PDE	EQ	ABDE	07:37-08:20	44	200:4/ 01
0258	82	11	10	314	13	23	16.8	33.983N	137.870E	NEAR S. COAST OF HONSHU JAPAN	347	4.6	0.0	PDE	EQ	ABD	13:24-13:48	17	200:4/ 02
0259	82	11	10	314	21	20	45.8	15.454S	176.822W	FIJI IS. REGION	33	5.5	5.7	PDE	EQ	A	21:23-21:34	12	200:4/ 03
0260	82	11	11	315	00	43	45.7	6.677S	101.671E	SOUTHWEST OF SUMATERA	46	6.4	5.2	PDE	EQ	ABDE	00:58-01:01	44	200:4/ 04
0261	82	11	11	315	01	55	37.2	44.237N	149.515E	KURIL IS.	41	5.0	0.0	PDE	EQ	ABDE	01:56-02:39	44	200:4/ 05
0262	82	11	11	315	02	01	15.1	44.338N	149.488E	KURIL IS.	41	5.0	0.0	PDE	EQ	ABDE	02:02-02:45	44	200:4/ 05
0263	82	11	11	315	02	52	09.3	44.113N	149.595E	KURIL IS.	41	5.3	5.2	PDE	EQ	ABDE	02:53-03:35	43	200:4/ 06
0264	82	11	11	315	04	14	34.6	44.217N	149.314E	KURIL IS.	33	5.0	0.0	PDE	EQ	ABDE	04:16-04:58	44	200:4/ 07
0265	82	11	11	315	11	55	58.9	6.190S	145.369E	EAST PAPUA NEW GUINEA REG.	49	5.4	0.0	PDE	EQ	ABD	11:57-12:43	47	200:4/ 08
0266	82	11	11	315	21	21	22.4	27.431S	176.735W	KERMADEC IS REGION	33	5.3	5.5	PDE	EQ	A	21:25-21:36	12	200:4/ 09
0267	82	11	12	316	12	16	06.2	1.478N	126.459E	MOLUCCA PASSAGE	44	5.5	4.6	PDE	EQ	A	12:19-12:30	12	200:4/ 10
0268	82	11	12	316	19	17	00.1	37.024N	116.832W	SOUTHERN NEVADA	0	4.4	0.0	PDE	NX	A	19:23-19:34	12	200:4/ 11
0269	82	11	12	316	22	08	54.0	43.753N	150.875E	KURIL IS. REGION	33	5.1	0.0	PDE	EQ	ABDE	22:10-22:52	43	200:4/ 12
0270	82	11	13	317	01	20	59.2	17.879S	176.386W	FIJI IS. REGION	33	5.0	4.9	PDE	EQ	A	01:23-01:35	13	200:4/ 13
0271	82	11	13	317	05	43	47.4	3.385S	146.835E	BISMARCK SEA	7	5.3	5.1	PDE	EQ	ABDE	05:45-06:28	44	200:4/ 14
0272	82	11	13	317	07	31	29.1	18.568S	167.241E	VANUATU ISLANDS	36	5.0	0.0	PDE	EQ	A	07:34-07:45	12	200:4/ 15
0273	82	11	13	317	10	21	13.4	6.872S	105.355E	SUNDA STRAIT	58	5.1	0.0	PDE	EQ	A	10:27-10:38	12	200:4/ 16
0274	82	11	13	317	12	14	03.1	44.944N	148.984E	KURIL ISLANDS	33	4.9	0.0	PDE	EQ	ABD	12:15-12:38	16	200:4/ 17
0275	82	11	13	317	15	44	46.1	44.385N	129.498W	OFF COAST OF OREGON	10	5.1	5.1	PDE	EQ	A	15:58-16:01	12	200:4/ 18
0276	82	11	13	317	18	22	58.8	11.978N	143.812E	SOUTH OF MARIANA IS.	15	5.3	5.8	PDE	EQ	ABDE	18:23-18:58	36	200:5/ 01
0277	82	11	13	317	18	28	16.6	12.849N	143.780E	SOUTH OF MARIANA IS.	17	5.5	4.9	PDE	EQ	ABDE	18:28-19:04	37	200:5/ 01
0278	82	11	14	318	08	29	18.8	52.977N	158.697E	NEAR EAST COAST OF KAMCHATKA	70	5.9	0.0	PDE	EQ	ABDE	08:31-09:19	49	200:5/ 02
0279	82	11	14	318	16	23	57.3	9.419S	122.584E	SAVU SEA	60	5.5	0.0	PDE	EQ	A	16:28-16:39	12	200:5/ 03
0280	82	11	14	318	17	29	24.2	0.988N	29.095W	CENTRAL MID-ATLANTIC RIDGE	10	5.1	5.1	PDE	EQ	A	17:38-17:58	21	200:5/ 04
0281	82	11	15	319	07	59	29.3	26.271N	124.905E	NORTHEAST OF TAIWAN	202	4.9	0.0	PDE	EQ	A	08:02-08:13	12	200:5/ 05
0282	82	11	15	319	14	15	25.4	25.500S	13.855W	SOUTH ATLANTIC RIDGE	10	5.2	5.0	PDE	EQ	A	14:24-14:44	21	200:5/ 06
0283	82	11	15	319	15	25	52.2	20.668N	130.078E	BONIN IS. REGION	319	4.7	0.0	PDE	EQ	ABD	15:26-15:41	16	200:5/ 07
0284	82	11	16	320	17	25	54.1	14.628S	168.848E	VANUATU IS.	33	5.9	5.5	PDE	EQ	ABDE	17:27-18:15	49	200:5/ 08
0285	82	11	16	320	17	41	05.9	14.588S	167.962E	VANUATU IS.	33	5.1	0.0	PDE	EQ	A	17:43-17:54	12	200:5/ 08
0286	82	11	17	321	09	43	42.4	5.887S	147.167E	EAST PAPUA NEW GUINEA REGION	78	5.5	0.0	PDE	EQ	ABDE	09:45-10:30	46	200:5/ 09
0287	82	11	17	321	17	08	29.3	6.113S	150.835E	NEW BRITAIN REGION	57	5.2	4.3	PDE	EQ	ABDE	17:09-17:52	44	200:5/ 10
0288	82	11	18	322	10	00	31.2	24.816N	125.862E	SOUTHWESTERN RYUKYU ISLANDS	33	5.0	0.0	PDE	EQ	A	10:03-10:14	12	200:5/ 11
0289	82	11	18	322	10	59	21.2	5.767S	152.367E	NEW BRITAIN REGION	33	4.7	0.0	PDE	EQ	ABD	11:00-11:15	16	200:5/ 12
0290	82	11	18	322	14	57	51.7	1.720S	76.741W	ECUADOR	195	6.0	0.0	PDE	EQ	A	15:07-15:26	20	200:5/ 13
0291	82	11	18	322	22	48	03.7	3.634S	149.870E	WEST IRIAN	71	5.5	0.0	PDE	EQ	A	22:42-22:53	12	200:5/ 14
0292	82	11	19	323	04	27	16.4	10.594S	74.753W	PERU	33	6.3	6.3	PDE	EQ	E	04:30-06:59	150	200:6/ 01
0293	82	11	19	323	07	52	43.7	1.283N	121.902E	MINAHASSSA PENINSULA	42	5.2	0.0	PDE	EQ	A	07:56-08:07	12	200:6/ 02
0294	82	11	19	323	23	05	24.7	45.964N	142.615E	HOKKAIDO, JAPAN REGION	325	4.4	0.0	PDE	EQ	ABD	23:06-23:23	18	200:6/ 03
0295	82	11	20	324	05	10	00.6	5.700S	149.730E	NEW BRITAIN REGION	134	5.2	0.0	PDE	EQ	ABDE	05:19-06:02	44	200:6/ 04
0296	82	11	20	324	07	50	46.0	34.610N	70.566E	AFGHANISTAN	31	5.7	5.2	PDE	EQ	A	08:06-08:17	12	200:6/ 05
0297	82	11	20	324	23	10	42.1	55.143N	162.752E	NEAR EAST COAST OF KAMCHATKA	33	4.8	0.0	PDE	EQ	ABD	23:21-23:37	17	200:6/ 06
0298	82	11	20	324	23	34	35.1	7.514S	128.476E	BANDA SEA	128	5.1	0.0	PDE	EQ	A	23:38-23:49	12	200:6/ 06
0299	82	11	21	325	14	46	18.2	52.713N	164.956E	OFF EAST COAST OF KAMCHATKA	33	5.2	4.2	PDE	EQ	ABDE	14:48-15:36	49	200:6/ 07
0300	82	11	21	325	20	37	09.2	41.981N	142.583E	HOKKAIDO, JAPAN REGION	65	4.9	0.0	PDE	EQ	ABD	20:38-20:54	17	200:6/ 08

KEY: INFORMATION SOURCES - PDE=NEIS PDECARD, MON=NEIS MONTHLY LIST, ICS=ICS LIST HEL=HELI.ORDER, OTH=OTHER
EVENT TYPE - EQ=EARTHQUAKE, NX=NUCLEAR EXPLOSION, SX=SCIENTIFIC EXPLOSION, O'=OTHER, UN=UNKNOWN
PHASES - A=P, B=PO, C=S, D=SO, E=T, F=OTHER

EVNT NO	ORIGIN TIME YR	MO	DA	JUL	HR	MN	SECS	COORDINATES LAT	LON	LOCATION DESCRIPTION	DEP KM	MA BDY	MI SRF	INF SRC	EV TP	PHASES	SAVED INTERVAL	MNS	STRIP TAPE/FILE
#301	82 11 21	325	23	27	11.7	55.432N	163.222E	OFF EAST COAST OF KAMCHATKA	35	5.7	6.1	PDE	EQ	ABDE	23:29-00:20	52	20016/ #9
#302	82 11 22	326	00	25	20.3	55.627N	163.153E	OFF EAST COAST OF KAMCHATKA	33	4.7	0.0	PDE	EQ	ABD	00:27-00:44	18	20016/ 10
#303	82 11 22	326	02	20	03.7	7.255S	132.145E	TANIMBAR ISL. REGION	85	5.5	5.8	PDE	EQ	A	00:31-02:42	12	20016/ 10
#304	82 11 22	326	01	07	59.0	39.712N	77.718E	SOUTHERN SINKIANG PROV., CHINA	33	5.1	5.0	PDE	EQ	A	01:15-01:26	12	20016/ 11
#305	82 11 22	326	01	26	27.7	55.667N	163.221E	OFF EAST COAST OF KAMCHATKA	33	4.7	0.0	PDE	EQ	ABD	01:28-01:45	18	20016/ 12
#306	82 11 22	326	05	32	51.2	23.744S	176.864W	SOUTH OF FIJI IS.	82	5.4	5.0	PDE	EQ	A	05:36-05:47	12	20016/ 13
#307	82 11 22	326	05	19	48.4	32.250S	178.273W	SOUTH OF KERMADEC IS.	30	5.3	5.0	PDE	EQ	A	06:24-06:35	12	20016/ 14
#308	82 11 22	326	23	00	04.6	32.283S	178.484W	SOUTH OF KERMADEC IS.	80	5.1	0.0	PDE	EQ	A	23:12-23:23	12	20017/ 01
#309	82 11 23	327	06	45	47.8	3.744S	101.788E	SOUTHERN SUMATERA	75	5.1	4.0	PDE	EQ	A	06:52-07:03	12	20017/ 02
#310	82 11 23	327	16	59	29.8	23.955S	175.478W	TONGA IS. REGION	30	5.2	5.0	PDE	EQ	A	19:03-19:14	12	20017/ 03
#311	82 11 25	329	07	31	13.9	3.307S	177.639E	GILBERT IS. REGION	33	5.2	0.0	PDE	EQ	ABDE	07:31-08:10	40	20017/ 04
#312	82 11 25	329	10	00	59.6	36.732N	71.474E	AFGHANISTAN-USSR BORDER REGION	124	4.7	0.0	PDE	EQ	A	10:16-10:27	12	20017/ 05
#313	82 11 25	329	18	55	29.1	30.006N	132.263E	SOUTHEAST OF SHIKOKU, JAPAN	30	4.8	0.0	PDE	EQ	ABD	18:57-19:13	17	20017/ 06
#314	82 11 26	330	16	00	27.3	11.857N	142.647E	SOUTH OF MARIANA IS.	33	4.4	0.0	PDE	EQ	ABD	16:09-16:22	14	20017/ 07
#315	82 11 26	330	16	52	01.0	5.820N	126.812E	MINDANAO, PHILIPPINE IS.	33	5.0	5.0	PDE	EQ	A	16:55-17:06	12	20017/ 08
#316	82 11 26	330	17	45	33.8	55.884S	144.228W	SOUTH PACIFIC CORDILLERA	10	5.7	5.3	PDE	EQ	A	17:53-18:04	12	20017/ 09
#317	82 11 27	331	02	19	09.0	32.463S	178.263W	SOUTH OF KERMADEC IS.	52	5.5	0.0	PDE	EQ	A	02:23-02:35	13	20017/ 10
#318	82 11 27	331	03	38	42.1	55.764S	144.389W	SOUTH PACIFIC CORDILLERA	10	5.3	5.0	PDE	EQ	A	03:38-03:49	12	20017/ 11
#319	82 11 27	331	09	55	38.8	50.174N	147.792E	SEA OF OKHOTSK	623	5.6	0.0	PDE	EQ	ABDE	09:56-10:06	51	20017/ 12
#320	82 11 27	331	11	13	51.3	5.296N	125.809E	MINDANAO, PHILIPPINE IS.	142	5.1	0.0	PDE	EQ	A	11:16-11:28	13	20017/ 13
#321	82 11 27	331	14	11	46.3	36.535N	71.069E	AFGHANISTAN-USSR BORDER REGION	187	4.2	0.0	PDE	EQ	A	14:19-14:30	12	20017/ 14
#322	82 11 27	331	17	02	44.2	23.544S	175.286W	TONGA IS. REGION	33	5.2	0.0	PDE	EQ	A	17:06-17:17	12	20017/ 15
#323	82 11 27	331	20	30	27.7	39.018N	140.830E	HONSHU, JAPAN	33	4.8	0.0	PDE	EQ	ABD	20:31-20:47	17	20017/ 16
#324	82 11 28	332	11	04	06.9	6.687S	150.523E	NEW BRITAIN REGION	33	5.2	5.0	PDE	EQ	ABDE	11:05-11:49	45	20017/ 17
#325	82 11 28	332	19	05	38.2	2.912S	129.481E	CERAM	33	5.0	5.0	PDE	EQ	A	19:08-19:20	13	20017/ 18
#326	82 11 29	333	14	02	58.6	6.464S	154.399E	SOLOMON IS.	33	0.0	0.0	PDE	EQ	ABD	14:04-14:19	16	20017/ 19
#327	82 11 30	334	02	16	43.9	20.436S	178.853W	FIJI IS. REGION	540	5.2	0.0	PDE	EQ	A	02:19-02:30	12	20017/ 20
#328	00 00 00	000	00	00	02.0	0.000N	2.000E	PROBABLY MARIANAS	2	0.0	0.0	HEL	EQ	BD	06:52-07:19	26	20017/ 21
#329	82 11 30	334	14	03	00.5	32.249S	178.133W	SOUTH OF KERMADEC IS.	30	5.2	0.0	PDE	EQ	A	14:07-14:18	12	20017/ 22
#330	82 11 30	334	18	54	20.6	8.449S	121.595E	FLORES IS. REGION	20	4.7	0.0	PDE	EQ	A	18:58-19:09	12	20017/ 23
#331	82 11 30	334	19	00	32.2	51.977N	158.918E	NEAR EAST COAST OF KAMCHATKA	33	4.7	0.0	PDE	EQ	ASD	19:10-19:26	17	20017/ 23
#332	82 12 01	335	08	39	44.4	31.847N	131.762E	KYUSHU, JAPAN	36	5.0	5.1	PDE	EQ	ABDE	08:41-05:29	49	20018/ 01
#333	82 12 02	336	03	20	14.1	1.199S	23.722W	CENTRAL MID-ATLANTIC RIDGE	10	5.2	4.9	PDE	EQ	A	03:29-03:48	20	20018/ 19
#334	82 12 02	336	09	43	53.7	51.927N	178.473W	FOX IS., ALEUTIAN IS.	33	5.5	4.7	PDE	EQ	ABDE	09:46-10:37	52	20018/ 02
#335	82 12 02	336	15	24	50.1	36.217N	142.629E	OFF EAST COAST OF HONSHU JAPAN	33	4.7	0.0	PDE	EQ	ABD	15:26-15:41	16	0/ 02
#336	82 12 02	336	19	36	56.4	4.542S	138.982E	WEST IRIAN	33	5.6	5.3	PDE	EQ	A	19:39-19:50	12	20018/ 03
#337	82 12 03	337	00	56	10.0	3.889S	151.969E	NEW IRELAND REGION	256	4.9	0.0	PDE	EQ	ABD	00:56-01:11	16	20018/ 04
#338	82 12 03	337	01	38	42.5	23.588S	175.762W	TONGA IS. REGION	33	5.3	5.9	PDE	EQ	A	01:42-01:53	12	20018/ 05
#339	82 12 03	337	16	49	56.6	9.257S	120.342E	SUMBA IS. REGION	30	5.1	0.0	PDE	EQ	A	16:54-17:05	12	20018/ 07
#340	82 12 03	337	22	30	00.1	13.350S	167.206E	VANUATU IS.	260	5.7	0.0	PDE	EQ	A	22:31-22:42	12	20018/ 06
#341	82 12 04	338	02	07	27.9	3.715S	140.022E	WEST IRIAN	33	5.1	0.0	PDE	EQ	A	02:09-02:20	12	20018/ 09
#342	82 12 04	338	07	45	03.4	4.944N	126.855E	TALAUD ISLANDS	180	5.0	0.0	PDE	EQ	A	07:48-07:59	12	20018/ 10
#343	82 12 04	338	23	23	44.4	22.937N	142.691E	VOLCANO IS. REGION	270	4.7	0.0	PDE	EQ	ABDE	23:23-23:59	37	20018/ 11
#344	82 12 05	339	01	03	49.9	0.259S	126.434E	MOLUCCA SEA	50	4.9	0.0	PDE	EQ	A	01:07-01:18	12	20018/ 12
#345	82 12 05	339	03	37	12.6	49.907N	78.843E	EASTERN KASAKH SSR	2	6.1	4.4	PDE	NX	A	03:44-03:55	12	20018/ 13
#346	82 12 05	339	05	48	24.1	9.874S	161.181E	SOLOMON ISLANDS	84	5.9	0.0	PDE	EQ	ABDE	05:49-06:32	44	20018/ 14
#347	82 12 05	339	09	04	53.5	23.659S	175.461W	TONGA ISLANDS REGION	30	5.0	5.0	PDE	EQ	A	09:08-09:19	12	20018/ 15
#348	82 12 05	339	13	42	12.0	11.089S	165.126E	SANTA CRUZ ISLANDS	35	5.4	0.0	PDE	EQ	A	13:43-13:55	13	20018/ 16
#349	82 12 05	339	15	00	36.0	23.624S	175.627W	TONGA ISLANDS REGION	33	5.4	5.2	PDE	EQ	A	15:24-15:15	12	20018/ 17
#350	82 12 05	339	15	52	22.6	23.489S	175.881W	TONGA ISLANDS REGION	33	5.5	5.7	PDE	EQ	A	15:56-16:07	12	20018/ 18
#351	82 12 06	340	14	03	31.6	36.321N	141.262E	NEAR EAST COAST OF HONSHU, JAP	59	4.7	0.0	PDE	EQ	ABD	14:04-14:19	16	20018/ 20
#352	82 12 07	341	09	43	49.6	36.025N	114.825W	SOUTHERN NEVADA	5	0.0	0.0	PDE	EQ	A	09:50-10:01	12	20018/ 21
#353	82 12 07	341	12	12	09.1	45.551N	146.885E	KURIL ISLANDS	117	4.8	0.0	PDE	EQ	ABD	12:13-12:29	17	20018/ 22
#354	82 12 08	342	02	41	34.1	14.235N	146.126E	MARIANA ISLANDS	66	4.9	0.0	PDE	EQ	ABD	00:41-00:54	14	0/ 00
#355	82 12 08	342	10	54	12.6	3.472S	177.577E	GILBERT ISLANDS REGION	33	5.1	0.0	PDE	EQ	A	10:54-11:06	13	0/ 00
#356	82 12 08	342	16	30	51.0	8.632N	119.918E	MINAHASSA PENINSULA	87	5.0	0.0	PDE	EQ	A	16:34-16:46	13	0/ 00
#357	82 12 08	342	18	04	47.1	41.364S	87.626W	WEST CHILE RISE	10	5.4	0.0	PDE	EQ	A	18:14-18:33	20	0/ 00
#358	82 12 09	343	01	41	37.6	29.009S	112.655W	EASTER ISLAND REGION	10	5.6	5.9	PDE	EQ	ABDE	01:58-03:42	113	0/ 00
#359	82 12 09	343	05	28	48.1	3.481S	177.616E	GILBERT ISLANDS REGION	33	5.6	5.2	PDE	EQ	ABDE	05:29-06:07	39	0/ 00
#360	82 12 09	343	10	39	48.3	21.825S	168.527E	LOYALTY ISLANDS	33	5.4	5.0	PDE	EQ	A	10:42-10:53	12	20019/ 23
#361	82 12 09	343	10	58	35.7	47.833N	155.246E	KURIL ISLANDS REGION	33	5.2	0.0	PDE	EQ	ABDE	19:00-19:43	44	20019/ 01
#362	82 12 10	344	14	49	35.7	45.177N	148.613E	KURIL ISLANDS	119	4.9	0.0	PDE	EQ	ABD	14:50-15:06	17	20019/ 02
#363	82 12 10	344	15	28	00.0	37.030N	116.872W	SOUTHERN NEVADA	0	4.0	0.0	PDE	NX	A	15:26-15:37	12	20019/ 03
#364	82 12 10	344	17	28	59.9	26.442S	176.570W	SOUTH OF FIJI ISLANDS	33	5.2	5.1	PDE	EQ	A	17:24-17:36	13	20019/ 04
#365	00 00 00	000	00	00	00.0	0.000N	0.000E	PROBABLE MARIANAS PO SO T	0	0.0	0.0	HEL	EQ	BDE	19:10-19:44	35	20019/ 05
#366	00 00 00	000	00	00	00.0	0.000N	0.000E	PROBABLE MARIANAS PO SO T	0	0.0	0.0	HEL	EQ	BDE	23:19-00:07	49	20019/ 06
#367	82 12 11	345	16	46	31.4	11.377S	119.813E	SOUTH OF SUMBA ISLAND	33	5.7	0.0	PDE	EQ	A	16:51-17:02	12	20019/ 07
#368	82 12 12	346	17	10	09.2	17.010N	145.616E	MARIANA ISLANDS	326	4.9	0.0	PDE	EQ	ABDE	17:09-17:42	34	20019/ 08
#369	82 12 13	347	02	50	51.6	63.275S	61.237W	SOUTH SHETLAND ISLANDS	33	5.7	5.4	PDE	EQ	A	03:00-03:19	20	20019/ 09
#370	82 12 13	347	09	12	49.4	14.750N	44.287E	WESTERN ARABIAN PENINSULA	10	5.9	6.0	PDE	EQ	AE	09:22-11:41	140	20019/ 10
#371	82 12 13	347	10	25	05.5	10.111S	178.476W	FIJI IS. REGION	645	4.7	0.0	PDE	EQ	A	10:27-10:38	12	20019/ 10
#372	82 12 14	348	02	37	10.5	20.535S	169.487E	VANUATU IS	207	5.2	0.0	PDE	EQ	A	02:39-02:51	13	20019/ 11
#373	82 12 14	348	12	02	05.0	23.653S	175.005W	TONGA IS. REGION	33	5.4	5.0	PDE	EQ	A	12:05-12:17	13	20019/ 12
#374	82 12 14	348	23	11	07.7	23.157S	178.612W	SOUTH OF FIJI IS.	548	5.9	0.0	PDE	EQ	A	23:13-23:25	13	20019/ 13
#375	82 12 15	349	10	17	21.8	18.177S	178.321W	FIJI IS. REGION	652	5.0	0.0	PDE	EQ	A	10:19-10:30	12	20019/ 14
#376	82 12 16	350	00	48	48.6	36.242N	69.896E	HINDU KUSH REGION	35	6.2	6.6	PDE	EQ	AE	00:48-02:33	106	20020/ 01
#377	82 12 16	350	05	27	53.1	36.356N	69.595E	HINDU KUSH REGION	33	5.0	0.0	PDE	EQ	A	05:35-05:46	12	20020/ 02
#378	82 12 16	350	09	56	38.0	11.689N	92.993E	ANDAMAN IS. REGION	86	5.3	0.0	PDE	EQ	A	09:03-09:14	12	20020/ 03
#379	82 12 16	350	17	04	26.9	1.342N	126.940E	MOLUCCA PASSAGE	69	5.4	0.0	PDE	EQ	A	17:07-17:18	12	20020/ 04
#380	82 12 16	350	21	01	38.2	36.174N	68.994E	HINDU KUSH REGION	33	5.0	4.0	PDE	EQ	A	21:09-21:20	12	20020/ 05
#381	82 12 17	351	02	43	01.9	24.642N	122.618E	TAIWAN REGION	73	6.2	0.0	PDE	EQ	A	02:46-02:57	12	20020/ 06
#382	82 12 17	351	11	52	57.7	3.582S	177.716E	GILBERT IS. REGION	33	5.0	0.0	PDE	EQ	ABDE	11:53-12:32	40	20020/ 07
#383	82 12 17	351	21	15	01.6	26.671S	176.277W	SOUTH OF FIJI ISLANDS	33	5.3	5.6	PDE	EQ	A	21:19-21:30	12	20020/ 08
#384	82 12 18	352	00	41	16.6	1.758N	126.634E	MOLUCCA PASSAGE	47	5.6	5.1	PDE	EQ	A	00:44-00:55	12	20020/ 09
#385	82 12 18	352	00	26	47.5	25.675S	176.574W	SOUTH OF FIJI ISLANDS	33	5.3	0.0	PDE	EQ	A	05:30-05:42	13	20020/ 10
#386	82 12 18	352	21	11	36.2	6.837S	125.117E	BANDA SEA	661	4.7	0.0	PDE	EQ	A	21:14-21:26	13	20020/ 11
#387	82 12 19	353	00	06	19.8	32.478S	178.457W	SOUTH OF KERMADEC ISLANDS	33	5.0	5.2	PDE	EQ	A	00:18-00:22	13	20020/ 12
#388	82 12 19	353	00	33	49.4	32.472S	178.323W	SOUTH OF KERMADEC ISLANDS	33	5.6	5.5	PDE	EQ	A	00:38-00:49	12	20020/ 13
#389	82 12 19	353	06	24	39.6	6.311S	100.784E	SOUTHWEST OF SUMATERA	33	5.4	0.0	PDE	EQ	A	06:31-06:42	12	20020/ 14
#390	82 12 19	353	13	00	15.4	24.255S	175.932W	SOUTH OF TONGA ISLANDS	33	5.5	5.6	PDE	EQ	A	13:03-13:15	13	20020/ 15
#391	82 12 19	353	17	43	55.9	24.188S	175.773W	SOUTH OF TONGA ISLANDS	33	6.0	7.7	PDE	EQ	ABDE	17:47-18:49	62	20020/ 16
#392	82 12 19	353	18	33	16.0	23.985S	175.421W	TONGA ISLANDS REGION	33	5.7	0.0	PDE	EQ	A	18:36-18:48	13	20020/ 16
#393	82 12 19	353	18	49	02.3	23.429S	175.224W	TONGA ISLANDS REGION	33	5.4	0.0	PDE	EQ	A	18:52-19:04	13	20020/ 17
#394	82 12 19	353	20	14	19.7	24.590S	175.483W	SOUTH OF TONGA ISLANDS	33	5.4	0.0	PDE	EQ	A	20:10-20:29	12	20020/ 18
#395	82 12 19	353	20	40	05.6	23.840S	175.766W	TONGA ISLANDS REGION	33	5.6	0.0	PDE	EQ	A	20:51-21:03	13	20020/ 19
#396	82 12 19	353	21	26	08.2	23.924S	175.565W	TONGA ISLANDS REGION	33	5.6	0.0	PDE	EQ	A	21:29-21:41	13	20020/ 20
#397	82 12 19	353	21	31	33.2	23.672S	175.810W	TONGA ISLANDS REGION	188	4.7	0.0	PDE	EQ	A	21:35-21:46	12	20020/ 20
#398	82 12 19	353	21	41	56.5	3.459S	127.760E	GILBERT ISLANDS REGION	33	5.1	0.0	PDE	EQ	ABDE	21:42-22:21	40	20020/ 20
#399	82 12 19	353	23	41	08.1	24.513S	175.826W	SOUTH OF TONGA ISLANDS	33	5.0	5.2	PDE	EQ	A	23:44-23:56	13	20021/ 01
#400	82 12 20	354	00	33	00.9	57.362S	25.692W	SOUTH SANDWICH ISL. REGION	33	6.0	5.1	PDE	EQ	A	00:42-01:01	20	20021/ 02

WAKE HYDROPHONE INFORMATION PROCESSING SYSTEM (WHIPS) EVENT LISTING 5 JUL 83

KEY: INFORMATION SOURCES - PDE=NEIS PDECARD, MON=NEIS MONTHLY LIST, ICS=ICS LIST, HEL=HELICORDER, OTH=OTHER
EVENT TYPE - EQ=EARTHQUAKE, NX=NUCLEAR EXPLOSION, SX=SCIENTIFIC EXPLOSION, OT=OTH.R, UN=UNKNOWN
PHASES - A=P, B=PO, C=S, D=SO, E=T, F=OTHER

EVNT NO	ORIGIN TIME YR	MO	DA	JUL	HR	MN	SECS	COORDINATES LAT	LON	LOCATION DESCRIPTION	DEP KM	MAGNI BDY	SRF	INF SRC	EV TP	PHASES	SAVED INTERVAL	MNS	STRIP TAPE/FILE
#481	82	12	28	354	#1	38	38.3	24.#6#S	175.5##W	SOUTH OF TONGA ISLANDS	33	5.5	6.#	PDE	EQ	AE	#1:34-#2:36	63	28#21/ #3
#482	82	12	28	354	#2	58	18.6	23.69S	176.#25W	SOUTH OF FIJI ISLANDS	33	5.7	6.3	PDE	EQ	AE	#3:#1-#4:#3	63	28#21/ #4
#483	82	12	28	354	#5	54	37.5	24.5#4S	175.985W	SOUTH OF TONGA ISLANDS	33	5.9	5.#	PDE	EQ	A	#5:58-[illegible] #9	12	28#21/ #5
#484	82	12	28	354	#7	14	28.7	24.6#4S	175.623W	SOUTH OF TONGA ISLANDS	33	5.3	#.#	PDE	EQ	A	#7:18-[illegible]:29	12	28#21/ #6
#485	82	12	28	354	#7	56	42.#	24.542S	175.989W	SOUTH OF TONGA ISLANDS	33	5.6	5.1	PDE	EQ	A	#7:#2-[illegible]:11	12	28#21/ #7
#486	82	12	28	354	12	34	59.3	24.6#2S	175.991W	SOUTH OF TONGA ISLANDS	33	5.5	5.6	PDE	EQ	A	12:36-[illegible]:52	13	28#21/ #8
#487	82	12	28	354	14	35	45.4	24.564S	175.848W	SOUTH OF TONGA ISLANDS	33	5.7	6.#	PDE	EQ	AE	14:39-[illegible]:41	63	28#21/ #9
#488	82	12	28	354	18	12	22.9	23.821S	175.631W	TONGA ISLANDS REGION	33	5.6	6.2	PDE	EQ	AE	18:16-[illegible]:17	62	28#21/ 10
#489	82	12	21	355	#1	10	16.1	42.255N	142.396E	HONSHU-HOKKAIDO JAPAN REGION	52	4.7	#.#	PDE	EQ	ABD	#1:19-[illegible]:35	17	28#21/ 11
#418	82	12	21	355	#2	19	29.#	24.672S	175.743W	SOUTH OF TONGA ISLANDS	33	5.2	5.4	PDE	EQ	A	#2:23-[illegible]:34	12	28#21/ 12
#411	82	12	21	355	#5	48	18.7	3.494S	142.925E	NEAR N COAST PAPUA NEW GUINEA	17	5.1	#.#	PDE	EQ	ABDE	#5:58-#6:35	46	28#21/ 13
#412	82	12	21	355	#5	18	23.1	16.172S	172.589W	SAMOA ISLANDS REGION	33	5.2	#.#	PDE	EQ	A	#5:19-#5:24	12	28#21/ 13
#413	82	12	21	355	#7	31	47.#	24.239S	175.787W	SOUTH OF TONGA ISLANDS	33	5.#	#.#	PDE	EQ	A	#7:35-#7:46	12	28#21/ 14
#414	82	12	21	355	12	#8	46.6	29.22IN	81.333E	NEPAL	33	4.7	#.#	PDE	EQ	A	12:16-[illegible]:27	12	28#21/ 15
#415	82	12	21	355	16	12	18.3	24.744S	175.776W	SOUTH OF TONGA ISLANDS	33	5.3	5.7	PDE	EQ	A	16:16-[illegible]:27	12	28#21/ 16
#416	82	12	21	355	18	#8	27.1	23.62#S	175.622W	TONGA ISLANDS REGION	33	5.3	5.2	PDE	EQ	A	18:04-[illegible]:15	12	28#21/ 17
#417	82	12	21	355	18	43	25.8	23.999S	175.#99W	TONGA ISLANDS REGION	33	5.1	#.#	PDE	EQ	A	18:47-[illegible]:58	12	28#22/ #1
#418	82	12	21	355	23	35	27.9	37.172N	71.743E	AFGHANISTAN-USSR BORDER REGION	168	4.#	#.#	PDE	EQ	A	23:42-[illegible]:54	13	28#22/ #2
#419	82	12	22	356	15	32	35.3	23.251S	179.#35E	SOUTH OF FIJI ISLANDS	573	5.5	#.#	PDE	EQ	A	15:35-[illegible]:46	12	28#22/ #3
#42#	82	12	23	357	##	1#	3#.1	24.479S	176.218W	SOUTH OF FIJI ISLANDS	33	5.6	5.3	PDE	EQ	A	#7:14-[illegible]:25	12	28#22/ #4
#421	82	12	23	357	#2	14	13.2	23.812S	175.949W	TONGA ISLANDS REGION	33	5.4	5.4	PDE	EQ	A	#2:17-[illegible]:29	13	28#22/ #5
#422	82	12	23	357	#3	2#	2#.#	24.587S	176.#9#W	SOUTH OF FIJI ISLANDS	33	5.4	5.3	PDE	EQ	A	#3:24-[illegible]:35	12	28#22/ #6
#423	82	12	23	357	#5	47	24.9	24.186S	175.#16W	SOUTH OF TONGA ISLANDS	33	5.1	#.#	PDE	EQ	A	#5:51-[illegible]:#2	12	28#22/ #7
#424	82	12	23	357	#9	41	47.#	23.778S	175.326W	TONGA ISLANDS REGION	33	5.3	5.1	PDE	EQ	A	#9:45-[illegible]:56	12	28#22/ #8
#425	82	12	23	357	13	#5	16.5	23.596S	175.445W	TONGA ISLANDS REGION	33	5.5	5.4	PDE	EQ	A	13:#8-[illegible]:2#	13	28#22/ #9
#426	82	12	24	358	#4	18	24.2	24.465S	176.1#3W	SOUTH OF FIJI ISLANDS	33	5.2	5.1	PDE	EQ	A	#4:22-[illegible]:33	12	28#22/ 10
#427	82	12	24	358	#6	47	1#.#	37.166N	71.794E	AFGHANISTAN-USSR BORDER REGION	148	4.6	#.#	PDE	EQ	A	#6:54-[illegible]:#5	12	28#22/ 11
#428	82	12	24	358	1#	1#	22.6	44.#96N	149.511E	KURIL ISLANDS	56	5.2	#.#	PDE	EQ	ABDE	1#:11-[illegible]:54	44	28#22/ 12
#429	82	12	24	358	23	31	#3.#	52.521N	173.311E	NEAR ISLANDS, ALEUTIAN ISLANDS	74	5.2	#.#	PDE	EQ	A	23:32-[illegible]:44	13	28#22/ 13
#43#	##	##	##	###	##	##	##.#	#.###N	#.###E	POSSIBLY NEAR WAKE ISLAND	#	#.#	#.#	HEL	EQ	BDE	##:#9-[illegible]:26	18	28#22/ 14
#431	82	12	25	359	#4	19	31.9	#.717S	134.871E	WEST IRIAN REGION	51	4.7	#.#	PDE	EQ	A	#4:22-#4:53	12	28#22/ 15
#432	82	12	25	359	#7	53	39.3	4.377S	131.454E	BANDA SEA	33	5.1	4.4	PDE	EQ	A	#7:56-[illegible]:#8	13	28#22/ 16
#433	82	12	25	359	12	28	#8.9	8.431S	123.#84E	FLORES ISLAND REGION	22	5.6	5.8	PDE	EQ	A	12:32-12:43	12	28#22/ 17
#434	82	12	25	359	16	51	47.3	26.575N	95.#4#E	BURMA-INDIA BORDER REGION	33	5.#	#.#	PDE	EQ	A	16:57-17:#9	13	28#22/ 18
#435	82	12	26	36#	##	29	36.5	45.252N	151.2##E	KURIL ISLANDS	33	5.#	#.#	PDE	EQ	ABDE	##:3#-[illegible]:3	44	28#22/ 19
#436	82	12	26	36#	#[illegible]	#2	#7.#	23.985S	175.174W	TONGA ISLANDS REGION	33	5.1	#.#	PDE	EQ	A	#2:23-[illegible]:3#	13	28#22/ 2#
#437	82	12	26	360	#2	42	#8.3	3.637S	177.692E	GILBERT ISLANDS REGION	33	4.9	#.#	PDE	EQ	ABDE	#2:42- [illegible]:21	4#	28#22/ 21
#438	82	12	26	36#	#3	35	14.3	5#.#7#N	79.#9#E	EASTERN KAZAKH SSR.	#	5.7	#.#	PDE	NX	A	#3:42-[illegible]:53	12	28#22/ 22
#439	82	12	26	36#	#5	29	34.#	41.#11N	61.693E	UZBEK SSR	33	4.9	#.#	PDE	EQ	A	#5:37-[illegible]:49	12	28#22/ 23
#44#	82	12	26	36#	#9	24	42.7	4.553S	143.858E	PAPUA NEW GUINEA	1#2	5.3	#.#	PDE	EQ	ABDE	#9:26-[illegible]:12	47	28#22/ 24
#441	82	12	26	36#	16	19	57.6	38.27#N	141.69#E	NEAR EAST COAST OF HONSHU JAPA	73	5.1	#.#	PDE	EQ	ABDE	16:21-[illegible]:#3	43	28#23/ #1
#442	82	12	26	36#	23	59	56.3	3.38#S	177.79#E	GILBERT ISLANDS REGION	33	4.7	#.#	PDE	EQ	ABDE	#2:#0-[illegible]:3#	39	28#23/ #2
#443	82	12	27	361	#1	32	57.6	19.##6N	145.##6E	MARIANA ISLANDS	6##	5.3	#.#	PDE	EQ	ABDE	#1:32-[illegible]:#5	34	28#23/ #3
#444	82	12	27	351	#1	58	42.8	11.439S	162.325E	SOLOMON ISLANDS	7#	5.#	#.#	PDE	EQ	ABDE	#1:52-[illegible]:56	45	28#23/ #3
#445	##	##	##	###	##	##	##.#	#.##2N	#.###E	PROBABLE MARIANAS PO,SO,T	#	#.#	#.#	HEL	EQ	BDE	#6:17-[illegible]:46	3#	28#23/ #4
#446	82	12	27	361	#7	#7	29.4	34.11KN	139.13#E	NEAR S. COAST OF HONSHU JAPAN	33	5.#	#.#	PDE	EQ	ABDE	#7:#6-[illegible]:51	44	28#23/ #5
#447	82	12	27	361	11	33	18.4	33.#23N	139.451E	SOUTH OF HONSHU JAPAN	21	5.2	5.#	PDE	EQ	ABDE	11:34-[illegible]:16	43	28#23/ #6
#448	82	12	27	361	14	#7	43.5	34.23#N	139.245E	NEAR S. COAST OF HONSHU JAPAN	33	5.#	#.#	PDE	EQ	ABDE	14:#8-[illegible]:51	44	28#23/ #7
#449	82	12	28	362	#1	23	47.6	33.#6N	139.361E	SOUTH OF HONSHU JAPAN	2#	5.#	4.1	PDE	EQ	ABDE	#1:25-[illegible]:#7	43	28#23/ #8
#45#	82	12	28	362	#1	52	31.3	33.7#7N	139.447E	SOUTH OF HONSHU JAPAN	21	5.3	5.5	PDE	EQ	ABDE	#1:53-[illegible]:35	43	28#23/ #8
#451	82	12	28	362	#2	12	14.1	33.57#N	139.54#E	SOUTH OF HONSHU JAPAN	15	5.2	#.#	PDE	EQ	ABDE	#2:13-[illegible]:55	43	28#23/ #8
#452	82	12	28	362	#6	37	42.#	33.739N	139.465E	SOUTH OF HONSHU JAPAN	2#	5.9	6.1	PDE	EQ	ABDE	#6:38-[illegible]:2#	43	28#23/ #9
#453	82	12	28	362	#7	3#	#7.5	22.355N	1##.86#E	BURMA-CHINA BORDER REGION	26	6.2	#.#	PDE	EQ	A	#7:35-[illegible]:46	12	28#23/ 1#
#454	82	12	28	362	#9	##	#3.1	25.577N	99.379E	YUNNAN PROVINCE, CHINA	3#	5.#	#.#	PDE	EQ	A	#8:#5-[illegible]:17	13	28#24/ #1
#455	82	12	28	362	1#	#3	46.3	18.#7N	145.76#E	MARIANA ISLANDS	217	4.6	#.#	PDE	EQ	ABDE	1#:#3-[illegible]:35	33	[illegible]#24/ #2
#456	82	12	28	362	13	49	29.5	19.95#N	121.423E	PHILIPPINE ISLANDS REGION	39	5.9	5.9	PDE	EQ	A	13:52-14:#4	13	28#24/ #3
#457	82	12	28	362	15	53	51.5	23.685S	175.7#2W	TONGA ISLANDS REGION	33	5.3	5.6	PDE	EQ	A	15:57-16:#8	12	28#24/ #4
#458	82	12	28	362	16	29	36.3	33.636N	139.674E	SOUTH OF HONSHU JAPAN	33	4.5	5.7	PDE	EQ	ABDE	16:3#-17:12	43	28#24/ #5
#459	82	12	28	362	21	19	#5.#	3.363S	177.713E	GILBERT ISLANDS REGION	33	5.1	#.#	PDE	EQ	ABDE	21:19-21:58	4#	28#24/ #6
#45#	82	12	28	362	21	51	#5.1	23.38#S	175.635W	TONGA ISLANDS REGION	33	5.#	#.#	PDE	EQ	A	21:54-22:#6	13	28#24/ #6
#461	82	12	28	362	23	37	#6.4	18.194S	178.514W	FIJI ISLANDS REGION	627	4.#	#.#	PDE	EQ	A	23:39-23:5#	12	28#24/ #7
#462	82	12	29	363	##	#9	28.#	3#.344N	79.#22E	TIBET-INDIA BORDER REGION	33	4.#	#.#	PDE	EQ	A	##:16-[illegible]:27	12	28#24/ #8
#463	82	12	29	363	#[illegible]	1#	55.#	17.717S	177.446W	FIJI ISLANDS REGION	419	5.1	#.#	PDE	EQ	A	##:13-[illegible]:24	12	28#24/ #8
#464	82	12	29	363	#7	#2	31.4	33.724N	139.255E	SOUTH OF HONSHU JAPAN	2#	5.5	6.3	PDE	EQ	ABDE	#7:#3-#7:45	43	28#24/ #9
#465	82	12	29	363	12	17	45.9	33.782N	139.296E	SOUTH OF HONSHU JAPAN	22	5.3	4.6	PDE	EQ	ABDE	12:19-13:#1	43	28#24/ 1#
#466	82	12	29	363	14	#5	4#.9	14.866N	12#.323E	LUZON PHILIPPINE ISLANDS	1#7	5.5	#.#	PDE	EQ	A	14:#9-14:2#	12	28#24/ 11
#467	82	12	29	363	15	14	59.6	34.849N	14#.396E	NEAR EAST COAST OF HONSHU JAPA	33	5.#	#.#	PDE	EQ	ABDE	15:16-15:57	42	28#24/ 12
#469	82	12	29	363	15	21	2#.9	29.94IN	7#.136E	PAKISTAN	33	5.#	4.9	PDE	EQ	A	15:29-15:4#	12	28#24/ 12
#469	82	12	29	363	16	5#	41.7	6.5#4S	154.529E	SOLOMON ISLANDS	33	5.1	#.#	PDE	EQ	ABDE	16:59-17:41	43	28#24/ 13
#47#	82	12	3#	364	##	51	21.#	24.154S	174.96#W	SOUTH OF TONGA ISLANDS	33	5.3	4.9	PDE	EQ	A	##:55-#1:#6	12	28#24/ 14
#471	82	12	3#	364	#8	37	16.1	25.95#N	91.64#E	INDIA-BANGLADESH BORDER REGION	64	4.9	#.#	PDE	EQ	A	#8:43-#8:54	12	28#24/ 15
#472	82	12	3#	364	12	29	25.7	26.361N	91.971E	EASTERN INDIA	33	5.#	#.#	PDE	EQ	A	12:35-12:47	13	28#24/ 16
#473	82	12	3#	364	17	5#	#9.4	6.237S	13#.458E	BANDA SEA	137	5.#	#.#	PDE	EQ	A	17:53-18:#4	12	28#24/ 17
#474	82	12	31	365	#9	58	#2.#	28.714N	128.463E	RYUKYU ISLANDS	33	5.#	5.4	PDE	EQ	A	1#:##-1#:11	12	28#24/ 18
#475	82	12	31	365	13	41	49.#	3.4#2S	177.668E	GILBERT ISLANDS REGION	26	5.3	4.4	PDE	EQ	ABDE	13:42-14:2#	39	28#25/ #1
#476	82	12	31	365	14	43	15.1	5.345N	126.913E	MINDANAO PHILIPPINE ISLANDS	185	5.1	#.#	PDE	EQ	A	14:46-14:57	12	28#25/ #2
#477	##	##	##	#C#	##	##	##.#	#.###N	#.###E	PROBABLE MARIANAS PO,SO,T	#	#.#	#.#	HEL	EQ	BDE	23:55-[illegible]:29	35	28#25/ #3
#478	83	#1	#1	#81	#5	31	54.6	17.3#7S	69.276W	PERU-BOLIVIA BORDER REGION	172	5.7	#.#	PDE	EQ	A	#5:41-#6:[illegible]	2#	28#25/ #4
#479	83	#1	#1	#81	1#	46	12.3	16.99#N	147.435E	MARIANA ISLANDS REGION	33	4.7	#.#	PDE	EQ	ABD	1#:45-1#:58	14	28#25/ #5
#48#	83	#1	#1	#81	11	1#	#7.6	61.33IN	147.156E	SOUTHERN ALASKA	55	5.3	#.#	PDE	EQ	A	11:21-11:32	12	28#25/ #6
#481	83	#1	#2	382	#6	52	32.#	12.14#S	166.792E	SANTA CRUZ ISLANDS	33	4.9	#.#	PDE	EQ	ABD	#6:54-#7:#9	16	28#25/ #7
#482	83	#1	#2	382	12	54	#6.9	9.76#S	159.76#E	SOLOMON ISLANDS	33	5.3	#.#	PDE	EQ	ABDE	12:55-13:3#	44	28#25/ #8
#483	83	#1	#2	382	18	29	47.2	1.916N	126.#6#E	MOLUCCA PASSAGE	64	5.4	#.#	PDE	EQ	A	18:33-18:44	12	28#25/ #9
#484	83	#1	#2	382	22	#9	#7.5	2#.753S	178.728W	FIJI ISLANDS REGION	621	5.2	#.#	PDE	EQ	A	22:11-22:22	12	28#25/ 1#
#485	83	#1	#2	382	23	58	11.9	6.722N	126.86#E	MINDANAO PHILIPPINE ISLANDS	55	5.2	#.#	PDE	EQ	A	##:#1-##:12	12	28#25/ 11
#486	83	#1	#3	383	#3	39	46.7	4.#83S	1#3.145E	SOUTHERN SUMATERA	56	5.5	5.2	PDE	EQ	A	#3:46-#3:57	12	28#25/ 12
#487	83	#1	#3	383	#6	#4	#8.7	59.5#2S	26.346W	SOUTH SANDWICH ISLANDS REGION	1#7	5.6	#.#	PDE	EQ	A	#6:13-#6:32	2#	28#25/ 13
#488	83	#1	#3	383	11	2#	14.#	24.2#7N	94.481E	BURMA-INDIA BORDER REGION	74	6.2	#.#	PDE	EQ	A	11:34-11:45	12	28#25/ 14
#489	83	#1	#3	383	18	53	29.#	41.472N	141.488E	HOKKAIDO JAPAN	33	4.9	4.4	PDE	EQ	ABD	18:55-19:1#	16	28#25/ 15
#49#	83	#1	#4	384	#3	#9	#3.3	3.155S	1#1.264E	SOUTHERN SUMATERA	56	5.5	#.#	PDE	EQ	A	#3:15-#3:26	12	28#25/ 16
#491	83	#1	#4	384	#7	#3	1#.#	42.174N	142.#5E	HOKKAIDO JAPAN REGION	36	5.2	#.#	PDE	EQ	ABDE	#7:#4-#7:49	46	28#25/ 17
#492	83	#1	#5	285	#1	44	16.5	6.73#N	126.924E	MINDANAO PHILIPPINE ISLANDS	185	5.1	#.#	PDE	EQ	A	#1:47-#1:58	12	#/ #2
#493	83	#1	#5	285	#2	#1	#3.3	54.748N	162.936E	NEAR EAST COAST OF KAMCHATKA	33	6.6	5.6	PDE	EQ	ABDE	#2:#3-#2:53	51	#/ #3
#494	83	#1	#5	285	#4	2#	1#.2	9.66#N	122.2#1E	NEGROS PHILIPPINE ISLANDS	33	5.5	5.5	PDE	EQ	A	#4:31-#4:42	12	#/ #2
#495	83	#1	#5	285	#7	1#	35.4	42.321N	142.631E	HOKKAIDO JAPAN REGION	41	5.1	#.#	PDE	EQ	ABDE	#7:2#-#8:#4	45	28#25/ 1#
#496	83	#1	#5	285	#7	3#	#7.6	9.63#N	122.366E	NEGROS PHILIPPINE ISLANDS	33	5.2	#.#	PDE	EQ	A	#7:41-#7:52	12	28#25/ 1#
#497	83	#1	#5	285	16	52	19.9	6.784S	11.741W	ASCENSION ISLAND REGION	1#	5.2	4.7	PDE	EQ	A	17:#1-17:21	21	28#25/ 19
#49#	83	#1	#5	285	16	59	51.2	9.57#N	122.2#5E	NEGROS PHILIPPINE ISLANDS	33	5.#	#.#	PDE	EQ	A	17:#3-17:14	12	28#25/ 19
#49[illegible]	83	#1	#5	285	##	##	##.#	#.##2N	#.###E	PROBABLE BONIN ISL. PO,SO,T	#	#.#	#.#	HEL	EQ	BDE	17:41-18:2#	4#	28#25/ 2#
25##	83	#1	#6	286	12	29	5#.6	44.58IN	148.191E	KURIL ISLANDS	84	5.3	#.#	PDE	EQ	ABDE	12:31-13:14	44	28#26/ #1

WAKE HYDROPHONE INFORMATION PROCESSING SYSTEM (WHIPS) EVENT LISTING 6 JUL 83

KEY: INFORMATION SOURCES - PDE=NEIS PDECARD, MON=NEIS MONTHLY LIST, ICS=ICS LIST, HEL=HELICORDER, OTH=OTHER
EVENT TYPE - EQ=EARTHQUAKE, NX=NUCLEAR EXPLOSION, SX=SCIENTIFIC EXPLOSION, OT=OTHER, UN=UNKNOWN
PHASES - A=P, B=PO, C=S, D=SO, E=T, F=OTHER

EVNT NO	ORIGIN TIME YR MO DA JUL HR MN SECS	COORDINATES LAT LON	LOCATION DESCRIPTION	DEP KM	MAGNI BDY	MAGNI SRF	INF SRC	EV TP	PHASES	SAVED INTERVAL	MNS	STRIP TAPE/FILE
#501	83 01 06 006 17:21:26.4	0.349N 147.327E	CAROLINE ISLANDS REGION	33	5.0	0.0	PDE	EQ	ABDE	17:21-17:55	35	20026/ 02
#502	83 01 06 006 18:02:38.0	14.060N 146.997E	MARIANA ISLANDS	33	4.5	0.0	PDE	EQ	ABD	18:02-18:14	13	20026/ 03
#503	83 01 06 006 19:56:44.9	19.668S 176.599W	FIJI ISLANDS REGION	205	5.1	0.0	PDE	EQ	A	19:59-20:10	12	20026/ 04
#504	83 01 06 006 20:29:30.4	31.356N 82.220E	TIBET	33	4.7	0.0	PDE	EQ	A	20:36-20:47	12	20026/ 05
#505	83 01 07 007 09:17:35.6	3.248N 126.857E	TALAUD ISLANDS	63	5.2	0.0	PDE	EQ	A	09:20-09:31	12	20026/ 06
#506	83 01 07 007 18:18:56.9	36.001N 139.747E	HONSHU JAPAN	67	5.0	0.0	PDE	EQ	ABDE	18:20-19:03	44	20026/ 07
#507	83 01 07 007 23:48:24.7	26.863S 176.653W	SOUTH OF FIJI ISLANDS	33	5.3	5.3	PDE	EQ	A	23:52-00:03	12	20026/ 08
#508	83 01 08 008 06:35:12.2	3.316S 177.675E	GILBERT ISLANDS REGION	33	4.9	0.0	PDE	EQ	ABD	06:36-06:50	16	20026/ 09
#509	83 01 08 008 08:18:34.8	17.958S 178.117W	FIJI ISLANDS REGION	601	5.1	0.0	PDE	EQ	A	08:12-08:24	13	20026/ 10
#510	83 01 08 008 10:51:33.3	36.453N 70.651E	HINDU KUSH REGION	195	4.8	0.0	PDE	EQ	A	10:59-11:10	12	20026/ 11
#511	83 00 00 000 00:00:00.0	0.000N 0.000E	PROBABLE BONIN ISLANDS	0	0.0	0.0	HEL	EQ	BDE	11:00-11:37	38	20026/ 11
#512	83 01 08 008 11:21:29.6	15.324S 173.397W	TONGA ISLANDS	33	6.1	6.3	PDE	EQ	AE	11:24-12:18	55	20026/ 11
#513	83 01 08 008 15:04:55.2	3.164S 148.255E	BISMARCK SEA	9	5.5	6.1	PDE	EQ	AE	15:06-15:46	43	20026/ 12
#514	83 01 08 008 16:21:14.2	55.265N 163.182E	OFF EAST COAST OF KAMCHATKA	33	5.0	0.0	PDE	EQ	ABDE	16:23-17:13	51	20026/ 13
#515	83 01 09 009 10:42:47.3	55.057N 163.225E	OFF EAST COAST OF KAMCHATKA	33	5.2	5.1	PDE	EQ	ABDE	10:45-11:35	51	20026/ 14
#516	83 01 09 009 12:44:07.3	43.929N 142.687E	HOKKAIDO JAPAN REGION	201	4.7	0.0	PDE	EQ	ABDE	12:45-13:31	47	20027/ 01
#517	83 01 09 009 18:36:53.5	35.922N 139.565E	NEAR S. COAST OF HONSHU JAPAN	106	5.0	0.0	PDE	EQ	ABDE	18:38-19:21	44	20027/ 02
#518	83 01 09 009 21:03:54.0	55.111N 163.381E	OFF EAST COAST OF KAMCHATKA	33	5.4	6.0	PDE	EQ	ABDE	21:06-21:56	51	20027/ 03
#519	83 01 10 010 01:57:55.7	1.944S 133.748E	WEST IRIAN REGION	33	5.3	5.7	PDE	EQ	ABDE	02:00-02:52	53	20027/ 04
#520	83 01 10 010 05:12:51.0	9.628N 122.887E	NEGROS PHILIPPINE ISLANDS	42	5.1	0.0	PDE	EQ	A	05:16-05:27	12	20027/ 05
#521	83 01 10 010 12:32:21.9	27.299S 63.399W	SANTIAGO DEL ESTERO PROV. ARGE	559	5.8	0.0	PDE	EQ	A	12:41-13:01	21	20027/ 06
#522	83 01 11 011 06:12:43.4	3.417S 177.640E	GILBERT ISLANDS REGION	33	4.9	0.0	PDE	EQ	ABD	06:13-06:27	15	20027/ 07
#523	83 01 11 011 18:49:00.0	3.365N 122.338E	CELEBES SEA	642	5.2	0.0	PDE	EQ	A	18:51-19:03	13	20027/ 08
#524	83 01 12 012 01:02:28.5	3.417S 177.597E	GILBERT ISLANDS REGION	33	4.7	0.0	PDE	EQ	ABD	01:03-01:17	15	20027/ 09
#525	83 01 12 012 03:28:25.0	27.031N 96.962E	BURMA-INDIA BORDER REGION	36	4.9	0.0	PDE	EQ	A	03:34-03:45	12	20027/ 10
#526	83 01 12 012 04:29:45.7	56.900N 162.481E	NEAR EAST COAST OF KAMCHATKA	33	4.7	0.0	PDE	EQ	ABD	04:32-04:49	18	20027/ 11
#527	83 01 12 012 09:51:52.0	24.481S 175.824W	SOUTH OF TONGA ISLANDS	33	5.3	5.1	PDE	EQ	A	09:55-10:06	12	20027/ 12
#528	83 01 12 012 12:22:25.6	26.848N 96.794E	BURMA	33	4.6	0.0	PDE	EQ	A	12:28-12:39	12	20027/ 13
#529	83 01 12 012 16:10:22.9	4.357S 150.248E	NEW BRITAIN REGION	567	4.7	0.0	PDE	EQ	ABDE	16:19-17:01	43	20027/ 14
#530	83 01 12 012 16:41:21.8	54.924N 162.869E	NEAR EAST COAST OF KAMCHATKA	33	4.9	0.0	PDE	EQ	ABD	16:43-17:02	18	20027/ 14
#531	83 01 13 013 09:23:47.5	35.780S 182.832W	SOUTHERN PACIFIC OCEAN	10	5.4	5.1	PDE	EQ	ABD	09:33-10:08	36	20027/ 15
#532	83 01 13 013 15:05:05.3	44.458N 148.150E	KURIL ISLANDS	33	5.1	0.0	PDE	EQ	ABDE	15:06-15:49	44	20027/ 16
#533	83 01 13 013 16:30:33.9	6.590S 154.157E	SOLOMON ISLANDS	33	4.8	0.0	PDE	EQ	ABD	16:31-16:46	16	20028/ 01
#534	83 01 14 014 18:28:53.3	56.854N 164.239W	KODIAK ISLAND REGION	33	5.6	5.9	PDE	EQ	ABDE	18:24-19:26	63	20028/ 02
#535	83 01 15 015 00:16:51.3	7.402N 124.592E	MINDANAO PHILIPPINE ISLANDS	35	5.6	4.6	PDE	EQ	A	00:20-00:31	12	20028/ 03
#536	83 01 15 015 02:39:32.3	33.264N 135.974E	NEAR S. COAST OF SOUTH. HONSHU	413	5.5	0.0	PDE	EQ	ABDE	00:48-01:25	46	20028/ 04
#537	83 01 15 015 02:49:54.3	52.839N 160.154E	OFF EAST COAST OF KAMCHATKA	33	5.6	0.0	PDE	EQ	ABDE	00:51-01:42	52	20028/ 04
#538	83 01 15 015 02:28:18.0	6.298S 131.117E	TANIMBAR ISLANDS REGION	46	5.3	0.0	PDE	EQ	A	02:23-02:34	12	20028/ 05
#539	83 01 15 015 16:55:30.6	2.742N 124.282E	CELEBES SEA	375	4.9	0.0	PDE	EQ	A	16:58-17:05	12	20028/ 06
#540	83 01 15 015 19:40:08.1	9.117S 124.157E	TIMOR	92	4.9	0.0	PDE	EQ	A	19:44-19:55	12	20028/ 07
#541	83 01 16 016 02:27:52.1	7.221S 129.491E	BANDA SEA	106	5.2	0.0	PDE	EQ	A	02:31-02:42	12	20028/ 08
#542	83 01 16 016 13:10:44.5	17.203S 176.929W	FIJI ISLANDS REGION	33	5.7	5.3	PDE	EQ	A	13:13-13:24	12	20028/ 09
#543	83 01 16 016 22:10:11.6	5.449S 147.055E	EAST PAPUA NEW GUINEA REGION	229	6.0	0.0	PDE	EQ	ABDE	22:11-22:56	46	20028/ 10
#544	83 01 17 017 09:40:16.0	5.485S 146.525E	EAST PAPUA NEW GUINEA REGION	174	5.4	0.0	PDE	EQ	ABDE	09:41-10:26	46	20028/ 11
#545	83 01 17 017 11:55:30.4	26.427N 126.241E	RYUKYU ISLANDS	33	5.1	0.0	PDE	EQ	A	11:57-12:09	13	20028/ 12
#546	83 01 17 017 12:41:29.3	38.892N 22.193E	GREECE	9	6.0	7.0	PDE	EQ	AF	12:45-14:44	120	20028/ 13
#547	83 01 17 017 19:06:08.3	25.666N 126.219E	RYUKYU ISLANDS	74	4.9	0.0	PDE	EQ	A	19:08-19:19	12	20028/ 14
#548	83 01 18 018 02:22:54.7	49.636S 114.920W	EASTER ISLAND CORDILLERA	10	5.1	5.3	PDE	EQ	ABD	02:31-03:05	35	20029/ 01
#549	83 01 18 018 15:23:33.0	58.023S 24.274W	SOUTH SANDWICH ISLANDS REGION	33	6.0	6.5	PDE	EQ	AF	15:28-17:27	120	20029/ 02
#550	83 01 18 018 17:42:04.2	6.812S 128.187E	BANDA SEA	310	5.0	0.0	PDE	EQ	A	17:45-17:56	12	20029/ 03
#551	83 01 18 018 22:51:56.3	36.368N 70.446E	HINDU KUSH REGION	208	4.4	0.0	PDE	EQ	A	22:59-23:10	12	20029/ 04
#552	83 01 19 019 11:50:10.3	10.618S 166.142E	SANTA CRUZ ISLANDS	153	5.0	0.0	PDE	EQ	ABDE	11:51-12:35	45	20029/ 05
#553	83 01 19 019 12:09:39.1	25.259N 91.853E	INDIA-BANGLADESH BORDER REGION	33	4.9	0.0	PDE	EQ	A	12:16-12:27	12	20029/ 05
#554	83 01 19 019 13:30:29.0	55.895N 160.762E	KAMCHATKA	50	5.0	0.0	PDE	EQ	ABDE	13:40-14:32	53	20029/ 06
#555	83 01 19 019 22:22:06.9	5.741S 154.378E	SOLOMON ISLANDS	112	5.4	0.0	PDE	EQ	ABDE	22:23-21:04	42	20029/ 07
#556	83 01 20 020 10:02:47.6	7.516S 120.848E	BANDA SEA	153	5.0	0.0	PDE	EQ	A	10:06-10:17	12	20029/ 08
#557	83 01 20 020 12:45:32.2	28.754N 142.379E	BONIN ISLANDS REGION	33	5.0	0.0	PDE	EQ	ABDE	12:46-13:23	38	20029/ 09
#558	83 01 20 020 22:22:27.6	51.362N 178.755W	ANDREANOF ISL., ALEUTIAN ISL.	69	4.5	0.0	PDE	EQ	ABD	22:24-22:48	17	20029/ 10
#559	83 01 21 021 05:04:42.0	4.263N 124.559E	CELEBES SEA	306	4.7	0.0	PDE	EQ	A	05:07-05:18	12	20029/ 11
#560	83 01 21 021 10:25:53.1	42.462N 143.034E	HOKKAIDO JAPAN REGION	72	5.2	0.0	PDE	EQ	ABDE	10:27-11:12	46	20029/ 12
#561	83 01 21 021 14:20:06.5	3.480S 141.274E	PAPUA NEW GUINEA	33	5.4	5.2	PDE	EQ	ABDE	14:22-15:09	46	20030/ 01
#562	83 01 21 021 10:01:06.8	3.556S 177.682E	GILBERT ISLANDS REGION	33	5.1	4.8	PDE	EQ	ABDE	10:01-10:42	40	20030/ 02
#563	83 01 22 022 01:24:33.9	6.654S 103.882E	SOUTHWEST OF SUMATERA	33	5.4	5.5	PDE	EQ	A	01:30-01:42	13	20030/ 03
#564	83 01 22 022 01:27:43.4	6.785S 103.813E	SOUTHWEST OF SUMATERA	33	5.4	0.0	PDE	EQ	A	01:34-01:45	12	20030/ 03
#565	83 01 22 022 06:44:36.5	6.753S 102.993E	SOUTHWEST OF SUMATERA	29	5.6	6.1	PDE	EQ	AF	06:46-06:17	90	20030/ 04
#566	83 01 22 022 06:56:25.2	6.875S 103.861E	SOUTHWEST OF SUMATERA	33	5.2	0.0	PDE	EQ	A	07:02-07:13	12	20030/ 04
#567	83 01 22 022 08:44:21.5	26.299S 178.745E	SOUTH OF FIJI ISLANDS	594	5.0	0.0	PDE	EQ	A	08:47-08:58	12	20030/ 05
#568	83 01 23 023 04:31:36.9	11.584N 141.732E	WEST CAROLINE ISLANDS	33	4.9	0.0	PDE	EQ	ABDE	04:32-05:09	38	20030/ 06
#569	83 01 23 023 08:08:36.6	46.319N 152.016E	KURIL ISLANDS	162	4.8	0.0	PDE	EQ	ABDE	08:09-08:54	46	20030/ 07
#570	83 01 23 023 10:46:53.7	2.838N 128.507E	HALMAHERA	33	5.0	0.0	PDE	EQ	A	10:49-11:01	13	20030/ 08
#571	83 01 23 023 16:36:38.7	37.277S 95.243W	SOUTHERN PACIFIC OCEAN	10	5.6	0.0	PDE	EQ	ABD	16:46-17:23	38	20030/ 09
#572	83 01 23 023 17:01:31.9	37.161S 95.147W	SOUTHERN PACIFIC OCEAN	10	5.1	0.0	PDE	EQ	ABD	17:10-17:48	39	20030/ 09
#573	83 01 24 024 08:17:30.6	16.184N 95.149W	OAXACA MEXICO	45	6.3	6.6	PDE	EQ	AE	08:26-10:18	113	20031/ 01
#574	83 00 00 000 02:00:00.0	0.000N 0.000E	POSSIBLE NUCLEAR TEST	0	0.0	0.0	HEL	NX	AE	08:45-09:09	25	20031/ 01
#575	83 01 24 024 13:02:37.1	51.342N 176.308E	RAT ISL., ALEUTIAN ISL.	33	5.4	5.7	PDE	EQ	ABDE	13:04-13:51	48	20031/ 02
#576	83 01 24 024 15:04:16.3	54.664N 160.435E	NEAR EAST COAST OF KAMCHATKA	33	4.7	0.0	PDE	EQ	ABDE	15:06-15:56	51	20031/ 03
#577	83 01 24 024 16:13:21.7	51.433N 176.262E	RAT ISL., ALEUTIAN ISL.	33	4.9	0.0	PDE	EQ	ABD	16:15-16:31	17	20031/ 04
#578	83 01 24 024 16:35:03.4	29.426N 142.014E	SOUTH OF HONSHU JAPAN	33	5.1	0.0	PDE	EQ	ABDE	16:35-17:13	39	20031/ 05
#579	83 01 24 024 23:09:21.5	12.952N 93.644E	ANDAMAN ISLANDS REGION	79	6.1	0.0	PDE	EQ	A	23:15-23:27	13	20031/ 06
#580	83 01 25 025 00:20:29.9	33.672N 141.827E	OFF EAST COAST OF HONSHU JAPAN	64	4.9	0.0	PDE	EQ	ABD	00:29-00:44	16	20031/ 07
#581	83 01 25 025 03:32:07.3	9.676S 161.123E	SOLOMON ISLANDS	92	4.6	0.0	PDE	EQ	ABD	03:33-03:48	16	20031/ 08
#582	83 01 25 025 06:00:09.0	3.618S 148.223E	WEST IRIAN	33	5.4	5.8	PDE	EQ	A	06:10-06:21	12	20031/ 09
#583	83 01 25 025 07:24:45.5	3.491S 148.269E	WEST IRIAN	33	5.3	0.0	PDE	EQ	A	07:26-07:38	13	20031/ 10
#584	83 01 25 025 07:34:48.6	45.711N 26.614E	ROMANIA	164	4.7	0.0	PDE	EQ	A	07:44-08:03	20	20031/ 11
#585	83 01 25 025 11:20:21.5	51.483N 176.320E	RAT ISL., ALEUTIAN ISL.	33	5.1	4.5	PDE	EQ	ABDE	11:30-12:17	48	20031/ 12
#586	83 01 25 025 16:42:09.4	3.454S 148.342E	WEST IRIAN	33	5.1	0.0	PDE	EQ	A	16:44-16:55	12	20031/ 13
#587	83 01 25 025 20:06:37.0	36.394N 70.888E	HINDU KUSH REGION	182	5.0	0.0	PDE	EQ	A	20:14-20:25	12	20031/ 14
#588	83 01 26 026 04:40:12.5	49.787S 114.873W	EASTER ISLAND CORDILLERA	10	5.1	0.0	PDE	EQ	ABD	04:49-05:23	35	20032/ 01
#589	83 01 26 026 04:43:10.7	49.751S 115.119W	EASTER ISLAND CORDILLERA	10	5.7	6.1	PDE	EQ	ABD	04:52-05:26	35	20032/ 01
#590	83 01 26 026 16:02:21.5	30.355S 179.427W	KERMADEC ISLANDS REGION	230	6.1	0.0	PDE	EQ	A	16:06-16:17	12	20032/ 02
#591	83 01 26 026 17:52:39.2	6.132S 150.852E	NEW BRITAIN REGION	47	5.7	0.0	PDE	EQ	ABDE	17:54-18:37	44	20032/ 03
#592	83 01 26 026 18:55:56.7	15.255S 173.416W	TONGA ISLANDS	33	5.4	5.0	PDE	EQ	A	18:58-19:10	13	20032/ 04
#593	83 01 26 026 20:23:30.7	7.234S 155.985E	SOLOMON ISLANDS	71	5.5	0.0	PDE	EQ	ABDE	20:24-21:06	43	20032/ 05
#594	83 01 27 027 04:05:09.2	44.572N 148.181E	KURIL ISLANDS	34	5.0	0.0	PDE	EQ	ABDE	04:06-04:58	45	20032/ 06
#595	83 01 27 027 09:07:33.1	35.715N 139.439E	NEAR S. COAST OF HONSHU JAPAN	77	4.8	0.0	PDE	EQ	ABD	09:08-09:24	17	20032/ 07
#596	83 01 27 027 09:42:39.2	35.578N 139.774E	NEAR S. COAST OF HONSHU JAPAN	33	4.6	0.0	PDE	EQ	ABD	09:43-09:59	17	20032/ 08
#597	83 01 27 027 15:36:47.2	6.975S 129.521E	BANDA SEA	166	5.1	0.0	PDE	EQ	A	16:48-16:51	12	20032/ 09
#598	83 01 28 028 03:15:10.1	2.684N 124.130E	CELEBES SEA	362	5.6	P 0	PDE	EQ	A	03:18-03:29	12	20032/ 10
#599	83 01 28 028 08:38:43.3	36.617N 94.772E	QINGHAI PROVINCE CHINA	33	4.8	0.0	PDE	EQ	A	08:44-08:55	12	20032/ 11
#600	83 01 28 028 11:17:32.0	18.325S 168.911E	VANUATU ISLANDS	214	4.8	0.0	PDE	EQ	A	11:19-11:31	13	20032/ 12

WAKE HYDROPHONE INFORMATION PROCESSING SYSTEM (WHIPS) EVENT LISTING 6 JUL 83

KEY: INFORMATION SOURCES - PDE=NEIS PDECARD, MON=NEIS MONTHLY LIST, ICS=ICS LIST, HEL=HELICORDER, OTH=OTHER
EVENT TYPE - EQ=EARTHQUAKE, NX=NUCLEAR EXPLOSION, SX=SCIENTIFIC EXPLOSION, OT=OTHER, UN=UNKNOWN
PHASES - A=P, B=PO, C=S, D=SO, E=T, F=OTHER

EVNT NO	ORIGIN TIME YR MO DA JUL HR MN SECS	COORDINATES LAT LON	LOCATION DESCRIPTION	DEP KM	MAGNI BDY	SRF	INF SRC	EV TP	PHASES	SAVED INTERVAL	MNS	STRIP TAPE/FILE
#601	83 #1 28 #28 14:23:#5.4	1#.74#S 165.#13E	SANTA CRUZ ISLANDS	79	5.6	#.#	PDE	EQ	ABDE	14:24-15:##	45	2##32/ 13
#602	83 #1 28 #28 15:#5:34.9	28.735N 139.318E	BONIN ISLANDS REGION	443	5.1	#.#	PDE	EQ	ABDE	15:#6-15:46	41	2##32/ 13
#603	83 #1 28 #28 21:#1:37.3	3.#3#S 177.857E	GILBERT ISLANDS REGION	33	4.9	#.#	PDE	EQ	ABD	21:#2-21:16	15	2##32/ 14
#604	83 #1 29 #29 ##:#7:#1.#	17.613S 179.869E	FIJI ISLANDS	634	4.8	#.#	PDE	EQ	A	##:##-##:28	13	2##32/ 15
#605	83 #1 29 #29 #2:44:1#.2	36.585N 141.4##E	NEAR E. COAST OF HONSHU JAPAN	58	5.#	#.#	PDE	EQ	ABDE	#2:45-#3:27	43	2##32/ 16
#606	83 #1 29 #29 09:54:57.2	48.214N 146.151E	SEA OF OKHOTSK	488	4.8	#.#	PDE	EQ	ABDE	#9:56-1#:44	49	2##33/ #1
#607	83 #1 29 #29 1#:#2:14.7	48.214N 146.177E	SEA OF OKHOTSK	478	4.9	#.#	PDE	EQ	ABDE	1#:#3-1#:51	49	2##33/ #1
#608	83 #1 29 #29 17:47:52.4	17.515S 179.886E	FIJI ISLANDS	63#	4.8	#.#	PDE	EQ	A	17:49-18:#1	13	2##33/ #2
#609	83 #1 3# #3# #1:26:#5.9	5.428N 94.942E	NORTHERN SUMATERA	#2	5.2	#.#	PDE	EQ	A	#1:32-#1:43	12	2##33/ #3
#61#	83 #1 3# #3# 13:29:54.2	1#.35#S 161.231E	SOLOMON ISLANDS	98	4.8	#.#	PDE	EQ	ABD	13:31-13:46	16	2##33/ #4
#611	83 #1 3# #3# 22:45:39.9	33.369N 14#.796E	SOUTH OF HONSHU JAPAN	49	5.7	5.1	PDE	EQ	ABDE	22:46-23:27	42	2##33/ #5
#612	83 #1 31 #31 #5:32:21.1	7.397S 128.743E	BANDA SEA	183	5.3	#.#	PDE	EQ	A	#5:35-#5:47	13	2##33/ #5
#613	83 #1 31 #31 21:17:31.4	3.39#S 177.616E	GILBERT ISLANDS REGION	29	5.8	5.3	PDE	EQ	ABDE	21:18-21:56	39	2##33/ #7
#614	## ## ## ### ##:##:##.#	#.###N #.###E	PROBABLE MARIANAS PO, SO, T	#	#.#	#.#	HEL	EQ	BDE	22:23-22:52	3#	2##33/ #8
#615	83 #2 #1 #32 #2:#7:#7.7	3.486S 14#.147E	WEST IRIAN	33	5.1	#.#	PDE	EQ	ABDE	#2:#9-#2:57	49	2##33/ #9
#616	83 #2 #1 #32 14:47:28.4	37.156N 135.#8#E	SEA OF JAPAN	374	4.2	#.#	PDE	EQ	ABDE	14:48-15:36	49	2##33/ 1#
#617	83 #2 #1 #32 15:3#:#6.#	4.675S 144.#42E	NEAR N COAST OF PAPUA NEW GUIN	68	5.3	#.#	PDE	EQ	ABDE	15:4#-16:25	46	2##33/ 11
#618	83 #2 #2 #33 23:44:#6.1	27.#32N 92.87#E	INDIA-CHINA BORDER REGION	33	5.2	#.#	PDE	EQ	A	2#:5#-21:#1	12	2##33/ 12
#619	83 #2 #4 #35 #6:31:16.3	1.513N 127.259E	HALMAHERA	15#	5.4	#.#	PDE	EQ	A	#6:34-#6:45	12	2##33/ 13
#62#	83 #2 #4 #35 15:21:57.#	4.386S 152.84#E	NEW BRITAIN REGION	43	5.4	#.#	PDE	EQ	ABDE	15:23-16:#3	41	2##33/ 14
#621	83 #2 #4 #35 19:#5:59.6	1#.393S 124.384E	TIMOR	33	5.4	#.#	PDE	EQ	A	19:1#-19:21	12	2##33/ 15
#622	83 #2 #5 #36 #3:51:58.#	5.584S 153.#19E	NEW IRELAND REGION	47	5.#	#.#	PDE	EQ	ABDE	#3:53-#4:34	42	2##34/ #1
#623	83 #2 #5 #36 15:47:19.6	6.52#S 154.#65E	SOLOMON ISLANDS	51	5.#	#.#	PDE	EQ	ABDE	15:48-16:3#	43	2##34/ #2
#624	83 #2 #5 #36 17:#7:53.1	3.375S 177.567E	GILBERT ISLANDS REGION	33	5.1	#.#	PDE	EQ	ABDE	17:#8-17:46	39	2##34/ #3
#625	83 #2 #5 #36 23:51:46.1	3.369S 177.678E	GILBERT ISLANDS REGION	33	5.8	5.6	PDE	EQ	ABDE	23:52-#0:3#	39	#/ ##
#626	83 #2 #6 #37 #1:52:33.5	36.187N 68.997E	HINDU KUSH REGION	89	5.1	#.#	PDE	EQ	A	#2:##-#2:11	12	#/ ##
#627	83 #2 #6 #37 16:15:29.6	3.314S 177.866E	GILBERT ISLANDS REGION	33	4.#	#.#	PDE	EQ	ABD	16:16-16:3#	15	#/ ##
#628	83 #2 #7 #38 #1:21:#2.#	1#.291S 161.#63E	SOLOMON ISLANDS	89	5.3	#.#	PDE	EQ	ABDE	#1:22-#2:#6	45	#/ ##
#629	83 #2 #7 #38 11:#7:26.9	26.495S 177.799W	SOUTH OF FIJI ISLANDS	181	5.3	#.#	PDE	EQ	A	11:11-11:22	12	2##34/ #4
#63#	83 #2 #7 #38 16:53:3#.3	49.331N 155.627E	KURIL ISLANDS	33	5.2	4.6	PDE	EQ	ABDE	16:55-17:48	46	2##34/ #5
#631	83 #2 #7 #38 16:56:33.8	7.#41S 129.##5E	BANDA SEA	18#	5.#	#.#	PDE	EQ	A	17:##-17:11	12	2##34/ #5
#632	## ## ## ### ##:##:##.#	#.###N #.###E	POSSIBLE NUCLEAR TEST	#	#.#	#.#	HEL	NX	A	17:59-18:13	15	2##34/ #6
#633	83 #2 #7 #38 18:23:54.2	29.78#S 178.464W	KERMADEC ISLANDS	4#3	5.7	#.#	PDE	EQ	A	18:27-18:38	12	2##34/ #7
#634	83 #2 #7 #38 21:26:##.#	33.718N 135.939E	NEAR S. COAST OF S. HONSHU	4#6	4.#	#.#	PDE	EQ	ABDE	21:27-22:12	46	2##34/ #8
#635	83 #2 #8 #39 #2:51:19.5	26.426N 126.156E	RYUKYU ISLANDS	135	4.5	#.#	PDE	EQ	A	##:53-#3:#5	13	2##34/ #9
#636	83 #2 #8 #39 #3:#2:46.#	19.358N 155.233W	HAWAII	27	4.7	#.#	PDE	EQ	ABDE	#2:#5-#2:54	5#	2##34/ 1#
#637	83 #2 #8 #39 #6:5#:42.9	51.675N 159.752E	OFF EAST COAST OF KAMCHATKA	33	5.7	5.6	PDE	EQ	ABDE	#7:##-#7:47	48	2##34/ 11
#638	83 #2 #8 #39 1#:19:5#.9	6.352S 147.627E	EAST PAPUA NEW GUINEA REGION	59	5.3	#.#	PDE	EQ	ABDE	1#:2#-11:#6	46	2##34/ 12
#639	83 #2 #8 #39 14:#6:19.2	45.926N 143.962E	HOKKAIDO JAPAN REGION	252	5.2	#.#	PDE	EQ	ABDE	14:#7-14:54	48	2##34/ 13
2642	83 #2 #8 #39 16:17:47.9	1.675S 96.473E	SOUTHWEST OF SUMATERA	15	5.3	#.#	PDE	EQ	A	16:24-16:35	12	2##35/ #1
#64:	83 #2 #8 #39 21:3#:52.1	2#.4#3S 177.867W	FIJI ISLANDS REGION	543	5.#	#.#	PDE	EQ	A	21:33-21:44	12	2##35/ #2
#642	83 #2 #9 #4# #5:43:36.#	19.546N 12#.488E	PHILIPPINE ISLANDS REGION	33	5.4	#.#	PDE	EQ	A	#5:47-#5:58	12	2##35/ #3
#643	83 #2 #9 #4# #5:54:##.9	19.569N 12#.535E	PHILIPPINE ISLANDS REGION	33	5.4	5.4	PDE	EQ	A	#5:57-#6:#8	12	2##35/ #3
#644	83 #2 #9 #42 #7:#2:31.6	7.592S 156.#78E	SOLOMON ISLANDS	36	5.6	5.7	PDE	EQ	ABDE	#7:#3-#7:45	43	2##35/ #4
#645	83 #2 #9 #48 13:31:34.1	19.534N 12#.43#E	PHILIPPINE ISLANDS REGION	33	5.1	#.#	PDE	EQ	A	13:34-13:46	13	2##35/ #5
#646	## ## ## ### ##:##:##.#	#.###N #.###E	PROBABLE BONIN ISLANDS	#	#.#	#.#	HEL	EQ	BDE	14:#1-14:3#	3#	2##35/ #6
#647	83 #2 11 #42 #1:33:#1.8	49.875N 153.933E	KURIL ISLANDS	177	4.7	#.#	PDE	EQ	ABDE	#1:34-#2:21	48	2##35/ #7
#648	83 #2 11 #42 #4:34:18.2	5.741S 133.762E	APOE ISLANDS REGION	33	5.6	4.5	PDE	EQ	A	#4:37-#4:48	12	2##35/ #8
#649	83 #2 11 #42 16:##:##.1	37.#51N 116.#45W	SOUTHERN NEVADA	#	#.#	#.#	PDE	NX	A	16:#6-16:17	12	2##35/ #9
#652	83 #2 11 #42 17:41:#2.7	2#.784S 178.283W	FIJI ISLANDS REGION	513	5.1	#.#	PDE	EQ	A	17:43-17:54	12	2##35/ 1#
#651	83 #2 12 #43 #5:17:1#.7	36.39#N 71.#53E	AFGHANISTAN-USSR BORDER REGION	27#	4.6	#.#	PDE	EQ	A	#5:24-#5:35	12	2##35/ 11
#652	83 #2 12 #43 #8:47:1# 8	5.618N 126.444E	MINDANAO PHILIPPINE ISLANDS	38	5.#	6.#	PDE	EQ	AE	#8:5#-#9:45	56	2##35/ 12
#553	83 #2 12 #43 11:2#:#7.1	5.52#N 125.565E	MINDANAO PHILIPPINE ISLANDS	33	5.#	#.#	PDE	EQ	A	11:31-11:42	12	2##35/ 13
#554	83 #2 12 #43 22:5#:24.5	23.789N 1#5.#86E	YUNNAN PROVINCE CHINA	33	4.6	#.#	PDE	EQ	A	23:#3-23:14	12	2##35/ 14
#555	83 #2 13 #44 #1:4#:13.2	39.988N 75.#97E	SOUTHERN SINKIANG PROV CHINA	33	5.6	6.2	PDE	EQ	AE	#1:47-#3:26	1##	2##35/ 15
#656	83 #2 13 #44 #1:52:52.2	39.992N 75.275E	SOUTHERN SINKIANG PROV CHINA	33	5.2	#.#	PDE	EQ	A	#2:##-#2:11	12	2##35/ 15
#657	83 #2 13 #44 #2:39:#3.3	39.916N 75.26#E	SOUTHERN SINKIANG PROV CHINA	33	4.4	#.#	PDE	EQ	A	#2:46-#2:57	12	2##35/ 15
#658	83 #2 13 #44 #4:1#:52.9	39.962N 75.12#E	SOUTHERN SINKIANG PROV CHINA	33	4.5	#.#	PDE	EQ	A	#4:26-#4:37	12	2##35/ 16
#559	83 #2 13 #44 #6:35:3#.#	13.836N 144.977E	MARIANA ISLANDS	1#9	5.6	#.#	PDE	EQ	ABDE	#6:35-#7:#9	35	2##35/ 17
#66#	83 #2 13 #44 #7:23:11.#	4#.#55N 75.137E	KIRGHIZ-SINKIANG BORDER REGION	33	4.9	#.#	PDE	EQ	A	#7:3#-#7:41	12	2##36/ #1
#661	83 #2 13 #44 14:23:#1.1	5.52#N 126.521E	MINDANAO PHILIPPINE ISLANDS	33	5.#	4.9	PDE	EQ	A	14:26-14:37	12	2##36/ #2
#662	83 #2 13 #44 15:1#:12.1	11.41#N 126.215E	PHILIPPINE ISLANDS REGION	33	5.1	#.#	PDE	EQ	A	15:13-15:24	12	2##36/ #3
#663	83 #2 14 #45 ##:23:1#.6	1#.479N 148.934E	WEST CAROLINE ISLANDS	33	5.#	5.#	PDE	EQ	ABDE	##:24-#1:#2	39	2##36/ #4
#664	83 #2 14 #45 #1:29:52.3	1.648N 126.4#9E	MOLUCCA PASSAGE	56	5.2	#.#	PDE	EQ	A	#1:33-#1:44	12	2##36/ #5
#665	83 #2 14 #45 #3:2#:#3.3	54.956N 159.191W	SOUTH OF ALASKA	33	5.9	6.3	PDE	EQ	AE	#3:23-#4:21	59	2##36/ #6
#666	83 #2 14 #45 #6:##:#1.3	22.412S 169.766E	LOYALTY ISLANDS REGION	75	5.#	#.#	PDE	EQ	A	#6:11-#6:22	12	2##36/ #7
#667	83 #2 14 #45 #8:1#:#3.7	54.971N 159.212W	SOUTH OF ALASKA	33	5.9	5.6	PDE	EQ	AE	##:13-#9:11	59	2##36/ #8
#668	83 #2 14 #45 23:48:12.#	51.#84N 175.571E	RAT ISLANDS, ALEUTIAN ISLANDS	91	4.6	#.#	PDE	EQ	ABD	23:5#-##:#6	17	2##36/ #9
#669	83 #2 15 #46 #1:14:35.4	1#.236S 161.388E	SOLOMON ISLANDS	78	5.2	#.#	PDE	EQ	ABDE	#1:15-#1:59	45	2##36/ 1#
#67#	83 #2 16 #47 #9:5#:35.3	25.329S 179.624E	SOUTH OF FIJI ISLANDS	47#	5.4	#.#	PDE	EQ	A	#9:53-1#:#4	12	2##36/ 11
#671	83 #2 17 #48 ##:16:#1.#	43.939N #3.#18E	NORTHERN SINKIANG PROV CHINA	33	5.1	#.#	PDE	EQ	A	##:22-##:34	13	2##36/ 12
#672	## ## ## ### ##:##:##.#	#.###N #.###E	PROBABLE BONIN ISL. PO SO T	#	#.#	#.#	HEL	EQ	BDE	15:2#-15:54	35	2##36/ 13
#673	83 #2 17 #48 16:1#:4#.7	21.378S 174.469W	TONGA ISLANDS	41	5.9	5.6	PDE	EQ	A	16:14-16:25	12	2##36/ 14
#674	83 #2 17 #48 17:##:##.#	37.163N 116.#63W	SOUTHERN NEVADA	#	4.#	#.#	PDE	NX	A	17:#6-17:17	12	2##36/ 15
#675	83 #2 18 #49 #3:53:37.6	23.#68N 143.959E	VOLCANO ISLANDS REGION	33	4.9	#.#	PDE	EQ	ABD	#3:53-#4:#7	15	2##36/ 16
#676	83 #2 18 #49 14:51:2#.9	7.3#7N 125.185E	MINDANAO PHILIPPINE ISLANDS	33	5.3	#.#	PDE	EQ	A	14:54-15:#5	12	2##36/ 17
#677	## ## ## ### ##:##:##.#	#.###N #.###E	POSSIBLE NUCLEAR TEST	#	#.#	#.#	HEL	NX	A	14:54-15:#8	15	2##36/ 17
#678	83 #2 18 #49 19:31:34.9	5.#55S 153.242E	NEW IRELAND REGION	33	5.2	#.#	PDE	EQ	ABDE	19:32-2#:13	42	2##36/ 18
#679	83 #2 19 #5# 15:57:19.2	24.#53N 122.629E	TAIWAN REGION	33	5.1	4.6	PDE	EQ	A	16:##-16:11	12	2##36/ 19
#68#	83 #2 19 #5# 2#:14:22.6	#.718N 124.#23E	MINDANAO PHILIPPINE ISLANDS	564	5.#	#.#	PDE	EQ	A	2#:16-2#:28	13	2##36/ 2#
#681	83 #2 19 #5# 21:4#:39.9	4.587S 137.#5E	WEST IRIAN	#1	4.#	#.#	PDE	EQ	ABD	21:43-22:##	18	2##37/ #1
#682	83 #2 2# #51 #1:21:35.6	43.448N 147.433E	KURIL ISLANDS	33	5.#	#.#	PDE	EQ	ABDE	#1:22-#2:#5	44	2##37/ #2
#683	83 #2 2# #51 #2:26:51.5	12.#81N 92.966E	ANDAMAN ISLANDS REGION	3#	5.2	4.4	PDE	EQ	A	#2:33-#2:44	12	2##37/ #3
#684	83 #2 2# #51 #4:49:#2.7	9.67#S 1##.156E	SOUTH OF JAVA	33	5.#	#.#	PDE	EQ	A	#4:55-#5:#6	12	2##37/ #4
#685	83 #2 2# #51 ##:19:25.9	11.5#1S 118.337E	SOUTH OF SUMBAWA ISLAND	33	4.#	#.#	PDE	EQ	A	##:24-##:35	12	2##37/ #5
#686	83 #2 2# #51 1#:49:54.5	5.#27N 126.316E	MINDANAO PHILIPPINE ISLANDS	67	5.#	#.#	PDE	EQ	A	1#:53-11:#4	12	2##37/ #6
#687	83 #2 2# #51 11:34:54.7	5.#38N 126.632E	MINDANAO PHILIPPINE ISLANDS	33	5.#	#.#	PDE	EQ	A	11:3#-11:49	12	2##37/ #7
#688	83 #2 2# #51 13:56:#1.#	5.#5#N 126.586E	MINDANAO PHILIPPINE ISLANDS	61	5.#	#.#	PDE	EQ	A	13:59-14:1#	12	2##37/ #8
#689	83 #2 2# #51 2#:46:58.5	12.3#9N 144.#89E	SOUTH OF MARIANA ISLANDS	37	5.2	5.1	PDE	EQ	ABDE	2#:47-21:22	36	2##37/ #9
#69#	83 #2 21 #52 12:51:#4.#	5.591N 126.615E	MINDANAO PHILIPPINE ISLANDS	33	5.1	#.#	PDE	EQ	A	12:54-13:#5	12	2##37/ 1#
#691	83 #2 21 #52 17:46:24.4	17.768S 172.588W	TONGA ISLANDS REGION	33	5.3	#.#	PDE	EQ	A	17:49-18:##	12	2##37/ 11
#692	83 #2 21 #52 18:26:56.#	45.786N 148.947E	KURIL ISLANDS	33	5.#	#.#	PDE	EQ	ABDE	18:28-19:12	45	2##37/ 12
#693	83 #2 22 #53 #2:48:52.3	35.637N 139.917E	NEAR S COAST OF HONSHU JAPAN	84	4.9	#.#	PDE	EQ	ABD	#2:5#-#3:#5	16	2##37/ 13
#694	83 #2 22 #53 #9:36:44.4	16.#41N 95.333W	OAXACA MEXICO	37	5.6	5.1	PDE	EQ	A	#9:45-#9:56	12	2##37/ 14
#695	83 #2 22 #53 14:49:41.5	17.952S 168.376E	VANUATU ISLANDS	182	5.1	#.#	PDE	EQ	A	14:51-15:#3	13	2##37/ 15
#696	83 #2 22 #53 18:43:29.9	29.78#N 67.378E	AFGHISTAN	33	4.7	#.#	PDE	EQ	A	18:51-19:#2	12	2##37/ 16
#697	83 #2 23 #54 14:13:36.5	4#.375N 63.626E	UZBEK SSR	33	5.#	4.2	PDE	EQ	A	14:21-14:32	12	2##37/ 17
#698	83 #2 23 #54 21:26:45.#	1.994N 125.663E	MOLUCCA PASSAGE	79	5.3	#.#	PDE	EQ	A	21:3#-21:41	12	2##37/ 18
#699	83 #2 24 #55 #9:44:56.2	5.297S 1#3.#56E	SOUTHERN SUMATERA	74	4.7	#.#	PDE	EQ	A	#9:51-1#:#2	12	2##37/ 19
#7##	83 #2 24 #55 18:23:24.#	23.672S 179.136E	SOUTH OF FIJI ISLANDS	651	5.5	#.#	PDE	EQ	A	18:26-18:37	12	2##37/ 2#

WAKE HYDROPHONE INFORMATION PROCESSING SYSTEM (WHIPS) EVENT LISTING 6 JUL 83

KEY: INFORMATION SOURCES - PDE=NEIS PDECARD, MON=NEIS MONTHLY LIST, ICS=ICS LIST, HEL=HELICORDER, OTH=OTHER
EVENT TYPE - EQ=EARTHQUAKE, NX=NUCLEAR EXPLOSION, SX=SCIENTIFIC EXPLOSION, OT=OTHER, UN=UNKNOWN
PHASES - A=P, B=PO, C=S, D=SO, E=T, F=OTHER

EVNT	ORIGIN TIME	COORDINATES	LOCATION	DEP	MAGNI	INF	EV	SAVED	STRIP
NO	YR MO DA JUL HR MN SECS	LAT LON	DESCRIPTION	KM	BDY SRF	SRC	TP	PHASES	INTERVAL MNS	TAPE/FILE
#701	83 #2 25 #56 #5:16:#6.1	23.547S 176.339W	SOUTH OF FIJI ISLANDS	33	5.# 4.6	PDE	EQ A	#5:19-#5:31	13	2##37/ 21
#702	83 #2 25 #56 #8:37:#8.1	35.#4#N 78.#38E	EASTERN KASHMIR	33	4.9 #.#	PDE	EQ A	#8:44-#8:55	12	2##37/ 22
#703	83 #2 25 #56 16:33:11.1	7.37#S 107.116E	JAVA	9#	5.# #.#	PDE	EQ A	16:39-16:5#	12	2##37/ 23
#704	83 #2 25 #56 22:#3:54.9	5.423S 146.#26E	EAST PAPUA NEW GUINEA REGION	222	6.# #.#	PDE	EQ ABDE	22:#5-22:5#	46	2##37/ 24
#705	83 #2 25 #56 22:49:52.1	18.757S 69.582W	NORTHERN CHILE	144	5.9 #.#	PDE	EQ A	22:59-23:18	2#	2##37/ 25
#706	83 #2 26 #57 #2:#5:36.9	22.418N 121.234E	TAIWAN REGION	37	5.1 4.5	PDE	EQ A	#2:#8-#2:2#	13	2##37/ 26
#707	83 #2 26 #57 #3:#1:26.4	31.931N 131.67#E	KYUSHU JAPAN	52	5.2 4.6	PDE	EQ ABDE	#3:#3-#3:51	49	2##38/ #1
#708	83 #2 26 #57 #5:32:#4.6	3.217S 136.653E	WEST IRIAN	33	4.# #.#	PDE	EQ ABD	#5:34-#5:51	18	2##38/ #2
#709	83 #2 26 #57 #6:#1:16.5	18.#38S 172.286W	TONGA ISLANDS REGION	33	5.1 #.#	PDE	EQ A	#6:#4-#6:15	12	2##38/ #3
#710	83 #2 26 #57 #7:1#:59.2	49.231N 155.617E	KURIL ISLANDS	57	6.# #.#	PDE	EQ ABDE	#7:12-#7:57	46	2##38/ #4
#711	83 #2 26 #57 11:42:4#.7	58.524S 162.796E	AUCKLAND ISLANDS REGION	1#	5.4 #.#	PDE	EQ A	11:49-12:#6	12	2##38/ #5
#712	## ## ## 2## ##:##:##.#	#.##2N #.##0E	UNKNOWN P PHASE	#	#.# #.#	HEL	UN A	16:25-16:34	1#	2##38/ #6
#713	83 #2 26 #57 2#:#7:4#.4	38.973N 73.815E	AFGHANISTAN-USSR BORDER REGION	33	5.3 5.1	PDE	EQ A	2#:15-2#:26	12	2##38/ #7
#714	83 #2 27 #58 1#:11:#4.7	36.#99N 141.982E	NEAR E COAST OF HONSHU JAPAN	33	4.7 #.#	PDE	EQ ABD	1#:12-1#:26	15	2##36/ #8
#715	83 #2 27 #58 12:14:19.1	35.#72N 139.948E	NEAR S COAST OF HONSHU JAPAN	64	5.9 #.#	PDE	EQ ABDE	12:15-12:58	44	2##38/ #9
#716	83 #2 27 #58 2#:33:#8.5	32.638N 76.567E	KASHMIR-TIBET BORDER REGION	52	5.3 4.9	PDE	EQ A	2#:4#-2#:5)	12	2##38/ 1#
#717	83 #2 28 #59 #5:44:24.3	44.164N 148.#39E	KURIL ISLANDS	41	5.# 5.9	PDE	EQ ABDE	#5:45-#6:29	45	2##36/ 11
#718	83 #2 28 #59 #9:#1:12.#	42.#24N 72.153E	KIRGHIZ SSR	33	4.9 #.#	PDE	EQ A	#9:#8-#9:2#	13	2##38/ 12
#719	83 #2 28 #59 18:33:14.3	28.182N 142.219E	BONIN ISLANDS REGION	33	5.# #.#	PDE	EQ ABDE	18:33-19:11	39	2##38/ 13
#720	83 #2 28 #59 22:17:58.6	4.#89S 142.344E	PAPUA NEW GUINEA	1#3	5.3 #.#	PDE	EQ ABDE	22:19-23:#7	49	2##38/ 14
#721	83 #3 #1 #6# #2:#2:19.5	39.168N 54.594E	TURKMEN SSR	33	4.# #.#	PDE	EQ A	#2:11-#2:22	12	2##36/ 15
#722	83 #3 #1 #6# #9:#2:17.3	31.#66N 141.637E	SOUTH OF HONSHU JAPAN	33	5.# 5.4	PDE	EQ ABDE	#9:#3-#9:41	39	2##36/ 16
#723	83 #3 #1 #6# 13:22:31.6	28.61#N 95.982E	INDIA-CHINA BORDER REGION	33	5.# #.#	PDE	EQ A	13:28-13:39	12	2##36/ 17
#724	83 #3 #1 #6# 19:26:45.4	5.715S 1#4.314E	SOUTHERN SUMATERA	33	5.# #.#	PDE	EQ A	19:32-19:44	13	2##38/ 18
#725	## ## ## #6# ##:##:##.#	#.##2N #.##2E	PROBABLE MARIANAS	#	#.# #.#	HEL	EQ BDE	#1:5#-#2:19	3#	2##39/ #1
#726	83 #3 #2 #61 #7:#7:41.4	11.595S 77.827W	NEAR COAST OF PERU	64	5.5 #.#	PDE	EQ A	#7:17-#7:36	2#	2##29/ #2
#727	83 #3 #2 #61 #9:11:22.1	37.249N 141.974E	NEAR E COAST OF HONSHU JAPAN	33	4.7 #.#	PDE	EQ ABD	#8:12-#8:27	16	2##39/ #3
#728	83 #3 #3 #62 #1:51:19.5	18.#19S 178.286W	FIJI ISLANDS REGION	55#	5.2 #.#	PDE	EQ A	#1:53-#2:#4	12	2##39/ #4
#729	83 #3 #3 #62 #2:#2:21.4	11.433N 139.873E	WEST CAROLINE ISLANDS	45	5.# #.#	PDE	EQ ABDE	#2:#3-#2:42	48	2##39/ #4
#732	83 #3 #3 #62 #2:3#:31.#	6.152S 1##.783E	SOUTHWEST OF SUMATERA	33	5.6 5.4	PDE	EQ A	#2:37-#2:48	12	2##29/ #4
#731	83 #3 #3 #62 #3:32:13.#	43.928N 86.697E	NORTHERN SINKIANG PROV CHINA	33	5.5 #.#	PDE	EQ A	#3:3#-#3:5#	13	2##29/ #5
#732	83 #3 #3 #62 16:42:54.6	41.763N 143.425E	HOKKAIDO JAPAN REGION	33	5.2 #.#	PDE	EQ ABDE	16:44-17:2#	45	2##39/ #6
#733	83 #3 #3 #62 17:43:##.4	39.413N 143.373E	OFF E COAST OF HONSHU JAPAN	33	4.9 #.#	PDE	EQ ABD	17:44-17:59	16	2##39/ #7
#734	83 #3 #4 #63 14:11:36.#	39.553N 143.132E	OFF E COAST OF HONSHU JAPAN	33	5.2 5.6	PDE	EQ ABDE	14:12-14:55	44	2##39/ #8
#735	83 #3 #4 #63 19:#6:12.9	14.265S 14.319W	SOUTH ATLANTIC RIDGE	1#	5.2 5.3	PDE	EQ ABD	19:15-2#:19	65	2##39/ #9
#736	## ## ## ### ##:##:##.#	#.##0N #.##0E	PROBABLE MARIANAS	#	#.# #.#	HEL	EQ BDE	23:5#-##:19	3#	2##39/ 1#
#737	83 #3 #5 #64 #9:57:#4.#	1#.794S 115.#54E	SOUTH OF BALI ISLAND	33	5.# 5.3	PDE	EQ A	#9:#2-#9:13	12	2#0#39/ 11
#738	83 #3 #5 #64 11:37:53.6	39.141N 64.586E	UZBEK SSR	33	4.# #.#	PDE	EQ A	11:46-11:57	12	2##39/ 12
#739	83 #3 #5 #64 16:41:47.1	22.653N 93.971E	BURMA-INDIA BORDER REGION	97	4.6 #.#	PDE	EQ A	16:47-16:59	13	2##29/ 13
#740	83 #3 #5 #64 21:32:2#.#	35.575N 136.147E	SOUTHERN HONSHU JAPAN	49	4.# #.#	PDE	EQ ABD	21:34-21:49	16	2##39/ 14
#741	83 #3 #5 #64 21:5#:#6.#	49.547N 152.7#2E	NORTHWEST OF KURIL ISLANDS	347	4.9 #.#	PDE	EQ ABDE	21:51-22:39	49	2##39/ 15
#742	83 #3 #6 #65 22:23:57.7	6.144S 147.3#8E	EAST PAPUA NEW GUINEA REGION	84	5.5 #.#	PDE	EQ ABDE	22:25-23:1#	46	2##42/ #1
#743	83 #3 #7 #66 #6:3#:26.1	9.561N 126.#71E	MINDANAO PHILIPPINE ISLANDS	87	5.# #.#	PDE	EQ A	#6:33-#6:44	12	2##42/ #2
#744	83 #3 #7 #65 15:12:22.3	18.297N 146.551E	MARIANA ISLANDS	7#	4.# #.#	PDE	EQ ABD	15:11-15:24	14	#/ ##
#745	83 #3 #8 #67 13:21:46.#	3.476S 177.631E	GILBERT ISLANDS REGION	33	5.# 5.#	PDE	EQ ABDE	13:22-14:#6	39	2##42/ #3
#746	83 #3 #8 #67 18:3#:#7.7	3.5#7S 177.7#7E	GILBERT ISLANDS REGION	33	5.1 #.#	PDE	EQ ABDE	18:3#-19:17	48	2##42/ #4
#747	83 #3 #8 #67 2#:24:25.2	13.77#N 144.747E	MARIANA ISLANDS	1##	5.# #.#	PDE	EQ ABDE	2#:24-2#:5#	35	2##42/ #5
#748	83 #3 #8 #67 23:27:57.5	7.#94S 129.261E	BANDA SEA	181	5.4 #.#	PDE	EQ A	23:31-23:42	12	#/ ##
#749	83 #3 #9 #68 ##:#5:46.2	7.238S 1#7.762E	JAVA	118	5.4 #.#	PDE	EQ A	##:11-##:22	12	#/ ##
#75#	83 #3 #9 #68 17:16:27.7	5.#58S 145.697E	EAST PAPUA NEW GUINEA REGION	2#2	5.# #.#	PDE	EQ ABDE	17:18-18:#3	46	2##48/ #6
#751	83 #3 1# #69 ##:27:49.4	43.#11N 147.441E	KURIL ISLANDS	42	6.2 5.#	PDE	EQ ABDE	##:29-#1:12	44	2##48/-#7
#752	83 #3 1# #69 #5:46:#6.#	14.645S 167.282E	VANUATU ISLANDS	33	5.3 #.#	PDE	EQ A	#5:48-#5:59	12	2##48/ #8
#753	83 #3 1# #69 11:5#:19.9	5.411N 126.76#E	MINDANAO PHILIPPINE ISLANDS	33	5.4 5.6	PDE	EQ A	12:#1-12:12	12	2##48/ #9
#754	83 #3 11 #7# #2:24:#9.3	1#.249S 13.438W	ASCENSION ISLAND REGION	1#	4.# #.#	PDE	EQ A	##:33-##:52	2#	#/ ##
#755	83 #3 11 #7# #3:1#:42.1	6.992S 147.374E	EAST PAPUA NEW GUINEA REGION	66	5.9 #.#	PDE	EQ ABDE	#3:12-#3:58	47	#/ ##
#756	83 #3 11 #7# 23:#2:36.5	5.372N 126.623E	MINDANAO PHILIPPINE ISLANDS	6#	5.2 #.#	PDE	EQ A	23:#5-23:16	12	2##42/-1#
#757	83 #3 12 #71 #2:44:44.6	36.435N 7#.959E	HINDU KUSH REGION	234	4.5 #.#	PDE	EQ AE	#2:52-#1:#3	12	2##42/-11
#758	83 #3 12 #71 #2:53:4#.2	4.#37S 127.914E	BANDA SEA	33	5.9 6.#	PDE	EQ AE	#2:57-#1:55	59	2##42/-11
#759	83 #3 12 #71 #1:36:36.6	4.1#3S 127.918E	BANDA SEA	22	6.# 6.5	PDE	EQ AE	#1:4#-#2:38	59	2##42/-11
#76#	83 #3 12 #71 #7:##:15.#	52.325N 17#.119W	FOX ISL, ALEUTIAN ISL.	33	5.3 5.2	PDE	EQ ABDE	#7:#2-#7:54	53	2##42/ 12
#761	83 #3 12 #71 #7:21:5#.2	5.395N 126.671E	MINDANAO PHILIPPINE ISLANDS	63	5.# #.#	PDE	EQ A	#7:24-#7:36	13	2##48/ 12
#762	83 #3 12 #71 #8:49:45.7	1#.#98S 168.128E	VANUATU ISLANDS	33	5.6 5.9	PDE	EQ A	#8:52-#9:#3	12	2##48/ 13
#763	83 #3 12 #71 12:3#:17.5	4.26#S 128.175E	BANDA SEA	33	5.# #.#	PDE	EQ A	12:33-12:45	13	2##48/ 14
#764	83 #3 12 #71 14:25:27.2	31.575N 1#4.239E	SICHUAN PROVINCE CHINA	33	4.# #.#	PDE	EQ A	14:3#-14:41	12	2##48/ 15
#765	83 #3 12 #71 14:45:17.#	4.1#5S 128.#58E	BANDA SEA	21	5.2 #.#	PDE	EQ A	14:4#-15:##	13	2##48/ 16
#766	83 #3 12 #71 21:#5:15.7	8.671N 93.#89E	NICOBAR ISLANDS REGION	33	5.# 4.5	PDE	EQ A	21:11-21:23	13	2##48/ 17
#767	83 #3 12 #71 22:14:15.4	21.733N 143.#7#E	MARIANA ISLANDS REGION	33	4.# #.#	PDE	EQ ABD	22:14-22:27	14	2##48/-18
#768	83 #3 13 #72 #2:54:1#.#	5.1#9S 147.61#E	EAST PAPUA NEW GUINEA REGION	31	5.2 5.1	PDE	EQ ABDE	#2:55-#3:39	45	2##48/-19
#769	83 #3 13 #72 #5:1#:56.#	52.371N 157.475E	KAMCHATKA	33	5.1 #.#	PDE	EQ ABDE	#5:2#-#6:#9	5#	2##49/ 2#
#77#	83 #3 13 #72 #9:##:51.6	42.22#N 142.6#6E	HOKKAIDO JAPAN REGION	4#	4.# #.#	PDE	EQ ABD	#9:1#-#9:25	16	2##49/ 21
#771	83 #3 13 #72 1#:#5:45.2	52.321N 157.398E	KAMCHATKA	33	4.6 #.#	PDE	EQ ABD	1#:#7-1#:24	18	2##49/ 22
#772	83 #3 13 #72 1#:#6:14.#	52.487N 157.478E	KAMCHATKA	33	4.# #.#	PDE	EQ ABD	1#:#8-1#:24	17	2##49/ 22
#773	83 #3 13 #72 2#:#5:57.7	54.117N 159.172E	NEAR E COAST OF KAMCHATKA	33	5.# #.#	PDE	EQ ABDE	2#:#9-2#:57	5#	2##41/ #8
#774	83 #3 13 #72 2#:2#:#8.#	41.563N 142.#5#E	HOKKAIDO JAPAN REGION	63	5.# #.#	PDE	EQ ABDE	2#:21-21:#6	46	2##41/ #8
#775	83 #3 13 #72 23:3#:14.6	51.973N 178.#63E	RAT ISL, ALEUTIAN ISL.	142	4.7 #.#	PDE	EQ ABD	23:32-23:45	17	2##41/-#9
#776	83 #3 14 #73 11:55:2#.2	39.292N 54.633E	TURKMEN SSR	33	4.9 4.#	PDE	EQ A	12:#4-12:15	12	2##41/ 1#
#777	83 #3 14 #73 12:12:4#.5	39.257N 54.522E	TURKMEN SSR	33	5.2 5.#	PDE	EQ A	12:21-12:32	12	2##41/ 11
#778	83 #3 14 #73 14:15:36.#	3.327S 177.524E	GILBERT ISLANDS REGION	33	5.# #.#	PDE	EQ ABDE	14:16-14:54	39	2##41/ 12
#779	83 #3 14 #73 19:#2:#6.5	4.175S 127.#24E	BANDA SEA	33	5.5 #.#	PDE	EQ A	19:#5-19:16	12	2##41/ 13
#78#	83 #3 14 #73 21:14:54.3	52.342N 17#.152W	FOX ISL, ALEUTIAN ISL.	33	5.1 #.#	PDE	EQ ABDE	21:17-22:#9	53	2##41/ 14
#781	83 #3 15 #74 12:37:53.2	7.#99N 123.#24E	MINDANAO PHILIPPINE ISLANDS	52	5.4 4.6	PDE	EQ A	12:41-12:52	12	2##41/ 15
#782	83 #3 15 #74 14:49:1#.4	39.297N 54.55#E	TURKMEN SSR	33	5.# 4.2	PDE	EQ A	14:57-15:#9	13	2##41/ 16
#783	83 #3 15 #74 17:27:24.9	34.78#N 137.566E	NEAR S COAST OF HONSHU JAPAN	31	5.4 4.9	PDE	EQ ABDE	17:2#-18:12	45	2##41/ 17
#784	83 #3 15 #74 19:5#:3#.7	5.34#N 126.6#9E	MINDANAO PHILIPPINE ISLANDS	47	5.7 6.6	PDE	EQ AE	2#:#1-2#:56	56	2##41/ 18
#785	83 #3 15 #74 22:27:#1.2	8.335S 122.642E	FLORES ISLAND REGION	172	4.6 #.#	PDE	EQ A	22:31-22:42	12	2##41/-19
#786	83 #3 16 #75 #5:2#:36.3	3.3#8S 14#.31#E	WEST IRIAN	11	5.1 #.#	PDE	EQ A	#5:3#-#5:42	13	2##41/ 2#
#787	83 #3 16 #75 #9:13:1#.7	3.44#N 95.7#1E	OFF W COAST OF NORTH SUMATERA	3#	5.3 #.#	PDE	EQ A	#9:19-#9:31	13	2##41/ 35
#788	83 #3 17 #76 #2:53:#8.#	12.287N 144.#34E	SOUTH OF MARIANA ISLANDS	36	5.7 5.4	PDE	EQ ABDE	#2:53-#3:2#	36	2##41/-36
#789	83 #3 17 #76 #7:11:3#.4	51.59#N 142.491E	SAKHALIN ISLAND	41	5.6 4.9	PDE	EQ A	#7:14-#7:25	12	2##41/ 37
#79#	83 #3 17 #76 1#:1#:48.4	12.#4#N 122.954E	LUZON PHILIPPINE ISLANDS	43	5.3 5.7	PDE	EQ A	1#:14-1#:25	12	2##41/ 38
#791	83 #3 17 #76 19:59:2#.3	41.796N 14#.76#E	HOKKAIDO JAPAN REGION	131	5.3 #.#	PDE	EQ ABDE	2#:##-2#:46	47	2##41/ 39
#792	83 #3 18 #77 ##:1#:39.5	44.#46N 139.179E	EASTERN SEA OF JAPAN	46	4.9 #.#	PDE	EQ ABD	##:2#-##:36	17	2##41/-4#
#793	83 #3 18 #77 #3:37:#3.#	22.443S 174.245W	TONGA ISLANDS REGION	4#	5.4 #.#	PDE	EQ A	##:4#-##:52	13	2##41/ 41
#794	83 #3 18 #77 #3:#5:5#.1	4.#57S 153.5#7E	NEW IRELAND REGION	##	6.4 7.#	PDE	EQ ABDE	#9:#6-#9:47	42	2##41/ 42
#795	83 #3 18 #77 17:32:#2.5	37.335N 7#.745E	AFGHANISTAN-USSR BORDER REGION	33	4.# #.#	PDE	EQ A	17:39-17:51	13	2##42/ #1
#796	83 #3 18 #77 17:5#:14.4	4.665S 153.54#E	NEW IRELAND REGION	9#	5.# #.#	PDE	EQ ABDE	17:51-18:31	41	2##42/ #1
#797	83 #3 19 #78 #5:#6:18.3	3#.91#N 1#2.515E	SICHUAN PROVINCE CHINA	33	4.5 #.#	PDE	EQ A	#6:11-#6:23	13	2##42/ #2
#798	83 #3 19 #78 11:46:24.2	51.6#1N 159.76#E	OFF EAST COAST OF KAMCHATKA	37	5.2 5.1	PDE	EQ ABDE	11:48-12:35	48	2##42/ #8
#799	83 #3 19 #78 13:4#:22.2	17.92#S 179.444W	FIJI ISLANDS REGION	625	4.6 #.#	PDE	EQ A	13:5#-14:#1	12	2##42/ #9
#8#2	83 #3 19 #78 17:13:27.6	4.26#S 152.765E	NEW BRITAIN REGION	17	5.3 5.4	PDE	EQ ABDE	17:14-17:54	41	2##42/ 1#

WAKE HYDROPHONE INFORMATION PROCESSING SYSTEM (WHIPS) EVENT LISTING 6 JUL 83

KEY: INFORMATION SOURCES - PDE=NEIS PDECARD, MON=NEIS MONTHLY LIST, ICS=ICS LIST, HEL=HELICORDER, OTH=OTHER
EVENT TYPE - EQ=EARTHQUAKE, NX=NUCLEAR EXPLOSION, SX=SCIENTIFIC EXPLOSION, OT=OTHER, UN=UNKNOWN
PHASES - A=P, B=PO, C=S, D=SO, E=T, F=OTHER

EVNT NO	ORIGIN TIME YR MO DA JUL HR MN SECS	COORDINATES LAT	LON	LOCATION DESCRIPTION	DEP KM	MAGNI BDY	MAGNI SRF	INF SRC	EV TP	SAVED PHASES	SAVED INTERVAL	SAVED MNS	STRIP TAPE/FILE
0001	83 03 19 070 22:59:47.1	4.826S	153.812E	NEW IRELAND REGION	119	4.8	0.0	PDE	EQ	ABD	23:00-23:15	16	20042/-11
0002	83 03 20 079 11:24:48.4	2.375N	126.000E	MOLUCCA PASSAGE	50	5.5	0.0	PDE	EQ	A	11:20-11:39	12	20042/ 12
0003	83 03 20 079 13:45:49.0	4.727S	153.125E	NEW IRELAND REGION	86	5.9	0.0	PDE	EQ	ABDE	13:46-14:27	42	20042/ 13
0004	83 03 20 079 16:24:13.3	18.827S	177.762W	FIJI ISLANDS REGION	632	5.0	0.0	PDE	EQ	A	16:26-16:37	12	20042/ 14
0005	83 03 20 079 17:44:07.1	18.804S	177.679W	FIJI ISLANDS REGION	634	4.9	0.0	PDE	EQ	A	17:46-17:57	12	20042/ 15
0006	83 03 21 080 04:06:24.0	5.031S	153.698E	NEW IRELAND REGION	80	5.5	0.0	PDE	EQ	ABDE	04:07-04:48	42	20042/-16
0007	83 03 21 080 07:44:17.6	21.660S	175.321W	TONGA ISLANDS	70	6.3	0.0	PDE	EQ	A	07:47-07:59	13	20042/ 17
0008	83 03 21 080 07:57:10.4	7.342S	128.920E	BANDA SEA	143	5.6	0.0	PDE	EQ	A	08:00-08:12	13	20042/ 17
0009	83 03 21 080 15:23:42.7	36.582N	70.593E	HINDU KUSH REGION	166	4.2	0.0	PDE	EQ	A	15:31-15:42	12	20042/ 18
0010	83 03 21 060 15:49:52.0	21.394S	175.452W	TONGA ISLANDS	70	5.4	0.0	PDE	EQ	A	15:53-16:04	12	20042/ 19
0011	83 03 22 081 01:32:20.6	51.297N	178.481W	ANDREANOF ISL. ALEUTIAN ISL.	33	4.9	0.0	PDE	EQ	ABD	01:34-01:50	17	20042/-20
0012	83 03 22 081 20:17:07.5	53.211N	162.259E	OFF EAST COAST OF KAMCHATKA	33	4.7	0.0	PDE	EQ	ABD	20:19-20:35	17	20042/ 21
0013	83 03 23 082 06:09:29.6	6.618S	154.612E	SOLOMON ISLANDS	41	5.7	6.2	PDE	EQ	ABDE	06:10-06:52	43	20042/ 22
0014	83 03 23 082 06:40:32.1	6.663S	154.559E	SOLOMON ISLANDS	55	5.2	0.0	PDE	EQ	ABDE	06:41-07:23	43	20042/ 22
0015	83 03 23 082 08:26:55.2	6.627S	154.585E	SOLOMON ISLANDS	35	5.4	5.6	PDE	EQ	ABDE	08:28-09:09	42	20042/ 23
0016	83 03 23 082 12:11:23.9	37.01N	71.487E	AFGHANISTAN-USSR BORDER REGION	122	5.2	0.0	PDE	EQ	A	12:18-12:38	13	20042/ 24
0017	83 03 23 082 14:04:52.1	6.780S	154.528E	SOLOMON ISLANDS	68	5.2	0.0	PDE	EQ	ABDE	14:06-14:47	42	20043/ 01
0018	83 03 23 082 16:07:21.2	3.375S	177.491E	GILBERT ISLANDS REGION	27	4.8	0.0	PDE	EQ	ABD	16:07-16:21	15	20043/ 02
0019	83 03 23 082 21:54:36.3	37.224N	138.125E	NEAR W COAST OF HONSHU JAPAN	54	4.6	0.0	PDE	EQ	ABD	21:56-22:11	16	20043/ 03
0020	00 00 00 000 00:00:00.0	0.000N	0.000E	LOCAL PO, SO, T	0	0.0	0.0	HEL	EQ	BDE	00:22-00:51	30	20043/ 04
0021	83 03 24 083 07:01:42.9	10.551S	159.822E	SOLOMON ISLANDS	151	4.9	0.0	PDE	EQ	ABD	07:03-07:18	16	20043/ 05
0022	83 03 24 083 07:24:12.5	7.615S	107.173E	JAVA	57	4.9	0.0	PDE	EQ	A	07:30-07:41	12	20043/ 06
0023	83 03 24 083 08:44:53.9	6.602S	154.564E	SOLOMON ISLANDS	52	5.1	0.0	PDE	EQ	ABDE	08:46-09:27	42	20043/ 07
0024	83 03 24 083 12:47:40.5	4.721S	153.336E	NEW IRELAND REGION	80	5.2	0.0	PDE	EQ	ABDE	10:48-11:29	42	20043/ 08
0025	83 03 24 083 12:24:35.2	10.814S	163.992E	SOLOMON ISLANDS	74	4.9	0.0	PDE	EQ	ABD	12:25-12:41	17	20043/ 09
0026	00 00 00 000 00:00:00.0	0.000N	0.000E	PROBABLE MARIANAS PO, SO, T	0	0.0	0.0	HEL	EQ	BDE	20:10-20:39	30	20043/ 10
0027	83 03 25 084 07:44:01.2	6.555S	130.006E	BANDA SEA	164	5.4	0.0	PDE	EQ	A	07:47-07:58	12	20043/ 11
0028	83 03 25 084 13:00:14.2	6.494S	151.722E	NEW BRITAIN REGION	45	5.3	0.0	PDE	EQ	ABDE	13:01-13:44	44	20043/ 12
0029	83 03 25 084 19:33:54.1	8.395S	124.608E	TIMOR	169	4.8	0.0	PDE	EQ	A	19:37-19:49	13	20043/ 13
0030	83 03 25 084 21:41:54.8	6.492S	155.118E	SOLOMON ISLANDS	123	5.1	0.0	PDE	EQ	ABDE	21:42-22:24	43	20043/ 14
0031	83 03 26 085 10:51:48.4	39.139N	44.542E	N.W. IRAN-USSR BORDER REGION	33	4.6	0.0	PDE	EQ	A	11:00-11:20	21	20043/ 15
0032	83 03 26 085 12:46:47.7	5.105S	153.597E	NEW IRELAND REGION	70	4.9	0.0	PDE	EQ	ABD	12:47-13:02	16	20043/ 16
0033	83 03 26 085 14:57:49.3	1.167N	126.586E	MOLUCCA PASSAGE	73	5.2	0.0	PDE	EQ	A	15:01-15:12	12	20043/ 17
0034	83 03 26 085 17:19:37.5	4.631S	143.870E	PAPUA NEW GUINEA	101	4.5	0.0	PDE	EQ	ABD	17:21-17:37	17	20043/ 18
0035	83 03 26 085 18:42:46.8	42.847N	141.795E	HOKKAIDO JAPAN REGION	00	4.4	0.0	PDE	EQ	ABD	18:44-19:00	17	20043/ 19
0036	83 03 26 085 20:20:00.0	37.301N	116.467W	SOUTHERN NEVADA	0	5.1	0.0	PDE	NX	A	20:26-20:37	12	20044/ 01
0037	83 03 27 086 02:42:41.4	34.260N	92.644E	QINGHAI PROVINCE CHINA	33	4.5	0.0	PDE	EQ	A	02:48-03:00	13	20044/ 02
0038	83 03 27 086 09:04:13.5	27.514N	141.378E	BONIN ISLANDS REGION	30	4.8	0.0	PDE	EQ	ABD	09:05-09:19	15	20044/ 03
0039	83 03 27 086 10:32:00.1	4.038S	153.568E	NEW IRELAND REGION	95	4.9	0.0	PDE	EQ	ABD	10:33-10:47	15	20044/ 04
0040	83 03 27 086 22:05:07.6	6.893S	148.454E	NEW BRITAIN REGION	33	5.0	0.0	PDE	EQ	ABDE	20:06-20:51	46	20044/ 05
0041	83 03 28 087 19:17:50.6	26.306N	127.311E	RYUKYU ISLANDS	62	5.3	0.0	PDE	EQ	A	19:20-19:31	12	20044/ 06
0042	83 03 28 087 23:30:27.2	12.986N	146.354E	SOUTH OF MARIANA ISLANDS	33	4.7	0.0	PDE	EQ	ABD	23:38-23:51	14	20044/ 07
0043	83 03 29 088 04:53:29.4	30.443N	131.508E	KYUSHU JAPAN	33	4.9	0.0	PDE	EQ	ABD	04:55-05:11	17	20044/ 08
0044	83 03 29 088 22:55:47.8	6.904S	154.807E	SOLOMON ISLANDS	33	5.1	0.0	PDE	EQ	ABDE	22:57-23:38	42	20044/ 09
0045	83 03 30 089 00:49:09.9	1.572N	122.513E	MINAHASSA PENINSULA	40	5.4	5.1	PDE	EQ	A	00:53-01:04	12	20044/ 10
0046	83 03 30 089 06:46:22.5	40.001N	75.033E	KIRGHIZ-XINJIANG BORDER REGION	33	4.9	4.9	PDE	EQ	A	06:53-07:05	13	20044/ 11
0047	83 03 30 089 12:02:52.3	6.637S	154.566E	SOLOMON ISLANDS	33	4.8	0.0	PDE	EQ	ABD	12:04-12:18	15	20044/ 12
0048	83 03 30 089 16:13:35.2	39.884N	75.488E	SOUTHERN XINJIANG CHINA	33	4.8	0.0	PDE	EQ	A	16:21-16:32	12	20044/ 13
0049	83 03 30 089 18:55:49.1	5.919S	142.220E	PAPUA NEW GUINEA	33	5.2	0.0	PDE	EQ	ABDE	18:58-19:46	49	20044/ 14
0050	83 03 31 090 13:24:45.6	34.201N	135.833E	NEAR S COAST OF SOUTH HONSHU	380	4.9	0.0	PDE	EQ	ABDE	13:25-14:11	47	20044/ 15
0051	83 04 01 091 01:04:59.0	18.534N	145.806E	MARIANA ISLANDS	102	5.1	0.0	PDE	EQ	ABDE	01:04-01:36	33	20044/ 16
0052	00 00 00 000 00:00:00.0	0.000N	0.000E	PROBABLE BONIN PO, SO, T	0	0.0	0.0	HEL	EQ	BDE	20:43-21:12	30	20044/ 17
0053	83 04 02 092 04:10:23.5	3.123S	135.287E	WEST IRIAN	33	5.0	0.0	PDE	EQ	A	04:20-04:32	13	20044/ 18
0054	83 04 02 092 05:09:10.3	54.899N	162.314E	NEAR EAST COAST OF KAMCHATKA	92	4.9	0.0	PDE	EQ	ABD	05:11-05:26	16	20044/ 19
0055	83 04 02 092 06:49:01.9	24.711S	176.196W	SOUTH OF FIJI ISLANDS	40	5.4	5.0	PDE	EQ	A	06:52-07:04	13	20044/ 20
0056	83 04 02 092 21:04:30.6	6.327S	154.533E	SOLOMON ISLANDS	44	4.6	0.0	PDE	EQ	ABD	21:05-21:20	16	20044/ 21
0057	83 04 02 092 21:55:44.0	36.393N	70.734E	HINDU KUSH REGION	215	4.8	0.0	PDE	EQ	A	22:03-22:14	12	20045/ 01
0058	83 04 03 093 02:58:00.7	8.731N	83.115W	COSTA RICA	33	6.6	7.2	PDE	EQ	AE	02:59-05:00	130	20045/ 02
0059	83 04 03 093 10:14:53.0	8.671N	124.181E	MINAHASSA PENINSULA	174	5.0	0.0	PDE	EQ	A	10:18-10:29	12	20045/ 03
0060	83 04 03 093 19:14:05.2	51.997N	179.256E	RAT ISL. ALEUTIAN ISL.	116	5.6	0.0	PDE	EQ	ABDE	19:16-20:04	49	20045/ 04
0061	83 04 03 093 19:26:24.5	51.889N	176.919W	ANDREANOF ISL. ALEUTIAN ISL.	60	5.3	0.0	PDE	EQ	ABDE	19:28-20:17	50	20045/ 04
0062	83 04 04 094 00:45:07.9	38.517N	70.334E	AFGHANISTAN-USSR BORDER REGION	33	4.9	0.0	PDE	EQ	A	00:52-01:04	13	20045/ 05
0063	83 04 04 094 02:51:34.9	6.736N	94.811E	NORTHERN SUMATERA	85	6.5	0.0	PDE	EQ	A	02:58-03:09	12	20045/ 06
0064	83 04 04 094 03:03:35.0	5.752N	94.798E	NORTHERN SUMATERA	74	5.8	0.0	PDE	EQ	A	03:10-03:21	12	20045/ 06
0065	00 00 00 000 00:00:00.0	0.000N	0.000E	PROBABLE BONIN'S PO, SO, T	0	0.0	0.0	HEL	EQ	BDE	05:25-05:54	30	20045/ 07
0066	83 04 04 094 06:50:59.5	5.585N	94.648E	NORTHERN SUMATERA	76	5.0	0.0	PDE	EQ	A	07:05-07:16	12	20045/ 08
0067	83 04 04 094 19:04:20.0	52.923N	159.916E	OFF EAST COAST OF KAMCHATKA	30	6.0	5.5	PDE	EQ	ABDE	19:06-19:54	49	20045/ 09
0068	83 04 04 094 19:40:04.1	7.057S	129.379E	BANDA SEA	144	5.0	0.0	PDE	EQ	A	19:51-20:02	12	20045/ 09
0069	83 04 04 094 23:12:47.0	49.399N	155.648E	KURIL ISLANDS	60	6.1	6.5	PDE	EQ	ABDE	23:14-23:59	46	20045/ 10
0070	83 04 04 094 23:50:59.6	15.819S	167.274E	VANUATU ISLANDS	127	6.1	0.0	PDE	EQ	ABDE	00:00-00:49	50	20045/ 10
0071	83 04 05 095 02:55:24.6	41.631N	70.763E	KIRGHIZ SSR	33	5.1	0.0	PDE	EQ	A	01:03-01:14	12	20045/ 11
0072	83 04 05 095 06:50:33.5	40.062N	75.285E	KIRGHIZ-XINJIANG BORDER REGION	33	5.4	5.6	PDE	EQ	A	06:57-07:09	13	20046/ 01
0073	83 04 05 095 07:07:23.5	39.874N	75.449E	SOUTHERN XINJIANG CHINA	33	4.8	0.0	PDE	EQ	A	07:14-07:26	13	20046/ 02
0074	83 04 05 095 07:40:30.3	5.438N	126.698E	MINDANAO PHILIPPINE ISLANDS	41	5.1	0.0	PDE	EQ	A	07:43-07:54	12	20046/ 03
0075	83 04 05 095 21:39:00.0	26.489N	126.488E	RYUKYU ISLANDS	121	4.7	0.0	PDE	EQ	ABD	21:41-21:58	18	20046/ 04
0076	83 04 06 096 00:50:23.7	6.171S	149.865E	NEW BRITAIN REGION	53	4.8	4.7	PDE	EQ	ABD	00:51-01:07	17	20046/ 05
0077	83 04 06 096 02:00:11.0	36.438N	71.477E	AFGHANISTAN-USSR BORDER REGION	101	4.7	0.0	PDE	EQ	A	02:16-02:27	13	20046/ 06
0078	83 04 06 096 10:30:36.6	5.548S	153.568E	NEW IRELAND REGION	68	4.6	0.0	PDE	EQ	ABD	10:31-10:46	16	20046/ 07
0079	83 04 06 096 12:49:20.4	39.974N	75.129E	SOUTHERN XINJIANG CHINA	33	4.7	0.0	PDE	EQ	A	12:56-13:07	12	20046/ 08
0080	83 04 06 096 18:00:00.2	21.614S	179.391W	FIJI ISLANDS REGION	636	4.9	0.0	PDE	EQ	A	18:10-18:21	12	20046/ 09
0081	83 04 06 096 21:17:32.1	2.020S	128.166E	CERAM SEA	33	5.0	0.0	PDE	EQ	A	21:20-21:32	13	20046/ 10
0082	83 04 06 096 22:18:47.5	38.046N	71.488E	AFGHANISTAN-USSR BORDER REGION	33	5.2	4.7	PDE	EQ	A	22:26-22:37	12	20046/-11
0083	83 04 07 097 05:04:22.3	5.996S	100.752E	SOUTHWEST OF SUMATERA	33	5.0	0.0	PDE	EQ	A	05:10-05:22	13	20046/ 12
0084	83 04 07 097 22:56:52.3	54.512N	160.929E	NEAR EAST COAST OF KAMCHATKA	33	5.1	0.0	PDE	EQ	ABDE	22:59-23:40	58	20046/-13
0085	83 04 08 098 02:20:25.5	11.448N	57.589E	ARABIAN SEA	10	5.0	6.2	PDE	EQ	F	02:30-04:29	120	20046/-14
0086	83 04 08 098 06:21:24.0	5.640N	94.719E	NORTHERN SUMATERA	76	4.8	0.0	PDE	EQ	A	06:28-06:39	12	20046/ 15
0087	83 04 08 098 14:10:53.3	49.636N	155.286E	KURIL ISLANDS	82	5.5	0.0	PDE	EQ	ABDE	14:12-14:58	47	20046/ 16
0088	83 04 09 099 22:00:36.6	41.919N	142.421E	HOKKAIDO JAPAN REGION	64	4.5	0.0	PDE	EQ	ABD	22:02-22:17	16	20046/ 17
0089	83 04 10 100 02:20:36.3	17.636S	174.640W	TONGA ISLANDS	33	5.4	5.3	PDE	EQ	A	02:23-02:34	12	20046/ 18
0090	83 04 10 100 05:30:47.7	40.026N	77.060E	KIRGHIZ-XINJIANG BORDER REGION	33	4.8	4.4	PDE	EQ	A	05:46-05:57	12	20046/ 19
0091	83 04 10 100 05:51:37.6	22.120S	179.709W	SOUTH OF FIJI ISLANDS	600	5.3	0.0	PDE	EQ	A	05:54-06:05	12	20046/ 19
0092	83 04 10 100 12:19:32.5	2.302N	126.795E	MOLUCCA PASSAGE	90	5.0	0.0	PDE	EQ	A	12:22-12:33	12	20046/ 20
0093	83 04 10 100 10:29:35.4	38.709N	141.952E	SOUTH OF HONSHU JAPAN	33	5.3	5.3	PDE	EQ	ABDE	10:30-10:00	30	20046/ 21
0094	83 04 11 101 00:10:10.3	10.449N	62.706W	NEAR COAST OF VENEZUELA	40	6.0	5.0	PDE	EQ	A	00:27-00:46	20	20046/ 22
0095	83 04 11 101 14:32:54.9	40.310N	53.800E	TURKMEN SSR	33	4.0	0.0	PDE	EQ	A	14:41-14:52	12	20046/ 23
0096	83 04 11 101 15:34:55.6	44.30N	147.775E	KURIL ISLANDS	90	5.7	0.0	PDE	EQ	ABDE	15:36-16:19	44	20046/ 24
0097	83 04 11 101 17:03:45.9	35.480S	179.383W	EAST OF NORTH ISLAND	04	5.7	0.0	PDE	EQ	A	17:00-17:19	12	20046/ 25
0098	83 04 12 102 03:41:05.2	49.815N	78.227E	EASTERN KAZAKH SSR	0	4.9	0.0	PDE	NX	A	03:48-03:59	12	20046/ 26
0099	83 04 12 102 12:07:54.6	4.865S	70.183W	PERU-ECUADOR BORDER REGION	107	6.5	[illegible]	PDE	EQ	A	12:17-12:36	20	20046/ 27
0100	83 04 12 102 16:00:56.4	12.168S	167.000E	SANTA CRUZ ISLANDS	291	5.1		PDE	EQ	A	16:02-16:13	12	20046/ 28

WAKE HYDROPHONE INFORMATION PROCESSING SYSTEM (WHIPS) EVENT LISTING 13 AUG 83

KEY: INFORMATION SOURCES - PDE=NEIS PDECARD, MON=NEIS MONTHLY LIST, ICS=ICS LIST, HEL=HELICORDER, OTH=OTHER
EVENT TYPE - EQ=EARTHQUAKE, NX=NUCLEAR EXPLOSION, SX=SCIENTIFIC EXPLOSION, OT=OTHER, UN=UNKNOWN
PHASES - A=P, B=PU, C=S, D=SO, E=T, F=OTHER

EVNT NO	ORIGIN TIME YR MO DA JUL HR MN SECS	COORDINATES LAT	LON	LOCATION DESCRIPTION	DEP KM	MAGNI BDY	SRF	INF SRC	EV TP	SAVED PHASES	INTERVAL	MNS	STRIP TAPE/FILE
#981	83 #4 12 182 22:44:49.5	5.151S	153.637E	NEW IRELAND REGION	55	5.3	5.5	PDE	EQ	ABDE	22:45-23:26	42	20247/ #1
#982	83 #4 13 183 14:44:#9.5	10.559S	161.603E	SANTA CRUZ ISLANDS REGION	33	5.#	4.9	PDE	EQ	A	14:45-14:56	12	20247/ #2
#983	83 #4 13 183 15:26:37.#	14.577N	146.9#4E	MARIANA ISLANDS	58	4.7	#.#	PDE	EQ	ABD	15:26-15:39	14	20247/ #3
#984	83 #4 13 183 19:41:24.5	46.941N	145.638E	NORTHWEST OF KURIL ISLANDS	354	4.5	#.#	PDE	EQ	ABDE	19:42-20:29	46	20247/ #4
#985	83 #4 13 183 21:#7:22.#	22.816N	94.537E	BURMA	13#	4.7	#.#	PDE	EQ	A	21:13-21:24	12	20247/ #5
#986	83 #4 14 184 #2:46:26.7	14.811N	146.967E	MARIANA ISLANDS	33	4.5	#.#	PDE	EQ	ABD	#2:46-#2:58	13	20247/ #6
#987	83 #4 14 184 #4:#3:48.3	10.431S	165.225E	SANTA CRUZ ISLANDS	33	5.#	4.4	PDE	EQ	A	#4:#5-#4:16	12	20247/ #7
#988	83 #4 14 184 #6:#9:38.4	36.368N	71.112E	AFGHANISTAN-USSR BORDER REGION	224	4.6	#.#	PDE	EQ	A	#6:17-#6:28	12	20247/ #8
#98#	83 #4 14 184 #9:12:#1.2	35.953N	69.969E	HINDU KUSH REGION	7#	4.7	#.#	PDE	EQ	A	#9:19-#9:31	13	20247/ #9
#9#8	83 #4 14 184 1#:24:12.2	22.126S	175.#2#W	TONGA ISLANDS REGION	33	5.2	5.1	PDE	EQ	A	1#:27-1#:39	13	20247/ 1#
#911	## ## ## ### ##:##:##.#	#.###N	#.##E	PROBABLE MARIANAS PO, SO, T	#	#.#	#.#	HEL	EQ	BDE	11:18-11:47	3#	20247/ 11
#912	83 #4 14 184 19:#5:## 1	37.#73N	116.#46W	SOUTHERN NEVADA	#	5.7	#.#	PDE	NX	A	19:11-19:22	12	20247/ 12
#913	83 #4 14 184 23:#1:12.2	#.275N	126.113E	MOLUCCA PASSAGE	64	5.#	#.#	PDE	EQ	A	23:#4-23:15	12	20247/ 13
#914	83 #4 15 185 ##:#9:36.1	19.#96S	175.611W	TONGA ISLANDS	249	5.7	#.#	PDE	EQ	A	##:12-##:23	12	20247/ 14
#915	83 #4 15 185 #4:44:##.7	6.5#2S	154.948E	SOLOMON ISLANDS	33	5.9	5.5	PDE	EQ	ABDE	#4:45-#5:26	42	20247/ 15
#916	83 #4 15 185 #9:23:59.1	14.954N	99.142E	SOUTHEAST ASIA	1#	5.3	#.#	PDE	EQ	A	#9:3#-#9:4:	12	20247/ 16
#917	83 #4 15 185 14:21:49.#	13.13#N	121.971E	MINDORO PHILIPPINE ISLANDS	33	5.3	5.1	PDE	EQ	A	14:25-14:36	12	20247/ 17
#918	83 #4 15 185 14:51:59.8	53.355N	163.#81E	NEAR EAST COAST OF KAMCHATKA	71	5.8	#.#	PDE	EQ	ABDE	14:54-15:42	49	20247/ 18
#919	83 #4 16 186 12:57:45.6	1#.186S	11#.892E	SOUTH OF JAVA	23	5.8	5.3	PDE	EQ	A	13:#3-13:14	12	20247/ 19
#92#	83 #4 16 186 17:23:29.5	4.795N	127.684E	TALAUD ISLANDS	83	5.1	#.#	PDE	EQ	A	17:26-17:37	12	20247/ 2#
#921	83 #4 16 186 17:28:31.2	41.475N	142.#4#E	HOKKAIDO JAPAN REGION	62	5.#	#.#	PDE	EQ	ABDE	17:29-18:14	46	20247/ 2#
#922	83 #4 17 187 13:##:14.1	1.779N	99.52#E	NORTHERN SUMATERA	178	4.5	#.#	PDE	EQ	A	13:#6-13:17	12	20247/ 21
#923	83 #4 17 187 14:#6:56.3	22.747S	169.183E	VANUATU ISLANDS	22	5.4	6.2	PDE	EQ	ABDE	14:#9-15:#4	56	20246/ #:
#924	83 #4 17 187 19:14:47.2	36.612N	71.#14E	AFGHANISTAN-USSR BORDER REGION	27#	4.5	#.#	PDE	EQ	A	19:22-19:33	12	20248/ #2
#925	83 #4 17 187 2#:#5:44.9	44.84#N	147.615E	KURIL ISLANDS	115	4.9	#.#	PDE	EQ	ABDE	2#:#7-2#:51	45	20248/ #3
#926	83 #4 17 187 23:16:34.5	22.##:N	94.327E	BURMA	1##	5.1	#.#	PDE	EQ	A	23:22-23:33	12	20246/ #4
#927	83 #4 18 188 #5:#1:19.4	19.894S	175.889W	TONGA ISLANDS	241	5.1	#.#	PDE	EQ	A	#5:#4-#5:15	12	20246/ #5
#928	83 #4 18 188 1#:58:47.9	27.721N	62.#58E	SOUTHERN IRAN	37	6.5	6.2	PDE	EQ	F	11:## 12:59	12#	20246/ #6
#925	83 #4 18 188 13:52:13.2	8.276S	119.638E	FLORES ISLAND REGION	191	6.#	#.#	PDE	EQ	A	13:56-14:#7	12	20248/ #7
#93#	83 #4 18 188 16:29:37.5	52.111N	159.137E	OFF EAST COAST OF KAMCHATKA	7#	4.7	#.#	PDE	EQ	ABD	16:31-16:47	17	20246/ #8
#931	83 #4 18 188 17:15:#4.#	13.639S	167.2#9E	VANUATU ISLANDS	213	5.1	#.#	PDE	EQ	A	17:16-17:27	12	20248/ #9
#932	83 #4 18 188 18:28:1#.#	43.524N	147.688E	KURIL ISLANDS	3#	4.9	#.#	PDE	EQ	ABD	18:29-18:44	16	20246/ 1#
#933	83 #4 19 189 #9:11:#1.1	4.389S	144.#69E	NEAR N COAST PAPUA NEW GUINEA	137	5.2	#.#	PDE	EQ	ABD	#9:12-#9:28	17	20246/ 11
#934	83 #4 19 189 14:17:59.#	21.49#N	145.777E	MARIANA ISLANDS REGION	33	4.3	#.#	PDE	EQ	ABD	14:17-14:3#	14	20246/ 12
#935	83 #4 19 189 14:26:29.1	14.823S	167.478E	VANUATU ISLANDS	149	5.#	#.#	PDE	EQ	ABDE	14:28-15:16	49	20248/ 12
#93#	83 #4 19 189 15:#5:41.2	29.359N	139.727E	SOUTH OF HONSHU JAPAN	464	4.5	#.#	PDE	EQ	ABDE	15:#6-15:47	42	20248/ 12
#937	83 #4 19 189 15:15:1#.7	7.253S	129.2#5E	BANDA SEA	186	5.#	#.#	PDE	EQ	A	15:18-15:29	12	20246/ 12
#938	83 #4 19 189 16:25:27.2	46.449N	153.131E	KURIL ISLANDS	33	4.5	#.#	PDE	EQ	ABD	16:26-16:42	17	20246/ 13
#939	83 #4 19 189 18:52:58.4	21.864S	138.941W	TUAMOTU ARCHIPELAGO REGION	#	5.6	#.#	PDE	NX	A	18:59-19:1#	12	20249/ 14
#94#	83 #4 19 189 19:12:48.7	63.372N	149.95#W	CENTRAL ALASKA	113	5.1	#.#	PDE	EQ	ABD	19:17-19:38	22	20249/ #:
#941	83 #4 2# 11# 11:#1:39.#	5.521S	129.449E	BANDA SEA	282	5.2	#.#	PDE	EQ	A	11:#4-11:15	12	20249/ #2
#942	83 #4 2# 11# 16:34:32.2	12.423N	143.7#1E	SOUTH OF MARIANA ISLANDS	5#	4.9	#.#	PDE	EQ	ABD	16:34-16:48	15	20249/ #3
#943	83 #4 21 111 13:39:24.5	15.539N	146.151E	MARIANA ISLANDS	95	5.#	#.#	PDE	EQ	ABDE	13:39-14:11	33	20249/ #5
#944	83 #4 21 111 1#:25:#9.#	#.#23N	125.965E	MOLUCCA PASSAGE	63	5.2	#.#	PDE	EQ	A	1#:28-1#:39	12	20249/ #4
#945	## ## ## ### ##:##:##.#	#.###N	#.###E	PROBABLE MARIANAS PO, SO, T	#	#.#	#.#	HEL	EQ	BDE	21:57-22:26	3#	20249/ #6
#946	83 #4 22 112 ##:37:4#.5	14.952N	99.#72E	SOUTHEAST ASIA	33	5.#	5.#	PDE	EQ	A	##:43-##:54	12	20245/ #7
#947	83 #4 22 112 #3:21:4#.6	14.962N	99.#61E	SOUTHEAST ASIA	33	5.2	4.4	PDE	EQ	A	#3:27-#3:38	12	20249/ #8
#948	83 #4 22 112 #3:56:26.6	39.321N	64.271E	UZBEK SSR	46	4.#	#.#	PDE	EQ	A	#4:#4-#4:15	12	20249/ #9
#949	83 #4 22 112 #7:51:49.#	6.152N	126.984E	MINDANAO PHILIPPINE ISLANDS	59	5.7	#.#	PDE	EQ	A	#7:54-#8:#5	12	20249 1#
#95#	83 #4 22 112 1#:32:41.7	39.258N	68.313E	TAJIK SSR	33	4.#	#.#	PDE	EQ	A	1#:4#-1#:51	12	20249 11

#951	83 #4 22 112 13:53:##.#	37.112N	116.#22W	SOUTHERN NEVADA	#	4.#	#.#	PDE	NX	A	13:59-14:1#	12	20249/ 12
#952	## ## ## ### ##:##:##.#	#.###N	#.#3#E	PROBABLE BONIN ISL, PO,SO,T	#	#.#	#.#	HEL	EQ	BDE	14:32-15:#1	3#	20249/ 13
#953	83 #4 22 112 18:28:24.5	42.369N	87.942E	NORTHERN XINJIANG CHINA	24	5.1	4.1	PDE	EQ	A	18:34-18:46	13	20249/ 14
#954	83 #4 23 113 ##:3#:5#.3	6.391S	151.853E	NEW BRITAIN REGION	33	5.#	#.#	PDE	EQ	ABDE	##:32-#1:14	43	20249/ 15
#955	83 #4 23 113 #4:23:55.6	3#.272N	67.945E	PAKISTAN	33	4.7	4.2	PDE	EQ	A	#4:22-#4:43	12	20249/ 16
#956	83 #4 23 113 #9:28:13.#	11.353S	118.841E	SOUTH OF SUMBAWA ISLAND	21	5.4	#.#	PDE	EQ	A	#9:25-#9:36	12	20249/ 17
#957	83 #4 23 113 18:49:54.#	29.529N	68.29#E	PAKISTAN	33	4.#	4.3	PDE	EQ	A	18:58-19:#9	12	20249/ 18
#958	83 #4 23 113 23:33:58.#	53.##9S	117.838W	EASTER ISLAND CORDILLERA	1#	5.#	5.5	PDE	EQ	ABD	23:42-##:16	35	#/ ##
#955	83 #4 24 114 #3:26:39.#	16.354S	177.694W	FIJI ISLANDS REGION	33	4.9	5.6	PDE	EQ	A	#3:29-#3:4#	12	#/ #2
#96#	83 #4 24 114 #3:29:18.2	23.918S	176.#29W	SOUTH OF FIJI ISLANDS	33	5.9	5.5	PDE	EQ	A	#3:32-#3:44	13	#/ #2
#961	83 #4 24 114 #4:48:13.#	35.839N	139.776E	NEAR S COAST OF HONSHU JAPAN	98	4.7	#.#	PDE	EQ	ABD	#4:49-#5:#4	16	#/ #2
#962	83 #4 24 114 #9:##:#5.6	13.239N	146.3#9E	SOUTH OF MARIANA ISLANDS	33	5.1	#.#	PDE	EQ	ABDE	#9:#8-#9:4#	33	20249/ 19
#963	83 #4 24 114 #9:##:49.#	8.912S	157.649E	SOLOMON ISLANDS	18	5.8	6.2	PDE	EQ	ABDE	#9:1#-#9:53	44	20249/ 19
#964	83 #4 24 114 15:56:33.1	19.#85S	173.219W	TONGA ISLANDS	51	5.1	#.#	PDE	EQ	A	15:59-16:11	13	20249/ 2#
#965	83 #4 25 115 #1:59:46.9	53.943N	159.368E	NEAR EAST COAST OF KAMCHATKA	111	4.4	#.#	PDE	EQ	ABDE	#2:#1-#2:51	51	20249/ 21
#966	83 #4 25 115 11:13:11.5	8.786S	157.396E	SOLOMON ISLANDS	33	5.#	#.#	PDE	EQ	ABDE	11:14-11:57	44	20250/ #1
#967	83 #4 25 115 13:55:58.#	46.391N	142.332E	SAKHALIN ISLAND	311	4.7	#.#	PDE	EQ	ABDE	13:57-14:45	49	20250/ #2
#968	83 #4 25 115 14:##:43.3	51.331N	156.928E	KAMCHATKA	97	5.2	#.#	PDE	EQ	ABDE	14:#2-14:49	48	20250/ #2
#969	83 #4 25 115 17:57:#1.#	5.456S	146.86#E	EAST PAPUA NEW GUINEA	241	5.1	#.#	PDE	EQ	ABDE	17:58-18:43	46	20250/ #3
#97#	83 #4 25 115 19:#3:47.#	12.777N	123.#42E	LUZON PHILIPPINE ISLANDS	23	5.#	4.5	PDE	EQ	A	19:#7-19:18	12	20250/ #4
#971	83 #4 25 115 23:24:2#.9	55.618N	160.675E	KAMCHATKA	168	4.7	#.#	PDE	EQ	ABDE	23:26-##:18	53	20250/ #5
#972	83 #4 26 116 11:15:37.6	15.891S	168.365E	VANUATU ISLANDS	33	5.6	5.5	PDE	EQ	ABD	11:17-11:34	18	20250/ #6
#973	83 #4 26 116 12:38:1#.7	6.493S	105.374E	SUNDA STRAIT	75	5.#	#.#	PDE	EQ	A	12:44-12:55	12	20250/ #7
#974	83 #4 26 116 15:26:4#.9	24.632N	122.545E	TAIWAN REGION	123	5.6	#.#	PDE	EQ	A	15:29-15:4#	12	20250/ #8
#975	83 #4 26 116 16:#2:17.5	40.6#6N	153.465E	KURIL ISLANDS	155	4.9	#.#	PDE	EQ	ABDE	16:#3-16:49	47	20250/ #9
#976	83 #4 26 116 18:15:37.#	24.22#N	121.741E	TAIWAN	67	4.9	#.#	PDE	EQ	A	18:18-18:3#	17	20250/ 1#
#977	83 #4 27 117 ##:46:51.6	6.318S	151.318E	NEW BRITAIN REGION	4#	4.9	#.#	PDE	EQ	ABD	##:48-#::#3	16	20250/ 11
#978	83 #4 27 117 16:28:19.3	36.22#N	7#.76#E	HINDU KUSH REGION	161	4.7	#.#	PDE	EQ	A	16:35-16:47	13	20250/ 12
#979	83 #4 27 117 17:2#:35.1	2#.969S	174.532W	TONGA ISLANDS	21	5.5	5.6	PDE	EQ	A	17:24-17:35	12	20250/ 13
#98#	83 #4 28 118 #8:58:#6.#	51.119N	156.331E	KAMCHATKA	12#	4.9	#.#	PDE	EQ	ABDE	#8:59-#9:46	46	20250/ 14
#981	83 #4 29 119 #6:11:#7.#	5.97#S	147.71#E	E. PAPUA NEW GUINEA REGION	1##	4.9	#.#	PDE	EQ	ABD	#6:12-#6:28	17	20250/ 15
#982	83 #4 29 119 13:39:11.1	35.334N	139.#1#E	NEAR S COAST OF HONSHU JAPAN	33	4.#	#.#	PDE	EQ	ABD	13:4#-13:55	16	20250/ 16
#983	83 #4 3# 12# #2:51:44.#	21.296S	174.333W	TONGA ISLANDS	33	5.#	5.5	PDE	EQ	A	#2:55-#3:#6	12	20251/ #1
#984	83 #4 3# 12# 14:#3:49.7	41.523N	143.784E	HOKKAIDO JAPAN REGION	33	6.5	6.3	PDE	EQ	ABDE	14:#5-14:4#	44	20251/ #2
#985	83 #4 3# 12# 15:5#:24.6	41.629N	143.5#7E	HOKKAIDO JAPAN REGION	33	4.#	#.#	PDE	EQ	ABD	15:51-16:#7	17	20251/ #3
#986	83 #4 3# 12# 15:57:#9.1	41.613N	143.672E	HOKKAIDO JAPAN REGION	33	4.#	5.1	PDE	EQ	ABD	15:58-16:13	16	20251/ #4
#987	83 #4 3# 12# 17:28:46.6	25.648N	96.843E	BURMA	33	4.5	#.#	PDE	EQ	A	17:34-17:45	12	20251/ #4
#988	83 #4 3# 12# 19:#4:3#.2	49.5#3N	155.742E	KURIL ISLANDS	46	5.3	5.1	PDE	EQ	ABDE	19:#6-19:51	46	20251/ #5
#989	83 #4 3# 12# 19:24:27.6	5.529S	129.316E	BANDA SEA	25#	4.#	#.#	PDE	EQ	A	19:27-19:38	12	20251/ #5
#99#	83 #5 #1 121 ##:14:24.3	18.#15S	178.296W	FIJI ISLANDS REGION	595	4.#	#.#	PDE	EQ	A	##:16-##:27	12	20251/ #6
#991	83 #5 #1 121 #8:44:1#.3	38.436N	144.476E	OFF E COAST OF HONSHU JAPAN	43	4.7	#.#	PDE	EQ	ABD	#8:45-#8:59	15	20251/ #7
#992	83 #5 #1 121 15:25:34.9	2.981N	124.691E	CELEBES SEA	296	4.5	#.#	PDE	EQ	A	15:28-15:39	12	20251/ #8
#993	83 #5 #1 121 18:1#:41.5	46.356N	153.497E	KURIL ISLANDS	33	6.1	6.#	PDE	EQ	ABDE	18:11-18:55	45	20251/ #9
#994	83 #5 #1 121 2#:11:58.6	46.363N	153.437E	KURIL ISLANDS	33	5.6	5.4	PDE	EQ	ABDE	2#:13-2#:56	44	20251 1#
#995	83 #5 #2 122 #1:22:17.7	5.874S	123.#41E	BANDA SEA	3#6	5.#	#.#	PDE	EQ	A	#1:25-#1:36	12	20251/ 11
#996	83 #5 #2 122 #6:59:58.6	8.65#S	1#7.36#E	SOUTH OF JAVA	33	5.3	5.2	PDE	EQ	A	#7:#6-#7:17	12	20251/ 12
#997	## #3 ## ### ##:##:##.#	#.###N	#.###E	UNKNOWN P	#	#.#	#.#	HEL	EQ	A	1#:##-1#:14	15	20251/ 13
#998	83 #5 #2 122 15:21:51.2	46.279N	153.615E	KURIL ISLANDS	33	5.1	5.1	PDE	EQ	ABDE	15:23-16:#6	44	20251/ 14
#999	83 #5 #2 122 21:22:44.#	46.265N	153.592E	KURIL ISLANDS	33	5.3	5.3	PDE	EQ	ABDE	21:24-22:#6	43	20251/ 15
1##9	83 #5 #2 122 23:42:37.9	36.242N	12#.381W	CENTRAL CALIFORNIA	12	6.2	6.5	PDE	EQ	ABDE	23:48-#1:1#	83	20252/ #1

WAKE HYDROPHONE INFORMATION PROCESSING SYSTEM (WHIPS) EVENT LISTING 13 AUG 83

KEY: INFORMATION SOURCES - PDE=NEIS PDECARD, MON=NEIS MONTHLY LIST, ICS=ICS LIST, HEL=HELICORDER, OTH=OTHER
EVENT TYPE - EQ=EARTHQUAKE, NX=NUCLEAR EXPLOSION, SX=SCIENTIFIC EXPLOSION, OT=OTHER, UN=UNKNOWN
PHASES - A=P, B=PO, C=S, D=SO, E=T, F=OTHER

EVNT NO	ORIGIN TIME YR MO DA JUL HR MN SECS	COORDINATES LAT LON	LOCATION DESCRIPTION	DEP KM	MAGNI BDY	MAGNI SRF	INF SRC	EV TP	SAVED PHASES	INTERVAL	MNS	STRIP TAPE/FILE
1801	83 05 03 123 02:38:15.4	46.489N 153.492E	KURIL ISLANDS	33	5.1	0.0	PDE	EQ	ABDE	02:39-03:22	44	20052/ 02
1802	83 05 03 123 15:39:39.3	20.212S 176.345W	FIJI ISLANDS REGION	593	5.5	0.0	PDE	EQ	A	15:41-15:53	13	20052/ 03
1803	83 05 03 123 18:37:13.4	46.297N 152.535E	KURIL ISLANDS	33	5.2	4.7	PDE	EQ	ABDE	18:38-19:21	44	20052/ 04
1804	83 05 03 123 21:02:15.2	3.886N 125.503E	TALAUD ISLANDS	64	5.8	0.0	PDE	EQ	A	21:05-21:16	12	20052/ 05
1805	83 05 04 124 07:58:25.4	9.443S 149.678E	EAST PAPUA NEW GUINEA REGION	15	5.8	4.9	PDE	EQ	ABDE	08:00-08:47	48	20052/ 06
1806	83 05 04 124 14:29:38.3	42.653N 142.979E	HOKKAIDO JAPAN REGION	107	4.3	0.0	PDE	EQ	ABDE	14:31-15:16	41	20052/ 07
1807	83 05 05 125 04:43:59.4	33.829S 179.383E	SOUTH OF KERMADEC ISLANDS	97	6.0	0.0	PDE	EQ	A	04:48-04:59	12	20052/ 08
1808	83 05 05 125 06:19:45.2	38.762N 72.354E	TAJIK SSR	33	4.9	0.0	PDE	EQ	A	06:27-06:38	12	20052/ 09
1809	83 05 05 125 07:14:19.9	3.187S 135.165E	WEST IRIAN REGION	33	5.4	0.0	PDE	EQ	A	07:17-07:28	12	20053/ 01
1810	83 05 05 125 15:20:00.0	37.812N 116.088W	SOUTHERN NEVADA	0	4.5	0.0	PDE	NX	A	15:26-15:37	12	20053/ 02
1811	83 05 06 126 04:16:15.2	43.187N 145.934E	KURIL ISLANDS	34	5.2	5.8	PDE	EQ	ABDE	04:17-05:00	44	20053/ 03
1812	83 05 06 126 11:59:41.4	21.324S 174.152W	TONGA ISLANDS	33	5.2	4.7	PDE	EQ	A	12:03-12:14	12	20053/ 04
1813	83 05 06 126 18:24:18.5	15.439N 121.691E	LUZON PHILIPPINE ISLANDS	33	5.6	5.6	PDE	EQ	A	18:27-18:38	12	20053/ 05
1814	83 05 07 127 06:11:24.1	6.848S 147.410E	EAST PAPUA NEW GUINEA REGION	119	5.2	0.0	PDE	EQ	ABDE	06:13-06:57	45	20053/ 06
1815	83 05 07 127 08:20:39.8	9.782S 159.584E	SOLOMON ISLANDS	33	5.8	0.0	PDE	EQ	ABDE	08:22-09:05	44	20053/ 07
1816	83 05 07 127 22:40:16.6	33.480N 144.884E	SOUTH OF HONSHU JAPAN	181	4.5	0.0	PDE	EQ	ABDE	22:41-23:22	42	20053/ 08
1817	83 05 07 127 23:58:01.9	24.654N 121.959E	TAIWAN	22	4.8	0.0	PDE	EQ	A	00:01-00:12	12	20053/ 09
1818	83 05 08 128 00:26:15.0	36.814N 70.980E	HINDU KUSH REGION	46	4.9	0.0	PDE	EQ	A	00:34-00:45	12	20053/ 10
1819	83 05 08 128 15:05:08.6	19.997N 109.340W	REVILLA GIGEDO ISLANDS REGION	10	5.3	5.0	PDE	EQ	A	15:12-15:23	12	20053/ 11
1820	83 05 08 128 21:30:48.5	43.81UN 146.898E	KURIL ISLANDS	33	5.2	0.0	PDE	EQ	ABDE	21:32-22:14	43	20053/ 12
1821	83 05 09 129 15:53:02.7	8.280N 82.925W	PANAMA-COSTA RICA BORDER REGN	36	5.5	6.1	PDE	EQ	AE	16:02-16:11	130	20053/ 13
1822	83 05 09 129 20:09:15.1	19.963N 109.453W	REVILLA GIGEDO ISLANDS REGION	10	5.5	6.2	PDE	EQ	AE	20:16-21:52	98	20054/ 01
1823	83 05 10 130 00:15:06.2	24.422N 121.586E	TAIWAN	33	5.7	5.4	PDE	EQ	A	00:18-00:29	12	20054/ 02
1824	83 05 10 130 01:10:59.2	24.545N 122.029E	TAIWAN REGION	33	5.0	0.0	PDE	EQ	A	01:22-01:33	12	20054/ 03
1825	83 05 10 130 11:02:34.7	5.358S 150.915E	NEW BRITAIN REGION	104	6.0	0.0	PDE	EQ	ABDE	11:03-11:46	44	20054/ 04
1826	83 05 10 130 18:27:30.6	4.790S 152.508E	NEW BRITAIN REGION	60	5.9	0.0	PDE	EQ	ABDE	18:28-19:09	42	20054/ 05
1827	83 05 10 130 18:56:04.8	14.569N 122.352E	LUZON PHILIPPINE ISLANDS	35	5.1	0.0	PDE	EQ	A	18:59-19:10	12	20054/ 06
1828	83 05 10 130 19:05:19.2	36.503N 70.151E	HINDU KUSH REGION	218	5.0	0.0	PDE	EQ	A	19:12-19:24	13	20054/ 07
1829	83 05 11 131 00:17:13.3	2.382N 128.346E	HALMAHERA	140	5.8	0.0	PDE	EQ	A	00:20-00:31	12	20054/ 08
1830	00 00 00 000 00:00:00.0	0.000N 0.000E	UNKNOWN PHASE	0	0.0	0.0	HEL	UN	F	01:04-01:14	11	20054/ 09
1831	83 05 11 131 03:26:50.0	37.211N 141.817E	NEAR E COAST OF HONSHU JAPAN	44	4.8	0.0	PDE	EQ	ABD	03:27-03:42	16	20054/ 10
1832	83 05 11 131 07:41:44.5	11.949N 143.264E	SOUTH OF MARIANA ISLANDS	35	5.3	4.4	PDE	EQ	ABDE	07:42-08:16	37	20054/ 11
1833	83 05 11 131 10:05:06.4	14.726S 167.051E	VANUATU ISLANDS	165	4.8	0.0	PDE	EQ	ABD	10:06-10:23	18	20054/ 12
1834	83 05 11 131 20:20:27.1	45.651N 122.820W	WASHINGTON-OREGON BORDER REGN	0	0.0	0.0	PDE	EQ	A	20:26-20:37	12	20054/ 13
1835	83 05 11 131 21:40:15.2	21.467S 173.461W	TONGA ISLANDS	33	5.9	5.3	PDE	EQ	A	21:51-22:03	13	20054/ 14
1836	83 05 12 132 14:52:02.0	7.870S 103.353E	SOUTHWEST OF SUMATERA	33	5.0	4.7	PDE	EQ	A	14:58-15:09	12	20054/ 15
1837	83 05 12 132 21:52:56.4	51.181N 179.150W	ANDREANOF ISLANDS	50	4.9	0.0	PDE	EQ	ABD	21:54-22:11	18	20054/ 16
1838	83 05 13 133 10:09:37.0	3.023N 126.090E	NORTH OF HALMAHERA	142	5.5	0.0	PDE	EQ	A	10:12-10:23	12	20054/ 17
1839	83 05 13 133 22:54:14.9	6.626S 154.437E	SOLOMON ISLANDS	49	5.0	3.7	PDE	EQ	ABDE	22:55-23:37	43	20054/ 18
1840	83 05 14 134 13:29:17.9	40.393N 139.190E	NEAR W COAST OF HONSHU JAPAN	34	5.1	0.0	PDE	EQ	ABDE	13:30-14:16	47	20055/ 01
1841	83 05 15 135 00:24:00.5	18.888S 175.719W	TONGA ISLANDS	36	5.0	6.5	PDE	EQ	AE	00:27-01:23	57	20055/ 02
1842	83 05 15 135 22:02:14.2	52.002N 179.666E	RAT ISL. ALEUTIAN ISL.	162	4.5	0.0	PDE	EQ	ABD	22:04-22:20	17	20055/ 03
1843	83 05 16 136 12:07:54.7	39.415N 64.324E	UZBEK SSR	33	4.0	0.0	PDE	EQ	A	12:16-12:27	12	20055/ 04
1844	83 05 16 136 16:30:02.8	43.756N 87.293E	NORTHERN XINJIANG CHINA	33	5.0	0.0	PDE	EQ	A	16:36-16:47	12	20055/ 05
1845	83 05 16 136 21:39:47.1	38.489N 144.530E	OFF E COAST OF HONSHU JAPAN	33	5.1	0.0	PDE	EQ	ABDE	21:40-22:21	42	20055/ 06
1846	83 05 17 137 11:50:24.4	6.636S 154.135E	SOLOMON ISLANDS	59	5.2	0.0	PDE	EQ	ABDE	11:51-12:33	43	20055/ 07
1847	83 05 17 137 20:33:25.3	14.991S 169.040E	VANUATU ISLANDS	51	5.4	4.9	PDE	EQ	ABDE	20:35-21:23	49	20055/-12
1848	83 05 17 137 21:02:13.4	30.683S 177.768W	KERMADEC ISLANDS	33	5.0	0.0	PDE	EQ	A	21:06-21:18	13	20055/-12
1849	83 05 17 137 23:26:33.2	5.432S 154.939E	NEW BRITAIN REGION	118	5.6	0.0	PDE	EQ	ABDE	23:27-00:10	44	20055/ 16
1850	83 05 18 138 07:23:23.6	3.366N 126.799E	TALAUD ISLANDS	33	4.7	0.0	PDE	EQ	A	07:26-07:37	12	20055/ 14
1851	83 05 18 138 08:21:31.4	0.592N 121.739E	MINAHASSA PENINSULA	131	5.3	0.0	PDE	EQ	A	08:25-08:36	12	20055/ 15
1852	83 05 18 138 18:45:24.0	8.359S 121.272E	FLORES ISLAND REGION	209	4.9	0.0	PDE	EQ	A	18:49-19:00	12	20055/ 17
1853	83 05 19 139 09:54:37.9	28.172N 133.122E	RYUKYU ISLANDS	33	4.8	0.0	PDE	EQ	ABD	09:56-10:13	18	20055/ 18
1854	83 05 19 139 17:48:37.0	51.432N 174.078W	ANDREANOF ISL. ALEUTIAN ISL.	39	5.0	0.0	PDE	EQ	ABDE	17:50-18:40	51	20055/ 19
1855	83 05 19 139 21:20:57.0	53.902N 161.299E	OFF EAST COAST OF KAMCHATKA	33	4.4	0.0	PDE	EQ	ABD	21:23-21:39	17	20055/ 20
1856	83 05 20 140 04:45:55.1	4.776S 153.524E	NEW IRELAND REGION	181	4.9	0.0	PDE	EQ	ABD	04:46-05:01	16	20055/ 21
1857	83 05 20 140 06:09:18.0	53.116N 171.641W	ANDREANOF ISL. ALEUTIAN ISL.	233	4.8	0.0	PDE	EQ	ABD	06:11-06:28	18	20055/ 22
1858	83 05 20 140 15:42:06.6	29.291N 132.488E	SOUTHEAST OF SHIKOKU JAPAN	33	4.9	0.0	PDE	EQ	ABD	15:44-15:59	16	20055/ 23
1859	83 05 21 141 09:55:44.7	25.315S 179.319E	SOUTH OF FIJI ISLANDS	550	4.9	0.0	PDE	EQ	A	09:58-10:10	13	20055/ 24
1860	83 05 21 141 10:46:37.0	35.286N 140.246E	NEAR E COAST OF HONSHU JAPAN	31	5.1	4.5	PDE	EQ	ABDE	10:47-11:25	43	20056/ 01
1861	83 05 21 141 10:06:25.2	6.313N 124.268E	MINDANAO PHILIPPINE ISLANDS	71	5.0	0.0	PDE	EQ	A	10:09-10:20	12	20056/ 02
1862	83 05 21 141 10:32:44.5	35.169N 140.377E	NEAR E COAST OF HONSHU JAPAN	33	4.5	0.0	PDE	EQ	ABD	10:33-10:48	16	20056/ 03
1863	83 05 22 142 11:44:19.4	9.378S 123.765E	TIMOR	93	5.0	0.0	PDE	EQ	A	11:48-11:59	12	20056/ 04
1864	83 05 22 142 12:15:18.4	29.897N 141.582E	SOUTH OF HONSHU JAPAN	33	4.8	0.0	PDE	EQ	ABD	12:16-12:30	15	20056/ 05
1865	83 05 22 142 17:02:46.0	13.577S 167.514E	VANUATU ISLANDS	33	5.2	0.0	PDE	EQ	A	17:04-17:15	12	20056/ 06
1866	83 05 22 142 17:13:18.9	45.689N 151.695E	KURIL ISLANDS	33	4.9	0.0	PDE	EQ	ABD	17:14-17:29	16	20056/ 06
1867	83 05 22 142 19:56:12.6	45.133N 146.292E	KURIL ISLANDS	183	4.4	0.0	PDE	EQ	ABD	19:57-20:13	17	20056/ 07
1868	83 05 23 143 06:54:37.9	13.821S 171.294E	VANJATU ISLANDS REGION	38	5.8	5.6	PDE	EQ	A	06:56-07:07	12	20056/ 08
1869	83 05 23 143 17:55:52.9	37.984N 141.945E	NEAR E COAST OF HONSHU JAPAN	33	5.3	5.0	PDE	EQ	ABDE	17:57-18:39	43	20056/ 09
1870	00 00 00 000 00:00:00.0	0.000N 0.000E	PROBABLE HOKKAIDO PO, SO, T	0	0.0	0.0	HEL	EQ	ABDE	05:03-05:47	45	20056/ 10
1871	83 05 24 144 05:09:07.7	24.431N 143.295E	VOLCANO ISLANDS REGION	33	5.1	4.7	PDE	EQ	ABDE	05:09-05:44	36	20056/ 10
1872	83 05 24 144 07:38:36.0	26.910N 142.038E	BONIN ISLANDS REGION	460	4.5	0.0	PDE	EQ	ABD	07:38-07:53	16	20056/ 11
1873	83 05 24 144 10:03:25.0	31.356S 178.541W	KERMADEC ISLANDS REGION	33	5.3	0.0	PDE	EQ	A	10:07-10:19	13	20056/ 12
1874	83 05 24 144 13:39:49.5	55.605N 162.484E	OFF EAST COAST OF KAMCHATKA	49	4.8	0.0	PDE	EQ	ABD	13:42-13:59	18	20056/ 13
1875	83 05 25 145 17:30:58.2	21.912S 130.936W	TUAMOTU ARCHIPELAGO REGION	0	5.9	0.0	PDE	NX	A	17:37-17:48	12	20056/-14
1876	83 05 26 146 03:00:00.6	48.378N 139.153E	NEAR W COAST OF HONSHU JAPAN	33	6.0	7.7	PDE	EQ	ABDE	03:01-03:47	47	20056/-15
1877	83 05 26 146 06:46:03.3	40.930N 139.851E	NEAR W COAST OF HONSHU JAPAN	33	4.6	0.0	PDE	EQ	ABD	06:47-07:03	17	20056/ 16
1878	83 05 26 146 09:35:31.4	41.158N 139.963E	HOKKAIDO JAPAN REGION	19	5.2	0.0	PDE	EQ	ABDE	09:37-10:23	47	20056/ 17
1879	83 05 26 146 10:12:27.3	41.231N 139.897E	HOKKAIDO JAPAN REGION	33	5.3	0.0	PDE	EQ	ABDE	10:14-11:00	47	20056/ 17
1880	83 05 26 146 12:07:14.6	22.417N 101.203E	BURMA-CHINA BORDER REGION	33	4.7	0.0	PDE	EQ	A	12:12-12:24	13	20056/ 18
1881	83 05 26 146 12:18:14.3	39.288N 65.674E	SOUTHEASTERN UZBEK SSR	33	4.8	0.0	PDE	EQ	A	12:26-12:37	12	20056/ 19
1882	83 05 26 146 13:13:23.2	39.574N 140.614E	HONSHU JAPAN	33	5.8	0.0	PDE	EQ	ABDE	13:14-13:59	46	20056/ 20
1883	83 05 26 146 14:12:23.0	40.284N 138.990E	EASTERN SEA OF JAPAN	28	5.6	4.3	PDE	EQ	ABDE	14:14-14:59	46	20057/ 01
1884	83 05 26 146 15:00:00.0	37.103N 116.086W	SOUTHERN NEVADA	0	4.3	0.0	PDE	NX	A	15:06-15:17	12	20057/ 02
1885	83 05 26 146 22:40:24.7	41.812N 139.481E	HOKKAIDO JAPAN REGION	24	5.1	0.0	PDE	EQ	ABDE	22:50-23:36	47	20057/ 03
1886	83 05 26 146 23:25:00.0	40.070N 138.987E	EASTERN SEA OF JAPAN	22	5.0	0.0	PDE	EQ	ABDE	23:26-00:12	47	20057/ 03
1887	83 05 27 147 04:16:52.3	40.769N 139.097E	NEAR W COAST OF HONSHU JJAPAN	20	5.1	0.0	PDE	EQ	ABDE	04:18-05:04	47	20057/ 04
1888	83 05 27 147 13:35:43.1	46.564N 135.876E	NEAR E COAST OF EASTERN USSR	381	4.6	0.0	PDE	EQ	ABDE	13:37-14:29	53	20057/ 05
1889	83 05 27 147 22:55:39.2	13.866N 120.080E	MINDORO PHILIPPINE ISLANDS	187	5.1	0.0	PDE	EQ	A	22:58-23:10	13	20057/ 06
1890	83 05 28 148 02:29:24.2	41.888N 139.139E	HOKKAIDO JAPAN REGION	20	5.4	4.9	PDE	EQ	ABDE	02:31-03:17	47	20057/ 07
1891	83 05 28 148 06:14:41.1	40.193N 139.968E	EASTERN SEA OF JAPAN	27	4.8	0.0	PDE	EQ	ABD	06:16-06:32	17	20057/ 08
1892	83 05 28 148 07:44:58.9	40.139N 139.398E	NEAR W COAST OF HONSHU JAPAN	33	4.9	0.0	PDE	EQ	ABD	07:46-08:02	17	20057/ 09
1893	83 05 28 148 09:13:35.1	40.931N 139.459E	NEAR W COAST OF HONSHU JAPAN	33	4.3	0.0	PDE	EQ	ABD	09:15-09:31	17	20057/ 10
1894	83 05 28 148 15:48:19.7	40.881N 139.163E	NEAR W COAST OF HONSHU JAPAN	33	4.8	0.0	PDE	EQ	ABD	15:50-16:05	16	20057/ 11
1895	83 05 28 148 16:03:37.1	40.381N 139.216E	NEAR W COAST OF HONSHU JAPAN	29	5.0	0.0	PDE	EQ	ABDE	16:05-16:50	46	20057/ 11
1896	83 05 28 148 16:18:43.0	40.000N 139.000E	NEAR W COAST OF HONSHU JAPAN	33	5.0	5.0	PDE	EQ	ABDE	16:12-16:58	47	20057/ 11
1897	83 05 28 148 17:49:36.7	1.906S 97.493E	SOUTHERN SUMATERA	26	5.3	4.8	PDE	EQ	A	17:56-18:07	12	20057/ 12
1898	83 05 28 148 19:32:42.1	15.52UN 121.975E	LUZON PHILIPPINE ISLANDS	33	5.0	0.0	PDE	EQ	A	18:36-18:47	12	20057/ 13
1899	00 00 00 000 00:00:00.0	0.000N 0.000E	POSSIBLE MARIANAS PO, SO, T	0	0.0	0.0	HEL	EQ	BDE	23:22-23:51	30	20058/ 01
1900	83 05 28 148 23:54:58.0	6.736S 154.216E	SOLOMON ISLANDS	33	4.6	0.0	PDE	EQ	ABD	23:56-00:11	16	20058/ 02

KEY: INFORMATION SOURCES - PDE=NEIS PDECARD, MON=NEIS MONTHLY LIST, ICS=ICS LIST, HEL=HELICORDER, OTH=OTHER
EVENT TYPE - EQ=EARTHQUAKE, NX=NUCLEAR EXPLOSION, SX=SCIENTIFIC EXPLOSION, OT=OTHER, UN=UNKNOWN
PHASES - A=P, B=PU, C=S, D=SO, E=T, F=OTHER

EVNT NO	ORIGIN TIME YR MO DA JUL HR MN SECS	COORDINATES LAT LON	LOCATION DESCRIPTION	DEP KM	MAGNI BDY	MAGNI SRF	INF SRC	EV TP	SAVED PHASES	SAVED INTERVAL	MNS	STRIP TAPE/FILE
1101	83 05 29 149 00:28:32.1	40.398N 137.809E	EASTERN SEA OF JAPAN	33	4.6	4.1	PDE	EQ	ABD	00:38-00:46	17	22058/ 03
1102	83 05 29 149 02:14:22.0	4.223N 122.622E	CELEBES SEA	611	5.5	0.0	PDE	EQ	A	02:17-02:28	12	22058/ 04
110d	83 05 29 149 04:45:39.6	49.255N 153.375E	KURIL ISLANDS	33	5.0	5.2	PDE	EQ	ABDE	04:47-05:32	46	22058/ 05
1104	83 05 29 149 05:26:51.0	36.066N 141.937E	NEAR E COAST OF HONSHU JAPAN	20	5.3	4.1	PDE	EQ	ABDE	05:27-05:09	43	22058/ 05
110b	83 05 29 149 06:55:32.9	40.442N 125.449W	OFF COAST OF NORTH CALIFORNIA	10	5.1	5.1	PDE	EQ	A	07:0[illegible]-07:12	12	22058/ 06
110c	83 05 29 149 07:15:29.6	40.40?N 137.966E	EASTERN SEA OF JAPAN	20	5.1	0.0	PDE	EQ	ABDE	07:17-08:03	47	22058/ 07
110f	83 05 29 149 20:53:57.7	42.710N 141.434E	HOKKAIDO JAPAN REGION	76	5.3	0.0	PDE	EQ	ABDE	20:55-21:40	46	22058/ 08
1103	83 05 29 149 22:01:49.4	40.67JN 139.361E	NEAR W COAST OF HONSHU JAPAN	33	5.6	4.7	PDE	EQ	ABDE	22:03-22:49	47	22058/ 09
1109	83 05 29 149 22:07 59.1	15.575S 174.977W	TONGA ISLANDS	382	5.5	0.0	PDE	EQ	A	22:10-22:21	12	22058/ 09
1110	83 05 30 150 02:25:28.5	41.069N 139.163E	HOKKAIDO JAPAN REGION	33	4.6	0.0	PDE	EQ	ABD	02:27-02:43	17	22059/ 10
1111	83 05 30 150 03:33:44.6	49.74?N 78.21?E	EASTERN KAZAKH SSR	0	5.4	0.0	PDE	NX	A	03:40-03:52	13	22059/ 11
1112	83 05 30 150 12:32:41.1	1.894N 125.549E	MOLUCCA PASSAGE	82	5.4	0.0	PDE	EQ	A	12:36-12:47	12	22059/ 12
1113	83 05 30 150 14:47:14.2	4.727S 103.232E	SOUTHERN SUMATERA	97	5.5	0.0	PDE	EQ	A	14:53-15:04	12	22059/ 13
1114	83 05 30 150 15:54:31.0	52.060N 177.698W	ANDREANOF ISL. ALEUTIAN ISL.	107	5.0	0.0	PDE	EQ	ABDE	15:56-16:45	50	22059/ 14
1115	83 05 31 151 00:17:33.8	40.595N 139.053E	NEAR W COAST OF HONSHU JAPAN	33	4.7	0.0	PDE	EQ	ABD	00:19-00:35	17	22059/ 15
1116	83 05 31 151 00:31:41.8	5.892S 146.572E	EAST OF PAPUA NEW GUINEA REGIO	33	4.7	0.0	PDE	EQ	ABD	00:33-00:49	17	22059/ 15
1117	83 05 31 151 06:18:09.2	4.768S 153.258E	NEW IRELAND REGION	119	4.5	0.0	PDE	EQ	ABD	06:19-06:33	15	22059/ 16
1118	83 05 31 151 21:05:44.1	34.602N 79.764E	KASHMIR-TIBET BORDER REGION	33	5.0	4.3	PDE	EQ	A	21:12-21:24	13	22059/ 21
1119	83 05 31 151 21:15:56.2	40.202N 139.948E	EASTERN SEA OF JAPAN	25	4.9	0.0	PDE	EQ	ABD	21:17-21:33	17	22059/ 21
1120	83 05 31 151 23:19:11.1	40.711N 139.473E	NEAR W COAST OF HONSHU JAPAN	18	5.3	0.0	PDE	EQ	ABDE	23:20-00:06	47	22059/ 22
1121	83 05 31 151 23:22:32.3	40.796N 139.428E	NEAR W COAST OF HONSHU JAPAN	25	5.3	0.0	PDE	EQ	ABDE	23:24-00:10	47	22059/ 22
1122	83 06 01 152 00:58:46.9	40.419N 139.171E	NEAR W COAST OF HONSHU JAPAN	33	4.9	0.0	PDE	EQ	ABD	01:00-01:16	17	22059/ 23
1123	83 06 01 152 01:37:02.7	13.760N 122.748E	MINDORO PHILIPPINE ISLANDS	260	5.5	0.0	PDE	EQ	A	01:40-01:51	12	22059/ 24
1124	83 06 01 152 02:00:00.1	16.996S 174.713W	TONGA ISLANDS	228	6.1	0.0	PDE	EQ	A	02:02-02:13	12	22059/ 25
1125	83 06 01 152 06:40:36.9	39.959N 138.897E	EASTERN SEA OF JAPAN	33	4.8	0.0	PDE	EQ	ABD	06:42-06:58	17	22059/ 06
1126	83 06 01 152 07:14:32.1	40.399N 139.133E	NEAR W COAST OF HONSHU JAPAN	33	4.7	0.0	PDE	EQ	ABD	07:16-07:33	17	22059/ 07
1127	83 06 01 152 07:30:33.9	51.722N 171.302W	FOX ISLANDS ALEUTIAN ISLANDS	32	4.7	0.0	PDE	EQ	ABD	07:33-07:49	17	22059/ 07
1128	83 06 01 152 10:58:42.8	15.922S 172.821W	SAMOA ISLANDS REGION	33	5.6	6.1	PDE	EQ	A	11:01-11:12	12	22059/ 09
1129	83 06 01 152 11:17:40.2	43.919N 80.576E	NORTHERN XINJIANG CHINA	32	5.1	0.0	PDE	EQ	A	11:24-11:35	12	22059/ 10
1130	83 06 01 152 13:13:59.0	17.037S 174.614W	TONGA ISLANDS	223	4.8	0.0	PDE	EQ	A	13:16-13:27	12	22059/ 11
1131	00 00 00 000 00:00:00.0	0.000N 0.000E	PROBABLE MARIANAS PO, SO, T	0	0.0	0.0	HEL	EQ	BDE	15:29-15:58	30	22059/ 12
1132	00 00 00 000 00:00:00.0	0.000N 0.000E	UNKNOWN P	0	0.0	0.0	HEL	UN	A	20:26-20:35	10	22059/ 13
1133	83 06 02 153 20:51:58.2	24.596S 179.585E	SOUTH OF FIJI ISLANDS	524	5.0	0.0	PDE	EQ	A	20:54-21:06	13	22059/ 14
1134	83 06 03 154 01:30:04.2	51.164N 177.164W	ANDREANOF ISL. ALEUTIAN ISL.	54	4.6	0.0	PDE	EQ	ABD	01:32-01:48	17	22059/ 15
1135	83 06 03 154 21:51:52.4	0.636N 119.917E	MINAHASSA PENINSULA	33	5.0	0.0	PDE	EQ	A	21:56-22:07	12	22059/ 16
1136	83 06 03 154 22:52:13.6	7.094S 129.164E	BANDA SEA	200	5.2	0.0	PDE	EQ	A	22:55-23:06	12	22059/ 17
1137	83 06 04 155 09:34:44.4	27.859N 103.322E	YUNNAN PROVINCE CHINA	33	5.1	0.0	PDE	EQ	A	09:42-09:51	12	22059/ 18
1138	83 06 04 155 11:37:40.9	37.391N 115.214W	SOUTHERN NEVADA	6	0.0	0.0	PDE	EQ	A	11:44-11:55	12	22059/ 19
1139	83 06 05 156 00:43:14.3	7.600S 127.621E	BANDA SEA	184	5.2	0.0	PDE	EQ	A	00:46-00:58	13	22059/ 20
1142	83 06 05 156 05:34:40.2	6.105S 146.126E	EAST PAPUA NEW GUINEA REGION	116	5.2	0.0	PDE	EQ	ABDE	05:36-06:22	47	22059/ 21
1141	83 06 05 156 10:39:38.7	39.235N 75.712E	SOUTHERN XINJIANG CHINA	33	4.9	4.5	PDE	EQ	A	10:47-10:56	12	22059/ 22
1142	83 06 05 156 13:23:34.2	16.098S 172.987W	SAMOA ISLANDS REGION	33	5.1	4.7	PDE	EQ	A	13:26-13:37	12	22059/ 23
1143	83 06 05 156 16:26:40.7	15.929S 173.017W	TONGA ISLANDS	33	5.3	5.1	PDE	EQ	A	16:29-16:40	12	22059/ 24
1144	83 06 05 156 22:17:03.2	39.433N 73.466E	YAJIK-XINJIANG BORDER REGION	33	5.0	0.0	PDE	EQ	A	22:24-22:35	12	22059/ 25
1145	83 06 06 157 03:18:01.4	20.545S 178.569W	FIJI ISLANDS REGION	620	4.9	0.0	PDE	EQ	A	03:20-03:31	12	22059/ 26
1146	83 06 06 157 21:40:17.5	45.365N 150.352E	KURIL ISLANDS	33	5.6	5.1	PDE	EQ	ABDE	21:41-22:24	44	22059/ 01
1147	83 06 07 158 00:11:32.5	23.951N 122.756E	TAIWAN REGION	33	5.1	0.0	PDE	EQ	A	00:14-00:25	12	22060/ 02
1148	83 06 07 158 06:31:34.3	5.433N 95.187E	NORTHERN SUMATERA	110	4.8	0.0	PDE	EQ	A	06:38-06:49	12	22060/ 03
1149	83 06 07 158 15:57:36.1	32.812N 130.921E	KYUSHU JAPAN	51	0.0	4.7	PDE	EQ	ABD	15:59-16:15	17	22060/ 04
1150	83 06 08 159 09:54:38.0	5.289S 102.853E	SOUTHERN SUMATERA	33	5.2	0.0	PDE	EQ	A	10:00-10:12	13	22060/ 05
1151	83 06 09 160 04:36:50.6	40.014N 139.170E	NEAR W COAST OF HONSHU JAPAN	33	4.9	0.0	PDE	EQ	ABD	04:38-04:54	17	22060/ 06
1152	83 06 09 160 04:51:00.7	3.876S 129.046E	CERAM	114	5.2	0.0	PDE	EQ	A	04:54-05:05	12	22060/ 06
1153	83 06 09 160 10:23:31.9	40.198N 139.003E	NEAR W COAST OF HONSHU JAPAN	33	5.4	0.0	PDE	EQ	ABDE	10:25-11:12	46	22060/ 07
1154	83 06 09 160 12:49:04.1	40.200N 139.054E	NEAR W COAST OF HONSHU JAPAN	33	6.3	5.6	PDE	EQ	ABDE	12:50-13:36	47	22060/ 08
1155	83 06 09 160 13:04:00.9	40.193N 139.026E	NEAR W COAST OF HONSHU JAPAN	33	6.3	5.6	PDE	EQ	ABDE	13:05-13:51	47	22060/ 08
1156	83 06 09 160 14:41:49.7	40.40?N 137.751E	EASTERN SEA OF JAPAN	33	5.0	0.0	PDE	EQ	ABDE	14:42-15:29	46	22060/ 09
1157	83 06 09 160 17:10:00.0	37.158N 116.069W	SOUTHERN NEVADA	0	4.6	0.0	PDE	NX	A	17:16-17:27	12	22060/ 10
1158	83 06 09 160 18:46:01.0	51.441N 174.161W	ANDREANOF ISL. ALEUTIAN ISL.	20	6.2	5.8	PDE	EQ	ABDE	18:48-19:37	50	22060/ 11
1159	83 06 09 160 20:26:51.0	5.995S 122.650E	SULAWESI	50	5.5	5.2	PDE	EQ	A	20:31-20:42	12	22060/ 12
1160	83 06 09 160 20:36:36.9	51.441N 174.148W	ANDREANOF ISL. ALEUTIAN ISL.	26	4.8	0.0	PDE	EQ	ABD	20:38-20:55	18	22060/ 12
1161	83 06 10 161 02:13:23.0	75.505N 122.662E	LAPTEV SEA	10	5.5	5.3	PDE	EQ	A	02:18-02:30	13	22060/ 13
1162	83 06 10 161 07:20:17.6	40.244N 139.050E	NEAR W COAST OF HONSHU JAPAN	33	5.1	0.0	PDE	EQ	ABDE	07:21-08:07	47	22060/ 14
1163	83 06 10 161 20:38:27.0	16.275N 146.078E	MARIANA ISLANDS	100	5.1	0.0	PDE	EQ	ABDE	20:38-21:10	33	22060/ 15
1164	83 06 10 161 22:39:07.3	24.271S 176.283W	SOUTH OF FIJI ISLANDS	33	5.7	5.4	PDE	EQ	A	22:42-22:54	13	22061/ 01
1165	00 00 00 000 00:00:00.0	0.000N 0.000E	UNKNOWN Po	0	0.0	0.0	HEL	EQ	B	23:26-23:45	20	22061/ 02
1166	83 06 11 162 00:28:13.1	1.615N 126.593E	MOLUCCA PASSAGE	62	5.1	0.0	PDE	EQ	A	00:31-00:42	12	22061/ 03
1167	83 06 11 162 03:09:53.9	36.261N 120.466W	CENTRAL CALIFORNIA	2	5.4	5.4	PDE	EQ	A	03:16-03:27	12	22061/ 04
1168	83 06 11 162 04:54:00.6	4.380S 122.536E	SULAWESI	634	5.3	0.0	PDE	EQ	A	04:57-05:06	12	22061/ 05
1169	83 06 11 162 22:01:26.0	40.712N 139.243E	NEAR W COAST OF HONSHU JAPAN	33	5.0	0.0	PDE	EQ	ABDE	22:03-22:49	47	22061/ 06
1170	83 06 12 163 02:36:43.5	49.894N 78.964E	EASTERN KAZAKH SSR	0	6.1	4.5	PDE	NX	A	02:43-02:55	13	22061/ 07
1171	83 06 12 163 09:14:10.6	12.844S 169.038E	SANTA CRUZ ISLANDS REGION	592	5.2	0.0	PDE	EQ	A	09:15-09:26	12	22061/ 09
1172	83 06 12 163 10:12:43.2	1.527N 127.278E	HALMAHERA	124	5.6	0.0	PDE	EQ	A	10:15-10:26	12	22061/ 09
1173	83 06 12 163 19:20:59.6	46.687N 152.637E	KURIL ISLANDS	33	5.0	0.0	PDE	EQ	ABDE	19:22-20:06	45	22061/ 10
1174	83 06 13 164 00:52:02.2	40.452N 143.885E	OFF E COAST OF HONSHU JAPAN	33	4.7	4.7	PDE	EQ	ABD	00:53-01:08	16	22061/ 11
1175	83 06 13 164 03:54:54.1	45.147N 152.543E	KURIL ISLANDS	33	5.0	0.0	PDE	EQ	ABDE	03:56-04:39	44	22061/ 12
1176	83 06 13 164 04:19:30.5	40.485N 143.781E	OFF E COAST OF HONSHU JAPAN	33	4.9	0.0	PDE	EQ	ABD	04:20-04:35	16	22061/ 12
1177	83 06 13 164 08:01:38.4	27.625N 66.274E	PAKISTAN	33	4.9	0.0	PDE	EQ	A	08:10-08:21	12	22061/ 13
1178	83 06 13 164 09:45:01.1	8.464S 122.623E	FLORES ISLAND REGION	179	5.0	0.0	PDE	EQ	A	09:49-10:00	12	22061/ 14
1179	83 06 14 165 00:59:28.6	53.580S 148.635E	WEST OF MACQUARIE ISLAND	10	5.2	0.0	PDE	EQ	A	01:06-01:17	12	22061/ 15
1180	83 06 15 166 06:05:55.5	34.189N 92.817E	QINGHAI PROVINCE CHINA	33	5.1	5.2	PDE	EQ	A	06:12-06:23	12	22061/ 16
1181	83 06 15 166 06:07:55.3	15.192S 172.686W	TONGA ISLANDS	40	5.5	5.5	PDE	EQ	A	06:10-06:22	13	22061/ 16
1182	00 00 00 000 00:00:00.0	0.000N 0.000E	PROBABLE MARIANAS Po, So, T.	0	0.0	0.0	HEL	EQ	BDE	07:21-07:50	30	22061/ 17
1183	83 06 15 166 07:33:43.6	5.387N 127.592E	PHILIPPINE ISLANDS REGION	53	5.4	5.0	PDE	EQ	A	07:36-07:47	12	22061/ 17
1184	83 06 15 166 13:34:06.5	39.320N 64.333E	UZBEK SSR	33	4.9	0.0	PDE	EQ	A	13:42-13:53	12	22061/ 18
1185	83 06 17 168 11:33:15.4	36.448S 97.443W	WEST CHILE RISE	10	5.5	5.5	PDE	EQ	A	11:42-12:01	20	22061/ 19
1186	83 06 17 168 20:55:32.6	41.280N 144.155E	HOKKAIDO JAPAN REGION	33	5.0	0.0	PDE	EQ	ABDE	20:57-21:43	47	22061/ 20
1187	83 06 17 168 22:02:31.6	52.234N 159.647E	OFF E COAST OF KAMCHATKA	33	5.6	5.0	PDE	EQ	ABDE	22:04-22:52	48	22061/ 21
1188	83 06 18 169 03:03:34.0	53.121N 155.748E	NEAR EAST COAST OF KAMCHATKA	33	5.0	0.0	PDE	EQ	ABDE	03:05-03:54	50	22062/ 02
1189	83 06 18 169 11:29:48.4	5.577S 131.266E	BANDA SEA	59	5.1	0.0	PDE	EQ	A	11:33-11:44	12	22062/ 03
1190	83 06 18 169 13:17:56.2	12.255N 143.004E	SOUTH OF MARIANA ISLANDS	52	4.9	0.0	PDE	EQ	ABD	13:18-13:31	14	22062/ 04
1191	83 06 18 169 19:31:12.7	8.247S 155.350E	SOLOMON ISLANDS	27	5.6	0.0	PDE	EQ	ABDE	19:32-20:15	44	22062/ 05
1192	83 06 18 169 21:29:33.5	33.517N 131.793E	KYUSHU JAPAN	71	5.1	0.0	PDE	EQ	ABDE	21:31-22:19	49	22062/ 05
1193	83 06 18 169 22:13:31.4	40.129N 139.965E	EASTERN SEA OF JAPAN	22	5.5	4.7	PDE	EQ	ABDE	22:15-23:00	45	22062/ 06
1194	83 06 19 170 04:35:50.7	40.086N 139.947E	EASTERN SEA OF JAPAN	33	4.9	0.0	PDE	EQ	ABD	04:37-04:53	17	22062/ 07
1195	83 06 19 170 06:45:16.7	16.584S 174.059W	TONGA ISLANDS	310	4.8	0.0	PDE	EQ	A	06:47-06:59	13	22062/ 08
1196	83 06 19 170 21:38:15.8	40.03?N 141.844E	OFF E COAST OF HONSHU JAPAN	33	4.9	0.0	PDE	EQ	ABD	21:39-21:54	16	22062/ 09
1197	83 06 20 171 02:43:25.6	40.96?N 139.[illegible]E	NEAR W COAST OF HONSHU JAPAN	25	5.3	4.5	PDE	EQ	ABDE	02:45-03:31	47	22062/ 10
1198	83 06 20 171 05:43:53.2	23.53?S 179.[illegible]W	SOUTH OF FIJI ISLANDS	548	5.6	0.0	PDE	EQ	A	05:46-05:57	12	22062/ 11
1199	83 06 20 171 15:14:32.2	44.577N 147.646E	KURIL ISLANDS	70	5.3	0.0	PDE	EQ	ABDE	15:15-15:59	45	22062/ 12
1200	83 06 21 172 03:44:49.4	17.473S 168.484E	VANUATU ISLANDS	201	5.1	0.0	PDE	EQ	A	03:46-03:58	13	22062/ 13

EOF..

WAKE HYDROPHONE INFORMATION PROCESSING SYSTEM (WHIPS) EVENT LISTING 13 AUG 83

KEY: INFORMATION SOURCES - PDE=NEIS PDECARD, MON=NEIS MONTHLY LIST, ICS=ICS LIST, HEL=HELICORDER, OTH=OTHER
EVENT TYPE - EQ=EARTHQUAKE, NX=NUCLEAR EXPLOSION, SX=SCIENTIFIC EXPLOSION, OT=OTHER, UN=UNKNOWN
PHASES - A=P, B=PU, C=S, D=SO, E=T, F=OTHER

EVNT NO	ORIGIN TIME YR MO DA JUL HR MN SECS	COORDINATES LAT LON	LOCATION DESCRIPTION	DEP KM	MAGNI BDY	MAGNI SRF	INF SRC	EV TP	SAVED PHASES	SAVED INTERVAL MNS	STRIP TAPE/FILE
1201	83 06 21 172 06:25:27.6	41.315N 139.136E	HOKKAIDO JAPAN REGION	13	6.6	6.0	PDE	EQ	ABDE	06:27-07:13	47	20863/ 01
1202	83 06 21 172 06:46:50.1	41.305N 139.345E	HOKKAIDO JAPAN REGION	33	5.4	0.0	PDE	EQ	ABDE	06:48-07:34	47	0/ 00
1203	83 06 21 172 07:04:22.2	41.350N 139.349E	HOKKAIDO JAPAN REGION	33	5.5	0.0	PDE	EQ	ABDE	07:06-07:52	47	0/ 00
1204	83 06 21 172 07:13:51.4	41.320N 139.270E	HOKKAIDO JAPAN REGION	33	5.4	0.0	PDE	EQ	ABDE	07:15-07:01	47	0/ 00
1205	83 06 21 172 09:12:15.3	41.300N 139.596E	HOKKAIDO JAPAN REGION	33	4.6	0.0	PDE	EQ	ABD	09:13-09:29	17	0/ 00
1206	83 06 21 172 10:16:05.7	41.300N 139.421E	HOKKAIDO JAPAN REGION	33	4.8	0.0	PDE	EQ	ABD	10:17-10:33	17	0/ 00
1207	83 06 21 172 10:26:26.0	5.483S 151.037E	NEW BRITAIN REGION	105	5.2	0.0	PDE	EQ	ABDE	10:27-11:10	44	0/ 00
1208	83 06 21 172 10:38:46.7	24.045N 122.853E	TAIWAN REGION	33	4.9	0.0	PDE	EQ	A	10:41-10:53	13	0/ 00
1209	83 06 21 172 11:29:55.5	41.735N 139.168E	HOKKAIDO JAPAN REGION	20	5.2	0.0	PDE	EQ	ABDE	11:31-12:10	40	0/ 00
1210	83 06 21 172 11:32:12.7	7.122S 129.983E	BANDA SEA	111	4.8	0.0	PDE	EQ	A	11:35-11:46	12	0/ 00
1211	83 06 21 172 11:36:57.5	15.436S 173.451W	TONGA ISLANDS	33	5.1	0.0	PDE	EQ	A	11:39-11:51	13	0/ 00
1212	83 06 21 172 14:31:50.9	24.077N 122.467E	TAIWAN REGION	32	5.3	4.7	PDE	EQ	A	14:34-14:46	13	0/ 00
1213	83 06 21 172 14:48:05.5	24.253N 122.488E	TAIWAN REGION	24	5.8	6.3	PDE	EQ	A	14:51-15:02	12	0/ 00
1214	83 06 21 172 15:49:41.9	6.260N 125.335E	MINDANAO PHILIPPINE ISLANDS	342	0.0	0.0	PDE	EQ	A	15:52-16:03	12	0/ 00
1215	83 06 21 172 16:02:21.3	41.521N 139.488E	HOKKAIDO JAPAN REGION	33	4.8	0.0	PDE	EQ	ABD	16:04-16:20	17	0/ 00
1216	83 06 21 172 17:06:52.1	29.705N 129.362E	RYUKYU ISLANDS	164	5.9	0.0	PDE	EQ	ABDE	17:06-17:56	51	0/ 00
1217	83 06 22 173 04:34:20.0	41.378N 139.277E	HOKKAIDO JAPAN REGION	33	5.0	0.0	PDE	EQ	ABDE	04:36-05:22	47	0/ 00
1218	83 06 22 173 04:36:34.3	41.047N 139.161E	HOKKAIDO JAPAN REGION	27	5.3	0.0	PDE	EQ	ABDE	04:38-05:24	47	0/ 00
1219	83 06 22 173 05:39:33.9	41.455N 139.361E	HOKKAIDO JAPAN REGION	33	4.8	0.0	PDE	EQ	ABD	05:41-05:57	17	0/ 00
1220	83 06 22 173 14:32:07.4	50.315N 142.257E	SAKHALIN ISLAND	33	4.8	0.0	PDE	EQ	ABD	14:34-14:51	18	0/ 00
1221	83 06 22 173 15:20:23.4	41.340N 139.224E	HOKKAIDO JAPAN REGION	18	5.1	0.0	PDE	EQ	ABDE	15:22-16:08	47	0/ 00
1222	83 06 22 173 20:15:46.0	42.033N 138.974E	EASTERN SEA OF JAPAN	17	5.3	4.1	PDE	EQ	ABDE	20:17-21:03	47	0/ 00
1223	83 06 22 173 21:38:27.0	41.165N 139.335E	HOKKAIDO JAPAN REGION	33	4.4	0.0	PDE	EQ	ABD	21:40-21:56	17	0/ 00
1224	83 06 23 174 01:45:03.5	51.366N 179.024W	ANDREANOF ISL. ALEUTIAN ISL.	33	4.8	0.0	PDE	EQ	ABD	01:47-02:03	17	0/ 00
1225	83 06 23 174 11:00:38.0	41.556N 141.956E	HOKKAIDO JAPAN REGION	79	4.9	0.0	PDE	EQ	ABD	11:02-11:17	16	0/ 00
1226	83 06 23 174 12:05:16.4	51.763N 139.599E	SOUTH OF AUSTRALIA	10	5.5	5.6	PDE	EQ	A	12:06-12:19	12	0/ 00
1227	83 06 23 174 19:40:23.1	26.706S 177.171W	SOUTH OF FIJI ISLANDS	64	5.0	4.8	PDE	EQ	A	19:44-19:55	12	0/ 00
1228	83 06 24 175 02:09:28.8	4.669S 102.562E	SOUTHERN SUMATERA	33	5.1	0.0	PDE	EQ	A	02:15-02:26	12	0/ 00
1229	83 06 24 175 07:18:21.9	21.723N 103.381E	SOUTHEAST ASIA	10	6.1	6.5	PDE	EQ	F	07:18-08:47	90	0/ 00
1230	83 06 24 175 09:06:46.7	24.197N 122.439E	TAIWAN REGION	54	6.0	0.0	PDE	EQ	A	09:09-09:21	13	0/ 00
1231	83 06 24 175 09:07:17.2	45.155N 146.921E	KURIL ISLANDS	97	4.9	0.0	PDE	EQ	ABD	09:08-09:24	17	0/ 00
1232	83 06 24 175 12:20:14.6	34.435N 69.629E	AFGHANISTAN	33	4.7	0.0	PDE	EQ	A	12:26-12:39	12	0/ 00
1233	83 06 24 175 19:55:20.9	23.993N 122.696E	TAIWAN REGION	33	5.0	0.0	PDE	EQ	A	19:56-20:09	12	0/ 00
EOF..												

1234	83 06 25 176 02:32:47.3	29.898S	177.351W	KERMADEC ISLANDS	33	5.1	0.0	PDE	EQ	A	02:38-02:49	12	20864--9
1235	83 06 25 176 10:03:17.6	32.804S	178.798W	SOUTH OF KERMADEC ISLANDS	46	5.6	5.6	PDE	EQ	A	10:07-10:19	13	20864-11
1236	83 06 25 176 11:59:45.6	18.868S	177.589W	FIJI ISLANDS REGION	595	5.1	0.0	PDE	EQ	A	12:01-12:13	13	20864-12
1237	83 06 25 176 13:50:25.3	32.277N	137.683E	SOUTH OF HONSHU JAPAN	377	5.1	0.0	PDE	EQ	ABDE	13:51-14:34	44	20864-14
1238	83 06 25 176 08:40:43.0	1.332N	99.918E	NORTHERN SUMATERA	205	4.9	0.0	PDE	EQ	A	08:46-08:57	12	20864-16
1239	83 06 25 176 14:12:54.9	23.103N	123.343E	SOUTHWESTERN RYUKYU ISLANDS	16	5.4	0.0	PDE	EQ	A	14:15-14:27	13	20864-14
1240	83 06 25 176 15:04:09.9	22.037S	177.465W	SOUTH OF FIJI ISLANDS	274	5.5	0.0	PDE	EQ	A	15:07-15:18	12	20864-13
1241	83 06 25 176 19:10:02.2	32.817S	178.679W	SOUTH OF KERMADEC ISLANDS	33	5.5	0.0	PDE	EQ	A	19:14-19:26	13	20864-15
1242	83 06 25 176 19:40:55.3	24.001N	122.552E	TAIWAN REGION	42	5.5	5.0	PDE	EQ	A	19:44-19:55	12	20864-16
1243	83 06 25 176 23:14:56.0	7.291S	106.017E	JAVA	56	5.2	0.0	PDE	EQ	A	23:21-23:32	12	20864-17
1244	83 06 26 177 02:31:16.2	23.005N	93.758E	BURMA-INDIA BORDER REGION	73	4.7	0.0	PDE	EQ	A	02:37-02:48	12	20864-18
1245	83 06 26 177 05:10:20.1	44.931S	167.277E	SOUTH ISLAND NEW ZEALAND	33	5.1	0.0	PDE	EQ	A	05:16-05:27	12	20864-**
1246	83 06 26 177 13:56:54.5	41.301N	139.386E	HOKKAIDO JAPAN REGION	29	4.9	0.0	PDE	EQ	ABD	13:58-14:14	17	20864-20
1247	83 06 26 177 15:54:23.5	17.855S	167.470E	VANUATU ISLANDS	45	5.2	5.2	PDE	EQ	A	15:56-16:09	13	20864-21
1248	83 06 26 177 17:45:11.1	20.893N	139.894E	BONIN ISLANDS REGION	281	4.9	0.0	PDE	EQ	ABDE	17:45-18:25	41	20865- 1
1249	83 06 27 178 00:25:13.2	18.188S	167.666E	VANUATU ISLANDS	50	5.0	0.0	PDE	EQ	A	00:27-00:39	13	20865- 2
1250	83 06 27 178 14:10:05.5	23.047S	179.955W	SOUTH OF FIJI ISLANDS	540	5.3	0.0	PDE	EQ	A	14:12-14:24	13	20865- 3
1251	83 06 28 179 03:25:16.6	60.250N	141.272W	SOUTHEASTERN ALASKA	15	5.9	5.4	PDE	EQ	ABDE	03:30-04:40	71	20865--4
1252	83 06 28 179 17:45:58.2	21.815S	178.958W	TUAMOTU ARCHIPELAGO REGION	0	5.4	0.0	PDE	NX	A	17:52-18:03	12	20865- 5
1253	83 06 28 179 21:55:46.1	22.734S	174.702W	TONGA ISLANDS REGION	33	5.2	4.9	PDE	EQ	A	21:59-22:10	12	20865- 6
1254	83 06 28 179 23:59:33.4	43.874N	84.875E	NORTHERN XINJIANG CHINA	33	5.1	4.5	PDE	EQ	A	00:06-00:17	12	20865- 7
1255	83 06 29 180 05:11:57.3	40.190N	139.822E	NEAR W COAST OF HONSHU JAPAN	33	5.1	0.0	PDE	EQ	ABDE	05:13-05:59	47	20865- 8
1256	83 06 29 180 10:55:40.6	36.602N	140.794E	NEAR E COAST OF HONSHU JAPAN	103	4.6	0.0	PDE	EQ	ABD	10:56-11:11	16	20865- 9
1257	83 06 29 180 12:51:37.9	6.916S	129.822E	BANDA SEA	193	4.2	0.0	PDE	EQ	A	12:55-13:06	12	20865-10
1258	00 00 00 000 00:00:00.0	0.000N	0.000E	PROBABLE BONIN ISL. PO,SO,T	0	0.0	0.0	HEL	EQ	BDE	16:14-16:53	40	20865-11
1259	83 06 29 180 22:10:22.6	41.277N	139.358E	HOKKAIDO JAPAN REGION	33	4.9	0.0	PDE	EQ	ABD	22:20-22:36	17	20865-12
1260	83 06 30 181 06:53:28.7	18.871N	121.313E	LUZON PHILIPPINE ISLANDS	75	5.1	0.0	PDE	EQ	A	06:56-07:07	12	20865-13
1261	83 06 30 181 13:39:04.5	44.032N	147.849E	KURIL ISLANDS	47	5.6	5.4	PDE	EQ	ABDE	13:40-14:23	44	20865-14
1262	83 06 30 181 14:11:23.2	18.540S	174.841W	TONGA ISLANDS	272	4.8	0.0	PDE	EQ	A	14:14-14:25	12	20865-14
1263	83 06 30 181 17:37:49.0	2.529N	128.265E	HALMAHERA	49	5.6	5.4	PDE	EQ	A	17:40-17:52	13	20865-15
1264	83 06 30 181 18:24:51.5	44.402N	149.519E	KURIL ISLANDS	33	5.3	5.1	PDE	EQ	ABDE	18:26-19:08	43	20866- 1
1265	83 06 30 181 23:03:58.1	6.910S	155.220E	SOLOMON ISLANDS	97	5.1	0.0	PDE	EQ	ABDE	23:05-23:46	42	20866- 2
1266	83 06 30 181 23:10:51.0	44.428N	149.498E	KURIL ISLANDS	48	5.1	0.0	PDE	EQ	ABDE	23:22-00:02	43	20866- 2
1267	83 06 30 181 23:42:16.9	44.310N	149.586E	KURIL ISLANDS	33	5.0	0.0	PDE	EQ	ABDE	23:43-00:26	44	20866- 2
1268	83 07 01 182 02:23:11.7	44.542N	149.410E	KURIL ISLANDS	60	5.4	0.0	PDE	EQ	ABDE	02:24-03:07	44	20866- 3
1269	83 07 01 182 06:35:56.0	32.262N	140.464E	SOUTH OF HONSHU JAPAN	76	4.8	0.0	PDE	EQ	ABD	06:36-06:51	16	20866- 4
1270	83 07 01 182 08:53:55.5	44.256N	149.580E	KURIL ISLANDS	33	5.0	4.8	PDE	EQ	ABDE	08:55-09:[illegible]	43	20866- 5
1271	83 07 01 182 10:46:54.7	44.374N	149.575E	KURIL ISLANDS	33	5.2	4.7	PDE	EQ	ABDE	10:48-11:30	43	20866- 6
1272	83 07 01 182 22:03:42.0	36.898N	141.057E	NEAR E COAST OF HONSHU JAPAN	53	5.5	0.0	PDE	EQ	ABDE	22:04-22:47	44	20866- 7
1273	83 07 01 182 23:32:00.4	39.961N	139.816E	NEAR W COAST OF HONSHU JAPAN	37	4.6	0.0	PDE	EQ	ABD	23:33-23:49	17	20866- 8
1274	83 07 02 183 05:32:42.6	40.860N	138.965E	EASTERN SEA OF JAPAN	33	5.1	0.0	PDE	EQ	ABDE	05:34-06:20	47	20867- 1
1275	00 00 00 000 00:00:00.0	0.000N	0.000E	UNKNOWN PO	0	0.0	0.0	HEL	EQ	B	07:18-07:47	30	20867- 2
1276	83 07 02 183 09:34:05.6	5.724N	94.779E	NORTHERN SUMATERA	98	5.7	0.0	PDE	EQ	A	09:40-09:51	12	20867- 3
1277	83 07 02 183 11:42:21.9	39.305N	64.381E	UZBEK SSR	33	4.9	0.0	PDE	EQ	A	11:50-12:01	12	20867- 4
1278	83 07 03 184 02:49:26.0	20.157N	122.418E	PHILIPPINE ISLANDS REGION	211	6.1	0.0	PDE	EQ	A	02:52-03:03	12	20867- 5
1279	83 07 03 184 06:11:35.7	5.589S	154.318E	SOLOMON ISLANDS	485	5.4	0.0	PDE	EQ	ABDE	06:12-06:53	42	20867- 6
1280	83 07 03 184 07:05:26.1	41.453N	139.347E	HOKKAIDO JAPAN REGION	33	5.0	0.0	PDE	EQ	ABDE	07:07-07:53	47	20867- 7
1281	83 07 03 184 08:01:22.0	13.893S	167.954E	VANUATU ISLANDS	33	4.9	0.0	PDE	EQ	A	08:03-08:14	12	20867- 8
1282	83 07 03 184 17:14:23.2	9.650N	83.644W	COSTA RICA	33	5.7	6.1	PDE	EQ	AE	17:23-19:31	129	20867- 9
1283	83 07 03 184 17:40:01.4	24.823N	141.012E	VOLCANO ISLANDS REGION	292	4.5	0.0	PDE	EQ	ABDE	17:48-18:26	39	20867- 9

KEY: INFORMATION SOURCES - PDE=NEIS PDECARD, MON=NEIS MONTHLY LIST, ICS=ICS LIST, HEL=HELICORDER, OTH=OTHER
EVENT TYPE - EQ=EARTHQUAKE, NX=NUCLEAR EXPLOSION, SX=SCIENTIFIC EXPLOSION, OT=OTHER, UN=UNKNOWN
PHASES - A=P, B=PO, C=S, D=SO, E=T, F=OTHER

EVNT NO	ORIGIN TIME YR MO DA JUL HR MN SECS	COORDINATES LAT	LON	LOCATION DESCRIPTION	DEP KM	MAGNI BDY	SRF	INF SRC	EV TP	SAVED PHASES	INTERVAL	MNS	STRIP TAPE-FIL
1284	83 07 03 184 20:24:41.5	24.372N	122.499E	TAIWAN REGION	65	5.2	0.0	PDE	EQ	A	20:27-20:39	13	20066- 1
1285	83 07 04 185 11:32:46.2	55.569S	27.942W	SOUTH SANDWICH ISLANDS REGION	33	5.5	4.6	PDE	EQ	A	11:42-12:01	20	20066- 2
1286	83 07 04 185 20:51:19.6	49.753N	155.618E	KURIL ISLANDS	40	5.0	0.0	PDE	EQ	ABDE	20:52-21:30	47	20068- 3
1287	83 07 04 185 22:00:34.0	4.415N	126.736E	TALAUD ISLANDS	100	5.1	0.0	PDE	EQ	A	22:03-22:14	12	20068- 4
1288	83 07 05 186 05:58:21.4	55.696S	123.453W	EASTER ISLAND CORDILLERA	10	5.3	6.0	PDE	EQ	AE	06:07-06:03	117	20066- 5
1289	83 07 05 186 08:54:48.0	26.431N	128.947E	RYUKYU ISLANDS	33	5.3	5.1	PDE	EQ	ABDE	08:57-09:46	50	20066- 6
1290	83 07 05 186 09:57:38.0	24.201S	174.894W	SOUTH OF TONGA ISLANDS	33	5.5	0.0	PDE	EQ	A	10:01-10:12	12	20066- 7
1291	83 07 05 186 11:11:41.1	22.551S	171.015E	LOYALTY ISLANDS REGION	45	6.0	6.4	PDE	EQ	AE	11:14-12:11	58	20068- 8
1292	83 07 05 186 11:49:02.0	22.718S	170.931E	LOYALTY ISLANDS REGION	33	5.1	0.0	PDE	EQ	A	11:52-12:03	12	20068- 8
1293	83 07 05 186 12:55:05.0	22.713S	171.042E	LOYALTY ISLANDS REGION	33	5.4	0.0	PDE	EQ	A	12:58-13:09	12	20068- 9
1294	83 07 05 186 16:37:06.0	57.821S	25.629W	SOUTH SANDWICH ISLANDS REGION	33	5.7	5.5	PDE	EQ	A	16:46-17:05	28	20069- 1
1295	83 07 06 187 03:24:15.4	22.921S	171.061E	LOYALTY ISLANDS REGION	33	5.2	0.0	PDE	EQ	A	03:27-03:36	12	20069- 2
1296	83 07 06 187 04:54:36.5	21.807S	174.822W	TONGA ISLANDS	40	5.3	5.0	PDE	EQ	A	04:58-05:09	12	20069- 3
1297	83 07 06 187 07:47:12.8	13.812N	144.759E	MARIANA ISLANDS	146	5.0	0.0	PDE	EQ	ABDE	07:47-08:21	35	20069- 4
1298	83 07 06 187 17:59:54.7	11.630S	166.347E	SANTA CRUZ ISLANDS	33	5.2	4.8	PDE	EQ	A	18:01-18:12	12	20069- 5
1299	83 07 06 187 18:19:31.7	1.715N	98.148E	NORTHERN SUMATERA	84	5.3	0.0	PDE	EQ	A	18:25-18:37	13	20069- 6
1300	00 00 00 000 00:00:00.0	0.000N	0.000E	UNKNOWN PO, SO, T	0	0.0	0.0	HEL	EQ	BDE	00:48-01:27	40	20069- 7
1301	83 07 07 188 01:02:57.0	22.633S	171.002E	LOYALTY ISLANDS REGION	55	5.3	5.0	PDE	EQ	A	01:06-01:17	12	20069- 7
1302	83 07 07 188 03:35:05.5	12.203N	125.749E	SAMAR PHILIPPINE ISLANDS	40	5.0	0.0	PDE	EQ	A	03:38-03:49	12	20069- 8
1303	83 07 07 188 05:29:48.4	22.613S	170.858E	LOYALTY ISLANDS REGION	64	5.1	0.0	PDE	EQ	A	05:32-05:44	13	20069- 9
1304	83 07 07 188 13:33:53.5	19.203S	177.301W	FIJI ISLANDS REGION	377	5.3	0.0	PDE	EQ	A	13:36-13:47	12	20069-10
1305	83 07 07 188 15:35:45.4	22.602S	170.961E	LOYALTY ISLANDS REGION	33	5.1	0.0	PDE	EQ	A	15:38-15:50	13	20069-11
1306	83 07 07 188 16:05:48.0	22.561S	170.722E	LOYALTY ISLANDS REGION	41	5.4	6.2	PDE	EQ	AE	16:08-17:05	56	20069-12
1307	83 07 08 189 00:58:11.7	2.398N	128.424E	HALMEHERA	157	5.3	0.0	PDE	EQ	A	01:01-01:12	12	20069-13
1308	83 07 08 189 10:05:00.1	21.820S	173.380W	TONGA ISLANDS	33	5.5	4.8	PDE	EQ	A	10:08-10:19	12	20070- 1
1309	83 07 08 189 13:38:12.1	19.472S	169.872E	VANUATU ISLANDS	152	5.2	0.0	PDE	EQ	A	13:42-13:52	13	20070- 2
1310	00 00 00 000 00:00:00.0	0.000N	0.000E	PROBABLE MARIANAS PO, SO, T	0	0.0	0.0	HEL	EQ	BDE	14:38-15:07	30	20070- 3
1311	83 07 09 190 18:30:39.0	6.432S	146.605E	EAST PAPUA NEW GUINEA REGION	110	5.1	0.0	PDE	EQ	ABDE	18:32-19:10	47	20070- 4
1312	83 07 10 191 03:59:57.0	51.327N	53.286E	EUROPEAN USSR	0	5.3	0.0	PDE	NX	A	04:06-04:19	12	20072- 5
1313	83 07 10 191 04:04:57.0	51.336N	53.298E	EUROPEAN USSR	0	5.4	0.0	PDE	NX	A	04:13-04:24	12	20072- 5
1314	83 07 10 191 04:09:57.1	51.357N	53.301E	EUROPEAN USSR	0	5.2	0.0	PDE	NX	A	04:18-04:29	12	20072- 5
1315	83 07 10 191 17:19:46.6	27.481N	128.386E	RYUKYU ISLANDS	58	5.4	0.0	PDE	EQ	A	17:22-17:33	12	20072- 6
1316	00 00 00 000 00:00:00.0	0.000N	0.000E	PROBABLE MARIANAS PO,SO,,T	0	0.0	0.0	HEL	EQ	BDE	01:01-01:30	30	20072- 7
1317	83 07 11 192 10:35:26.0	41.340N	139.495E	HOKKAIDO JAPAN REGION	33	4.6	0.0	PDE	EQ	ABD	10:37-10:53	17	20072- 8
1318	83 07 11 192 12:56:28.1	60.896S	52.935W	SOUTH SHETLAND ISLANDS	10	6.1	6.9	PDE	EQ	AE	13:05-15:45	161	20072- 9
1319	83 07 11 192 21:10:23.0	40.522N	77.625E	KIRGHIZ-XINJIANG BORDER REGION	33	5.0	0.0	PDE	EQ	A	21:25-21:36	10	20072-10
1320	83 07 12 193 14:56:55.3	38.033N	141.895E	NEAR E COAST OF HONSHU JAPAN	33	4.7	0.0	PDE	EQ	ABD	14:56-15:13	16	20072-11
1321	83 07 12 193 15:10:03.3	61.033N	147.379W	SOUTHERN ALASKA	37	6.1	6.3	PDE	EQ	ABDE	15:14-16:22	69	20072-11
1322	83 07 13 194 11:09:42.2	36.320N	70.991E	HINDU KUSH REGION	131	4.7	0.0	PDE	EQ	A	11:17-11:26	10	20072-12
1323	83 07 13 194 15:07:40.8	6.622S	106.342E	JAVA	127	5.0	0.0	PDE	EQ	A	15:13-15:24	12	20071- 1
1324	83 07 14 195 09:48:36.8	18.957S	175.699W	TONGA ISLANDS	275	5.1	0.0	PDE	EQ	A	09:51-10:02	12	20071- 2
1325	83 07 14 195 19:47:46.5	5.532N	126.486E	MINDANAO PHILIPPINE ISLANDS	43	5.8	6.0	PDE	EQ	AE	19:50-20:46	57	20071- 3
1326	83 07 15 196 03:10:03.1	18.965S	168.363E	VANUATU ISLANDS	33	5.1	0.0	PDE	EQ	A	03:20-03:32	13	20071- 4
1327	83 07 15 196 03:55:53.9	52.288N	176.913W	ANDREANOF ISL. ALEUTIAN ISL.	127	5.2	0.0	PDE	EQ	ABDE	03:57-04:47	51	20071- 5
1328	83 07 15 196 04:46:56.5	21.799N	103.425E	SOUTHEAST ASIA	33	5.0	5.0	PDE	EQ	A	04:54-05:05	12	20071- 6
1329	83 07 15 196 07:48:59.4	60.282N	140.897W	SOUTHEASTERN ALASKA	15	5.1	0.0	PDE	EQ	A	07:53-08:05	13	20071- 7
1330	83 07 15 196 10:39:08.3	23.005N	121.439E	TAIWAN	36	5.0	0.0	PDE	EQ	A	10:42-10:53	12	20071- 8
1331	83 07 15 196 10:45:38.2	5.465N	126.542E	MINDANAO PHILIPPINE ISLANDS	47	5.6	5.6	PDE	EQ	A	10:48-10:59	12	20071- 8
1332	83 07 16 197 02:32:16.0	5.495N	126.538E	MINDANAO PHILIPPINE ISLANDS	30	5.2	5.2	PDE	EQ	A	02:35-02:46	12	20072-20
1333	83 07 16 197 07:55:24.6	7.186S	129.361E	BANDA SEA	150	5.4	0.0	PDE	EQ	A	07:58-08:10	13	20071-10
1334	83 07 16 197 11:25:11.7	7.704S	126.744E	BANDA SEA	176	5.2	0.0	PDE	EQ	A	11:28-11:40	13	20071-11
1335	83 07 16 197 14:09:47.5	0.156S	121.706E	MINAHASSA PENINSULA	71	5.2	0.0	PDE	EQ	A	14:13-14:24	12	20071-12
1336	83 07 16 197 15:50:07.3	18.901S	177.556E	FIJI ISLANDS	11	6.0	4.4	PDE	EQ	A	15:52-16:04	13	20071-13
1337	83 07 16 197 17:19:22.2	44.876N	148.871E	EASTERN SEA OF JAPAN	246	4.8	0.0	PDE	EQ	ABDE	17:20-18:08	49	20071-14
1338	83 07 16 197 18:17:11.4	0.141S	121.664E	MINAHASSA PENINSULA	49	5.0	0.0	PDE	EQ	A	18:21-18:32	12	20071-15
1339	83 07 16 197 23:28:22.7	7.418S	108.323E	JAVA	138	4.9	0.0	PDE	EQ	A	23:34-23:45	12	20071-16
1340	83 07 17 198 01:33:40.1	0.104S	121.679E	MINAHASSA PENINSULA	54	5.0	0.0	PDE	EQ	A	01:37-01:48	12	20071-17
1341	83 07 17 198 01:56:52.0	49.230N	155.669E	KURIL ISLANDS	96	5.0	0.0	PDE	EQ	ABDE	01:58-02:43	46	20071-18
1342	83 07 17 198 05:22:52.0	5.379N	126.555E	MINDANAO PHILIPPINE ISLANDS	45	5.3	4.1	PDE	EQ	A	05:26-05:37	12	20071-19
1343	83 07 17 198 05:44:45.5	0.115S	121.665E	MINAHASSA PENINSULA	54	5.2	0.0	PDE	EQ	A	05:48-05:59	12	20071-20
1344	83 07 17 198 06:29:19.0	18.479S	177.784W	FIJI ISLANDS REGION	591	5.1	0.0	PDE	EQ	A	06:31-06:42	12	20071-21
1345	83 07 17 198 10:14:26.1	0.056S	121.727E	MINAHASSA PENINSULA	51	5.2	0.0	PDE	EQ	A	10:18-10:29	12	20071-22
1346	83 07 17 198 10:21:54.0	7.144S	129.546E	BANDA SEA	103	4.9	0.0	PDE	EQ	A	10:25-10:36	12	20071-22
1347	83 07 17 198 13:15:52.6	0.024S	121.771E	MINAHASSA PENINSULA	33	5.0	0.0	PDE	EQ	A	13:19-13:31	13	20071-23
1348	83 07 17 198 14:47:05.6	23.508S	179.051E	SOUTH OF FIJI ISLANDS	554	5.0	0.0	PDE	EQ	A	14:49-15:01	13	20072- 1
1349	83 07 17 198 16:01:54.1	0.083S	121.763E	MINAHASSA PENINSULA	52	5.2	0.0	PDE	EQ	A	16:05-16:17	13	20072- 2
1350	83 07 17 198 19:04:19.3	0.081S	121.748E	MINAHASSA PENINSULA	62	5.4	0.0	PDE	EQ	A	19:08-19:19	12	20072- 3
1351	83 07 17 198 21:06:24.7	36.335N	70.838E	HINDU KUSH REGION	216	4.9	0.0	PDE	EQ	A	21:13-21:25	13	20072- 4
1352	83 07 17 198 21:56:21.4	31.256S	178.283W	KERMADEC ISLANDS REGION	87	5.3	0.0	PDE	EQ	A	22:00-22:12	13	20072- 5
1353	83 07 17 198 22:10:23.1	0.079S	121.689E	MINAHASSA PENINSULA	49	5.4	0.0	PDE	EQ	A	22:14-22:25	12	20072- 6
1354	83 07 17 198 23:02:49.7	22.767S	178.130W	SOUTH OF FIJI ISLANDS	335	5.2	0.0	PDE	EQ	A	23:05-23:17	13	20072- 7
1355	83 07 18 199 01:35:19.6	0.042N	121.641E	MINAHASSA PENINSULA	51	5.1	0.0	PDE	EQ	A	01:39-01:50	12	20072- 8
1356	83 07 18 199 03:14:14.7	0.118S	121.697E	MINAHASSA PENINSULA	62	5.4	0.0	PDE	EQ	A	03:18-03:29	12	20072- 9
1357	83 07 18 199 05:11:25.1	37.253N	141.613E	NEAR E COAST OF HONSHU JAPAN	42	5.2	0.0	PDE	EQ	ABDE	05:12-05:54	43	20072-10
1358	83 07 18 199 05:28:06.5	0.128S	121.727E	MINAHASSA PENINSULA	62	5.0	0.0	PDE	EQ	A	05:32-05:43	12	20072-10
1359	83 07 18 199 07:27:56.0	0.114S	121.787E	MINAHASSA PENINSULA	62	5.4	0.0	PDE	EQ	A	07:31-07:43	13	20072-11
1360	83 07 18 199 09:41:28.2	0.040S	121.742E	MINAHASSA PENINSULA	54	5.1	0.0	PDE	EQ	A	09:45-09:56	12	20072-12
1361	83 07 18 199 12:49:33.2	0.178S	121.692E	MINAHASSA PENINSULA	63	5.0	0.0	PDE	EQ	A	12:53-13:04	12	20072-13
1362	83 07 18 199 13:40:26.3	0.031S	121.649E	MINAHASSA PENINSULA	76	5.3	0.0	PDE	EQ	A	13:44-13:55	12	20072-14
1363	83 07 18 199 14:57:52.6	0.066S	121.743E	MINAHASSA PENINSULA	62	5.1	0.0	PDE	EQ	A	15:01-15:13	13	20072-15
1364	83 07 18 199 18:09:03.6	33.677N	136.739E	NEAR S COAST OF SOUTH HONSHU	366	5.0	0.0	PDE	EQ	ABDE	18:10-18:54	45	20072-16
1365	83 07 18 199 18 18:20.0	0.017S	121.748E	MINAHASSA PENINSULA	43	5.1	0.0	PDE	EQ	A	18:1[illegible]-18:25	12	20072-16
1366	83 07 18 [illegible] 23:31:47.7	0.084N	121.730E	MINAHASSA PENINSULA	46	5.1	0.0	PDE	EQ	A	23:35-23:46	12	20072-17
1367	83 07 19 200 02:01:01.4	0.199S	121.672E	MINAHASSA PENINSULA	78	5.1	0.0	PDE	EQ	A	02:05-02:16	12	20072-18
1368	83 07 19 200 06:09:20.6	18.950S	177.598E	FIJI ISLANDS	33	5.1	4.8	PDE	EQ	A	06:12-06:23	12	20072-19
1369	83 07 19 200 08:03:46.0	0.043S	121.661E	MINAHASSA PENINSULA	57	5.1	0.0	PDE	EQ	A	08:07-08:18	12	20072-21
1370	83 07 19 200 10:00:03.0	0.132S	121.733E	MINAHASSA PENINSULA	44	5.2	0.0	PDE	EQ	A	10:04-10:15	12	20072-22
1371	83 07 19 200 11:42:06.6	0.096S	121.627E	MINAHASSA PENINSULA	65	5.1	0.0	PDE	EQ	A	11:46-11:57	12	20072-23
1372	83 07 19 200 12:42:56.1	0.086S	121.655E	MINAHASSA PENINSULA	57	5.0	0.0	PDE	EQ	A	12:46-12:58	13	20072-24
1373	83 07 19 200 14:10:08.6	0.093S	121.718E	MINAHASSA PENINSULA	55	5.0	0.0	PDE	EQ	A	14:22-14:33	12	20072-25
1374	83 07 19 200 15:11:02.3	0.138S	121.612E	MINAHASSA PENINSULA	64	5.0	0.0	PDE	EQ	A	15:15-15:26	12	20072-26
1375	83 07 19 200 17:07:06.9	38.368N	138.465E	SOUTH OF HONSHU JAPAN	435	4.6	0.0	PDE	EQ	ABDE	17:07-17:49	43	20072-27
1376	83 07 19 200 18:22:24.1	0.170S	121.674E	MINAHASSA PENINSULA	58	5.1	0.0	PDE	EQ	A	18:26-18:37	12	20072-28
1377	00 00 00 000 00:00:00.0	0.000N	0.000E	PROBABLE MARIANAS PO,SO,T.	0	0.0	0.0	HEL	EQ	BDE	20:33-21:02	30	20073- 1
1378	83 07 19 200 23:14:38.0	0.152S	121.646E	MINAHASSA PENINSULA	56	5.0	0.0	PDE	EQ	A	23:18-23:29	12	20073- 2
1379	83 07 19 200 23:49:19.1	1.800N	123.880E	MINAHASSA PENINSULA	299	5.5	0.0	PDE	EQ	A	23:52-00:03	12	20073- 3
1380	83 07 20 201 10:33:53.0	0.020S	121.640E	MINAHASSA PENINSULA	53	5.0	0.0	PDE	EQ	A	10:37-10:49	13	20073- 4
1381	83 07 20 201 22:57:17.8	5.953N	127.491E	PHILIPPINE ISLANDS REGION	34	5.6	5.1	PDE	EQ	A	23:00-23:11	12	20073- 5
1382	83 07 21 202 13:17:51.5	0.057S	121.682E	MINAHASSA PENINSULA	42	5.2	0.0	PDE	EQ	A	13:21-13:33	13	20073- 6
1383	83 07 22 203 01:32:17.9	6.171S	154.474E	SOLOMON ISLANDS	51	4.8	0.0	PDE	EQ	ABD	01:33-01:48	16	20073- 7

WAKE HYDROPHONE INFORMATION PROCESSING SYSTEM (WHIPS) EVENT LISTING 19 DEC 83

KEY: INFORMATION SOURCES - PDE=NEIS PDECARD, MON=NEIS MONTHLY LIST, ICS=ICS LIST, HEL=HELICORDER, OTH=OTHER
EVENT TYPE - EQ=EARTHQUAKE, NX=NUCLEAR EXPLOSION, SX=SCIENTIFIC EXPLOSION, OT=OTHER, UN=UNKNOWN
PHASES - A=P, B=PO, C=S, D=SO, E=T, F=OTHER

EVNT NO	ORIGIN TIME YR MO DA JUL HR MN SECS	COORDINATES LAT	LON	LOCATION DESCRIPTION	DEP KM	MAGNI BDY	SRF	INF SRC	EV TP	SAVED PHASES	INTERVAL	MNS	STRIP TAPE-FIL
1384	83 07 22 203 02:25:48.2	8.852S	121.717E	MINAHASSA PENINSULA	53	5.0	0.0	PDE	EQ A	02:29-02:48	12	12	22873- 8
1385	83 07 22 203 02:36:43.9	14.662S	167.251E	VANUATU ISLANDS	193	5.4	0.0	PDE	EQ ABDE	02:38-03:26	49	29	22873- 9
1386	83 07 22 203 02:39:55.3	36.223N	120.395W	CENTRAL CALIFORNIA	7	6.0	5.7	PDE	EQ ABD	02:46-02:10	25	24	22873- 8
1387	83 07 22 203 06:36:14.6	0.190S	121.670E	MINAHASSA PENINSULA	32	5.1	0.0	PDE	EQ A	06:48-06:51	12	29	22873- 9
1388	83 07 23 204 08:29:48.0	0.143S	121.619E	MINAHASSA PENINSULA	46	5.2	0.0	PDE	EQ A	08:33-08:44	12	22	22873-10
1389	83 07 23 204 08:56:13.4	0.223S	121.596E	MINAHASSA PENINSULA	62	5.1	0.0	PDE	EQ A	09:00-09:11	12	22	22873-11
1390	83 07 23 204 15:06:48.4	12.441N	144.001E	SOUTH OF MARIANA ISLANDS	41	4.9	0.0	PDE	EQ ABD	15:07-15:20	14	25	22873-12
1391	83 07 23 204 22:57:24.2	0.133S	121.681E	MINAHASSA PENINSULA	62	5.1	0.0	PDE	EQ A	23:01-23:12	12	22	22873-13
1392	83 07 24 205 00:52:25.5	27.904S	176.488W	KERMADEC ISLANDS REGION	73	5.3	0.0	PDE	EQ A	00:56-01:07	12	22	22873-14
1393	83 07 24 205 05:59:35.2	43.693N	150.370E	KURIL ISLANDS REGION	33	5.0	0.0	PDE	EQ ABDE	06:00-06:42	43	29	22873-15
1394	83 07 24 205 09:40:44.1	6.183S	154.634E	SOLOMON ISLANDS	414	4.9	0.0	PDE	EQ ABDE	09:41-10:22	43	29	22873-16
1395	83 07 24 205 10:58:37.8	51.921N	158.926E	NEAR EAST COAST OF KAMCHATKA	65	4.6	0.0	PDE	EQ ABD	11:00-11:16	17	25	22873-17
1396	83 07 24 205 14:52:33.3	39.739N	139.453E	NEAR W COAST OF HONSHU JAPAN	190	5.2	0.0	PDE	EQ ABDE	14:53-15:39	47	24	22873-18
1397	83 07 24 205 17:50:07.4	19.356S	176.876W	FIJI ISLANDS REGION	288	4.8	0.0	PDE	EQ A	17:52-16:04	13	24	22873-19
1398	83 07 24 205 23:07:30.7	53.852N	158.391E	NEAR EAST COAST OF KAMCHATKA	181	6.1	0.0	PDE	EQ ABDE	23:09-23:59	51	29	22873-20
1399	83 07 24 205 23:38:08.3	8.167S	119.579E	FLORES ISLANDS REGION	33	5.8	5.9	PDE	EQ A	23:42-23:54	13	24	22873-21
1400	83 07 25 206 22:31:42.8	36.220N	120.390W	CENTRAL CALIFORNIA	8	5.6	5.3	PDE	EQ A	22:37-22:48	12	24	22874- 1
1401	83 07 25 206 23:17:44.1	40.102N	139.001E	NEAR W COAST OF HONSHU JAPAN	33	5.0	0.0	PDE	EQ ABDE	23:19-00:05	47	24	22874- 2
1402	83 07 26 207 11:01:59.2	0.044S	121.776E	MINAHASSA PENINSULA	57	5.2	4.0	PDE	EQ A	11:05-11:17	13	24	22874- 3
1403	83 07 26 207 20:14:51.6	0.655N	120.876E	MINAHASSA PENINSULA	43	5.3	4.5	PDE	EQ A	20:19-20:30	12	24	22874- 4
1404	83 07 28 209 01:40:33.3	28.149S	176.255W	KERMADEC ISLANDS REGION	31	5.6	5.4	PDE	EQ A	01:44-01:56	13	24	22874- 5
1405	83 07 28 209 03:00:59.0	0.685N	120.090E	MINAHASSA PENINSULA	41	5.0	0.0	PDE	EQ A	03:05-03:16	12	24	22874- 6
1406	83 07 28 209 09:58:11.1	43.725N	147.668E	KURIL ISLADS	34	5.2	5.0	PDE	EQ ABDE	09:59-10:42	44	24	22874- 7
1407	83 07 28 209 15:06:44.4	42.805N	142.647E	HOKKAIDO JAPAN REGION	59	5.5	0.0	PDE	EQ ABDE	15:08-15:52	45	24	22874- 8
1408	83 07 28 209 19:28:24.1	22.403S	171.430E	LOYALTY ISLANDS REGION	129	5.2	0.0	PDE	EQ A	19:31-19:42	12	24	22874- 9
1409	83 07 29 210 11:25:27.8	6.752S	105.629E	SUNDA STRAIT	33	6.5	5.4	PDE	EQ A	11:31-11:42	12	24	22874-10
1410	83 07 29 210 13:26:54.3	14.328N	146.518E	MARIANA ISLANDS	89	0.0	0.0	PDE	EQ ABD	13:26-13:39	14	24	22874-11
1411	83 07 29 210 14:21:35.6	4.917S	145.376E	NEAR N COAST PAPUA NEW GUINEA	161	4.8	0.0	PDE	EQ ABD	14:23-14:38	16	24	22874-12
1412	83 07 29 210 19:24:23.6	32.322N	140.087E	SOUTH OF HONSHU JAPAN	51	5.0	0.0	PDE	EQ ABDE	19:25-20:05	41	24	22874-13
1413	83 07 29 210 20:25:58.7	5.394N	126.567E	MINDANAO PHILIPPINE ISLANDS	50	5.2	4.5	PDE	EQ A	20:29-20:40	12	24	22874-14
1414	83 07 30 211 03:35:09.6	0.159S	121.720E	MINAHASSA PENINSULA	75	5.0	0.0	PDE	EQ A	03:39-03:50	12	24	22874-15
1415	83 07 30 211 07:07:14.6	0.144S	121.709E	MINAHASSA PENINSULA	63	5.0	0.0	PDE	EQ A	07:11-07:22	12	24	22874-16
1416	83 07 30 211 08:09:52.6	52.451N	170.580W	FOX ISLANDS ALEUTIAN ISLANDS	50	5.2	4.3	PDE	EQ ABDE	08:12-09:03	52	24	22874-17
1417	83 07 30 211 11:24:41.7	56.414N	162.001E	NEAR EAST COAST OF KAMCHATKA	33	4.6	0.0	PDE	EQ ABD	11:27-11:44	18	24	22874-18
1418	83 07 31 212 04:00:24.9	0.616N	120.103E	MINAHASSA PENINSULA	33	5.3	4.4	PDE	EQ A	04:12-04:23	12	24	22874-19
1419	83 07 31 212 09:09:21.3	0.964N	123.931E	MINAHASSA PENINSULA	272	5.1	0.0	PDE	EQ A	09:12-09:23	12	24	22874-20
1420	83 07 31 212 10:26:00.2	20.142S	126.869W	SOUTH PACIFIC OCEAN	10	6.0	5.3	PDE	EQ ABD	10:33-11:02	29	24	22874-21
1421	83 07 31 212 11:57:50.0	20.120S	127.000W	SOUTH PACIFIC OCEAN	10	5.4	0.0	PDE	EQ ABD	12:05-12:32	26	25	22875- 1
1422	83 07 31 212 16:32:33.9	5.620N	94.784E	NORTHERN SUMATERA	96	5.0	0.0	PDE	EQ A	16:39-16:52	12	25	22875- 2
1423	83 07 31 212 21:05:10.5	19.247N	145.435E	MARIANA ISLANDS	163	5.0	0.0	PDE	EQ ABDE	21:04-21:37	34	29	22875- 3
1424	83 08 01 213 03:14:55.7	16.921N	147.190E	MARIANA ISLANDS REGION	52	5.2	4.8	PDE	EQ ABDE	03:14-03:45	32	25	22875- 4
1425	83 08 08 000 00:00:00.0	0.000N	0.000E	PROBABLE MARIANAS PO, SO, T	0	0.0	0.0	HEL	EQ BDE	04:15-04:44	30	25	22875- 5
1426	83 08 01 213 06:01:57.1	3.391S	145.835E	NEAR N COAST PAPUA NEW GUINEA	33	5.0	5.1	PDE	EQ ABDE	06:03-06:47	45	25	22875- 6
1427	83 08 01 213 11:14:42.9	0.086S	121.678E	MINAHASSA PENINSULA	62	5.2	0.0	PDE	EQ A	11:18-11:29	12	25	22875- 7
1428	83 08 02 214 02:17:48.6	20.462N	122.170E	PHILIPPINE ISLANDS REGION	156	6.1	0.0	PDE	EQ A	02:20-02:31	12	25	22875- 8
1429	83 08 02 214 06:00:00.2	45.174N	153.482E	KURIL ISLANDS REGION	68	5.4	0.0	PDE	EQ ABDE	06:09-06:51	43	25	22875- 9
1430	83 08 02 214 12:43:39.2	7.191S	117.398E	BALI SEA	500	5.4	0.0	PDE	EQ A	12:47-12:58	12	25	22875-10
1431	83 08 02 214 13:15:10.3	16.469S	177.615E	FIJI ISLANDS	33	5.1	0.0	PDE	EQ A	13:17-13:29	13	25	22875-11
1432	83 08 02 214 22:07:54.7	27.370N	128.447E	RYUKYU ISLANDS	49	5.4	0.0	PDE	EQ A	22:10-22:21	12	25	22875-12
1433	83 08 03 215 07:12:33.2	11.205S	162.380E	SOLOMON ISLANDS	33	4.9	0.0	PDE	EQ ABD	07:14-07:29	16	25	22875-13
1434	83 08 03 215 13:33:00.0	37.119N	116.000W	SOUTHERN NEVADA	0	4.2	0.0	PDE	NX A	13:39-13:50	12	25	22875-14
1435	83 08 03 215 18:17:44.3	17.360S	167.703E	VANUATU ISLANDS	49	5.4	5.5	PDE	EQ ABDE	18:20-19:10	51	29	22875-15
1436	83 08 03 215 27:29:44.6	22.288S	7.463E	S ATLANTIC OCEAN GOOD ANTIPODE	10	5.1	0.0	PDE	EQ A	22:38-22:57	20	29	22875-16
1437	83 08 03 215 23:10:29.6	21.624N	143.048E	MARIANA ISLANDS REGION	389	5.0	0.0	PDE	EQ ABDE	23:10-23:53	36	29	22875-17
1438	83 08 03 215 23:25:27.6	21.669N	143.054E	MARIANA ISLANDS REGION	385	4.8	0.0	PDE	EQ ABDE	23:25-00:00	36	29	22875-17
1439	83 08 04 216 15:15:16.0	8.274S	128.270E	TIMOR SEA	50	5.4	0.0	PDE	EQ A	15:19-15:30	12	29	22875-18
1440	83 08 05 217 00:33:44.7	52.967N	159.770E	OFF EAST COAST OF KAMCHATKA	33	5.4	4.7	PDE	EQ ABDE	00:35-01:24	50	29	22876- 1
1441	83 08 05 217 05:25:43.7	17.276S	167.791E	VANUATU ISLANDS	33	5.3	5.7	PDE	EQ ABDE	05:28-05:18	51	29	22876- 2
1442	83 08 05 217 06:21:42.4	3.589S	62.171W	WESTERN BRAZIL	21	5.5	5.3	PDE	EQ A	06:31-06:50	20	29	22876- 3
1443	83 08 05 217 07:02:41.3	17.216S	167.827E	VANUATU ISLANDS	33	5.2	5.2	PDE	EQ ABDE	07:05-07:55	51	29	22876- 4
1444	83 08 05 217 08:29:32.3	7.727S	123.548E	BANDA SEA	274	4.8	0.0	PDE	EQ A	08:33-08:44	12	29	22876- 5
1445	83 08 06 218 02:26:49.3	16.134N	93.886W	CHIAPAS MEXICO	86	5.6	0.0	PDE	EQ A	02:35-02:46	12	29	22876- 6
1446	83 08 06 218 15:43:52.6	40.176N	24.728E	AEGEAN SEA	10	6.3	7.1	PDE	EQ AF	15:46-17:47	122	29	22876- 7
1447	83 08 06 218 22:06:03.9	44.413N	149.100E	KURIL ISLANDS	33	5.2	0.0	PDE	EQ ABDE	22:07-22:50	44	29	22876- 8
1448	83 08 06 218 22:37:54.9	6.556S	130.127E	BANDA SEA	161	5.0	0.0	PDE	EQ A	22:41-22:52	12	29	22876- 8
1449	83 08 07 219 02:40:21.7	6.336S	149.236E	NEW BRITAIN REGION	54	4.9	4.4	PDE	EQ ABD	02:49-03:05	17	29	22876- 9
1450	83 08 07 219 06:27:25.3	31.112N	140.540E	SOUTH OF HONSHU JAPAN	127	4.8	0.0	PDE	EQ ABD	06:28-06:42	15	29	22876-10
1451	83 08 08 220 03:47:50.0	35.466N	138.911E	HONSHU JAPAN	33	5.0	5.3	PDE	EQ ABDE	03:49-04:32	44	29	22876-11
1452	83 08 08 220 16:54:11.2	27.521S	13.332W	SOUTH ATLANTIC RIDGE	10	5.2	0.0	PDE	EQ A	17:03-17:22	20	29	22876-12
1453	83 08 09 221 00:23:59.0	7.532S	128.273E	BANDA SEA	173	5.0	0.0	PDE	EQ A	00:27-00:38	12	29	22877- 1
1454	83 08 09 221 10:21:10.6	0.399S	132.590E	WEST IRIAN REGION	33	5.2	5.0	PDE	EQ ABDE	10:23-19:16	54	29	22877- 2
1455	83 08 09 221 22:33:36.2	5.794S	110.439E	JAVA SEA	600	5.1	0.0	PDE	EQ A	22:36-22:49	12	29	22877- 3
1456	83 08 10 222 00:59:59.3	56.660N	152.362W	KODIAK ISLAND REGION	33	5.1	0.0	PDE	EQ ABDE	02:59-02:02	64	29	22877- 4
1457	83 08 10 222 20:05:48.0	23.713S	176.824W	SOUTH FIJI ISLANDS	33	5.4	5.4	PDE	EQ A	20:09-20:20	12	29	22877- 5
1458	83 08 11 223 01:35:39.8	25.955N	123.754E	NORTHEAST OF TAIWAN	206	5.0	0.0	PDE	EQ A	01:38-01:49	12	29	22877- 6
1459	83 08 11 223 02:10:48.7	10.007S	118.775E	SOUTH OF SUMBAWA ISLAND	33	5.1	4.3	PDE	EQ A	02:15-02:26	12	29	22877- 7
1460	83 08 11 223 12:03:01.0	18.014N	120.947E	LUZON PH'LIPPINE ISLANDS	39	5.4	5.4	PDE	EQ A	12:06-12:17	12	29	22877- 8
1461	83 08 11 223 21:35:41.7	42.001N	142.245E	HOKKAIDO JAPAN REGION	71	4.9	0.0	PDE	EQ ABD	21:37-21:52	16	29	22877- 9
1462	83 08 11 223 22:56:11.6	1.036N	127.335E	HALMAHERA	189	5.7	0.0	PDE	EQ A	22:59-23:10	12	29	22877-10
1463	83 08 12 224 07:42:12.5	14.960N	119.842E	LUZON PHILIPPINE ISLANDS	33	5.0	5.1	PDE	EQ A	07:45-07:57	13	29	22877-11
1464	83 08 13 225 02:27:48.5	53.513N	160.339E	NEAR EAST COAST OF KAMCHATKA	33	4.0	0.0	PDE	EQ ABD	02:29-02:46	18	29	22877-12
1465	83 08 13 225 15:39:32.4	7.124S	129.477E	BANDA SEA	189	5.5	0.0	PDE	EQ A	15:43-15:54	12	29	22877-13
1466	83 08 13 225 22:28:19.3	8.722S	111.237E	JAVA	79	5.9	0.0	PDE	EQ A	22:33-22:45	13	29	22877-14
1467	83 08 14 226 12:01:45.5	4.719S	153.180E	NEW IRELAND REGION	69	4.9	0.0	PDE	EQ ABD	12:02-12:17	16	29	22877-15
1468	83 08 14 226 14:11:43.0	12.990S	109.832W	NORTHERN EASTER I. CORDILLERA	10	5.3	0.0	PDE	EQ ABD	14:20-14:50	31	29	22877-16
1469	83 08 14 226 16:20:12.6	17.201S	178.778W	FIJI ISLANDS REGION	524	5.1	0.0	PDE	EQ A	16:22-16:33	12	29	22877-17
1470	83 08 14 226 19:56:39.2	63.336S	169.466E	BALLENY ISLANDS REGION	10	5.4	6.9	PDE	EQ A	20:04-20:15	12	29	22877-18
1471	83 08 14 226 22:26:11.6	9.896S	123.775E	TIMOR	119	5.0	0.0	PDE	EQ A	22:30-22:41	12	29	22877-19
1472	83 08 15 227 04:49:54.7	47.357N	153.169E	KURIL ISLANDS	92	5.0	0.0	PDE	EQ ABDE	04:51-05:35	45	29	22877-20
1473	83 08 15 227 19:44:41.7	17.096S	174.594W	TONGA ISLANDS	211	5.5	0.0	PDE	EQ A	19:47-19:58	12	29	22877-21
1474	83 08 16 228 00:33:44.7	12.290N	143.136E	SOUTH OF MAPIANA ISLANDS	66	5.2	0.0	PDE	EQ ABDE	00:34-01:10	37	29	22877-22
1475	83 08 16 228 05:20:29.6	8.073S	123.967E	MINAHASSA PENINSULA	126	5.2	0.0	PDE	EQ A	05:24-05:35	12	29	22878- 1
1476	83 08 16 228 13:37:19.0	36.638N	141.167E	NEAR E COAST OF HONSHU JAPAN	63	5.1	0.0	PDE	EQ ABDE	13:38-14:20	43	29	22878- 2
1477	83 08 16 228 16:29:01.3	4.780S	103.199E	SOUTHERN SUMATERA	59	5.1	0.0	PDE	EQ A	16:35-16:46	12	29	22878- 3
1478	83 08 17 229 01:11:13.4	18.758N	145.374E	MARIANA ISLANDS	213	4.5	0.0	PDE	EQ ABDE	01:10-01:43	34	29	22878- 4
1479	83 08 17 229 06:03:53.1	14.891S	166.886E	VANUATU ISLANDS	50	5.0	0.0	PDE	EQ ABDE	06:05-06:52	48	29	22878- 5
1480	83 08 17 229 09:29:48.6	8.775S	111.125E	JAVA	61	5.4	0.0	PDE	EQ A	09:35-09:46	12	29	22878- 6
1481	83 08 17 229 10:55:52.8	55.786N	161.212E	NEAR EAST COAST OF KAMCHATKA	55	6.5	6.7	PDE	EQ ABDE	10:58-11:49	52	29	22878- 7
1482	83 08 17 229 12:17:55.9	18.159N	120.982E	LUZON PHILIPPINE ISLANDS	30	6.2	6.7	PDE	EQ ABDE	12:21-13:19	59	29	22878- 8
1483	83 08 17 229 12:59:10.3	22.546S	174.330W	TONGA ISLANDS REGION	33	5.1	0.0	PDE	EQ A	13:02-13:14	13	29	22878- 8

WAKE HYDROPHONE INFORMATION PROCESSING SYSTEM (WHIPS) EVENT LISTING 19 DEC 83

KEY: INFORMATION SOURCES - PDE=NEIS PDECARD, MON=NEIS MONTHLY LIST, ICS=ICS LIST, HEL=HELICORDER, OTH=OTHER
EVENT TYPE - EQ=EARTHQUAKE, NX=NUCLEAR EXPLOSION, SX=SCIENTIFIC EXPLOSION, OT=OTHER, UN=UNKNOWN
PHASES - A=P, B=PO, C=S, D=SO, E=T, F=OTHER

EVNT NO	ORIGIN TIME YR MO DA JUL HR MN SECS	COORDINATES LAT LON	LOCATION DESCRIPTION	DEP KM	MAGNI BDY	MAGNI SRF	INF SRC	EV TP	SAVED PHASES	SAVED INTERVAL	MNS	STRIP TAPE-FIL
1484	83 08 18 230 08:30:10.2	19.416S 172.779W	TONGA ISLANDS REGION	33	5.3	5.0	PDE	EQ	A	08:33-08:44	12	20078- 9
1485	83 08 18 230 09:42:30.1	3.835S 151.293E	NEW IRELAND REGION	33	5.2	0.0	PDE	EQ	ABDE	09:43-10:24	42	20076-10
1486	83 08 18 230 16:05:40.3	3.748S 151.344E	NEW IRELAND REGION	33	5.2	0.0	PDE	EQ	ABDE	16:06-16:47	42	20078-11
1487	83 08 18 230 16:09:58.6	73.373N 54.039E	NOVAYA ZEMLYA	0	5.9	4.1	PDE	NX	A	16:17-16:28	12	20078-11
1488	00 00 00 000 00:00:00.0	0.000N 0.000E	PROBABLE MARIANAS PO SO T	0	0.0	0.0	HEL	EQ	BDE	17:37-18:06	30	20076-12
1489	83 08 18 230 19:46:49.6	3.786S 151.190E	NEW IRELAND REGION	33	5.2	4.9	PDE	EQ	A	19:47-19:59	13	20076-13
1490	83 08 19 231 14:35:34.3	2.175N 127.078E	MOLUCCA PASSAGE	55	5.2	4.3	PDE	EQ	A	14:38-14:49	12	20076-14
1491	00 00 00 000 00:00:00.0	0.000N 0.000E	PROBABLE BONIN ISL. PO SO T	0	0.0	0.0	HEL	EQ	BDE	00:54-01:30	37	20076-15
1492	00 00 00 000 00:00:00.0	0.000N 0.000E	PROBABLE JAPAN PO SO T	0	0.0	0.0	HEL	EQ	BDE	05:24-06:05	42	20079- 1
1493	83 08 20 232 06:19:28.2	8.558S 117.569E	SUMBAWA ISLAND REGION	134	5.5	0.0	PDE	EQ	A	06:24-06:35	12	20079- 2
1494	83 08 20 232 13:08:31.7	27.866N 141.807E	BONIN ISLANDS REGION	35	5.8	5.5	PDE	EQ	ABDE	13:09-13:46	38	20079- 3
1495	83 08 20 232 14:48:30.2	58.865N 156.160E	KURIL ISLANDS	120	5.0	0.0	PDE	EQ	ABDE	14:50-15:37	48	20079- 4
1496	83 08 20 232 17:15:06.6	18.117S 179.734W	FIJI ISLANDS REGION	659	4.7	0.0	PDE	EQ	A	17:17-17:28	12	20079- 5
1497	83 08 20 232 17:15:24.4	39.328N 73.611E	TAJIK-XINJIANG BORDER REGION	33	4.9	4.4	PDE	EQ	A	17:22-17:34	13	20079- 6
1498	83 08 21 233 06:18:55.0	4.519N 127.789E	TALAUD ISLANDS	83	5.0	0.0	PDE	EQ	A	06:21-06:33	13	20079- 6
1499	83 08 21 233 08:34:45.8	3.714N 126.620E	TALAUD ISLANDS	48	5.8	5.6	PDE	EQ	A	08:37-08:49	13	20079- 7
1500	83 08 21 233 17:21:13.6	7.384S 121.185E	FLORES SEA	541	5.1	0.0	PDE	EQ	A	17:25-17:36	12	20079- 8
1501	83 08 21 233 18:58:19.2	28.782S 112.653W	EASTER ISLAND REGION	10	5.4	5.5	PDE	EQ	A	19:06-19:18	13	20079- 9
1502	83 08 21 233 22:57:31.4	23.481S 177.188W	SOUTH OF FIJI ISLANDS	169	5.5	0.0	PDE	EQ	A	23:00-23:12	13	0- 0
1503	83 08 22 234 04:58:11.9	31.888N 141.710E	SOUTH OF HONSHU JAPAN	33	4.5	0.0	PDE	EQ	ABD	04:59-05:13	15	0- 0
1504	83 08 22 234 05:53:26.8	14.827S 166.969E	VANUATU ISLANDS	112	5.5	0.0	PDE	EQ	ABDE	05:55-06:43	49	0- 0
1505	83 08 22 234 09:09:42.3	7.819S 130.811E	TANIMBAR ISLANDS REGION	33	5.8	0.0	PDE	EQ	A	09:13-09:24	12	20080- 1
1506	83 08 22 234 12:30:21.4	7.208N 34.422W	CENTRAL MID-ATLANTIC RIDGE	10	5.1	0.0	PDE	EQ	A	12:47-13:07	21	20080- 2
1507	83 08 22 234 12:39:06.7	53.861N 160.493E	NEAR EAST COAST OF KAMCHATKA	33	5.4	0.0	PDE	EQ	ABDE	12:41-13:30	50	20080- 2
1508	83 08 22 234 23:00:42.5	16.209S 167.903E	VANUATU ISLANDS	185	5.1	0.0	PDE	EQ	ABDE	23:02-23:52	51	20080- 3
1509	83 08 22 234 23:16:30.0	3.587S 146.644E	BISMARCK SEA	29	5.4	5.5	PDE	EQ	ABDE	23:18-00:01	44	20080- 3
1510	83 08 23 235 11:15:16.9	5.917S 150.996E	NEW BRITAIN REGION	52	5.1	4.0	PDE	EQ	ABDE	11:16-11:59	44	20080- 4
1511	83 08 23 235 12:12:16.9	24.567N 95.200E	BURMA	126	5.1	0.0	PDE	EQ	A	12:18-12:29	12	20080- 5
1512	83 08 23 235 23:39:41.0	5.912S 151.068E	NEW BRITAIN REGION	51	5.3	5.8	PDE	EQ	ABDE	23:41-00:23	43	20080- 6
1513	83 08 24 236 13:36:30.9	40.305N 124.767W	NEAR COAST OF NORTHERN CALIF	30	5.5	5.7	PDE	EQ	ABDE	13:42-14:59	78	20080- 7
1514	83 08 24 236 20:19:51.3	3.627N 122.258E	CELEBES SEA	621	4.8	0.0	PDE	EQ	A	20:22-20:33	12	20080--8
1515	83 08 25 237 00:12:50.0	5.427S 150.919E	NEW BRITAIN REGION	112	5.1	0.0	PDE	EQ	ABDE	00:14-00:56	43	20080--9
1516	83 08 25 237 07:03:00.3	5.945S 151.000E	NEW BRITAIN REGION	40	5.5	0.0	PDE	EQ	ABDE	07:04-07:47	44	20080-10
1517	83 08 25 237 11:05:30.0	39.152N 74.052E	SOUTHERN XINJIANG CHINA	33	5.0	4.9	PDE	EQ	A	11:13-11:24	12	20080-11
1518	83 08 25 237 20:23:32.6	33.490N 131.430E	KYUSHU JAPAN	121	6.1	0.0	PDE	EQ	ABDE	20:25-21:14	50	20080-12
1519	00 00 00 000 00:00:00.0	0.000N 0.000E	PROBABLE BONIN ISL. PO SO T	0	0.0	0.0	HEL	EQ	BDE	01:13-01:52	40	20081- 1
1520	83 08 26 238 02:34:34.0	2.847S 139.097E	NEAR N COAST OF WEST IRIAN	76	5.4	0.0	PDE	EQ	A	02:36-02:47	12	20081- 2
1521	83 08 26 238 08:18:15.1	3.684N 127.143E	TALAUD ISLANDS	33	5.2	0.0	PDE	EQ	A	08:21-08:32	12	20081- 3
1522	83 08 26 238 18:20:32.8	20.705S 169.583E	VANUATU ISLANDS	100	5.3	0.0	PDE	EQ	ABDE	18:23-19:17	55	20081--4
1523	00 00 00 000 00:00:00.0	0.000N 0.000E	PROBABLE MARIANAS PO SO T	0	0.0	0.0	HEL	EQ	BDE	01:49-02:29	41	20081- 5
1524	83 08 27 239 04:14:20.8	20.642S 178.823W	FIJI ISLANDS REGION	620	4.7	0.0	PDE	EQ	A	04:16-04:28	13	20081- 6
1525	83 08 27 239 11:50:29.8	8.174N 126.005E	MINDANAO PHILIPPINE ISLANDS	55	5.2	0.0	PDE	EQ	A	11:53-12:04	12	20081- 7
1526	83 08 27 239 12:31:40.9	85.517N 90.603E	NORTH OF SEVERNAYA ZEMLYA	10	4.7	4.8	PDE	EQ	A	12:38-12:49	12	20081--8
1527	83 08 27 239 18:49:50.3	8.186N 125.962E	MINDANAO PHILIPPINE ISLANDS	33	5.5	6.0	PDE	EQ	ABDE	18:50-19:49	60	20081- 9
1528	83 08 28 240 11:30:14.7	46.197N 151.544E	KURIL ISLANDS	75	5.5	0.0	PDE	EQ	ABDE	11:31-12:15	45	20081-10
1529	83 08 28 240 13:19:32.5	44.972N 148.771E	KURIL ISLANDS	33	5.0	0.0	PDE	EQ	ABDE	13:20-14:04	45	20081-**
1530	83 08 29 241 05:19:24.5	3.430S 148.891E	BISMARCK SEA	33	5.2	5.0	PDE	EQ	ABDE	05:20-06:02	43	20081-12
1531	83 08 29 241 10:10:31.0	35.830N 121.353W	CENTRAL CALIFORNIA	0	5.3	0.0	PDE	EQ	ABDE	10:16-11:37	82	20082- 1
1532	00 00 00 000 00:00:00.0	0.000N 0.000E	PROBABLE KURILS	0	0.0	0.0	HEL	EQ	BDE	10:12-10:54	43	20082- 1
1533	83 08 29 241 15:36:13.6	9.561N 126.337E	MINDANAO PHILIPPINE ISLANDS	49	5.3	4.1	PDE	EQ	A	15:39-15:50	12	0- 0
1534	83 08 30 242 05:57:01.5	6.360S 130.485E	BANDA SEA	136	5.1	0.0	PDE	EQ	A	06:00-06:11	12	0- 0
1535	83 08 30 242 06:50:16.6	16.683S 172.075W	SAMOA ISLANDS REGION	35	6.1	5.7	PDE	EQ	ABD	08:53-09:11	19	0- 0
1536	83 08 30 242 10:39:27.3	25.071N 94.722E	BURMA-INDIA BORDER REGION	63	5.6	0.0	PDE	EQ	A	10:45-10:56	12	0- 0
1537	83 08 30 242 22:15:59.6	9.558S 158.818E	SOLOMON ISLANDS	76	5.0	0.0	PDE	EQ	ABDE	22:17-23:00	44	0- 0
1538	83 09 01 243 19:40:11.2	12.514N 144.238E	SOUTH OF MARIANA ISLANDS	33	4.3	3.9	PDE	EQ	ABDE	19:40-20:15	36	0- 0
1539	83 08 31 243 22:20:07.4	53.503N 163.622W	UNIMAK ISLAND REGION	33	5.1	0.0	PDE	EQ	A	22:23-22:34	12	0- 0
1540	00 00 00 000 00:00:00.0	0.000N 0.000E	PROBABLE MARIANAS	0	0.0	0.0	HEL	EQ	BDE	09:21-09:54	34	0- 0
1541	83 09 01 244 14:00:02.0	37.273N 116.355W	SOUTHERN NEVADA	0	5.4	0.0	PDE	NX	A	14:06-14:17	12	0- 0
1542	83 09 02 245 03:05:40.2	36.624N 140.932E	NEAR E COAST OF HONSHU JAPAN	60	5.1	0.0	PDE	EQ	ABDE	03:06-03:49	44	0- 0
1543	83 09 02 245 04:09:39.0	52.363N 175.517W	ANDREANOF ISL. ALEUTIAN ISL.	112	4.7	0.0	PDE	EQ	ABD	04:11-04:28	18	0- 0

EOF..

END

FILMED

3-84

DTIC